Earth-Science Reviews

Loess landscapes of Europe – mapping, geomorphology, and zonal differentiation

--Manuscript Draft--

Manuscript Number:	
Article Type:	Review Article
Keywords:	Aeolian deposits; Quaternary sediments; loess map; loess facies; dust deposition; conceptual loess formation model
Corresponding Author:	Frank Lehmkuhl, Prof. Dr. RWTH Aachen University: Rheinisch-Westfalische Technische Hochschule Aachen Aachen, GERMANY
First Author:	Frank Lehmkuhl, Prof. Dr.
Order of Authors:	Frank Lehmkuhl, Prof. Dr.
	Janina J. Nett, Dr.
	Stephan Pötter
	Philipp Schulte, Dr.
	Tobias Sprafke, Dr.
	Zdzislaw Jary, Prof. Dr.
	Pierre Antoine, Prof. Dr.
	Lara Wacha, Dr.
	Daniel Wolf, Dr.
	Andrea Zerboni, Prof. Dr.
	Jan Hošek, Dr.
	Slobodan B. Marković, Prof. Dr.
	Igor Obreht, Dr.
	Pál Sümegi, Prof. Dr.
	Daniel Veres, Dr.
	Christian Zeeden, Dr.
	Bruno J. Boemke
	Viktor Schaubert
	Jonas Viehweger
	Ulrich Hambach, Dr.
Abstract:	Paleoenvironmental reconstructions on a (supra-)regional scale have gained attention in Quaternary sciences during the last decades. In terrestrial realms, loess deposits and especially intercalations of loess and buried soils, so called loess-paleosol sequences (LPS) are important archives in order to unravel the terrestrial response to e.g. climatic fluctuations and reconstruct paleoenvironments during the Pleistocene. The analysis of LPS requires the knowledge of several key factors, such as the distribution of the aeolian sediments, their location relative to (potential) source areas, the climate conditions that led to their emplacement and the topography of the sink area. These factors strongly influence the sedimentological and paleoenvironmental characteristics of LPS and show broad variations throughout Europe, leading to a distinct distribution pattern throughout the continent. In our study, we present a new map of the distribution of aeolian sediments (mainly loess) and major potential source areas for Europe. The map was compiled combining geodata of different mapping approaches. Most of the used geodata stems from national maps of 27 different countries, which are highly accurate. Problematic aspects

	such as different nomenclatures across administrative borders were carefully investigated and revised. The result is a seamless map, which comprises pedological, geological, and geomorphological data and can be used for paleoenvironmental and archeological studies and other applications. We use the map and geomorphological cross-sections to discuss the various influences of geomorphology and paleoenvironment on the deposition and preservation of loess throughout Europe. We divided the loess areas into 6 main loess domains and 17 subdomains, in order to understand and explain the factors controlling their distribution. For the subdivision we used the following criteria: (1) influence of silt production areas, (2) affiliation to subcatchments, as rivers are very important regional silt transport agents, (3) occurrence of past periglacial activity with characteristic overprinting of the deposits. Additionally, the sediment distribution is combined with elevation data, to investigate the loess distribution statistically as well as visually. Throughout Europe, the variations and differences of the loess domains are the results of a complex interplay of changing paleoenvironmental conditions and related geomorphologic processes, controlling dust sources, transport, accumulation, preservation, pedogenesis, and simultaneous erosional and reworking events. Climatic, paleoclimatic, and pedoclimatic gradients are on the continental scale an additional important factor, since there are e.g. latitudinal differences of permafrost and periglacial processes, an increase in continentality from west to east and in aridity from northwest to southeast and south, strongly affecting sedimentary and geomorphic dynamics. We propose three main depositional regimes for loess formation in Europe: (1.) periglacial and tundra loess formation with periglacial processes and permafrost in the high latitude and mountainous regions; (2.) steppe and desert margin loess formation in the (semi-)arid regions; and (3.) loess and soil formation in temperate and subtropical regions. Loess deposits of (1.) and (2.) show coarser, sandier particle distributions toward the glacial and desert regions. In the humid areas (3.), forest vegetation limited dust production and accumulation, therefore, there is an increase in finer grain sizes due to the increase in weathering.
Suggested Reviewers:	Jef Vandenberghe, Prof jef.vandenberghe@vu.nl Expert on European loess and plaeoclimate
	Randell Schaetzl, Prof Michigan State University soils@msu.edu Loess expert with international knowledge
	Gábor Újvári senior researcher, Hungarian Academy of Sciences Institute of Experimental Medicine: Magyar Tudomanyos Akademia Kiserleti Orvostudomanyi Kutatointezet ujvari.gabor@csfk.mta.hu Expert on loess especially in Central and SE Europe
	Huayu Lu Nanjing University huayulu@nju.edu.cn Expert on Chinese loess
Opposed Reviewers:	

Dear editors,

We would like to submit the following review and research paper for the ESR:

Loess landscapes of Europe – mapping, geomorphology and zonal differentiation

Our submission presents first a new seamless map of the distribution of aeolian sediments (mainly loess) and major potential source areas for loess Europe. The map was compiled combining geodata of different mapping approaches from 27 different countries, which are highly accurate. We review the European loess landscapes and divided them in six domains and 17 subdomains. In addition, we show geomorphologic aspects of loess regions including 3-D images of selected loess landscapes. Finally we propose three main depositional regimes for loess formation in Europe in a new conceptual model of loess genesis. We will provide all data of this new map on our CRC website for free download and provide funding for golden access of this paper.

All authors have made substantial contributions to the submission. We confirm that each co-author was involved in the paper and have approved the final version of the manuscript: FL: Conceptualization, writing original draft, funding acquisition. JN: Project administration, methodology, validation, writing introduction, Chapter 3.3 and part of the discussion, review & editing. SP: Methodology, validation, data curation, writing regional part, Chapter 3.2, and part of the discussion. TS, PS, ZJ: Data curation, writing regional part, writing – review PA, JH, LW, DW AZ: Resources, data curation, writing regional part. SM, IO, DV. Data curation, writing regional part BB: Investigation, data curation, methodology VS: Visualization, formal analysis. JV: Investigation, data curation, software. UH: validation, partially designing and contributing to conceptual model, writing regional part, validation, review & editing.

Potential reviewers could be:
Prof. J. Vandenberghe, VU Amsterdam
Prof. R. Schaetzl, Michigan State University, USA
Prof. Lu Huayu, Nanjing University, China
Dr. Gábor Újvári, Hungarian Academy of Sciences, Hungary

On behalf of all authors

Yours sincerely,

Frank Lehmkuhl

Loess landscapes of Europe – mapping, geomorphology, and zonal differentiation

Lehmkuhl, F.[1*], Nett, J.J.[1], Pötter, S.[1], Schulte, P.[1], Sprafke, T.[2], Jary, Z.[3], Antoine, P.[4], Wacha, L.[5], Wolf, D.[6], Zerboni, A.[7], Hošek, J.[8,9], Marković, S.B.[10], Obreht, I.[1,11], Sümegi, P.[12], Veres, D.[13], Zeeden, C.[1,14], Boemke, B[1], Schaubert, V.[1], Viehweger, J.[1], Hambach, U.[15]

Abstract

Paleoenvironmental reconstructions on a (supra-)regional scale have gained attention in Quaternary sciences during the last decades. In terrestrial realms, loess deposits and especially intercalations of loess and buried soils, so called loess-paleosol sequences (LPS) are important archives in order to unravel the terrestrial response to e.g. climatic fluctuations and reconstruct paleoenvironments during the Pleistocene. The analysis of LPS requires the knowledge of several key factors, such as the distribution of the aeolian sediments, their location relative to (potential) source areas, the climate conditions that led to their emplacement and the topography of the sink area. These factors strongly influence the sedimentological and paleoenvironmental characteristics of LPS and show broad variations throughout Europe, leading to a distinct distribution pattern throughout the continent.

In our study, we present a new map of the distribution of aeolian sediments (mainly loess) and major potential source areas for Europe. The map was compiled combining geodata of different mapping approaches. Most of the used geodata stems from national maps of 27 different countries, which are highly accurate. Problematic aspects such as different nomenclatures across administrative borders were carefully investigated and revised. The result is a seamless map, which comprises pedological, geological, and geomorphological data and can be used for paleoenvironmental and archeological studies and other applications.

We use the map and geomorphological cross-sections to discuss the various influences of geomorphology and paleoenvironment on the deposition and preservation of loess throughout Europe. We divided the loess areas into 6 main loess domains and 17 subdomains, in order to understand and explain the factors controlling their distribution. For the subdivision we used the following criteria: (1) influence of silt production areas, (2) affiliation to subcatchments, as rivers are very important regional silt transport agents, (3) occurrence of past periglacial activity with characteristic overprinting of the deposits. Additionally, the sediment distribution is combined with elevation data, to investigate the loess distribution statistically as well as visually.

Throughout Europe, the variations and differences of the loess domains are the results of a complex interplay of changing paleoenvironmental conditions and related geomorphologic processes, controlling dust sources, transport, accumulation, preservation, pedogenesis, and simultaneous erosional and reworking events. Climatic, paleoclimatic, and pedoclimatic gradients are on the continental scale an additional important factor, since there are e.g. latitudinal differences of permafrost and periglacial processes, an increase in continentality from west to east and in aridity from northwest to southeast and south, strongly affecting sedimentary and geomorphic dynamics.

We propose three main depositional regimes for loess formation in Europe: (1.) periglacial and tundra loess formation with periglacial processes and permafrost in the high latitude and mountainous regions; (2.) steppe and desert margin loess formation in the (semi-)arid regions; and (3.) loess and soil formation in temperate and subtropical regions. Loess deposits of (1.) and (2.) show coarser, sandier particle distributions toward the glacial and desert regions. In the humid areas (3.), forest vegetation limited dust production and accumulation, therefore, there is an increase in finer grain sizes due to the increase in weathering.

Loess landscapes of Europe – mapping, geomorphology, and zonal differentiation

Lehmkuhl, F.[1*], Nett, J.J.[1], Pötter, S.[1], Schulte, P.[1], Sprafke, T.[2], Jary, Z.[3], Antoine, P.[4], Wacha, L.[5], Wolf, D.[6], Zerboni, A.[7], Hošek, J.[8,9], Marković, S.B.[10], Obreht, I.[1,11], Sümegi, P.[12], Veres, D.[13], Zeeden, C.[1,14], Boemke, B[1], Schaubert, V.[1], Viehweger, J.[1], Hambach, U.[15]

[1] Department of Geography, RWTH Aachen University, Germany

[2] Institute of Geography, University of Bern, Switzerland

[3] University of Wroclaw, Institute of Geography and Regional Development, Wrocław, Poland

[4] CNRS-Université Paris I UPEC, Laboratoire de Géographie Physique, Environnements quaternaires et actuels, Meudon, France

[5] Croatian Geological Survey, Zagreb, Croatia

[6] Department of Geography, TU Dresden, Germany

[7] Dipartimento di Scienze della Terra "A. Desio", Università degli Studi di Milano, Milano, Italy

[8] Czech Geological Survey, Prague, Czech Republic

[9] Center for Theoretical Study, Charles University and the Academy of Sciences, Jilská 1, 110 00 Praha 1, Czech Republic

[10] Department of Physical Geography, Faculty of Sciences,University of Novi Sad, Trg Dositeja Obradovića 3, 21000 Novi Sad, Serbia

[11] Organic Geochemistry Group, MARUM-Center for Marine Environmental Sciences and Department of Geosciences, University of Bremen, Bremen, Germany.

[12] Department of Geology and Paleontology, University of Szeged, Hungary & Institute of Geography and Earth Sciences, University of Szeged, Hungary

[13] Institute of Speleology, Romanian Academy, Cluj-Napoca, Romania

[14] Leibniz Institute for Applied Geophysics, Stilleweg 2, 30655 Hannover, Germany

[15] BayCEER & Chair of Geomorphology, University of Bayreuth, Germany

**Corresponding author: Prof. Dr. Frank Lehmkuhl, flehmkuhl@geo.rwth-aachen.de*

Abstract

Paleoenvironmental reconstructions on a (supra-)regional scale have gained attention in Quaternary sciences during the last decades. In terrestrial realms, loess deposits and especially intercalations of loess and buried soils, so called loess-paleosol sequences (LPS) are important archives in order to unravel the terrestrial response to e.g. climatic fluctuations and reconstruct paleoenvironments during the Pleistocene. The analysis of LPS requires the knowledge of several key factors, such as the distribution of the aeolian sediments, their location relative to (potential) source areas, the climate conditions that led to their emplacement and the topography of the sink area. These factors strongly influence the sedimentological and paleoenvironmental characteristics of LPS and show broad variations throughout Europe, leading to a distinct distribution pattern throughout the continent.

In our study, we present a new map of the distribution of aeolian sediments (mainly loess) and major potential source areas for Europe. The map was compiled combining geodata of different mapping approaches. Most of the used geodata stems from national maps of 27 different countries, which are highly accurate. Problematic aspects such as different nomenclatures across administrative borders were carefully investigated and revised. The result is a seamless map, which comprises pedological, geological, and geomorphological data and can be used for paleoenvironmental and archeological studies and other applications.

We use the map and geomorphological cross-sections to discuss the various influences of geomorphology and paleoenvironment on the deposition and preservation of loess throughout Europe. We divided the loess areas into 6 main loess domains and 17 subdomains, in order to understand and explain the factors controlling their distribution. For the subdivision we used the following criteria: (1) influence of silt production areas, (2) affiliation to subcatchments, as rivers are very important regional silt transport agents, (3) occurrence of past periglacial activity with characteristic overprinting of the deposits. Additionally, the sediment distribution is combined with elevation data, to investigate the loess distribution statistically as well as visually.

Throughout Europe, the variations and differences of the loess domains are the results of a complex interplay of changing paleoenvironmental conditions and related geomorphologic processes, controlling dust sources, transport, accumulation, preservation, pedogenesis, and simultaneous erosional and reworking events. Climatic, paleoclimatic, and pedoclimatic gradients are on the continental scale an additional important factor, since there are e.g. latitudinal differences of permafrost and periglacial processes, an increase in continentality from west to east and in aridity from northwest to southeast and south, strongly affecting sedimentary and geomorphic dynamics.

We propose three main depositional regimes for loess formation in Europe: (1.) periglacial and tundra loess formation with periglacial processes and permafrost in the high latitude and mountainous regions; (2.) steppe and desert margin loess formation in the (semi-)arid regions; and (3.) loess and soil formation in temperate and subtropical regions. Loess deposits of (1.) and (2.) show coarser, sandier particle distributions toward the glacial and desert regions. In the humid areas

(3.), forest vegetation limited dust production and accumulation, therefore, there is an increase in finer grain sizes due to the increase in weathering.

Highlights

- New seamless loess map of Europe including related Late Pleistocene sediments
- Review on European loess landscapes divided in six domains and 17 subdomains
- Geomorphology of loess regions including 3-D images of selected loess landscapes
- New conceptual model of loess genesis in Europe
- Paleoenvironmental variations determine spatial pattern of loess formation and domain subdivision

Keywords

Aeolian deposits, Quaternary sediments, loess map, loess facies, dust deposition, conceptual loess formation model

1. Introduction and general approach

Loess is one of the most extensively distributed Pleistocene sedimentary deposits in the northern hemisphere and Europe, representing the main archive of glacial periods (Bertran et al., 2016; Haase et al., 2007; Marković et al., 2015; Rousseau et al., 2013). The so-called loess-paleosol sequences (LPS) composed of the alternation of loess and buried soil (paleosol) horizons developed in response to climatic changes, and are key-archives in order to unravel paleoclimate (eg. Gallet et al., 1996; Obreht et al., 2017; Torre et al., 2020), paleoenvironments (eg. Hatté et al., 2013; Liu and Liu, 2017; Schaetzl et al., 2018; Schatz et al., 2011), and paleolandscapes (eg. Hughes et al., 2010; Lehmkuhl et al., 2016; Leonova et al., 2015). The fertile topsoils of loess landscapes have been heavily employed in agricultural practices with highly specialized past to present agricultural use of the loess lowlands already during the Neolithic, 7000 years ago (Bellwood, 2005; Whittle and Whittle, 1996). The Late Pleistocene loess steppe and loess tundra also play an important role in understanding early modern human migration and the occupation of Europe (Chu, 2018; Haesaerts et al., 2004; Hauck et al., 2017; Neugebauer-Maresch et al., 2014; Obreht et al., 2017; Zeuner, 1956). Stratigraphic and pedostratigraphic records across European LPS exhibit a more or less constant pattern including marker horizons (especially paleosols and paleosols complexes) that can be followed over long distances (Antoine et al., 2019, 2016; Haesaerts et al., 2004). This pattern demonstrates that LPS are formed in response to at least supra-regional climatic forcing at various time-scales from glacial-interglacial (Bronger, 2003; Kukla, 1977) to millennial-scale cycles (e.g. Dansgaard-Oeschger cycles, Antoine et al., 2009a; Moine et al., 2017; Rousseau et al., 2011, 2007; Zeeden et al., 2018). To understand the environments under which loess deposits form, it is crucial to know their occurrence and distribution, the geomorphological setting they formed in, and the climate conditions present during their formation (e.g. Pécsi and Richter, 1996; Smalley and Leach, 1978). To comprehend and analyze these environments, maps of the distribution of Quaternary aeolian sediments in western Eurasia mid-latitudes show not only their abundance, but also their distance to potential source areas and their relationship to elevation and relief (Lehmkuhl et al., 2018a, 2018b; Lindner et al., 2017). As early as the first half of the 20th century, the climatic importance of Scandinavian and Alpine ice sheets for the zonal evolution of loess deposits in Europe was understood and implications for a zonal distribution of loess facies were proposed (e.g. Zeuner, 1937). Generally, the distribution of loess and especially the development of LPS in Europe were controlled by relief, climate, the distance to large river systems, past continental ice sheets and the exposed shelf area of the North Sea may have been a key factor (Antoine et al., 2016; Lehmkuhl et al., 2016).

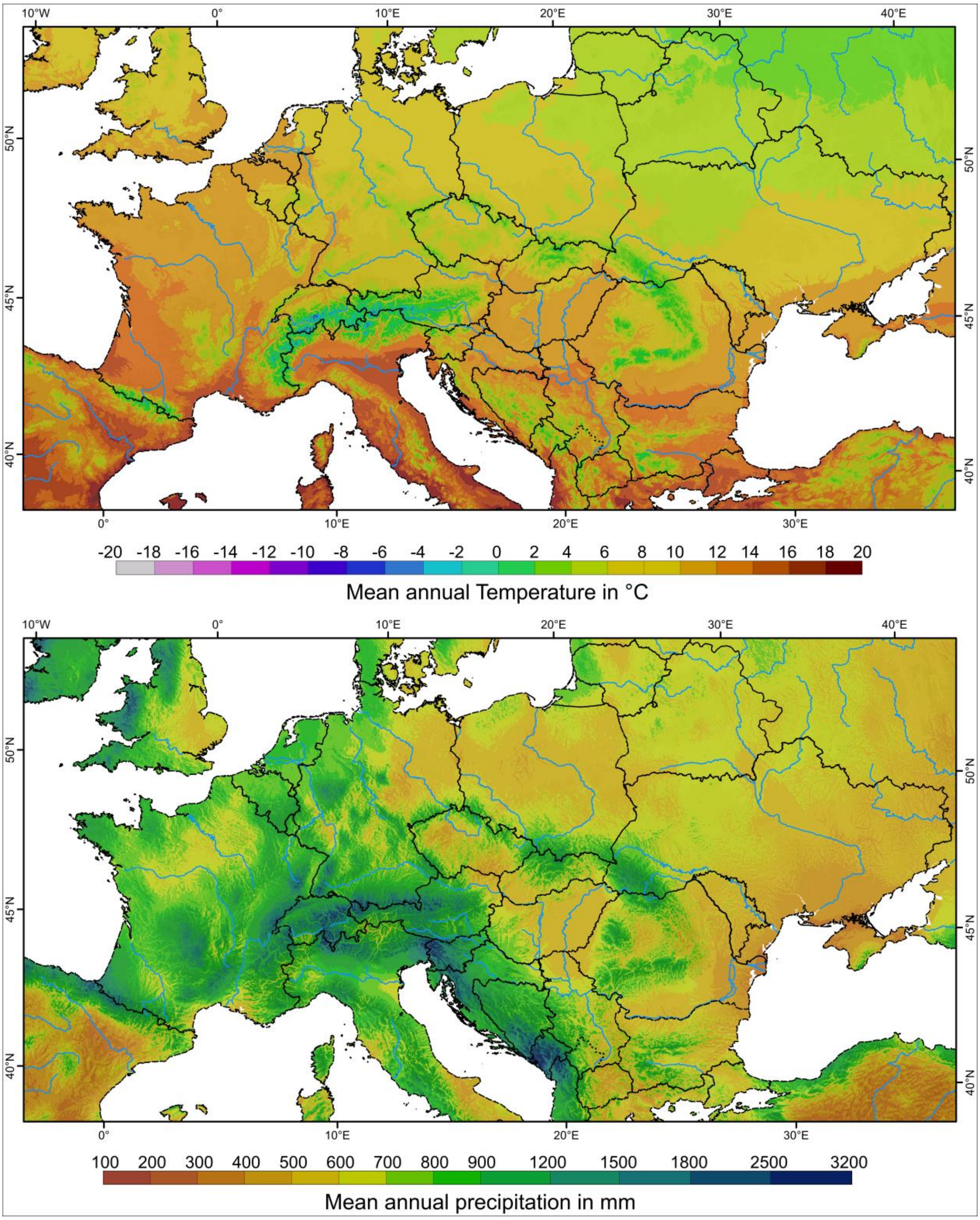

Figure 1: Modern climatic conditions in Europe. Mean annual air temperature on the upper panel, annual precipitation on the lower panel. Data adapted from Karger et al. (2017).

Maps highlighting the distribution of Quaternary aeolian deposits are an important tool to understand paleoenvironments in a spatial manner and context, and to deduce source and sink relationships at greater geomorphological scales. Maps are also useful tool in paleoecology and to reconstruct the dynamic of past human groups. The first loess maps at the European scale were produced by Grahmann (1932) and Fink et al. (1977). Later, a digital European Loess Map was published by Haase et al. (2007). More recently, Bertran et al. (2016) generated a map of European Pleistocene aeolian deposits based on topsoil textural data from the Land Use and Cover Area frame Statistical survey database (LUCAS, Orgiazzi et al., 2018; Tóth et al., 2013). Lastly, Li et al. (2020) prepared global distribution maps of provenance and transport pathways of major loess areas and discussed their genesis. Although several examples of loess maps exist, most mapping approaches encounter difficulties related to scale and availability of geodata. The choice of scale depends on the research question at hand. Most maps are either very detailed on a local scale or are presented at a larger scale and lack precision. Combining several national or regional maps can circumvent this problem but this often leads to artificial spatial breaks within the geodata, which can only be amended by evaluation and generalization of the geodata sets (e.g. Lehmkuhl et al., 2018a, 2018b).

While gathering and processing continent-wide geodata for an updated, seamless map of aeolian sediments in Europe, we already compiled three regional-scale maps. The loess map of Hungary and western Romania is based on geological and pedological data (Lindner et al., 2017). The subsequent map of the entire Carpathian Basin, combines geodata sources from ten different countries (Lehmkuhl et al., 2018a). Several cross-border problems arose due to different terminologies and definitions of loess and related sediments, which are a consequence of the complex genesis of loess sediments and the fundamental lack of representative genetic formation models (Lehmkuhl et al., 2018a; Smalley et al., 2011; Sprafke and Obreht, 2016). Such difficulties are not only restricted to national borders, but are sometimes even present within one country, as shown in the map of loess and other Quaternary sediments in Germany (Lehmkuhl et al., 2018b). Due to the federal system in Germany, artificial breaks between different states could only be avoided by combining loess and loess derivates in one mapping unit (Lehmkuhl et al., 2018b).

The present study builds upon this experience and uses continent-wide geodata to present a map of the distribution of Late Pleistocene aeolian sediments for the entire European continent. We follow a two-pillar approach, in which the mapping based multi-national geodata forms the starting point of a conceptual model of loess genesis. The continent-wide spatial synthesis of loess distribution provides the genetic basis of our geographically and geoecologically derived loess formation and distribution model. As already done for our previous publications, this map presents the late last glacial environment, mainly referring to Last Glacial Maximum (LGM ~26.5 to 19 ka; cf. Clark et al., 2009) environments (e.g. ice sheet margins, permafrost boundary, alluvial plains, dry shelfs) to comprehend the complex conditions during the last main period of loess formation in western Europe. Additionally, we divided the map into six domains and 17 subdomains of different loess regions to differentiate depositional environments and areas. We visualize our analysis using cross-sections and 3-D images. To put the loess map into context and give an overview of the present day environmental setting, Figure 1 depicts the modern climatic conditions of the European loess covered regions (after Karger et al., 2017).

We demonstrate and discuss the influence of topography, the distance to ice margins and potential source areas, as well as paleoclimatic patterns, such as the distribution of permafrost, on the distribution and depositional facies of loess deposits in Europe. For this we compile different LPS of

Europe. In addition, the data will be compared to the existing maps of Haase et al. (2007) and the pedological approach by Bertran et al. (2016). Finally, we propose a conceptual model of loess genesis with three main deposition (paleoenvironmental) regimes for loess formation, and discuss some aspects of changes in loess formation though time. We envisage our approach will have strong implications in better assessing the distributions and importance of aeolian and especially loess deposits in Europe, including their paleoclimate and chronostratigraphic relevance.

2. Material and methods

2.1. Source maps, spatial data, and processing

Spatial geodata from 27 different European countries was compiled, processed, and unified in order to create a seamless map of the distribution of Late Pleistocene aeolian sediments and their potential sources. In most cases, this included georeferencing and digitizing printed national and regional geological, pedological, and geomorphological maps. The source maps were chosen on a case-by-case basis, depending on the respective availability, age and quality of the maps, e.g. in respect to the differentiation between Quaternary sediments in geological maps. The used source data are described in the following and summarized in Supplementary Table S1.

The published map of Quaternary sediments in the Carpathian Basin (Lehmkuhl et al., 2018a; Lindner et al., 2017) combines harmonized soil, geomorphological and geological data from 10 countries (**Austria, Bosnia and Herzegovina, Croatia, Czech Republic, Hungary, Romania, Serbia, Slovakia, Slovenia** and **Ukraine**). The map of loess and other Quaternary sediments for **Germany** uses geological data of 16 federal geological surveys and data from the Federal Geological Survey (Lehmkuhl et al., 2018b). The geodata of these published maps are used without major changes in the new European loess map. Only the geodata from Austria and Croatia were re-evaluated and altered in comparison to Lehmkuhl et al. (2018a). For easier cross-border comparison, we unite loess and loess derivates as one class in the new European map.

For the Carpathian Basin (Lehmkuhl et al., 2018a), only the eastern part of **Austria** was mapped, based on the loess distribution in the geological map of Austria (scale 1:750,000) by Vetters (1933). This reference is sufficiently precise in continental northeastern Austria, with loess sediments rich in carbonate, whereas loess derivates in more humid northwest and southeast Austria are not represented. The geological maps (scale 1:200,000) of Upper Austria (Krenmayr et al., 2006), Burgenland (Pascher, 1999), and Styria (Flügel and Neubauer, 1984), representing these regions do not show the widespread loess derivates or indicate their joint occurrence with fluvial terraces (mainly in northeastern Austria) or pre-Quaternary Pannonian Basin sediments (in southeast Austria). Local geological maps (scale 1:50,000) have different degrees of detail and are incompatible with our approach. The map of Quaternary sediments (scale 1:1,000,000) by Fink and Nagl (1979) shows three classes of loess sediments, each in continuous or discontinuous distribution. Next to typical loess widespread in northeastern Austria these are 'Braunlöß' (German for 'brown loess') and 'Staublehm' (German for 'dusty loam'), both representing loess derivates widespread in northwestern and southeastern Austria. Our new loess map combines the loess distribution according to Vetters (1933) and the continuous loess derivates of Fink and Nagl (1979). To be compatible with mapping standards of neighboring countries, we exclude discontinuous loess derivates shown on the map of the Carpathian Basin for the lowland from southeastern Austria into eastern Hungary and northern Slovenia (Lehmkuhl et al., 2018a).

The data source for **Croatia** was updated compared to Lehmkuhl et al. (2018a). Here the basic geological map of the Republic of Croatia (scale 1:300,000) was used (Croatian Geological Survey, 2009). It differentiates between typical loess and marshy loess. Both were reclassified as 'loess and loess derivates' for the European loess map. Furthermore, the coastal areas of Croatia were complemented by the data from Italy (see below). Mapping on the Croatian site of the Carpathian Basin between Sava and Drava was problematic as the geological map of former Yugoslavia (1:500,000; Federal Geological Institute, 1970) did not always differentiate the Quaternary. This is in some parts of the region quite difficult due to the high sedimentological similarities between Neogene Pannonian lake deposits and Quaternary sediments in general.

The loess sediments in the **United Kingdom** are based on a national loess map (Catt, 1985). The source map differentiates between variations in loess thickness. For the European map, only loess with a thickness greater than 1 meter from Catt (1985) was used to keep the different data sets comparable. The alluvial fill and fluvial deposits are based upon superficial deposits in the BGS Geology 625k map (scale 1:625,000), with the permission of the British Geological Survey (2013). For **Belgium**, the national soil map (scale 1:500,000) was used to map both aeolian sediments and potential sediment sources (Marechal and Tavernier, 1970). The distribution of aeolian sediments and sediment sources in the **Netherlands** is based on the geological map (scale 1:600,000; Zagwijn and Van Staalduinen, 1975). It distinguished between loess, dunes and cover sands. For **France**, a map of loess and other aeolian sediments (Antoine et al., 1999a; scale 1:1,000,000) based on various geological and geomorphological maps, initially compiled in the 1970’ for the first INQUA loess map of Europe (Fink et al., 1977), was digitized. For **Switzerland**, the national general geological map (Christ, 1944, 1942; Christ and Nabholz, 1950) was used as the most recent terminologically consistent country-wide representation of loess (scale 1:200,000). In this case, georeferenced raster files were available from which a map unit representing loess and loess derivates was vectorized. The geodata for **Spain** contains information about the spatial distribution of loess, aeolian sand and alluvial plains for central and northeastern Spain (Wolf et al., 2019) and is based on the geological maps (scale 1:50,000; de San José Mancha, 1973) and the work by Balasch et al. (2019).

For **Italy**, the loess distribution – considered as ‘loess derivates' for the European loess map – is based on data collected by many scholars and summarized in Cremaschi (2004, 1990a, 1987) and data collected to draw an updated loess map (Zerboni et al., 2018). Moreover, the litho-paleoenvironmental maps of Italy prepared by the CLIMEX Group (Antonioli and Vai, 2004) and the national soil map (Costantini et al., 2012) have been considered. For this compilation, geomorphological units suitable for loess accumulation and preservation have been selected and compared to the distribution of investigated sequences and already mapped loess covers. In details, we considered the occurrence of stable flat surfaces, such as terraces at the margins of Po Plain, pre-LGM moraines and isolated hills, allowing the production of an integrated map of loess distribution (Badino et al., 2019). The distribution of loess was interpolated from known locations of loess by spatial analysis of environmental and geomorphological variables.

For **Romania**, the national geological maps (Ovejanu et al., 1968, scale 1:200,000; Săndulescu et al., 1978, scale 1:1,000,000) albeit distinguish several loess chronostratigraphic units, do not always show a very good lateral representation of loess. Therefore, the approach by Lindner et al. (2017), that investigated western Romania, was extended to the whole country. The main source map analyzed is the soil map of Romania (Florea et al., 1971, scale 1 : 500,000), with which different soils and soil textures were translated into different corresponding loess probability classes. For example, dark Chernozems were assigned a loess probability class 3, while podzolic soils were assigned a loess probability class 0. These loess probability classes were then combined to achieve a homogenous classification of loess along the border region between Romania and Bulgaria. For **Bulgaria**, the geological map of Bulgaria (Cheshitev et al., 1989, scale 1:500,000) was digitized.

National soil maps were digitized for **Poland** (Dobrzański et al., 1974), **Moldova** (Krupenikov et al., 1969) and **Ukraine** (Sokolovsky et al., 1977a). The maps for Poland and Ukraine specifically stated which soils occur on loess or loess-like sediments. The Moldavian soil map provided a class solely for the substratum on which the different soils were formed. In this case, the two classes *loess loam* and *eluvial-diluvial light clays and loams* were reclassified as loess and loess derivates, respectively. For the loess distributions for Belarus and western Russia, the European loess map by Haase et al. (2007) was modified to fit the improved accuracy and scale. For this purpose, the map was compared to the ALOS digital elevation model (JAXA EORC, 2016). The loess distribution was aligned to the Pleistocene terraces and other geomorphological features determined via the elevation data. Afterwards, these terraces were vectorized as alluvial fill and fluvial deposits.

In addition to the national data sets, pan-European data sets for potential aeolian Pleistocene sediment sources were evaluated and added to the map to substitute missing and deficient national datasets and add complementary map units. This includes *inter alia* Late Pleistocene and Holocene fluvial deposits, derived from the EUSR5000 soil map with a scale of 1:5,000,000 (BGR [Bundesanstalt für Geowissenschaften und Rohstoffe], 2005). This data set was primarily used to substitute the missing national data sets of fluvial deposits for the Netherlands, France, Spain, Italy, Belarus, and Russia. In some places, it was compared to the digital elevation model and modified to fit the Late Pleistocene terraces. In addition to alluvial fill and fluvial deposits, the modified Late Pleistocene dry continental shelf (Willmes, 2015) that represents the main source for aeolian sediments was added to the map. In order to pinpoint the main sediment sources and paths on the dry continental shelf, paleochannels on the shelves such as e.g. the Channel River were extracted using the European bathymetry data set EMODnet (2019). For an evaluation of the channel widths, estimates about discharge were made in comparison to recent rivers and paleoriver channels on the recent landmass. In the North Sea, areas with Holocene tidal sediment accumulation were corrected accordingly. As additional important paleoenvironmental factors we inserted the LGM northern timberline (mod.

acc. to Grichuk, 1992), the LGM boundaries of continuous and discontinuous permafrost (Vandenberghe et al., 2014a), the modified ice extent during the LGM (Ehlers et al., 2011), and the major rivers (current course; available at www.naturalearthdata.com). However, especially the limits of permafrost and the northern timberline are estimates and they are still a matter of debate. For example, a careful and comprehensive revision of paleoclimate proxies and periglacial features suggests that the lowland territory of the Carpathian Basin (or Pannonian Basin) was outside the continuous permafrost zone even during the most severe climate phases of the late Quaternary (Ruszkiczay-Rüdiger and Kern, 2015). These paleoenvironmental factors and recent rivers fit the pan-European scale and are no references for national or regional scale studies.

To harmonize and generalize the combined national and regional data sets, an automated tool was used. The tool is similar to the one used in Lehmkuhl et al. (2018b) and was applied to address cross-map-problems like misalignments that can occur due to different scales and mapping approaches in the used maps. The tool consists of a 5-step-algorithm for aggregation, simplification and smoothing and was adjusted to fit an average national mapping scale (see scheme in Supplementary Figure S1).

The result of this approach is a seamless map of Late Pleistocene aeolian sediments and potential sediment sources in Europe (Figure 2). Since it is mostly based on national and regional maps and data sets, the final resolution and accuracy is very high for a pan-European approach and a scale of approximately 1 : 1,000,000. A detailed table of the sources and a statistical analysis for each mapped country can be found in the supplementary material (Supplement Tab. S1).

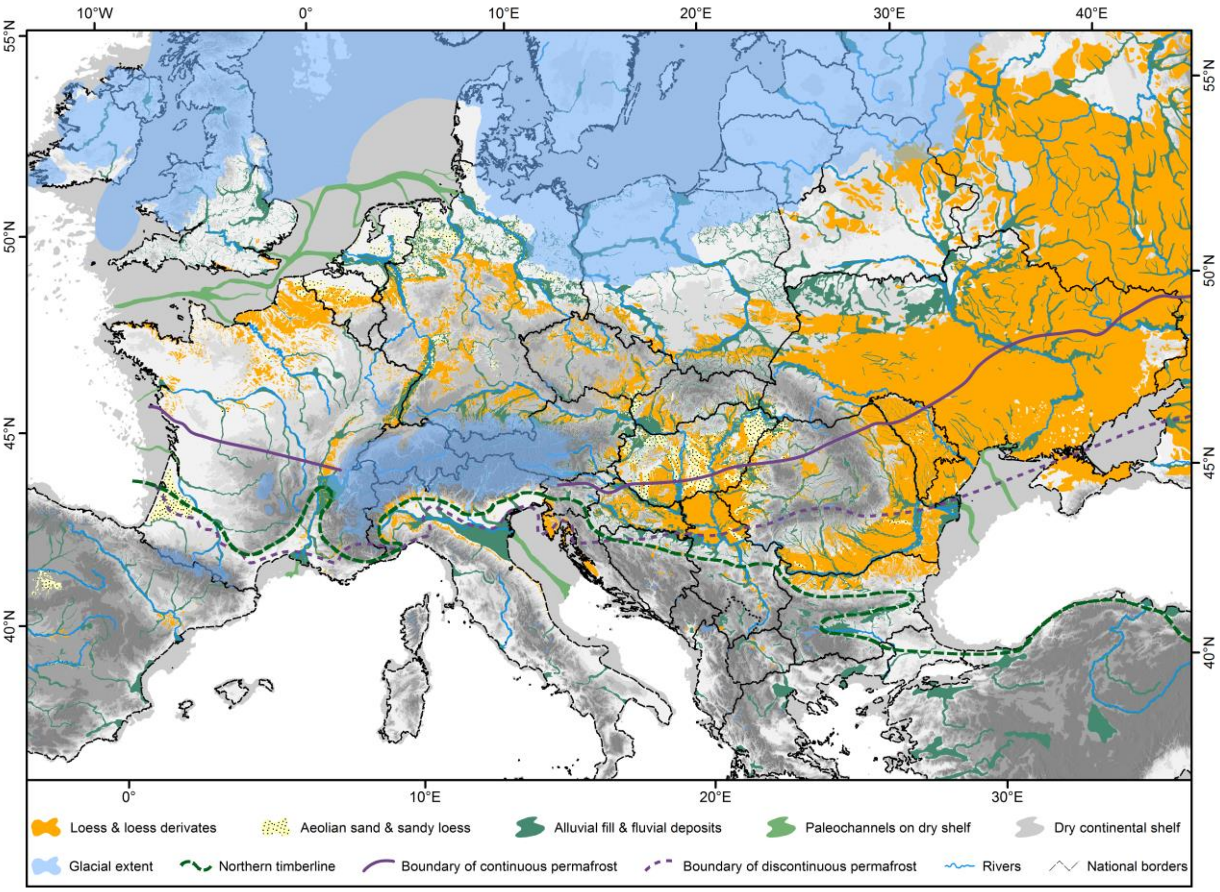

Figure 2: Distribution of loess and selected Late Pleistocene sediments in Europe. The LGM extent of glaciers (Ehlers et al., 2011) and dry continental shelves (Willmes, 2015), as well as the northern timberline (modified after Grichuk, 1992) and the boundaries of continuous and discontinuous permafrost (Vandenberghe et al., 2014a) are also mapped.

2.2. Visualization: Cross sections and 3-D images

In order to outline the influence of the topography on the distribution of Late Pleistocene aeolian sediments, four north-south running cross sections were derived using the new map and the ALOS digital elevation model (JAXA EORC, 2016). To do so, polylines were interpolated based on the elevation data. The interpolated lines were superelevated by the factor 100 and intersected with the sediment distribution, glacial extents as well as the boundaries of (dis-) continuous permafrost and the northern timberline. Moreover, six block diagrams (3-D images) were created using ESRI ArcScene 10.6.1. The different 3-D images were superelevated with varying factors of 1 to 20, depending on the topography. The distribution of all mapped sediments was rasterized and superelevated to gain spatial and topographic impressions of selected areas within the differentiated loess domains. In some 3-D images, a further distinction between mapped sediments as e.g. Late Pleistocene fluvial deposits and Holocene alluvial fill or loess and loess derivates was possible due to the differing data sources. Key sites and major cities were displayed for orientation purposes.

2.3. Statistics

To analyze the distribution of loess in Europe, we extracted information on the surface and height distribution. For the area statistics, the area of each mapped unit in each (sub-)domain was calculated via the 'calculate geometry'-function in ArcMap 10.6.1. This was also done for each country in order to estimate the proportion of the national data sets.

The ALOS digital elevation model (JAXA EORC, 2016) was clipped by the shapefiles representing ‘loess and loess derivates’ as well as ‘aeolian sand and sandy loess’. The resulting raster data sets were analyzed using the 'Zonal Statistics as Table' and the 'Zonal Histogram' tool with the vectorized (sub-) domains as feature zone data. The zonal histograms were used to calculate the relative surface percentage of each respective sediment unit at each elevation in meters above sea level (m a.s.l.). The outputs of the 'Zonal Statistics as Table' tool were used to assess main values such as minimum, maximum, mean, and median of the height distribution. In addition to the zonal statistics and histograms, the attribute tables of each clipped raster were exported for further analysis via RStudio. The data was then used to create boxplots, which illustrate the heights at which the corresponding sediments are distributed. To exclude extreme outliers, the upper and lower limit in the whisker was set to 1%. These outliers are probably related to misalignments between the loess shapefiles and the DEM, the scale of the source data or the smoothing process.

2.4. Software

Mapping, processing and statistical analysis were done using ESRI ArcMap10.6.1 in the focus of reproducibility and the broad availability of this software. Block diagrams were created using

ArcScene 10.6.1 and post-processed using Adobe Illustrator. Statistics were analyzed using R 3.4.1 (R Core Team, 2014) via the software RStudio 1.1.442 and Microsoft Excel 2016. Main graphics were created using R 3.4.1 or Adobe Illustrator.

3. Spatial distribution of European loess landscapes

The new map shows that loess is widely distributed in Europe (Figure 2). It spreads along the southern limit of the Pleistocene British and Fennoscandian ice sheets, spanning from southern England, through northern France, Germany, Poland and the Carpathian Basin to the Eastern European Plain. Within the Baltic part of Russia and northern Belarus, some loess patches can be found, which overlap with the LGM ice extend. These patches are part of the Late Pleistocene and late glacial sheets of aeolian sands and silts deposited after the ice receded. Several intramontane basins of the Central European low mountain ranges (German: Mittelgebirge), the valleys of large river systems such as the Rhône, Po, Rhine and Danube, and the lowlands of the Middle and Lower Danube Basin and the northern shore of the Black Sea are important loess covered areas. Some smaller spots reach the Mediterranean part of Europe and the Balkan Peninsula. The new map also depicts major alluvial and fluvial deposits. Here, the delta regions of the Rhône, Po and Danube rivers show an extremely wide Late Pleistocene and Holocene alluvial fill. These vast fluvial accumulations are the result of sea level rise after the deglaciation period and thus contains late glacial to Holocene deposits (e.g. Bruno et al., 2020).

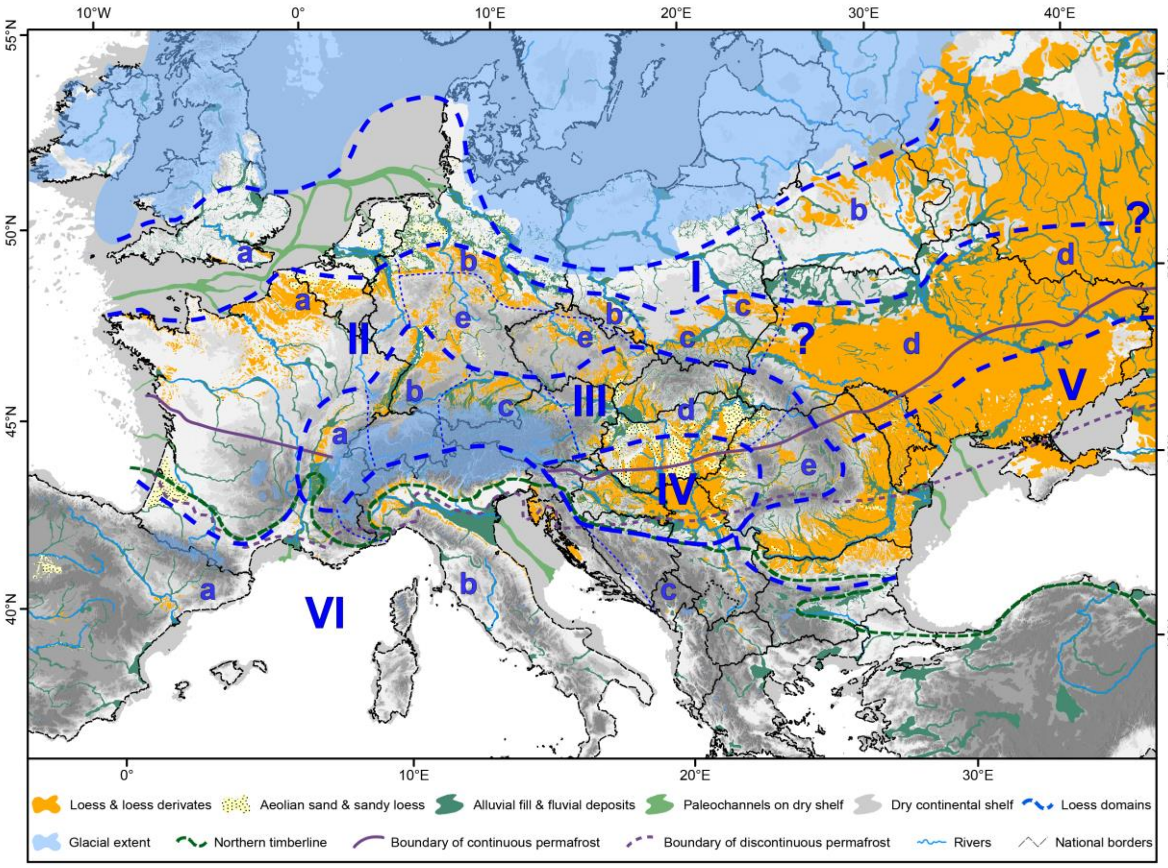

Figure 3: Major domains (roman numerals) and subdomains (lowercase letters) of loess and loess derivates for the LGM loess landscapes as shown in Figure 2.

As the last glacial cycle comprises the last period of major loess deposition (Marković et al., 2015), we focus on that time period and added to our map the LGM extent of glaciers (modified according to Ehlers et al., 2011), the contemporaneously dry continental shelves (modified according to Willmes, 2015), as well as the northern timberline (modified after Grichuk, 1992) and the boundaries of continuous and discontinuous permafrost (Vandenberghe et al., 2014a, Figure 2).

We divided the European loess distribution in six major domains and 17 subdomains (Figure 3). For the differentiation we used the following criteria that determine the loess facies: (1) Influence of potential silt production areas (North European / Alpine ice sheets with glacial grinding and periglacial areas with frost weathering vs. drylands with soluble salts and prevailing insolation weathering). (2) Catchment areas, as rivers are very important regional silt transport agents and river valleys act both as sinks and sources of sedimentary particles. (3) Paleoenvironmental factors influencing the formation, preservation and transformation of loess deposits, such as past periglacial activity with characteristic overprinting of the deposits.

The six major domains are (I) the Weichselian marginal or protogenetic zone; (II) the northern European loess belt; (III) the loess adjacent to Central European high altitude mountain ranges (northern fringe of the Alpine ice sheets and Carpathians); (IV) the Middle Danube Basin loess; (V) the eastern (Pontic) European loess; and (VI) the Mediterranean loess. Here we use the term **'loess facies'** to describe its properties. This term should be seen in particularly in context of proximity to source as well as the type and intensity of weathering processes. Loess facies characteristics e.g. are influenced by factors such as the parent material of the deposits, distance of transport, and (post-) depositional milieus (Pécsi and Richter, 1996). There are large variations between loess deposited proximally to ice margins or more distally. Loess formation and preservation are among others factors strongly influenced by the environment. In western Europe, for example, sediment layers occur which show characteristics of laminated niveo-aeolian deposits (e.g. Antoine et al., 2016, 2001; Haesaerts et al., 2016), while in southeastern Europe, loess formation was rather homogeneous and more continuous sedimentation took place (Marković et al., 2015; Obreht et al., 2019; Zeeden et al., 2016). Different potential major sources of aeolian deposits are the outwash plains of the British and Fennoscandian ice sheets, of alpine glaciations and the alluvial deposits of river systems. Sources and loess facies can also vary on a local scale. In southern Germany for example, we distinguish between loess linked to sources from the Swiss Alps (Upper Rhine Plain or Graben, subdomain IIIb) and from the Black Forest and the Eastern Alps (Upper Danube, subdomain IIIc). The most important (paleo-) environmental factors dividing the subdomains are (1) the boundaries of the (dis-) continuous permafrost, which strongly influences the preservation of loess, and (2) hydroclimatic factors, especially continentality which generally increases from west to east and strongly changes the chemical weathering and pedogenesis intensity. Both processes result in syndepositional/early diagenetic de-calcification, hydromorphic overprinting, and decomposition of organic compounds in humid and cold areas. On the contrary, in semi-arid regions, the preservation of dry, calcareous loess composed of almost pristine silty mineral dust dominates. Regarding pedogenesis, Chernozem-like (paleo-) soils are formed in the steppic areas, Greyzems (grey forest soils) in forest-steppe zones and more rubified (paleo-) soils (e.g. chromic Cambisols or Terra Rossa) are found in areas under the Mediterranean climatic influence, whereas under Atlantic and boreal climatic environments Luvisols and Cambisols (brown soils) are predominant (European Soils Bureau Network, 2005).

In the following, the six major domains and 17 subdomains are explained in detail to display the differences in aeolian sediment dynamics during the Late Pleistocene. The domains are described roughly from north to south. Figure 4 provides four loess landscapes transects that visualize the interplay of relief and loess in the various suggested subdomains across Europe (more information given in Chapter 3.7). In addition, we show a map with selected European loess sections as an orientation for the reader to locate the given examples in the text in Supplementary Figure 2. The figure is accompanied by Supplementary Table S2, which lists the referenced loess sections.

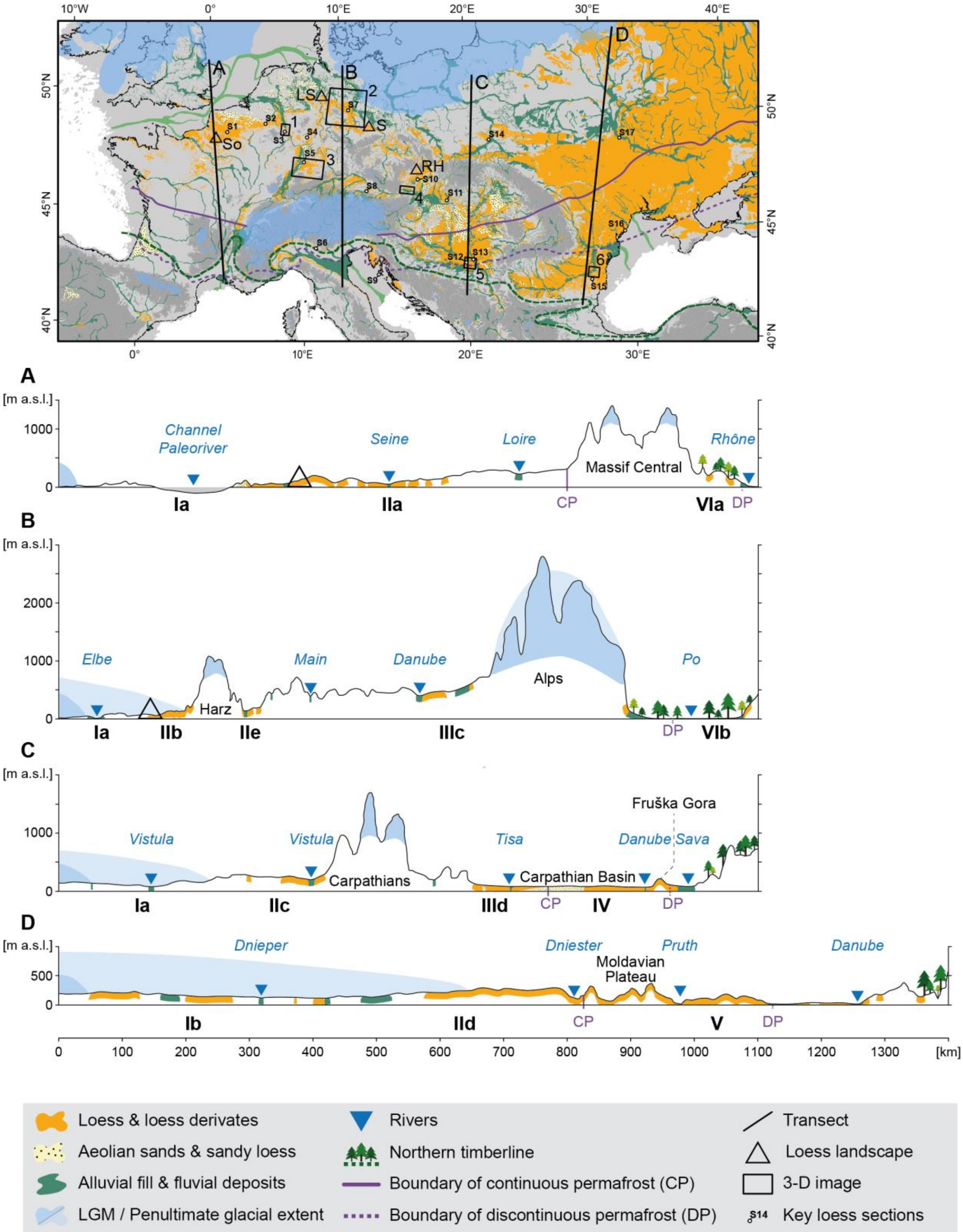

Figure 4: N-S transects showing four exemplary loess landscapes across Europe. The location of the transects, the 3-D images (Figs. 7, 8, 10, 11, 13, 14), and the meso-scale loess landscapes is shown in the top map. Meso-scale loess landscape: Valley sections (So = Somme, Northern France Figure 6 and RH = Red Hill, Czech Republic, Figure 12) loess-edge ramp (LS = Lower Saxony, S = Saxony, both Germany, Figure 9).

3.1. Loess domains and subdomains

I: Weichselian marginal or protogenetic zone

Following the suggestion by Łanczont and Wojtanowicz (2009) and Gozhik et al. (2014), we call the northernmost domain 'Weichselian marginal or protogenetic zone'. However, this term and especially the associated genetic interpretation is used differently by Łanczont and Wojtanowicz (2009), who suggest that silty and silty-sandy deposits in this zone were created mainly as a result of cryogenic weathering. We use the geographical attribution and the name and interpret this as geographic transport and accumulation zone. Loess and loess derivates cover an area of ~248,000 km². This domain comprises patches of sandy loess, sand sheets and cover sands (total ~15,000km²). The domain is divided further into two subdomains: Ia the western and Ib the eastern protogenetic subdomain.

Ia: Western protogenetic subdomain

This subdomain stretches between the Weichselian British Isles and Fennoscandian ice sheets and the northern European loess belt from southern England until the main drainage divide between the Vistula (Wisła) and Dnieper (Dnieper) rivers. In southern England loess deposits are usually found in rather thin covers with a maximum thickness of 4 m in local sedimentary traps (Catt, 1985, 1977). The new map only shows mapped loess deposits >2 m thick in Kent, Hampshire and Essex. For southern England such loess and loess derivates are described by Antoine et al. (2003). A recent review concerning loess in England is given in Assadi-Longroudi (2019).

Sandy deposits form a belt spanning from Belgium, through the Netherlands, Germany, Poland up to northwestern Ukraine. Kozarski and Nowaczyk (1991) reported a relatively frequent occurrence of isolated loess and sandy loess patches in lower Oder (Odra) and Warta region (northwestern Poland). Within this belt, the aeolian sediments reach various thicknesses, up to several meters. However, quite many of these regional sand sheets have thicknesses less than 2 m. As our data is mainly based on geological maps, sediments with a thickness of less than 2 m are not all included in our map. The grain size decreases with increasing distance from the Weichselian ice sheets: aeolian sand and sandy loess can be found in proximity to the source areas (e.g. in Germany east of Hamburg and south of Berlin, respectively), whereas loess and loess derivates can be found in distal positions further south (domain II). There are also aeolian sand covers that are overlapping with the maximum extent of the Weichselian glaciation. This indicates a post-LGM sedimentation during the late glacial or even early Holocene (Hilgers et al., 2001b; Koster, 2005; Küster and Preusser, 2010; Zeeberg, 1998). Vandenberghe (in Schaetzl et al., 2018) gives a summary of these periglacial aeolian sands and their transition to loess. Most of the loess deposits in this subdomain can be found at elevations between 27 m and 101 m, with its maximum at 229 m (cf. Chapter 3.3).

Ib: Eastern protogenetic subdomain

Subdomain Ib comprises the loess deposits on the plains of Belarus and Russia. Loess is found in elevations up to 285 m a.s.l. The southern border of this domain is the border between continuous and discontinuous loess mantle as suggested by Velichko (1990) along the line from Lviv through Kyiv to Ryazan. Towards the north from this line up to the limits of Valdai (Weichselian) ice sheet, loess occurs rather sporadically (subdomain Ib) with the largest patches found in the vicinity of the cities of Minsk, Smolensk, Moscow and Vladimir. South of this line the loess forms an almost continuous mantle (domains II and V) stretching up to the coasts of Black and Azov Seas (cf. Gozhik et al., 2014).

Discontinuous loess of subdomain Ib was deposited mainly during the Late Pleistocene (Velichko et al., 2006). The key loess sections in this area contain pedogenic marker horizons in the form of two well developed paleosol complexes assigned to Marine Isotope Stage (MIS) 5 and MIS 3, respectively, and are stratigraphically comparable to other marker paleosol complexes in European loess areas (Little et al., 2002; Rutter et al., 2003; Velichko, 1990). However, the particular feature of loess sequences in this subdomain are stratigraphically consistent and frequently repeating periglacial features indicating the impact of permafrost conditions and changing hydroclimate of the last glacial period (Morozova and Nechaev, 1997; Velichko et al., 2006). Loess deposits in this subdomain are found up to 277 m a.s.l. with a median of 199 m a.s.l. (cf. Chapter 3.3).

II: Northern European loess belt

The northern European loess belt preserves the most diversified pedo-sedimentary records in Europe. These deposits were strongly influenced by periglacial processes and environments and thus show a complex stratigraphy including erosional unconformities and permafrost features such as ice wedge casts or cryoturbation features as well as thermokarst erosion processes. This domain extends from western France through Belgium, Germany, and Poland to Ukraine and Russia. Geochemical results and heavy mineral signatures show that most material has its origin in northern Europe delivered by the British and Scandinavian ice sheets and contains also recycled material (Nawrocki et al., 2019; Rousseau et al., 2014; Skurzyński et al., 2020). In addition, there is a redistribution of the particles by periglacial braided rivers in the southern North Sea and eastern Channel, far from the original zone of production by glacial grinding (glacial fronts and outwash plain) (Antoine et al., 2009a). We divided this domain into five subdomains: three (IIa-c) from west to east along the front of the Central European low mountain ranges stretching to western Ukraine and gradually passing on towards subdomain IId in northern Ukraine and Russian uplands. Towards the south, the subdomains IIa-c are mainly restricted by the Central European low mountain ranges. In subdomain IId there is a gradual transition towards domain V with no or less influence of permafrost and periglacial features towards the south. The last subdomain (IIe) includes basins within the Central European low mountain ranges with elevations between 200 and 600 m a.s.l.. Loess and loess derivates occur here rather in isolated patches covering mostly wide river terraces (in most cases older than the last glacial cycle).

The northern boundary of the domain II with continuous loess distribution probably coincides with the northern fringe of past vegetation (biome) zones, as the vegetation influenced and enhanced the dust deposition. Due to the North Atlantic influence, loess in northern Europe has a rich stratigraphy that is generally similar in the whole domain from Normandy to Ukraine (Antoine et al., 2013, 2009b; Buggle et al., 2009; Jary and Ciszek, 2013; Lehmkuhl et al., 2018b, 2016; Rousseau, 1987; Rousseau et al., 2017, see Figure 5). There is a gradual transition from the subdomains IIa to IIc due to enhanced continentality and less humidity towards the east. In addition, the distance to and extent of the last and penultimate Fennoscandian ice sheets influence the loess facies and thickness in these subdomains.

This domain mainly contains loess that was deposited during the last glacial cycle. During this period, environmental conditions were highly variable and included erosive processes (slope wash and deflation, desert pavements) and periglacial processes (solifluction, involution, permafrost; Vandenberghe et al., 2014a; Zens et al., 2018). For example the Middle Pleniglacial (MPG) loess is rarely preserved due to several large erosion phases in contrary to the most recent loess (Upper Pleniglacial, UPG), that still occurs over a large area and exhibits the highest loess accumulation rates of the entire last glacial cycle (e.g. Frechen et al., 2003; Zens et al., 2018). Supra-regional attribution to past environmental conditions remains difficult (Kadereit et al., 2013; Sauer et al., 2016). However, long LPS sequences with a total thickness of more than 10 m, even including the whole Middle Pleniglacial (MPG) are locally preserved as cover deposits overlying high or middle fluvial terraces as in the Seine and Somme rivers (Grâce-Autoroute: Antoine et al., 2003; Saint-Pierre-lès-Elbeuf: Coutard et al., 2018; Lautridou, 1987) or in dissolution sinkholes in the chalk bedrock (Coutard et al., 2018). In addition, recent improvement in dating allowed for evidencing a detailed succession of interstadial soil horizons for MPG or ~MIS3 in sections from the Rhine area, such as Nussloch (cf. Figure 5; Moine et al., 2017; Prud'homme et al., 2016) or at Remagen (Frechen and Schirmer, 2011; Schirmer, 2012) and other sections (e.g. Zens et al., 2018).

Erosional unconformities are common features in this domain, which would make stratigraphic interpretations and correlations challenging (Antoine et al., 2001; Zöller and Semmel, 2001), but if they appear at supra-regional scale in response to global climate events they also offer strong marker levels for correlation (Antoine et al., 2016; Schirmer, 2016; Zens et al., 2018). The distribution of loess and related aeolian sediments was also influenced by sediment availability (e.g., proximity to the dry shelf, larger river systems, and the ice sheet margins itself), and prevailing wind directions. As a result, the thickness and temporal resolution of LPS can vary locally as well as between different loess regions (from < 2 to more than 10 m for the same time span). In our map, loess deposits in domain II cover an area of ~454,000 km², while aeolian sand and sandy loess are mapped on ~20,500 km² (see Chapter 3.3).

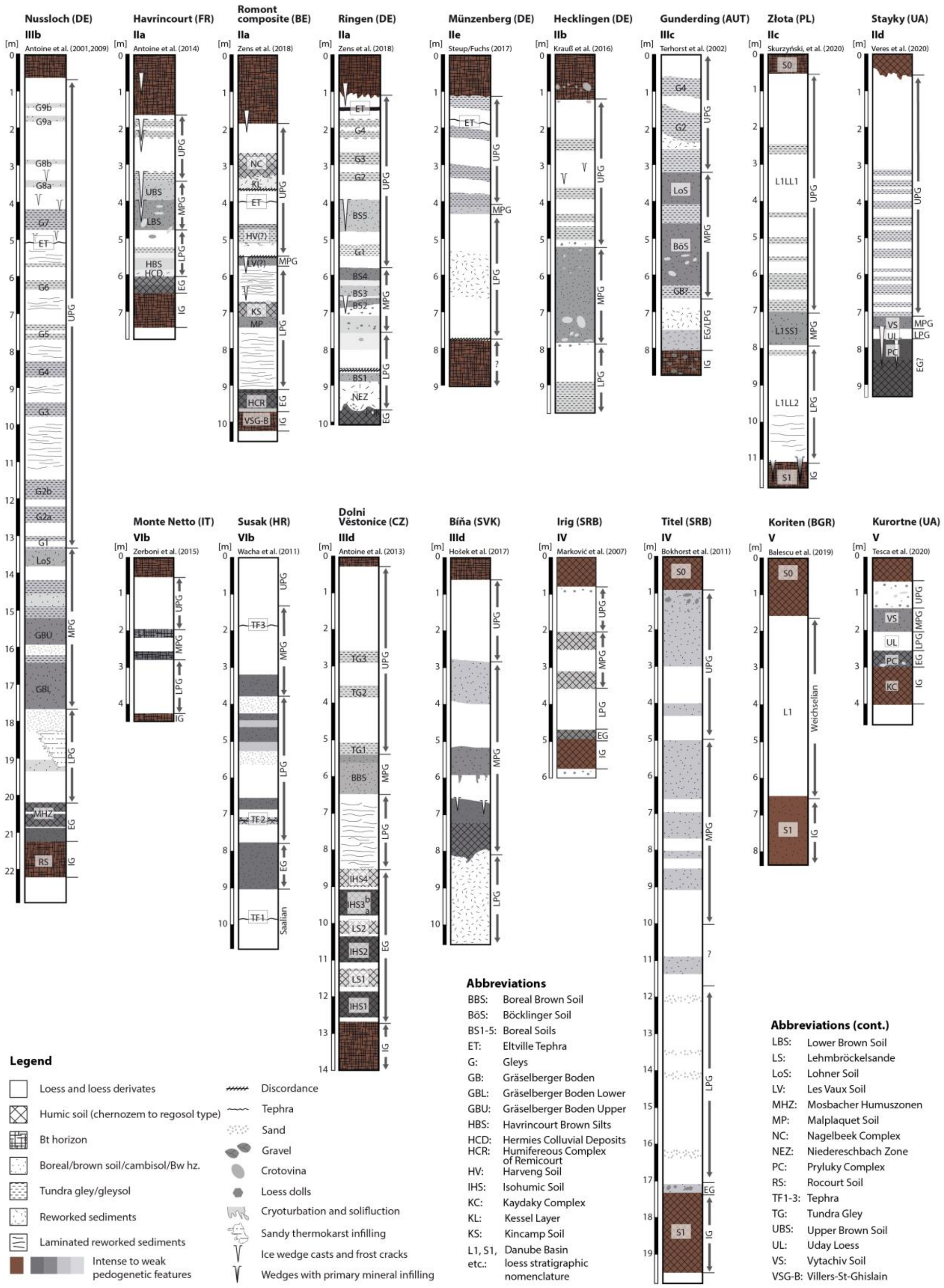

Nussloch (DE)
IIIb
Antoine et al. (2001,2009)
Havrincourt (FR)
IIa
Antoine et al. (2014)
Romont composite (BE)
IIa
Zens et al. (2018)
Ringen (DE)
IIa
Zens et al. (2018)
Münzenberg (DE)
IIe
Steup/Fuchs (2017)
Hecklingen (DE)
IIb
Krauß et al. (2016)
Gunderding (AUT)
IIIc
Terhorst et al. (2002)
Złota (PL)
IIc
Skurzyński, et al. (2020)
Stayky (UA)
IId
Veres et al. (2020)
Monte Netto (IT)
VIb
Zerboni et al. (2015)
Susak (HR)
VIb
Wacha et al. (2011)
Dolni Věstonice (CZ)
IIId
Antoine et al. (2013)
Bíňa (SVK)
IIId
Hošek et al. (2017)
Irig (SRB)
IV
Marković et al. (2007)
Titel (SRB)
IV
Bokhorst et al. (2011)
Koriten (BGR)
V
Balescu et al. (2019)
Kurortne (UA)
V
Tesca et al. (2020)
[m]
UPG
MPG
LPG
EG
IG
Weichselian
Saalian
Legend
Loess and loess derivates
Humic soil (chernozem to regosol type)
Bt horizon
Boreal/brown soil/cambisol/Bw hz.
Tundra gley/gleysol
Reworked sediments
Laminated reworked sediments
Intense to weak pedogenetic features
Discordance
Tephra
Sand
Gravel
Crotovina
Loess dolls
Cryoturbation and solifluction
Sandy thermokarst infilling
Ice wedge casts and frost cracks
Wedges with primary mineral infilling
Abbreviations
BBS: Boreal Brown Soil
BöS: Böcklinger Soil
BS1-5: Boreal Soils
ET: Eltville Tephra
G: Gleys
GB: Gräselberger Boden
GBL: Gräselberger Boden Lower
GBU: Gräselberger Boden Upper
HBS: Havrincourt Brown Silts
HCD: Hermies Colluvial Deposits
HCR: Humifereous Complex of Remicourt
HV: Harveng Soil
IHS: Isohumic Soil
KC: Kaydaky Complex
KL: Kessel Layer
KS: Kincamp Soil
L1, S1, etc.: Danube Basin loess stratigraphic nomenclature
Abbreviations (cont.)
LBS: Lower Brown Soil
LS: Lehmbröckelsande
LoS: Lohner Soil
LV: Les Vaux Soil
MHZ: Mosbacher Humuszonen
MP: Malplaquet Soil
NC: Nagelbeek Complex
NEZ: Niedereschbach Zone
PC: Pryluky Complex
RS: Rocourt Soil
TF1-3: Tephra
TG: Tundra Gley
UBS: Upper Brown Soil
UL: Uday Loess
VS: Vytachiv Soil
VSG-B: Villers-St-Ghislain

Figure 5: Transect of 17 selected LPS from northern France to eastern Bulgaria, which span the last glacial cycle in the respective subdomains. For correlation, all sections schematically divided in chrono-climatic units of European loess sequences (Haesaerts and Mestdagh, 2000, Antoine et al., 2013): (Saalian), Interglacial (IG), Earlyglacial (EG), Lower Pleniglacial (LPG), Middle Pleniglacial (MPG) and Upper Pleniglacial (UPG). The interglacials are shown in brown and the glacials in grey scales. The hatchings indicate the soil types. The individual OSL ages can be obtained from the references given above the sequences; countries and subdomain are given as abbreviations. Danube Basin loess stratigraphic nomenclature follows Marković et al. (2015).

IIa: Western European maritime (Atlantic) subdomain

This subdomain contains the loess deposits in northern France, Belgium, the Netherlands, and the Lower Rhine Embayment in western Germany. Since the 1950s several loess stratigraphies based on paleosols and specific sedimentary units were developed for different subregions of this subdomain. The latest updates were recently published for central Belgium by Haesaerts et al. (2016), the Lower Rhine Embayment by Schirmer (2016), Lehmkuhl et al. (2016), and Fischer et al. (2019). A recent summary of the loess sequences in northern France and Belgium is given by Antoine et al. (2016). The studies include detailed descriptions of single units, their most important properties, and their chronostratigraphic position.

In northern France, the Weichselian loess cover is represented by a semi-continuous mantle up to 8 m in thickness in favored sediment traps such as leeward slopes or fluvial terraces (see Figure 6; Antoine et al., 2016). The LPS from the last interglacial-glacial cycle exhibit a particularly constant pattern, including well-identified pedological and periglacial marker horizons that can be followed in Belgium and towards western Germany (Antoine et al., 2016). In this Atlantic subdomain, more humid conditions enhanced the erosive periglacial processes, but also led also to preservation in favorable accumulative positions (Antoine et al., 2016; Lehmkuhl et al., 2016).

For the whole area from Northern Brittany to Belgium the general stratigraphy of the last glacial period (115-11.7 ka) can be summarised as follows (Antoine et al., 2016, 2001; Zens et al., 2018): The Weichselian sequence starts above the truncated last interglacial brown leached soil complex (Rocourt / Elbeuf I) and can be further subdivided by four main chronoclimatic phases: (1) Early glacial (115-72 ka) consisting of a phase with grey forest soils (early glacial A) and a phase with steppe-like soils (early glacial B); (2) Lower Pleniglacial (LPG, ≈70-58 ka): first typical homogeneous loess deposits marking the first occurrence of typical periglacial conditions; (3) Middle Pleniglacial (MPG, ≈58-32): Loess deposition was strongly diminished and frequent phases of erosion reduced the resolution of MPG sediments in most LPS (Antoine et al., 2001). As a result of the relocation, the older units are redeposited in colluviums. A brown soil complex and very weak aeolian deposits have been preserved only in positions which are less affected by erosion; (4) Upper Pleniglacial (UPG, ≈32-15 ka): characterised by a drastic increase in loess sedimentation and the formation of tundra-gley horizons and large ice wedge casts occur, especially between 30 and 23 ka (Antoine et al., 2016; Zens et al., 2018).

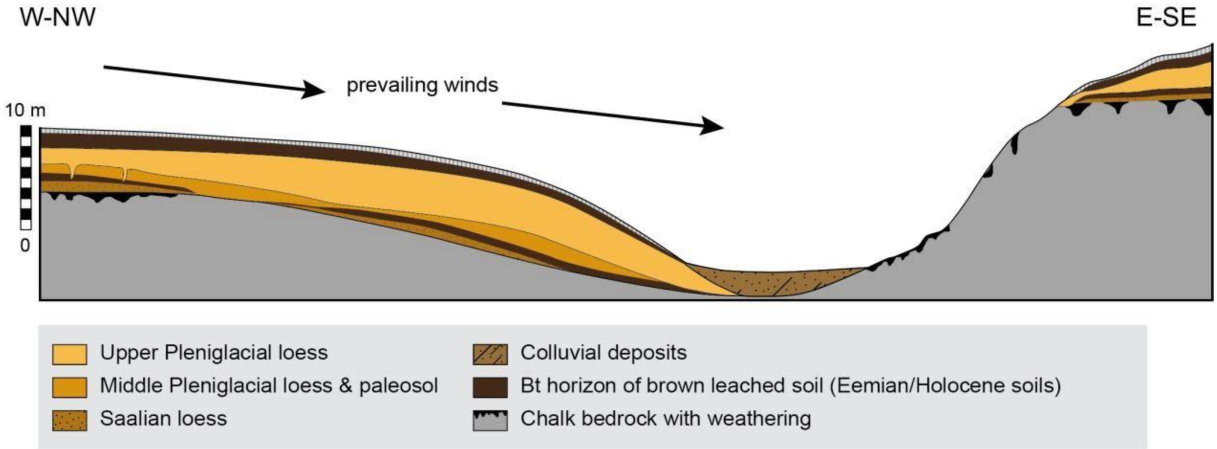

Figure 6: Loess stratigraphy in northern France (subdomain IIa) controlled by asymmetric valley topography (modified according to Antoine et al., 2016).

The Belgian and Dutch parts of Limburg are partly covered by loess (van Baelen, 2017; Zagwijn and Van Staalduinen, 1975) and the deposits have a continuous thickness of 2 to 6 m (Antoine et al., 2003, 1999a; Henze, 1998; Kels, 2007; Meijs, 2002). Both, Weichselian and Saalian loess deposits have been preserved (Kolfschoten et al., 1993; Meijs et al., 2013; van Baelen, 2017; Vancampenhout et al., 2013). The LPS Romont (cf. Figure 5), located between the villages Bassenge and Eben-Emael 5 km southwards of Maastricht in Belgian Limburg (Haesaerts et al., 2011) is defined as a stratotype in Belgium because the sequence is the type locality of the Eben-Zone (Schirmer, 2003) and the Rocourt Tephra (Juvigné et al., 2008).

The Lower Rhine Embayment shows clear differences in the presence and properties of loess related to the (meso-) relief. Loess sections in plateau-like positions are usually shorter and more affected by erosion than sections in depressions, paleochannels, on stretched slopes and slope toes. The latter ones are characterized by reworked sediments of older paleosols redeposited as heterogeneous, finely laminated colluvium (Lehmkuhl et al., 2016; Schirmer, 2016 and references therein). After the Eemian interglacial, Chernozem-like humic soils were formed under steppe-like environmental conditions. This was followed by a transition to colder and more continental conditions, which are reflected in the respective loess stratigraphies (eg. Haesaerts et al., 2016; Schirmer, 2016; Semmel, 1998). The first phases of the last glacial cycle are characterized by redeposited finely laminated sediments while the loess packages contain several thin and weakly developed tundra gleys and humic soils (cf. Figure 5; Zens et al., 2018). The most recent loess layer in this subdomain can be divided into two sedimentary facies: the niveo-aeolian (cold-humid) and the homogenous loess (cold-arid). They were termed Hesbaye and Brabant loess in Belgium and the Lower Rhine Embayment (e.g. Haesaerts et al., 2016; Schirmer, 2016) and can be also observed in northern France (Antoine et al., 2016).

Figure 7 shows the clear boundary of loess from the lowlands in the southern part of the Lower Rhine Embayment against the northern margins of the Eifel Mountains as part of the Rhenish Massif. Its restriction to lower elevations in the foreland is a typical feature for this subdomain. Loess in this subdomain is distributed on elevations up to 316 m with a median at 117 m (cf. Chapter 3.3).

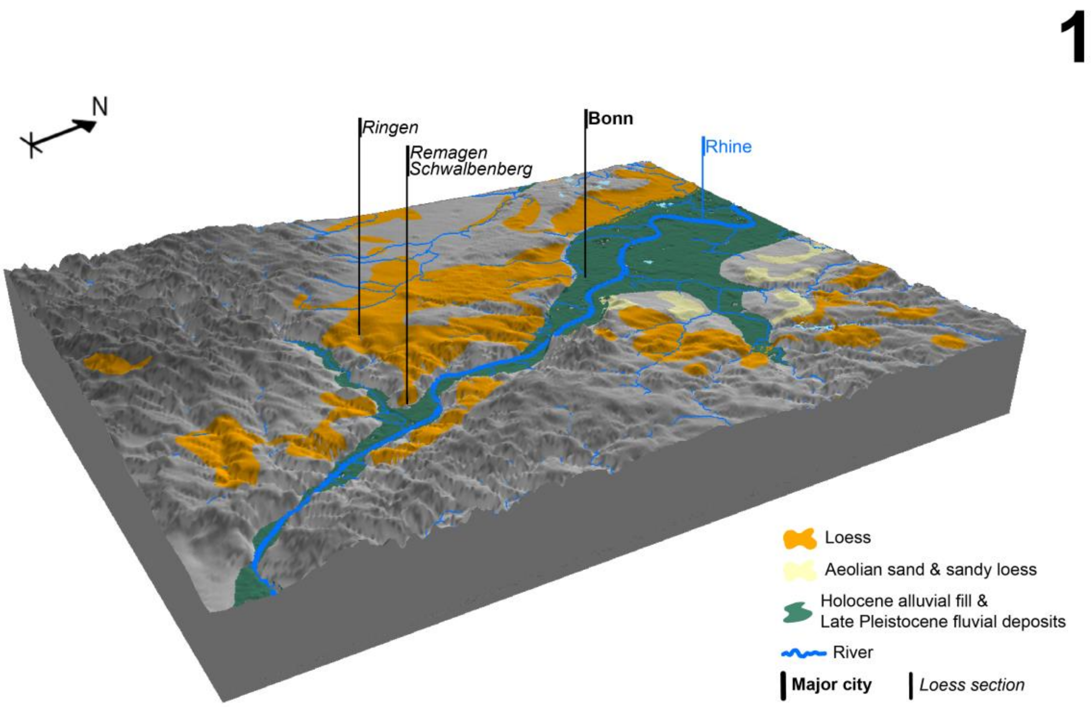

Figure 7: 3-D image of the distribution of loess, sandy deposits, and the late Quaternary floodplain in the southern part of the Lower Rhine Embayment. The size of the 3-D image is 40 x 55 km. Superelevated by factor 1 (no superelevation).

IIb: Western European continental subdomain

The subdomain IIb is situated in northern Germany on the northern margin of the Central European low mountain ranges from the foreland of the Rhenish Massif east of the Rhine River towards the eastern part of the foreland of the Harz Mountains close to the Elbe River. Further to the east it includes the loess region of Saxony north of the Ore Mountains, the northernmost part of Bohemia in the Czech Republic, and parts of western Poland up to the Odra (Oder) River. Here, thick loess sequences are mainly preserved in the eastern part of this subdomain, especially in parts of Saxony. In the western parts, e.g. in the foreland of the Harz Mountains, a more undulating relief developed on bedrock is covered with a generally thin loess cover. This is due to the advances and fluctuations of the ice sheets during the Saalian glacial period into this region and thus resulting in the absence of older LPS. Lehmkuhl et al. (2016) summarized the differences and similarities of LPS in the transition from more humid areas in the Lower Rhine Embayment towards drier areas in the east. In the foreland of the Harz Mountains, more continental climate condition lead to less intensive periglacial slope processes and solifluction, which is expressed by more complete preservation and less pronounced erosion and erosional discordances (Lehmkuhl et al., 2016). Figure 8 shows a 3-D visualization of the loess distribution surrounding the Harz Mountains including the two selected sections of Hecklingen and Zilly. Recent papers provide a summary for selected sections in the northern foreland of the Harz Mountains (Krauß et al., 2016; Lehmkuhl et al., 2016). A stratigraphy is depicted in Figure 5.

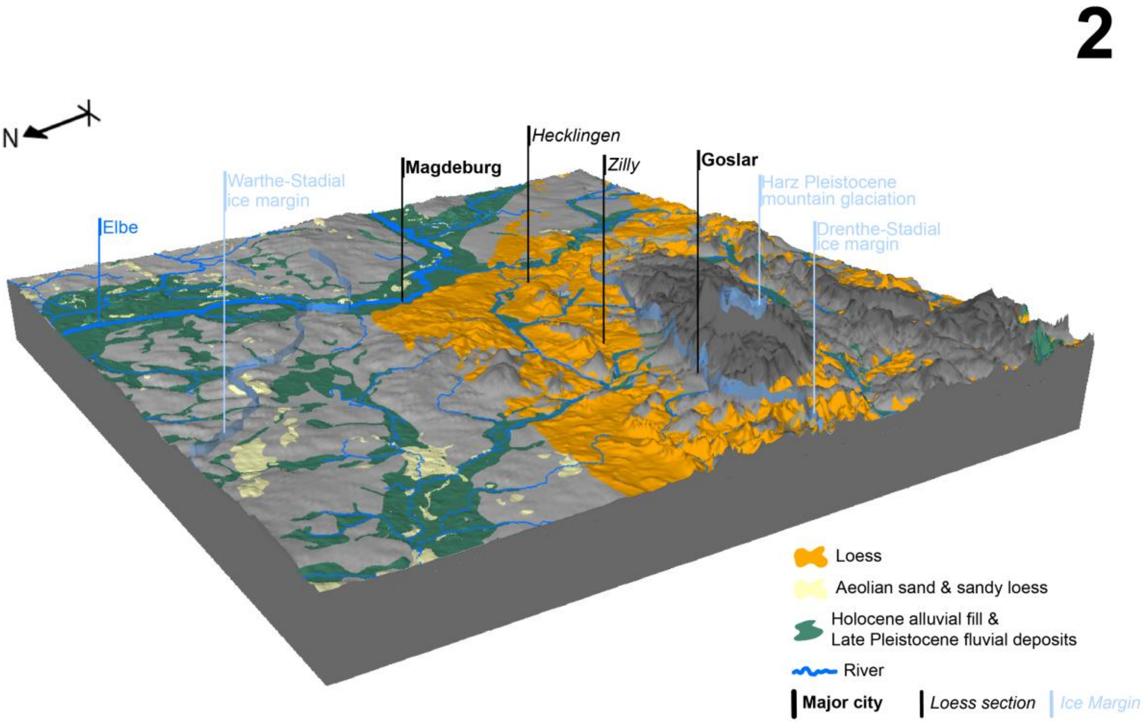

Figure 8: 3-D image of the distribution of loess, sandy deposits, and the late Quaternary floodplain surrounding the Harz Mountains in northern Germany. The size of the 3-D image is 180 x 190 km. Superelevated by factor 20.

The northern margin of the loess in this subdomain is in some areas a sharp, rectilinear boundary. Sections at this loess boundary show a distinct succession of loess, sandy loess and loess with sand layers, which were later modified by aeolian and cryogenic processes (Gehrt, 1994; Gehrt and Hagedorn, 1996). In Figure 9, the general composition of the so-called loess-edge ramp (Leger, 1990) (German: 'Lössrandstufe') and the stratigraphy in Lower Saxony and Saxony is summarized (redrawn and modified according to Gehrt (1994) and personal communication by E. Gehrt, 2020). Luminescence dating from sections of the loess-edge ramp leads to the assumption that the latest, northernmost loess formation occurred until the late glacial period. The time span covered by luminescence ages sedimentation starts at ~28 ka and lasts with the sandier sediments from about 15 until 8 ka with the averages concentrated at ~11 ka. These findings confirm earlier suggestions that the northernmost loess deposits in northern Germany represent the return of strong aeolian processes (westerly winds) under the cold and dry conditions during the late glacial shaping this northern loess boundary (Hilgers et al., 2001a).

In Saxony, the thickness of the loess deposits increases from south to north and reaches a maximum of around 8-12 m close to the northern boundary. Northwards, there is an abrupt change from loess deposits to coarser-grained aeolian, glacial or glaciofluvial sediments (Haase et al., 1970; Meszner et al., 2014, 2013). The so-called loess-edge ramp, comparable, but still distinct to those in Lower Saxony, marks in parts of Saxony this clear northern border. With a step of around 10 m, it is significantly higher than the one in Lower Saxony (see Figure 9, redrawn and modified according to Haase et al., 1970). Meszner et al. (2013) conclude from sedimentological patterns and grain size distributions that dominantly westerly winds delivered the dust.

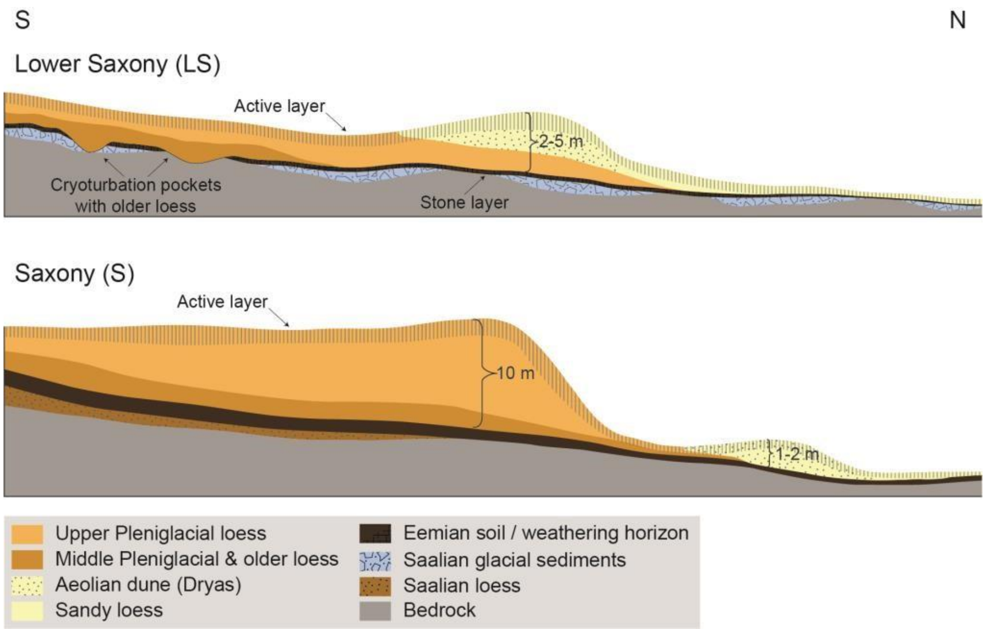

Figure 9: Loess-edge ramp ("Lößrandstufe") in Germany: Examples from Lower Saxony (redrawn and simplified according to Gehrt (1994) and personal communication by E. Gehrt, 2020) and Saxony (redrawn and modified according to Haase et al., 1970).

Loess in southwestern Poland is distributed in several isolated patches differing in sediment thickness, stratigraphy and basic physical properties (Jary, 2010, 1996; Jary et al., 2016, 2002). Its aeolian origin was recognized early by Orth (1872). Thin, discontinuous patches of loess and loess-derived sediments prevails but there are also thick loess covers (up to 10-15 m) with well-defined stratigraphy of the last glacial period (Jary, 2007; Moska et al., 2019, 2012, 2011). Aeolian silt was derived and deposited within a relatively narrow corridor between the Weichselian Ice Sheet and Sudetes Mountains. The loess material was presumably redistributed by the Great Odra Valley fluvial system (Badura et al., 2013) and then blown to the adjacent elevations by strong winds from the NW. The loess-edge ramp occurs both on the left and right side of the Odra river valley confirming the role of the river as a main transport and redistribution medium before the final aeolian event. Loess in this subdomain is distributed on elevations up to 381 m with a median of 160 m a.s.l. (cf. Chapter 3.3).

IIc: Central European continental subdomain

The third loess subdomain (IIc) is the continuation of the northern European loess belt to the east on the area of Vistula (Wisła) basin stretching within the widening corridor between the Carpathian mountain ranges in the south and the protogenetic zone in the north towards western Ukraine (Badura et al., 2013). There is a gradual shift from subdomain IIb to more continental conditions of subdomain IIc. This also affected the periglacial processes with more frequent cryoturbation horizons and larger ice wedge casts in the east (Jary, 2009; Jary and Ciszek, 2013). Compared to subdomain IIb this area has a greater distance to the Weichselian ice sheet and due to the absence of Saalian ice in most parts also pre-Weichselian loess deposits occur. Close to the state boundary between Poland and Ukraine there is a transitional area to the eastern European continental subdomain (IId). We draw this eastern border at the main drainage divide between the rivers that drain toward the Baltic Sea and those that drain towards the Black Sea. In addition, the maximum extent of the Saalian ice sheet is also close to this border (Figure 21). This subdomain includes also lowlands (~ 270 m asl) of Oder (Odra) River basin in the northeastern part of Czech Republic (south Silesia, the vicinity of Ostrava city) where up to 15 m thick Middle and Upper LPSs are preserved in isolated patches (Macoun et al., 1965). In comparison with southerly situated loess cover of Morava valleys (domain III), the loess is usually completely decalcified and signs of periglacial processes are more frequent. In many sites, textural and structural features of the loess (e.g. significant laminated structure or abundant ox/redox. signs) together with the specific combination of wetland and aquatic mollusc assemblages indicate an ephemeral swamp or limnic environment, in which dust was deposited (so called 'swamp loess' or 'Sumpflöss'). This facies corresponds to large proglacial lakes and wetlands existing in the region during the Saalian and Elsterian glaciations.

In Poland, Maruszczak (1991, 1985) distinguishes three regions of loess occurrence within the southern Polish upland region (in the vicinity of Kraków, Sandomierz and Lublin) and two foothill regions in the foreground of the Sudetes (subdomain IIb) and the Carpathians (subdomain IIc). A typical feature of the Polish loess areas is their occurrence as isolated patches and its transitional position between subdomains IIb (SW Poland) and IIc (SE Poland). Many authors claimed that the loess covers in Poland reflect present and past regional climatic conditions: continental in the east and more oceanic in the west (Cegła, 1972; Jersak, 1973; Maruszczak, 1991). The thickness, continuity and stratigraphic differentiation of loess cover increase towards the east (Jary, 2009; Jary and Ciszek, 2013). These isolated loess patches are composed of units of different ages; Late Pleistocene loess, however, predominates in the area of loess occurrence. In eastern Poland, loess of several glacial cycles formed thick sequences, locally up to 40 m thickness. A fundamental rule of loess arrangement in Poland is the connection of this deposit with a specified hypsometric level of 180-300 m a.s.l.. Locally, the lower limit drops to 150 m whereas the upper limit of loess occurrence may exceed 400 m a.s.l. (Jersak, 1973; Maruszczak, 1991, 1985, 1969). The thick loess mantles are often limited by distinct morphologic margins controlled by primary accumulation. The main dust sources for loess formation in Poland are usually related to the Pleistocene Fennoscandian ice sheets (e.g. Jahn, 1950; Jary and Kida, 2000; Smalley and Leach, 1978; Tutkovsky, 1899). However, some authors stress the role of local sources (e.g. Malicki, 1950; Maruszczak, 1991) and/or the significance of fluvial processes delivering material for aeolian deposits through the Vistula River and its tributaries (e.g. Jersak, 1973; Maruszczak, 1991). Most of the loess in this subdomain is found at elevations between 218and 292 m a.s.l., with a minimum and maximum at 169 m and 438 m a.s.l., respectively (cf. Chapter 3.3).

IId: Eastern European continental subdomain

Loess in eastern Europe stretches from northern Russia and Belarus towards Ukraine, Romania and Bulgaria in the south, until the shore of the Black Sea, and covers including domain V and the Volga loess outside of our map more than one million square kilometers. This loess transitions gradually eastwards into the (Central) Asian steppe belt. South of the latitude of Kyiv, a virtually continuous and thick loess cover begins (Gozhik et al., 2014). We separated this subdomain from domain V because of the decreasing influence of periglacial processes (and Mid Pleistocene glacial deposits) and the increasing dust deposition towards the south. A recent example for Late Pleistocene loess in the Central Russian Upland is given in Sycheva et al. (2020).

Important source areas of this loess subdomain and also for domain V were the alluvial and lacustrine plains that formed in front of the advancing and retreating Pleistocene ice sheets (Buggle et al., 2008; Makeev, 2009; Velichko, 1990; Velichko et al., 2006). The outwash material was transported by north-south flowing rivers (e.g. Dneiper, Dniester, Volga) or by frequent northerly winds. The loess cover in this subdomain is very thick (usually 10-20 m , Haase et al., 2007; Li et al., 2020 report local occurrences up to 50 m). In this area, dust accumulated in more tundra-like environments. In some regions there are older glacial tills from the maximum extent of the Elsterian (Oka) and Saalian (Dnieper) glaciations even intercalated into the loess deposits. Especially the deposits of the Dnieper glaciation in the middle Dnieper basin are an important stratigraphic marker horizon, that is found approx. as far south as the latitude of Dnepropetrovsk (Gozhik et al., 2014). They occur either at the base of the loess cover or as an intercalated layer within loess sequences (cf. Figure 5; Rousseau et al., 2011). In addition, periglacial features are visible in the sections of this region (Veres et al., 2018). There is a gradual transition between this subdomain and domain V following the direction of the permafrost boundary. This transition is gradual because of the fluctuation of the ice margins and permafrost distribution during the Pleistocene. Most of the loess in this subdomain is distributed in elevations between 141 m and 225 m a.s.l. with maximum of 372 m a.s.l. (cf. Chapter 3.3).

IIe: Central European low mountain ranges and basins subdomain

The fifth subdomain of the northern European loess belt is located in basins of the German and northern Czech low mountain ranges. As described by Lehmkuhl et al. (2016, 2018b), there is a topographic limitation of these basins and the distribution pattern of their deposits is rather fragmentary. Exceptions are the lowlands of Lower Franconia (Germany) east of Frankfurt am Main (e.g. Roesner, 1990) or the Wetterau as a part of Hessian basin between Frankfurt am Main and Gießen (see stratigraphy in Figure 5; Steup and Fuchs, 2017). We attributed the loess downstream of the Alps in the eastern vicinity of the Rhine River in southwestern Germany to subdomain IIIc.

The loess sections further to the east in Bohemia (western part of Czech Republic) have more similarities with sections of the northern European loess belt (domain II) than those in the south Moravia (the southeastern part of the Czech Republic (domain III)), as apparent e.g. from geochemical and rock magnetic investigations conducting on the reference Late Pleistocene LPS (Hošek et al., 2015). The data reveal stronger leaching of central Bohemian compared to south Moravian loess and paleosols suggesting more humid conditions in the more northwesterly situated Bohemia. Consequently, these findings suggest that the transitional zone between the two climate regions, or the two different modes, of the Late Pleistocene climate in central Europe could be quite narrow. Bohemia was and is under the direct influence of Atlantic cyclones whereas south Moravia belongs geographically to the Pannonian Basin, which was marked in the Late Pleistocene by continuous dry continental climate conditions, under the effects of a temperate sub-Mediterranean climatic influence (Krolopp and Sümegi, 2002; Marković et al., 2007). In addition, the region benefits from its rain shadow position in the southeast of the Bohemian Massif and its proximity to the Carpathian Basin from where dry and warm air masses can penetrate. Therefore, we attribute the Bohemian area to IIe and the Moravian loess to the subdomain IIId. Most of the loess in this subdomain is distributed in elevations between 228 m and 326 m a.s.l. with a minimum and maximum of 125 m and 480 m a.s.l. (cf. Section 3.3).

Marker features and horizons allowing correlation in domains II and III

The complexity of the pedosedimentary and stratigraphical evolution of the last glacial cycle loess is particularly high in subdomain IIa and decreases towards domain V, while the loess thickness increases on average (Figure 5). Nevertheless, also in domain V there are situations in which significantly less sediment was deposited, but where many time phases can be traced in various proxy data (e.g. Kurortne). By using pedostratigraphical units as markers, a correlation over the whole European loess area is possible. During phases of strong erosion (visible by unconformities) in the LPG and UPG, especially but not exclusively on slope sites the Interglacial and MPG soil complexes were eroded. Romont and Mützenberg show the patchiness of some profiles and situations and Nussloch is rather an exception concerning preservation conditions and high resolution. In order to cover as many phases of the last glacial cycle as possible, for some subdomains more than one representative profile was selected.

Marker features such as the Eltville tephra, or the Eben unconformity allow the inter-section correlation of individual profiles, and also the correlation between subdomains and domains, especially in-between domain II and III. In these domains, the homogenous uppermost loess package often starts above a periglacial marker horizon: the Nagelbeek tongue horizon (Haesaerts et al., 1981) or Nagelbeek Complex (E4 Soil) (Haesaerts et al., 2016; Schirmer, 2016, 2003). This important marker horizon follows a major unconformity (Eben discordance) which is continuously traceable in the western and Central European loess region (Krauß et al., 2016; Pouclet and Juvigne, 2009; Zens et al., 2018, 2017). The niveo-aeolian laminated loess below contains several tundra gleys (Gelic Cryosols) and the Eltville Tephra (Pouclet and Juvigne, 2009; Zens et al., 2017), which also allows correlations beyond different domains (Zens et al. 2017). This laminated loess facies is a marker-facies found from western France to Belgium and even to the Czech Republic in Dolní Věstonice (Antoine et al., 2013; Fuchs et al., 2013; Kukla, 1977) for the period between about 28 -23 ka (Moine et al., 2017). For the MPG, the main pedostratigraphic pattern which allows correlation (Zens et al., 2018) is the occurrence of various interstadial soils with varying intensities and pedogenetic (Saint-Acheul-Villiers-Adam; Antoine et al., 2003) or Lower and Upper Brown Soils (Antoine et al., 2016) in France, Les Vaux Soil in Belgium (Haesaerts et al., 2016); Lohne Soil, Böcking Soil, Boreal Soil 2 and 4 (Zens et al., 2018; Zöller and Semmel, 2001), Remagen-1 to 5 Soils (Frechen and Schirmer, 2011), and Boreal Brown Soil (Antoine et al., 2013) in Germany. Due to low sedimentation rates, the MPG soils are generally condensed to a polygenetic brown soil complex, which represents the entire period. However, these are often preserved in domain II and the adjacent. During the Lower Pleniglacial the first Weichselian loess deposit (60-70 ka) can be considered as a very good level-mark for correlation through the area (Haesaerts et al., 2016). Below this loess layer follows a Boreal brown soil called Havrincourt Brown Silt in France (cf Figure 5; Antoine et al., 2014), Boreal Soil 1 (Zens et al., 2018) or Malplaquet Soil in Belgium (Haesaerts et al., 2016), and Jackerath Soil (Regosol-Cambisol) in the Lower Rhine Embayment (Schirmer, 2016). Finally, a characteristic humic soil complex, the Humiferous complex of Remicourt (Haesaerts et al., 2016), Saint-Sauflieu Soil Complex (Antoine et al., 2016), Mosbacher Humus Zone (cf Figure 5, Zens et al., 2018), Isohumic Soil (Antoine et al., 2013), Pryluky complex (Tecsa et al., 2020 and references therein) developed under early glacial conditions and including up to four distinct layers is traceable from northern France towards Ukraine (Antoine et al., 2013; Haesaerts et al., 2016; Haesaerts and Mestdagh, 2000). Due to its widespread distribution this soil complex serves as one of the major marker units of the last glacial (Figure 5).

The preservation of the markers, especially the tephra layers, is often achieved by high aeolian accumulation rates at the time of their deposition. Therefore, for example at Ringen five individual bands of the Eltville tephra can be differentiated (Zens et al., 2017). In Susak, the loess is interfingered with rapidly deposited laterally strongly varying aeolian sands as well as three tephra layers (Wacha et al., 2011b).

III: Loess adjacent to Central European high-altitude mountain ranges (northern Alps and Carpathians)

This domain comprises the western, northern and northeastern margins of the European Alps, the northern part of the Carpathian Basin and Transylvania and the adjacent basins and catchment areas that drain these areas. During the LGM this domain was influenced by periglacial activity indicated by tundra gley soils and cryogenic features in the LPS. The resulting subdomains are located in the valleys of the Saône and Rhône River, the Upper Rhine graben and the upper reaches of the Danube including adjacent areas. Additionally, we enclose the northern part of the Carpathian Basin (southern slopes of the northern Carpathian Mountain ranges) and Transylvania, as the sequences of this area are also influenced by periglacial processes. These areas are strongly impacted by the mentioned major rivers, originating in the Alps (Rhône and Rhine), the Black Forest (the Danube major tributaries, like Inn River, draining the central Alps), and the northeastern Carpathian Mountains (Tisa, Somes, Mures), which are responsible for the silt transport from the Pleistocene alpine glaciers. All these areas are still influenced by periglacial conditions during loess accumulation and therefore the LPS of this domain are usually comparable with those from the northern European loess belt (domain II). A west-east trend in increasing climate continentality, modulated by regional topographic variations, can be recognized in the character of the intercalated interglacial and interstadial paleosols. Our map shows ~53,000 km² loess, ~15,500 km² aeolian sand and sandy loess, and ~79,000 km² alluvial fill and fluvial deposits in this domain.

IIIa: Saône to lower Rhône subdomain

This subdomain in the Saône and lower Rhône catchments in southeastern France stretches from the confluence of the Rhône with the Saône River northward towards the Vosges. The source of the Rhône is close to the Pleistocene Rhône glacier and other smaller alpine glaciers along the western margin of the Alps. The climatic conditions along this north-to-south trending region represent a gradient from a humid-temperate to a Mediterranean climate today or warmer temperate climatic condition without permafrost during the LGM, respectively. Because the area south of Valence (~45°N) has been strongly influenced by the Mediterranean climate conditions we categorized this part to subdomain VIa (Bosq et al., 2020a, 2018). Recent studies investigate the Pleistocene loess of these areas, highlighting the Rhône River as the major dust source in the area. The (paleo-)wind direction in the southern part, the Rhône graben, is north-south since air masses are channelled and concentrated by the topography. The more Mediterranean influenced loess sequences of the southern Rhône valley and the Provence seem to have their source area more in ophiolitic areas of the Alp massif (Bosq et al., 2020a). Most of the loess in this subdomain is distributed in elevations between 204 m and 272 m a.s.l. with a minimum and maximum of 131 m and 515 m a.s.l. (cf. Chapter 3.3).

IIIb: Upper Rhine subdomain

This subdomain comprises loess in the Upper Rhine Plain (Graben) and adjacent areas, such as the Kraichgau and Neckar Basin to the east. Common features of this subdomain are (1) the Pleistocene glaciations of the Alps and the higher mountains of Jura, Vosges and Black forest as proximal areas for glacial silt production, (2) periglacial silt production and regional sediment transport of the Rhine River and its tributaries until the northern end of the Upper Rhine plain and aeolian transport from the wide Pleistocene braided river plain, and (3) features of periglacial overprinting of the LPS.

Switzerland was largely covered by ice during the last glaciations. Loess deposits of few meters in thickness are present on high terraces and hills in the lowlands close to Aarau and along the Rhine River (Christ, 1944, 1942; Christ and Nabholz, 1950; Gouda, 1962). In the Upper Rhine Plain, the Rhine developed a large braided river system during the Pleistocene providing abundant material for mineral dust deflation. In the marginal hills of the southern Upper Rhine Plain and at the Kaiserstuhl, loess reaches in places thicknesses of more than 25 m (Guenther, 1987). Figure 10 indicates locations of important LPS in the Rhine-Neckar region, including the European reference LPS Nussloch located in a loess greda (dune-like morphology), characterized by an exceptional high last glacial dust accumulation rate (see Figure 5, Antoine et al., 2009b, 2001; Moine et al., 2017 and references therein). This 3-D image illustrates the distribution of alluvial fill and aeolian sediments from the middle Upper Rhine Graben and the adjacent eastern shoulders with elevations between 300 and 600 m a.s.l. (e.g. the Kraichgau and Neckar Basin). Aeolian sands are located close to the Rhine, indicating their local transport by westerly winds. Further east widespread loess covers indicate large-scale silt transport from the dry riverbeds of the Rhine, with a clear Alpine contribution. Antoine et al. (2009a) further assume significant deposition of dust from the English Channel and northern France in the region close to Heidelberg. Upstream the Neckar and its tributaries we assume next to the contribution from the glaciated Black Forest regional periglacial silt sources. Loess formation in subdomain IIIb occurred mainly under the cold and dry periglacial condition in a cold tundra environment (recent publications and references therein: Kadereit et al., 2013; Krauß et al., 2017; Zens et al., 2018). The lowlands in this region are slightly dryer compared to the neighboring regions in the north and west, but there are also a lot of similarities to the northern European loess belt including tundra gley soils (Gelic Cryosols) and some of the same marker soil horizons.

Swiss LPS are few and poorly studied. Most known is probably the c. 17 m thick Middle to Late Pleistocene section formerly exposed in the brickyard of Allschwil near Basel (Zollinger, Gaby, 1991). 23 km upstream the Rhine, drillings revealed more than 6 m thick last glacial loess deposits, recently studied by Gaar and Preusser (2017). Close to Freiburg, at Heitersheim and Riegel, 20 to 30 m of loess contain one or more interglacial Bt horizons (Guenther, 1987). There are also thick loess sequences on the western side of the Rhine River in France; the most prominent site is Achenheim, including three interglacial paleosols along a more than 30 m thick LPS and which contains also Paleolithic findings (see Rousseau and Puisségur, 1990 and references therein). The LPS of the Rhein-Neckar region are shown in Figure 10 (see also Bibus, 2002). The 23 m thick LPS Nussloch is well known as highly resolved Upper Pleniglacial loess record of central Europe (see Figure 5). At Mainz-Weisenau, at the northern end of the Upper Rhine Plain, an over 6 m thick profile exposed the last interglacial soil and three early glacial humus zones (Bibus et al., 2002). Most of the loess in this subdomain is distributed in elevations between 186 m and 349 m a.s.l., with a minimum and maximum of 107 m and 577 m a.s.l. (cf. Chapter 3.3).

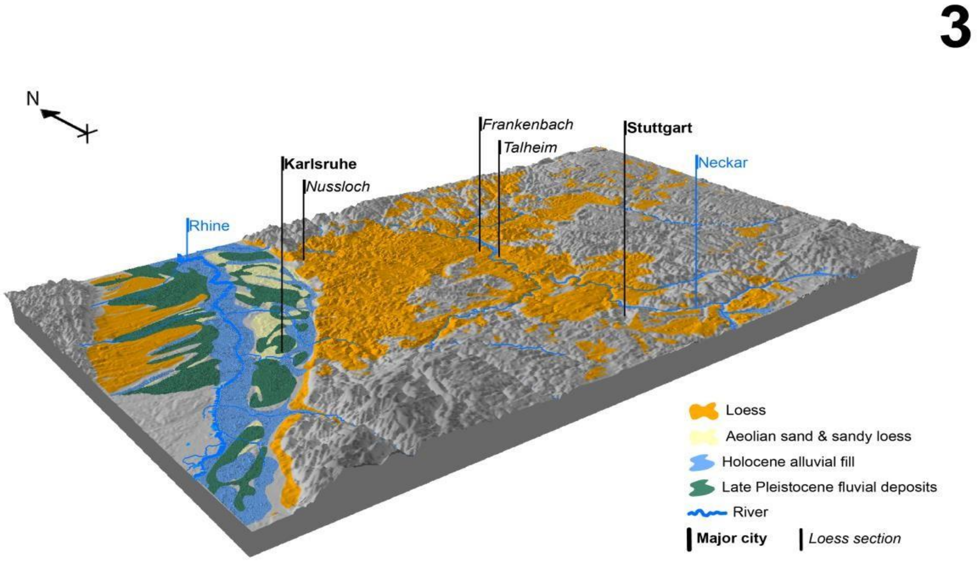

Figure 10: 3-D image of the distribution of loess, sandy deposits, the Late Pleistocene fluvial deposits and Holocene floodplain in the Upper Rhine Graben, the Kraichgau and Neckar Basin. The size of the 3-D image is 95 x 155km. Superelevated by factor 1 (no superelevation).

IIIc: Northern margin of the European Alps subdomain (upper Danube)

Subdomain IIIc comprises loess in southern Germany and northeastern Austria, which stretches mainly along the Danube River and its southern tributaries. These are primarily the water and sediment-rich rivers coming from the Alps, respectively the front of the alpine Würmian ice margin. Loess deposits are mainly found directly next to the (glaci)fluvial source areas and are widely distributed on terraces older than the last glacial. Very little silt contribution comes from the non-glaciated highlands north of the Danube (Swabian-Franconian Alb, Bohemian Massif). This subdomain ends at the southern end of the Bohemian Massif, where the Danube tributaries are no longer draining former glacial areas. Furthermore, the Bohemian Massif acts as a barrier for moisture brought by the Westerlies, resulting in a change of loess facies. Carbonate-bearing loess in subdomain IIIc is largely restricted to the thickest last glacial deposits and the lowest altitudes of this region, whereas loess sediments in subdomain IIId usually have high carbonate contents (Fink, 1965). Closer to the Alps, with increasing moisture, the decalcified loess shows redoximorphic features, which corresponds to the brown loess and dust loam facies, respectively (Fink and Nagl, 1979; section 2.1. Most of the loess and loess derivates in subdomain IIIc are located at elevations between 378 and 488 m, with minimum and maximum values of 290 m and 638 m (see Chapter 3.3).

Upper terrace gravel pits expose up to 5-10 m thick last glacial LPS, for example Bobingen in southwestern Bavaria (Mayr et al., 2017) or Gunderding in northeastern Austria (Terhorst et al., 2015). LPS of 10-15 m thickness reaching back into the Middle Pleistocene (with several Bt horizons) could be found in loam pits, usually on older Terrace levels (Deckenschotter) and in the Neogene

Alpine molasse hills, e.g. at Hagelstadt in Central Bavaria (Strunk, 1990) or Wels-Aschet in NE Austria (Terhorst, 2013).

IIId: Eastern margin of the European Alps and northern Carpathian Basin (including adjacent basins) subdomain

This subdomain comprises the loess in the eastern parts of the Bohemian Massif, the eastern and southeastern margin of the Alps and the widespread loess covers east of the uplands reaching from northeast Austria and southeast Czech Republic (Moravia) into the northern part of the Carpathian Basin (southern Slovakia, northern Hungary and Romania). Silt sources are mainly periglacial low mountain areas and the Danube with large amounts of Alpine glacial material. Smalley and Leach (1978) specify flysch rocks of the Carpathian Mountains as significant regional silt source and point to the possibility of silt transport from northern European glaciations through the Moravian gate in the northeastern part of the Czech Republic. Additionally, the authors indicate that regions far downstream the Alps contain significant proportions of reworked older loess, remobilized by wind and water.

In northeast Austria, loess sediments are widespread along the higher terraces of the Danube and adjacent hills (Figure 11) locally reaching almost 40 m thickness at Krems, where the Danube leaves the narrow valley cutting through the Bohemian Massif (Wachau). Within the Wachau and at the eastern margin of the Bohemian Massif loess deposits are highly variable in age and thickness and often contain fragments of local rock mixed in by slope processes (Sprafke, 2016; Sprafke and Obreht, 2016). A high carbonate content (c. 20-25 %) and loess-like structure made Vetters (1933) map these silt-dominated deposits as loess, whereas decalcified aeolian silts in northwestern and southeastern Austria remain largely ignored on geological maps (see section 2). Thick loess deposits in northwestern Austria and Moravia can be found in the lowlands of the larger tributaries of the Danube (Morava/Thaya), but on the eastern side of these rivers on the border to the Slovakian Republic, large areas of aeolian sand are formed, which indicates that the wind mainly deflated dry floodplain deposits from western directions. Notable loess covers of variable thickness are present in the rolling hills between the larger rivers, but the highest altitudes between Danube and Thaya remain free of loess (Figure 11).

LPS close to the Bohemian Massif and in the hills of northeastern Austria are variable in age and temporal resolution. Interglacial paleosols in the Krems-region are often polygenetic or missing completely because of reworking or partially erosion, especially at ending phases of interglacials, which renders pedostratigraphical approaches rather difficult (Sprafke, 2016). The classical LPS of Krems-Schießstätte (shooting range) and Stranzendorf are unique loess records of the Early Pleistocene paleoclimatic cycles (Fink and Kukla, 1977; Kukla and Cílek, 1996). The LPS Paudorf and Göttweig near Krems expose Middle Pleistocene to last interglacial pedocomplexes (Sprafke et al., 2014). Thick calcified last glacial loess packages in the Wachau and Krems region are also famous for Upper Paleolithic cultural layers, e.g. at Willendorf (Wachau) (Nigst et al., 2014), Krems-Hundsteig (Neugebauer-Maresch, 2008) and Krems–Wachtberg (Einwögerer et al., 2006) and Stratzing (Neugebauer-Maresch, 1993).

4

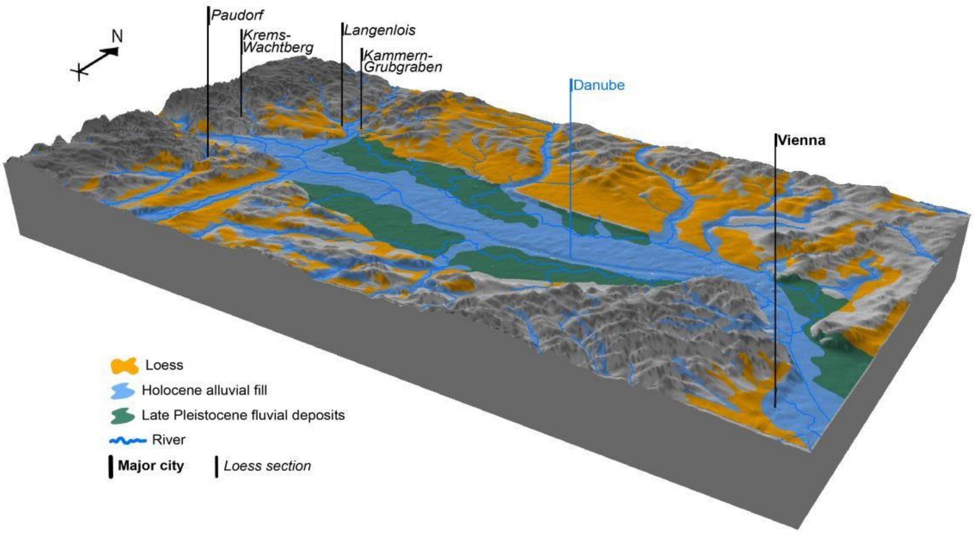

Figure 11: 3-D image of the distribution of loess, sandy deposits, the Late Pleistocene fluvial deposits and Holocene floodplain in Lower Austria. The size of the 3-D image is 35 x 70 km. Superelevated by factor 1 (no superelevation).

Well-resolved MIS 5 pedocomplexes are exposed close to the Thaya and Morava rivers at the classical LPS Dolní Věstonice (Antoine et al., 2013; Fuchs et al., 2013 and references therein) and Stillfried (Fink, 1954; Terhorst et al., 2011), with nearby loess containing important Upper Paleolithic sites. In south Moravia (Czech Republic) loess sediments are mainly found in the lowland river basins where they cover mostly Pleistocene river terraces. Figure 12 provides an example from the famous Červený kopec (Red Hill) section at Brno, Czech Republic (Kukla, 1978, 1977). Based on this typical staircase of loess covered terraces (CK 1 -5) Kukla (1977) developed the classical European glacial stages in loess and the correlation with deep-sea sediments. The paleosols of Middle and Late Pleistocene age that are often missing in the Krems-region were better preserved here (Fink and Kukla, 1977; Kukla and Cílek, 1996).

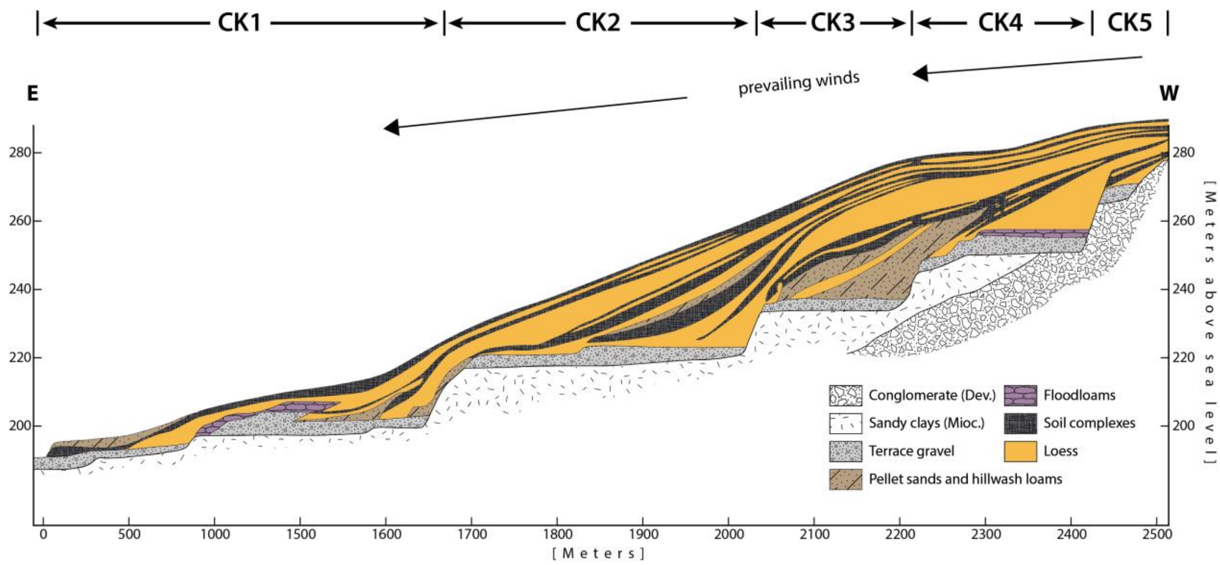

Figure 12: Redrawn and modified sketch from Kukla (1977, 1978) showing the Červený kopec (Red Hill) section at Brno Czech Republic with the terraces CK 1 -5 covered with LPS. The section was exposed in an excavation front of a brickyard pit and in boreholes.

Cumulative loess thickness can reach up to 50 m in south Moravia, especially towards the Bohemian Massif foothills (Hošek et al., 2017, 2015; Lehmkuhl et al., 2018a; Zeman et al., 1986, 1980). The above-mentioned profile Červený Kopec at Brno (southeastern edge of Bohemian Massif) is an exclusive example of such accumulation. This classical loess section, intercalated by fourteen pedocomplexes, provides the most complete record in central Europe, covering last 1 Ma, i.e. MIS 25 – MIS 2 (Kukla, 1975).

In southwestern Slovakia Middle and Late Pleistocene loess covers a vast area of Danube and Záhoří lowlands, reaching up to 40 m in thickness (Šajgalík and Modlitba, 1983). Towards to the north (higher elevation along the western Carpathians) and east (East Slovakian lowlands) loess becomes coarser than in southwestern Slovakia and they are mainly decalcified and polygenetic with strongly (pseudo)gleyed paleosols (Košťálik, 1989; Lehmkuhl et al., 2018a; Šajgalík and Modlitba, 1983; Vaškovský, 1977). Some smaller patches of loess and loess derivates can also be found at the Carpathian foothills in western Ukraine, which also belong to this subdomain.

Loess and its derivates and coarser variants, as well as aeolian sand, are widely distributed in (northern) Hungary (Pécsi, 1987) and northwestern Romania. Loess deposits are distributed along the Danube and Tisa rivers. Several famous loess sections are part of this subdomain such as the LPS Basaharc (Sümegi et al., 2011), Mende (Borsy et al., 1979; Frechen et al., 1997; Marton, 1979; Wagner and M, 1979), Albertirsa (Novothny et al., 2002) and Süttő (Figure 5; Barta, 2014; Koeniger et al., 2014; Novothny et al., 2011, 2009; Profe et al., 2018a; Rolf et al., 2014). Most of the investigated loess sequences are located within the basin along the major rivers, but also in northeastern Hungary two sites were investigated: Bodrogkeresztúr and Tokaj (Bösken et al., 2019; Schatz et al., 2015a, 2015b, 2012, 2011; Sümegi et al., 2016b, 2000). These sites highlight the more humid paleoenvironmental conditions at the Carpathian foothills.

Geomorphological processes in the northern part of Carpathian Basin were controlled by strong northern and northwestern winds during glacial times (Sebe et al., 2011). Most of the loess in this subdomain is distributed in elevations between 131 m and 261 m a.s.l. with a minimum and maximum of 84 m and 538 m a.s.l. (cf. Chapter 3.3).

IIIe: Transylvanian subdomain

Loess is distributed in one greater area in the western Transylvanian Plateau and several small isolated patches along the rivers in the rest of the basin. Due to the high elevations and the proximity to the (partly) glaciated Carpathian Mountains, the relatively steep slopes resulting from significant basin-wide neotectonic activity (including salt and gas diapirism), the Quaternary sediments were strongly influenced and overprinted by permafrost features (Pendea et al., 2008). Additionally, the sequences in Transylvania are often disturbed by slope processes, resulting in colluviated loess and loess derivates (Jakab, 2007; Pendea et al., 2009). These deposits are an archive for the landscape evolution and history of the area, but it is challenging to use them as paleoclimate archives. Please note that we adapt the permafrost boundary from Vandenberghe et al. (2014a) and in Transylvania this boundary is probably situated further south than shown in our map due to areas with higher elevation. Most of the loess in this subdomain is distributed in elevations between 334 m and 456 m a.s.l. with a minimum and maximum of 209 m and 705 m a.s.l., in thicknesses up to 20 m, especially along the Aries and Mures river cuesta (cf. Chapter 3.3).

IV: Middle Danube loess

The loess domain of the Middle Danube Basin has a long tradition of loess research (Marković et al., 2016) and contains some of the thickest European loess sequences (at least >50 m in outcrops and approx. >100m recorded from drillings), preserving a quasi-continuous paleoenvironmental record extending to the Early Pleistocene (Buggle et al., 2013; Marković et al., 2011, 2015; Schaetzl et al., 2018). In this domain we include the central and southern part of the Carpathian Basin (Middle Danube Basin). The southern limit of the extensive spatial loess distribution in this domain follows the valley of the Great Morava River and is bounded to the south by the foothills of the Dinaric and Carpatho-Balkan mountain ranges. South of these areas, loess distribution is characterized by many isolated deposits that essentially originate from local sources (see subdomain VIc).

The loess deposits of the Carpathian Basin and adjacent areas are not as homogeneous as one might expect. In the western part of domain IV between southwestern Austria and Croatia the distinction between Neogene Pannonian Basin silts and loess is not always clear, which is complicated by redoximorphic features overprinting these sediments, i.e. dust loam according to Fink & Nagl (1979) and pseudogleyed loess derivates after Rubinić et al. (2018). Yet, these poorly mapped and investigated loess deposits can reach 10 m thickness at the northern side of the Mur River draining the Alps. There is a gradual transition towards the southern part of domain IV that is reflected in slight shifts in (paleo-)vegetation and environment from periglacial conditions with tundra and forest-steppe towards drier steppe conditions. The boundary between domain III and IV follows approximately the southern limit of continuous permafrost (Figure 2). Thus, loess from the central and southern part of the Carpathian Basin does not belong to the same loess facies as the northern part (i.e. Moravia, the eastern parts of Austria and the northern Hungarian plain). Loess deposits from domain IV share more commonalities with the loess deposits of the Lower Danube Basin (domain V). However, modern and Pleistocene climate conditions differed between the Carpathian Basin (Middle Danube Basin) and the Lower Danube Basin: both are rather continental but the aridity is more pronounced in the latter one (Botti, 2018; Obreht et al., 2017).

Generally, LPSs in the Middle Danube basin reflect typical loess plateau deposition (e.g. Marković et al., 2018a). Characteristics of these LPS also indicate a paleoclimatic gradient towards warmer and drier conditions from northwest to southeast (Sümegi and Krolopp, 2002). Drier conditions indicated better preservation of more complete LPS in the southeastern part of the Carpathian Basin (Marković et al., 2015, 2008) and also higher sedimentation rates (Antoine et al., 2009a; Bokhorst et al., 2009; Sümegi et al., 2013; Újvári et al., 2017, 2010). The domain is positioned in an important geographic location, being close enough to the Atlantic Ocean to record its weakened influence, but at the same time isolated inland by surrounding mountains and partly protected from intensive cold Arctic air masses. Because of the geographic setting, climate and environmental conditions in the southeastern Carpathian Basin region were more stable than those elsewhere, as indicated by other European late Pleistocene loess-paleosol records (Antoine et al., 2001, 1999b; Rousseau, 2001; Rousseau et al., 1998; Vandenberghe et al., 1998). The mechanisms behind dust accretion in loess plateaus seem to be restricted to steppe environments in which seasonal droughts during late summer and early autumn occur (Buggle et al., 2014, 2013). In those climates of Cfb to Cfa type (Walter, 1974) biological loess crusts and mats play an important role serving as dust traps and possibly also facilitating loessification and transforming this way the semi-continuous accretion of dust to stable LPS (Svirčev et al., 2019). Together with the flora of the semi-desert to steppe environments the biocrusts effectively protect LPS from erosion and deflation leading to plateau deposits which record Pleistocene environmental history since the late Lower Pleistocene at least.

The loess plateaus of domain IV are mainly located between the floodplains of the Danube River and its major tributaries, such as Tisa, Drava, Sava and Timis/Tamiš. Loess plateaus are remarkably thick at the confluences of the rivers, where deflatable material from both sides was deposited (Fitzsimmons et al., 2012; Marković et al., 2008). This indicates that the Danube River and its tributaries were important source areas during the Pleistocene, at least for the relatively coarse-grained silt and sand fractions (Bokhorst et al., 2011; Buggle et al., 2008; Smalley and Leach, 1978; Újvári et al., 2008), while smaller particles potentially can be of far-distance origin (Varga et al., 2019; Zeeden et al., 2016). Figure 13 provides an overview of different loess landscapes and loess sections along the Danube in the southern part of the Carpathian Basin and their geomorphological situation. Loess and loess derivates are distinguished according to Lehmkuhl et al. (2018a). The lowermost and youngest terraces of the Tisa, Sava, and Danube rivers and their tributaries are covered by loess-like sediments and loess derivates and are therefore often referred to as loess terraces. The famous Titel loess plateau, which is situated in the Danube-Tisa-interfluve, can be clearly distinguished in the figure. Next to the Titel LPS (Bokhorst et al., 2009), also the 20 m thick Surduk LPS on the opposite bank of the Danube exhibits a very detailed record of the last interglacial-glacial cycle (Antoine et al., 2009a; Fuchs et al., 2008). Surduk is located at the edge of the Srem loess plateau, which has been formed between the Danube and Sava rivers at the southern and eastern slopes of the tectonically uplifted Fruška Gora Mountains. These mountains are surrounded to the south by a system of loess covered alluvial fans, with decreasing loess thickness upslope. This geomorphic situation influences e.g. the stratigraphic succession and the characteristics of paleosols (Vandenberghe et al., 2014b). Whereas the upslope section of Irig shows pure aeolian set-up, the downslope section of Ruma comprises a loess facies also characterized by intense sediment relocation (Marković et al., 2007, 2006; Vandenberghe et al., 2014b). The plateaus continue west of the Fruška Gora Mountains in eastern Croatian, where loess is regarded as generally pure or unaltered. Quaternary limnic, alluvial and marsh sediments are overlain by aeolian deposits in the Croatian part of the Carpathian Basin (e.g. Marković et al., 2009; Galović et al., 2011). .

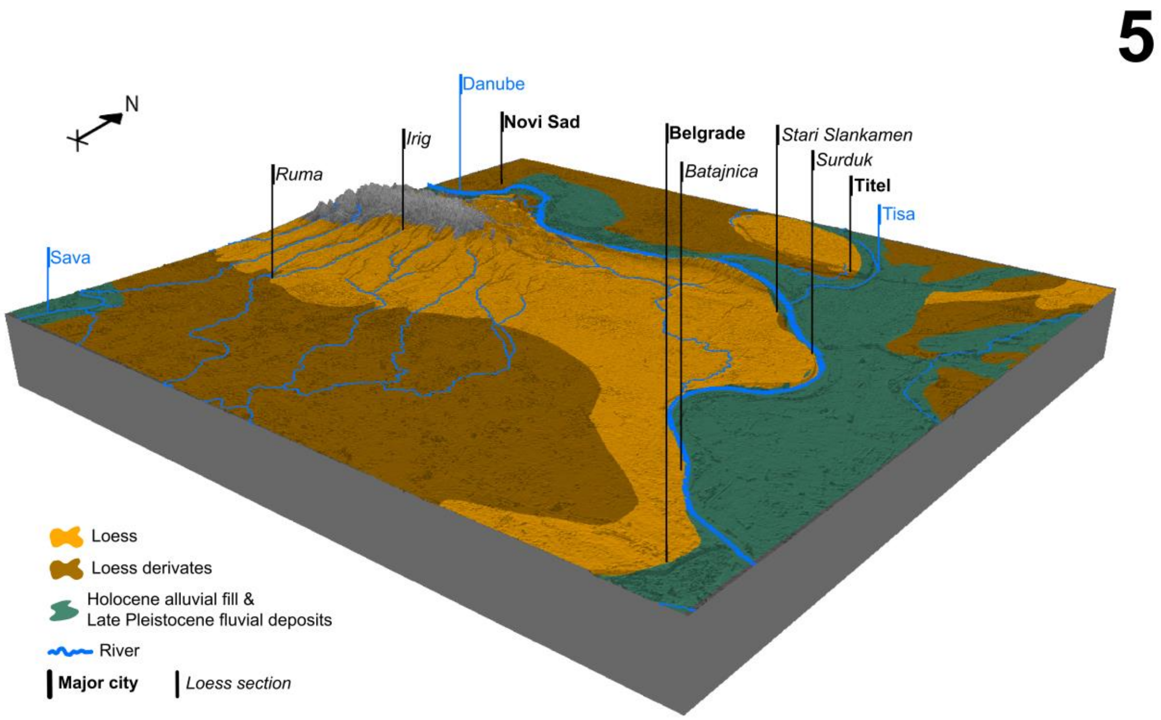

Figure 13: 3-D image of the loess landscape in the Vojvodina (northern Serbia) showing the distribution of loess, loess derivates, the late Quaternary floodplain and numerous investigated loess sequences. The size of the 3-D image is 53 x 57 km. Superelevated by factor 1 (no superelevation).

Loess and loess derivates continue into Slavonija-Srijem/Srem area in Croatia, along the Danube-Drava-Sava interfluves where several LPS were described. This region can be regarded as the southernmost border of the loess in the Carpathian Basin. Loess mostly covers alluvial river terrace sediments and forms smaller plateaus in the river interfluve. There are several LPS described, e.g. Šarengrad, Vukovar, Erdut and Zmajevac (Banak et al., 2016; Fenn et al., 2020; Galović et al., 2009;

Wacha et al., 2013; Wacha and Frechen, 2011). The paleosols intercalating the loess are mostly Chernozem-type soils and brown forest soils (Bronger, 2003). The provenance of the material is similar to the Pannonian basin region with an evident, more local influence from southern provinces (e.g. Sava River southern tributaries originating from the Dinaride Ophiolite zone; (Galović, 2016)). A gradual increase in humidity is observed in the loess sequences going across the Pannonian region of Croatia towards the west. This increase persisted throughout all (or most) climatic shifts from the late glacial to today (Rubinić et al., 2018). A particularity of paleosols (mainly Stagnosols) in the western part of the Pannonian region in Croatia is that the increased distance to the source allowed pedogenesis to outcompete loess accumulation, so that no unaltered loess can be found in this area. Rubinić et al. (2018) concluded that Croatian pseudogleys could be considered as soils that had reached their quasi-equilibrium stage thousands of years ago and they have continued to form throughout the Holocene. Loess in this domain is distributed in elevations up to 393 m a.s.l. with a median of 98 m a.s.l. (cf. Chapter 3.3). The map shows ~60,500 km² loess and loess derivates, ~17,000 km² aeolian sand and sandy loess, and ~37,000 km² alluvial fill and fluvial deposits. Most of the loess and loess derivates are located in elevations between 81 and 136 m a.s.l. with a maximum of 285 m a.s.l.

V: Pontic East European domain

Domain V consists of the vast and laterally continuous aeolian deposits of southern Ukraine, Russia, Moldova, the Moldavian Plateau and the Lower Danube Basin in Romania and Bulgaria, including the Dobrogea. The most comprehensive studies of LPS in eastern Europe are located in this domain and they contain a rich archive of paleoclimatic changes for at least the Middle and Late Pleistocene (Antoine et al., 2019; Buggle et al., 2013; Chen et al., 2020; Haesaerts et al., 2003; Liang et al., 2016; Lomax et al., 2019; Necula et al., 2015a; Obreht et al., 2017; Rousseau et al., 2020, 2013, 2001; Tecsa et al., 2020; Tsatskin et al., 1998; Velichko et al., 2009; Zeeden et al., 2018). In this area, there are no indications of permafrost and loess deposits developed under forest steppe and steppe conditions. This is also reflected in the distribution of modern topsoils, with recent Luvisols in the former forest steppes and Chernozems in the steppe areas (e.g. Velichko, 1990). Loess deposits are strongly influenced by the Danube River, the Carpathian Mountains and the Black Sea, but also the Don, Dniester, Dneiper and Volga run through this domain. Another relevant dust source are the drylands around the Caspian Sea and further east and dust might have been transported by the Easterlies to domain V (see e.g. Obreht et al., 2017 and references therein). This loess domain covers different bioclimatic zones: continental conditions in the Lower Danube Basin, sub-Mediterranean Black and Azov Sea coasts, and more semi-arid and desert conditions towards the east. Similar to domain IV, the dominating depositional mode is the accretion of dust in plateau deposits over the entire Pleistocene. At the western and northern shores of the Black Sea, the Sea of Azov and the Caspian Basin loess deposits are influenced by desert margin conditions with dust input from the East including endorheic basins and alluvial fans at the foot slopes of mountain ranges which both delivered deflatable silt (Vandenberghe et al., 2006). Interestingly thicknesses of paleosol and loess intervals are similar and grain sizes are getting finer in this area indicating continuous and steady input of far travelled dust (Chen et al., 2020). Towards the Caspian Basin, the loess cover gets generally thinner. The shelf of the Black Sea is not a dominant source area as LPS are thinning towards the coast (Jipa, 2014). This domain shows features which are commonly found in more arid landscapes e.g. in Central Asia, such as alkaline lakes, which are frequent in the rain shadow of the Carpathian Mountains in Lower Danube Basin and even north of the Black Sea coast.

The southern part of this domain is dominated by the Lower Danube Basin (LDB) and the Dobrogea uplands. The LDB is strongly influenced by the Danube River and its tributaries, draining the eastern and southern Carpathians, as well as the Balkans. The basin is characterized by vast aeolian plateaus nested between major river valleys, and can be subdivided into the Wallachian Plain, the Bulgarian Plain, the forelands of Carpathians and Balkans, the Moldavian Plateau as well as the Dobrogea uplands (Jipa, 2014). The plains are usually covered with thick (tens of meters) Quaternary loess mantles, smoothing the landscape. In these areas the sediment covers are dissected by rivers forming loess bluffs at their banks (e.g. LPS Vlasca, Figs. 14). In contrast, the Dobrogea uplands consist of a limestone plateau, which shows a dendritic fluvial system which is mostly covered by loess deposits in variable thickness. Here, the thickest sections are usually available in abandoned quarries (e.g. LPS Mircea Voda and Urluia, Figure 14) or also as loess bluffs along valleys (e.g. LPS Rasova, Figure 14) or even in cliffs along the Danube and the Black Sea coast. In general, the sequences of the LDB show a broad variability in thickness and age: whereas some sections cover several glacial cycles (Costinești, Constantin et al., 2014; Mostiștea, Necula et al., 2015b; Urluia, Obreht et al., 2017). Albeit loess records in the region are laterally very consistent chronostratigraphically, thicknesses can also vary significantly. Additionally, several LPS preserve tephra layers (Italian, Carpathian Caucasian), in places in considerable thickness (Anechitei-Deacu et al., 2014; Antoine et al., 2019; Constantin et al., 2012; Lomax et al., 2019; Obreht et al., 2017; Veres et al., 2013; Zeeden et al., 2018).

In addition to the paleoenvironmental preconditions, close to the Carpathian bending the area is also influenced by tectonic subsidence, leading to thick Pliocene-Pleistocene sediment fillings, e.g. in the Focşani Basin comprising up to 7 km thick Pliocene-Pleistocene fluvial and aeolian deposits (Matenco et al., 2016). Most of the loess in this subdomain is distributed in elevations between 46 m and 139 m a.s.l. with a maximum of 139 m a.s.l. (cf. Chapter 3.3). The map shows ~246,000 km² loess and loess derivates, ~1,600 km² aeolian sand and sandy loess, and ~46,000 km² alluvial fill and fluvial deposits. Most of the loess deposits are found in elevations between 46 m and 138 m a.s.l. with a maximum of 308 m a.s.l.

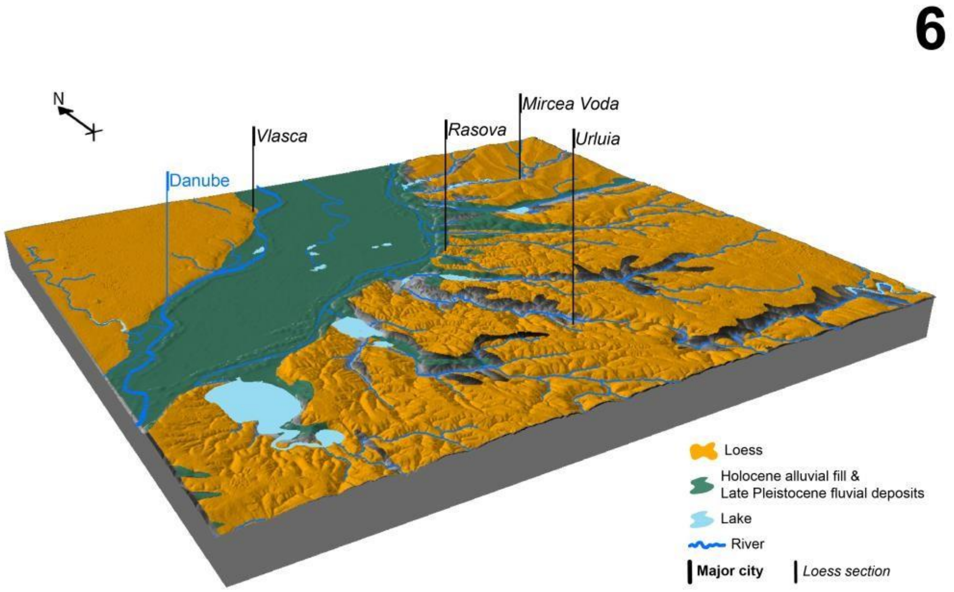

Figure 14: 3-D image of the distribution of loess and late Quaternary floodplain deposits in the Lower Danube Basin. The size of the 3-D image is 50 x 55 km. Superelevated by factor 1 (no superelevation).

VI: Mediterranean loess

This domain comprises loess and loess-like sediments in the Mediterranean area. Periglacial processes are limited to discontinuous evidence of soil freezing and ice lensing recorded at the margin of the Po Plain (Cremaschi et al., 2015, 1990; Cremaschi and Van Vliet-Lanoë, 1990). Recent studies suggest that Pleistocene loess covers vast areas in the (peri) Mediterranean regions (Boixadera et al., 2015; Bosq et al., 2020a; Wacha et al., 2018; Wolf et al., 2019; Zerboni et al., 2018). Loess in these regions does not reach the thickness of loess in central and eastern Europe and is often preserved as (relocated and weathered) loess-derivates. We present three subdomains: the western Mediterranean subdomain (VIa), the northern Mediterranean subdomain (VIb) and the eastern Mediterranean subdomain (VIc). A possible source for aeolian material besides globally distributed dust are the rivers (such as Ebro or Po), glacial and pro-glacial system at the margin of southern Alps, and glacial grinding from several paleoglaciation in the Mediterranean (Ehlers et al., 2011), especially on the Iberian Peninsula (summary in Oliva et al., 2019) and the Dinaric mountain ranges (e.g. Hughes et al., 2011). Moreover, periglacial weathering processes in the mountains and regional desert-like conditions and insolation weathering in the lowlands produced silt-sized particles. Dry emerged shelves are a further source of loess along shorelines. The map shows ~18,000 km² of loess and loess derivates, ~2,800km² of aeolian sand and silty loess and ~82,000 km² alluvial fill and fluvial deposits in this domain (see Chapter 3.3).

VIa: Western Mediterranean subdomain

Loess in southwestern Europe is mostly concentrated on the Iberian peninsula (e.g. Bertran et al., 2016). Aeolian deposits can be found in the lower Ebro Basin in northeastern Spain (Boixadera et al., 2015) and the upper Tagus Basin in central Spain (Wolf et al., 2019, 2018). Boixadera et al. (2015) reported about loess deposits in the Ebro Basin that are generally 3-4 m thick and consist of well-sorted fine sands and silts, i.e., coarser than typical loess. Loess in central Spain is distributed along the upper Tagus River in elevations between 500 and 700 m a.s.l., covering fluvial terraces and depressions nearby. The Tagus loess reaches thicknesses of around 8 m and reveals high contents of calcium carbonate (between 30 and 40%) and soluble salts (~10 %) indicating that Tagus River deposits and weathered local marls were important loess sources during the Pleistocene (Wolf et al., 2019). In contrast to other European loess areas, paleosols generally show reddish colors and can be rated as Mediterranean Cambisols. In addition, there are some areas in the southern part of the lower Rhône and Rhône delta region, which can be attributed to this subdomain (see IIIa). Especially in the region of the Provence, Mediterranean influences on loess derivates lead to indicative soil formation such as Terra Rossa (Bosq et al., 2020a). Loess in this subdomain is distributed in elevations up to 707 m, with a median of 286 m (cf. Chapter 3.3).

VIb: Northern Mediterranean subdomain

In this subdomain, loess formation is widely recorded along the margins of the Po Plain (Cremaschi et al., 2015) and the coastline of the northern and eastern Adriatic Sea and on the islands of Croatia (Cremaschi, 1990a; Wacha et al., 2018, 2011b). These deposits are summarized as the Po plain loess basin (Cremaschi, 2004, 1990a, 1987; Zerboni et al., 2018). Moreover, loess is discontinuously distributed along the shorelines of the southern Adriatic, where it is mostly preserved at the top of limestone plateau (eventually recycled by pedogenesis) and within caves and rock shelters (Cremaschi, 2004; Cremaschi and Ferraro, 2007) and was occasionally described along the Tyrrhenian shorelines (Boretto et al., 2017). Loess in Italy originates from the deflation of the Upper Pleistocene fluvioglacial and fluvial deposits at the southern margin of the Alps, along the northern fringe Apennines and along the Adriatic shelf. Along the southern Adriatic and Tyrrhenian shorelines a further silt source are secondary tephra clasts deposited along the emerged shelf and later deflated inland (Cremaschi and Ferraro, 2007; Hirniak et al., 2020). It is also often overprinted by pedogenesis and thus its extent and paleoenvironmental significance were underestimated (Amit and Zerboni, 2013). A variety of soils are interbedded within loess sequences, including Chernozems, Alfisols, Cambisols and Luvisols, and occasionally layers of reworked loess are also present. Only a few sequences of thick, unweathered loess (e.g. the Val Sorda of Torino Hill sequence) and some complex pedosequences (e.g. Monte Netto) can be found in northern Italy (Cremaschi et al., 1990; Ferraro, 2009; Forno, 1990; Zerboni et al., 2015). The Val Sorda sequence, for instance, was preserved because it was capped by glacial deposits formed at the final LGM advance of the Garda Lake Glacier. The majority, however, is deposited as sheets of wind-blown silt. Loess deposits are recurrent at several geomorphological settings along the southern margin of the Alps and the northern margin of the Apennines. These locations correspond to dissected fluvial terraces, pre-LGM glacial deposits, uplifted isolated hills and karst plateaus (Cremaschi, 2004; Zerboni et al., 2018). Occasionally, loess bodies can be found on top of polygenetic paleosols, inside sinkholes and trapped within caves and rock shelters, embedding anthropogenic deposits (Peresani et al., 2008).

Additionally to the Italian loess deposits, this subdomain also consists of loess on the Adriatic coast of Croatia (e.g. Istrian Penisula: Zhang et al., 2018), including the islands of the Kvarner Bay (Profe et al., 2018b; Wacha et al., 2018). These deposits originate from Alpine glacial outwash plains in the Po Plain (Cremaschi, 1990a; Mikulčić Pavlaković et al., 2011), but are strongly influenced by Mediterranean climate (Profe et al., 2018b). The large glacio-fluvial outwash plains from the Pleistocene alpine glaciers in the northern Po Plain and the dry shelf of the Adriatic Sea provide additional dust sources. Heavy mineral assemblages of loess sequences from the two opposite sides of the Adriatic Sea (Monte Conero and Susak Island) suggest the same source of wind sediments, corresponding to the Upper Pleistocene alluvial plain of the Po River, today submerged by the Adriatic Sea (Cremaschi, 1990b).

Loess along the eastern Adriatic coast and on the islands directly covers the Cretaceous carbonate basement. The loess deposits are mostly coarser in grain size due to local winds than the loess in domain IV. At Susak, for example, the grain size is shifted toward fine sand (Wacha et al., 2018). On a more recent geological map of Croatian loess, Susak was mapped as sandy loess (Fuček et al., 2014). It contains more paleosols compared to loess in eastern Croatia (domain IV). The soils are also more reddish in color, highlighting the Mediterranean climate influence (see stratigraphy in Figure 5). The thickness of the loess and loess derivates in the Adriatic region is quite small (Susak being the exception with ca. 30 m thick loess deposits) and for that reason they were mostly not presented on older maps. Its distribution is discontinuous and patchy. The loess in Istria, on the other hand, is finer grained compared to the Susak loess, and therewith more similar to typical loess in domain IV, but it also shows a higher degree of pedogenetic overprinting. The loess in the Adriatic region is mainly of last glacial age (Cremaschi et al., 2015; Wacha et al., 2011a; Zhang et al., 2018), but it is suggested that red paleosols below the loess on Susak formed on even older loess (Durn et al., 2018) as well as buried paleosols at Monte Netto (Delpiano et al., 2019; Zerboni et al., 2015). Loess in this subdomain is distributed in elevations up to 698 m, with a median of 188 m (cf. Chapter 3.3).

VIc: Eastern Mediterranean subdomain

There are several small patches of loess deposits in the basins and river valleys of the Balkans, especially in Bosnia-Herzegovina, southern Serbia, Montenegro, and North Macedonia. These are scarcely described in the literature. However, these deposits exhibit unique geophysical and geochemical properties, reflecting the stronger influence of Mediterranean climate with more intensive weathering (Basarin et al., 2011; Bösken et al., 2017; Obreht et al., 2016, 2014). Based on the strong geochemical fingerprints of the silt originating from mafic rocks of surrounding mountains, the most plausible major source areas are local rivers (Obreht et al., 2016). An illustrative example for the alternating influence of the local rivers as a dust source is the Stalać LPS (Bösken et al., 2017; Obreht et al., 2016), which lies in the vicinity of the confluence of the South (Južna) Morava and the West (Zapadna) Morava rivers into the Great (Velika) Morava River. This setting of three river basins served as local dust source, making loess accumulation possible. This makes this section exceptional since it preserves several glacial-interglacial cycles (Bösken et al., 2017; Kostić and Protić, 2000; Obreht et al., 2016), while others usually cover just a part of the last glacial cycle (Basarin et al., 2011; Obreht et al., 2014). Consequently, the occurrence of the small patches of loess deposits in this subdomain is highly influenced by the local geomorphology and the extent of glaciers in the Balkan mountain ranges (Obreht et al., 2016). Results from LPS of the region show that the central Balkans are still under the influence of the westerlies from the Atlantic Ocean, but most prominently more continental and Mediterranean climatic conditions prevail in this region. Investigations showed that the climatic boundaries are sharp and fluctuated in the course of the Pleistocene. These fluctuations are e.g. imprinted in indicative (paleo-) soil properties (Obreht et al., 2016). However, the transitional region from the Balkans to the Carpathian Basin is characterized by loess that is more similar to plateau loess in domain IV with some characteristic of Mediterranean loess, e.g. Nosak and Smedarevo (Marković et al., 2014). Loess in this subdomain is distributed in elevations up to 1,307 m, with a median of 374 m (cf. Chapter 3.3).

3.2. Relief and loess: Visualization with four north-south transects

The north-south transects were chosen in a longitudinal distance of approx. 400 km. They were spread across Europe to visualize the interplay of relief and loess in various domains and subdomains. The geographic location of transects are depicted in the top panel of Figure 4.

Transect A shows a cross section from the southern margin of the British Isles ice sheet, through southern England, France, and the Massif Central towards the Mediterranean coast near the Rhône delta. It depicts the broad area of the dry English Channel, which acted together with the exposed North Sea shelf during glacial periods as deflation area and therefore major source of aeolian sediments deposited further south (subdomain IIa). The nowadays French-Belgium coast in direct vicinity to the source area is characterized by aeolian sands and dunes. To the south, broad and extensive loess areas with a hilly relief adjoin. The Seine Basin, known for vast loess deposits, is also visible and it is intersected by several fluvial systems (subdomain IIa). The central uplands with the Loire valley are free of loess and aeolian sediments. They are bounded to the south by the Massif Central. This boundary also coincides with the boundary of the continuous permafrost (Vandenberghe et al., 2014a). Towards the Rhône delta, just small patches of Mediterranean loess occur (subdomain VIa).

Transect B runs from the southwestern margin of the Fennoscandian ice sheet through northern Germany, the Harz Mountains, the Central European low mountain ranges, the Danube valley, across the Alps towards the Po plain in Italy. The protogenetic zone (subdomain Ia) is dominated in this area by broad glaciofluvial sediments and sparse aeolian sediments, mainly sands. In the foreland of the Harz Mountains, the sharp northern boundary of loess subdomain IIb (loess-edge ramp, see chapter 3.1) is visible. The foothills of the Harz Mountains are covered by a thinning loess cover, reaching up to an elevation of approx. 300 m. This area was also influenced by the advances of the penultimate (Saalian) glaciation. Thus, the loess-edge ramp at the northern loess margin covers Saalian glacial tills (Figure 9). The glaciated mountain range is bounded to the south by the loess covered Thuringian

Basin (subdomain IIe), which is adjoined by the central German low mountain ranges, where loess is only found sparsely in basins and depressions. Along the German stretches of the Danube River (subdomain IIIc), loess can be found in higher elevations and is intersected by alluvial plains of the Danube River and its tributaries, which act as local dust sources. The (glacio-) fluvial deposits from the Würmian Pleistocene glaciation of the Alps act as additional dust source and are mainly not loess covered (cf. Lehmkuhl et al., 2018b). Within the transect loess distribution rapidly declines south of the LGM-timberline, indicating reduced dust deposition in forested areas. Only the southern slopes of the Alps and the northern slopes of the Apennines are covered with a loess blanket (subdomain VIb).

Transect C runs from the southern margin of the Fennoscandian ice sheet southwards through Poland, crossing the Western Carpathians and their forelands, the Carpathian Basin and ends on the northern foothills of the Dinaric mountain ranges. The northern part (subdomain Ia) was strongly influenced by the Weichselian and especially the Saalian ice sheet advances. The latter is also true for subdomain IIb. Therefore, hardly any aeolian sediments can be found in this area. Southwards, the loess regions of southern Poland adjoin (subdomain IIc), which are bounded by the Tatra Mountains, as a part of the Western Carpathians. The mountain ranges of northern Hungary, such as the Bükk Mountains, are free of aeolian sediments, which reoccur on their southern slopes. The northern Carpathian Basin is dominated by vast deposits of loess and loess derivates (subdomain IIId). Further to the south in the Danube-Tisa-interfluve, the aeolian sediments are coarser, forming sandy loess deposits and large bodies of aeolian cover sands and dunes. The southern part of the basin is again covered by loess (domain IV) until the foothills of the Dinaric mountain ranges. The timberline during the LGM did not play a role in loess distribution in the Carpathian Basin, since it was located at higher elevations. The southern Carpathian Basin acted as a refugium for several mammal species (Stojak et al., 2015) and warmth-loving gastropod taxa (Sümegi et al., 2017) and especially the mountain regions are regarded as biogeographical refugium with transitional zones in the loess steppe (Marković et al., 2018b, 2008; Sümegi et al., 2016a).

Transect D starts at the eastern margin of the ice sheet near the Russian-Belarusian border, going slightly tilted towards southwest through the Eastern European Plain, Moldova, southeast Romania and northern Bulgaria to the eastern foothills of the Balkans. The northern fringe is slightly influenced by last glacial ice advances. Southwards, the vast and flat East European Plain adjoins (subdomain Ib), where loess and loess derivates are found in large extents. These are intersected by the large river systems of the Dnieper. In subdomain Ib and IId, the area was strongly influenced by ice advances of the penultimate glacial (MIS 6). The loess sequences in this area show in some cases intercalations of glacial sediments (Lindner et al., 2002). The Moldavian Plateau south of the Dniester is heavily intersected by fluvial erosion. It was still influenced by discontinuous permafrost during the LGM and shows a hilly relief. Further to the south, the Lower Danube Basin with its flat topography and vast extents of aeolian deposits is located (domain V). Within the foothills of the Balkans, loess only occurs in patches within depressions and basins.

3.3. Statistical analysis

In Europe more than 1 Mio km² are covered by loess and loess derivates, ~72,000 km² are covered by aeolian sand and sandy loess deposits, and ~500,000 km² in the map shows alluvial fill and fluvial deposits (Tab. 1). Loess and loess derivates cover vast areas of subdomains Ib, IId, and domain V, while most of the aeolian sand and sandy loess is shown in domains Ia, IIa, IIId and IV, while in other subdomains none are mapped. Large areas of alluvial fill and fluvial deposits cover domains I, IId, IIId, V, and VI.

Table 1: Surface statistics of the distribution of loess and selected Late Pleistocene sediments in Europe (Figure 2) per domain and subdomain.

Domain & subdomain	**Surface area [km²]**		
	Loess & loess derivates	Aeolian sand & sandy loess	Alluvial fill & fluvial deposits
I	248,379	14,769	137,794
Ia	1,875	14,769	59,735
Ib	246,504	0	78,059
II	453,713	20,457	116,767
IIa	46,718	16,723	27,067
IIb	18,813	1,624	9,180
IIc	21,316	0	15,776
IId	351,082	509	54,865
IIe	15,784	1,601	9,878
III	53,249	15,563	79,232
IIIa	3,295	0	10,936
IIIb	9,955	987	10,131
IIIc	7,297	92	18,182
IIId	29,075	14,245	33,952
IIIe	3,626	239	6,031
IV	60,428	17,140	36,754
V	245,978	1,588	45,810
VI	17,916	2,843	81,887
VIa	2,532	2,843	45,323
VIb	13,276	0	28,245
VIc	2,108	0	8,319
Total	1,079,663	72,359	498,244

Figure 15 indicates that loess and loess derivates are distributed up to an elevation of 1307 m a.s.l.. While half of the loess in each subdomain is clustered in a narrow elevation band for most domains, the subdomains of domain VI show very broad distributions. Especially the upper limit was often very far from the mean values, which is a reason why we only show 98% of the distribution (considering that small misalignments between the loess distribution and the DEM with a resolution of ~30 m might lead to big differences in steep terrain). The highest elevation is found in domain VIc with 1307 m.

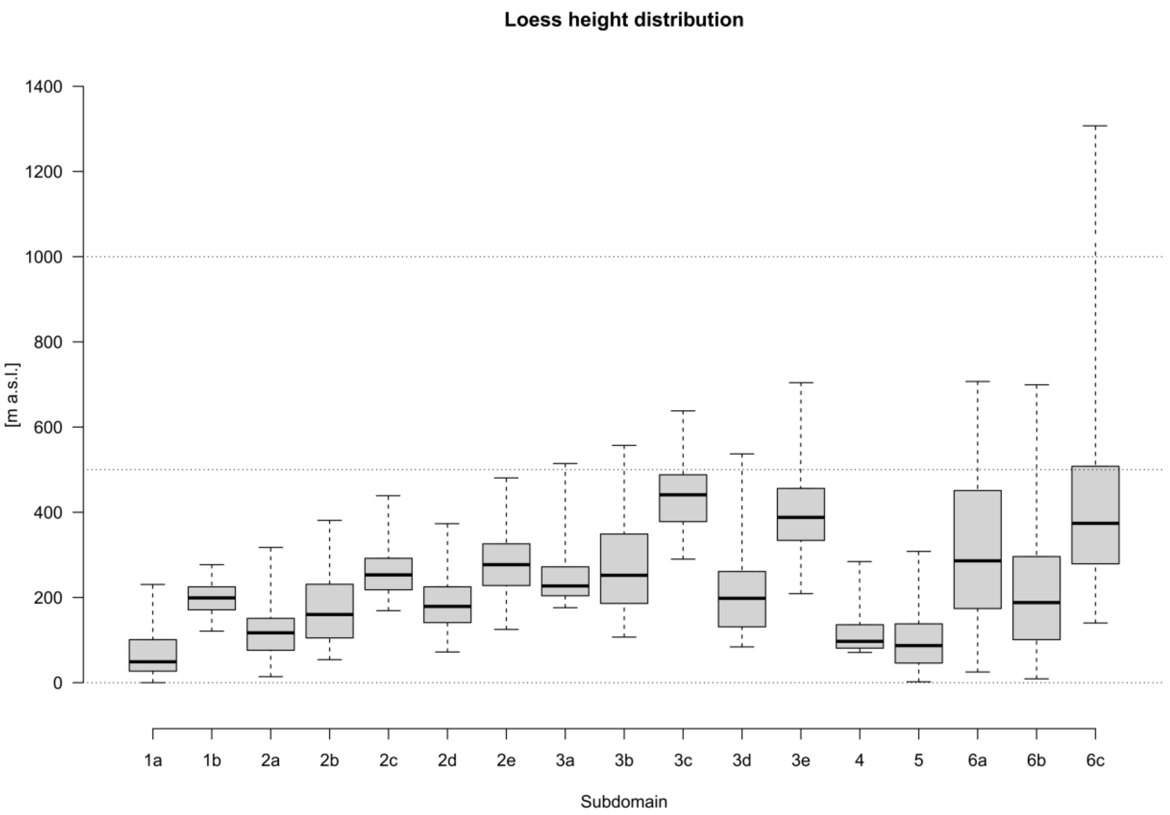

Figure 15: Box plots of the elevation (ordinate) of loess and loess derivates in Europe per subdomain (abscissae). To exclude extreme outliers, the upper and lower limit in the whisker was set to 1% (cf. Supplementary Tab. S3).

It is evident from Figure 16 that the sediments are not normally distributed in their height. While some subdomains such as domain IV show a very narrow height distribution, most of the loess is spread over several hundred m a.s.l. The broadest spectrum is observed in domain VI where loess and loess derivates are found between 25 m and 1307 m. Domain IV shows a very sharp lower boundary of loess distribution that is likely related to the flat landscape in the Carpathian Basin. In domain II, subdomains IIa and IIb show a similar distribution, as do IIc and IIe. Some subdomains can be almost distinguished by their height (e.g. Ia and Ib), but usually there is quite some overlap (IIIa, IIIb, IIIe).

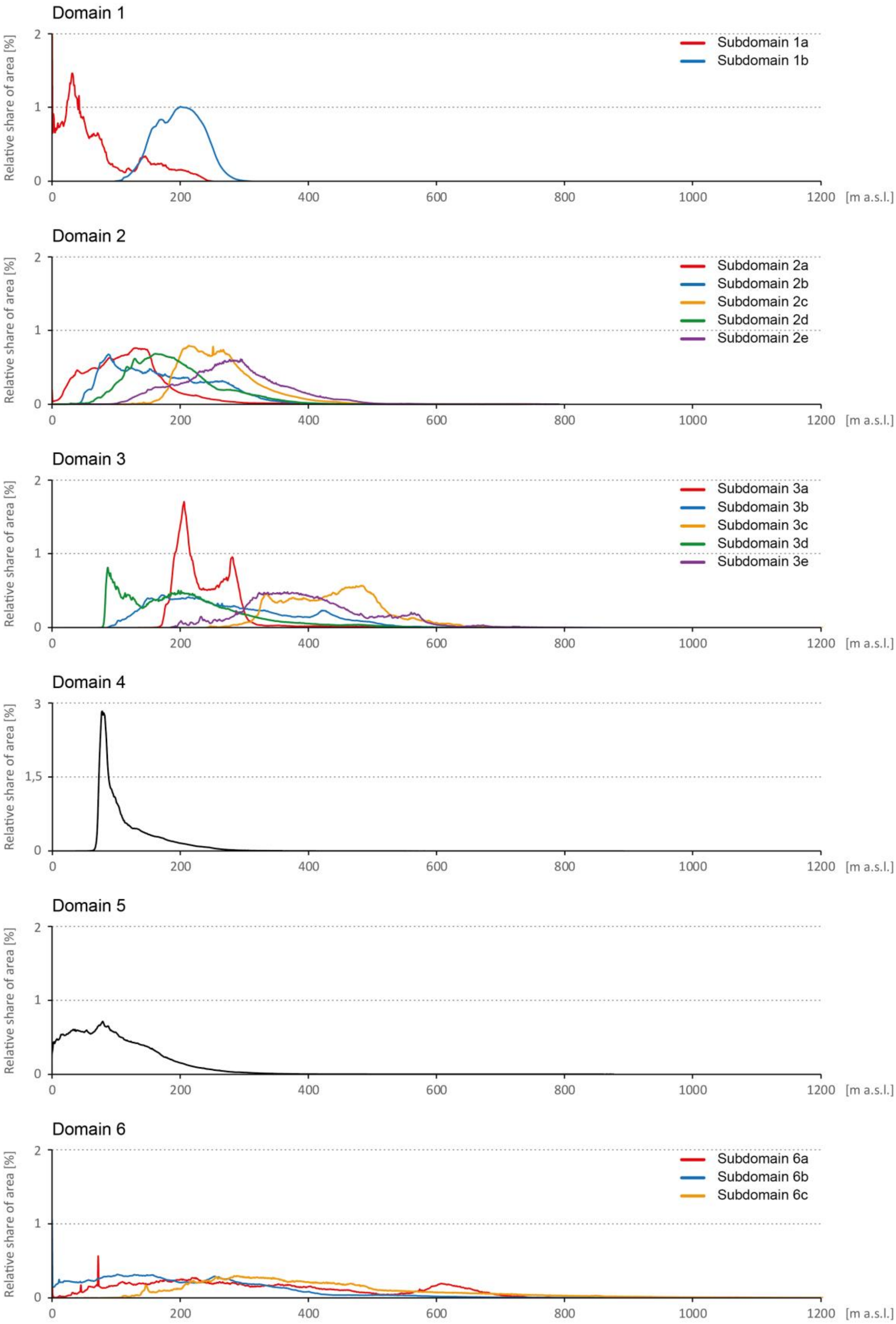

Figure 16: Frequency distributions of the elevation of loess and loess derivates per main and subdomain. The ordinate shows the relative proportion of each elevation that is depicted on the horizontal axis. A color legend is given for the subdomains. Note that the ordinated of domain 4 uses a different scale.

4. Discussion

4.1. Comparison to other methodological approaches

Maps of the distribution of aeolian sediments in Europe, either on a regional or continental scale, were compiled for almost a century (e.g. Antoine et al., 2003; Bertran et al., 2016; Fink et al., 1977; Fink and Nagl, 1979; Flint, 1971; Grahmann, 1932; Haase et al., 2007; Lehmkuhl et al., 2018a, 2018b; Lindner et al., 2017; Zerboni et al., 2018). Especially the pan-European approaches are widely recognized and used as a basis for geospatial analysis and interpretation (e.g. Buggle et al., 2013, 2008; Fitzsimmons et al., 2012; Franc et al., 2017; Iovita et al., 2012; Lehmkuhl et al., 2016; Nawrocki et al., 2018; Sprafke and Obreht, 2016). Besides mapping approaches based on geological and pedological data or field observations, potential dust emission and deposition areas can be determined using numerical models (Schaffernicht et al., 2020; Sima et al., 2009). In the following subchapters, we compare our map to the most widely used European loess map by Haase et al. (2007), which combined several existing data sets and a more recent approach by Bertran et al. (2016), where the distribution of aeolian sediments was derived from topsoil data. Finally, we discuss our data with the results of the model-simulated dust deposition by Schaffernicht et al. (2020).

4.1.1. Comparison with the map of Haase et al. (2007)

One of the most commonly used maps of European loess is the one provided by Haase et al. (2007). This map has a resolution of 1:2,500,000 and is based on data compilation carried out in the 1970s, 1980s and the 2000s. This collaborative effort was carried out by the INQUA Loess Commission under guidance of J. Fink. Similar to our approach, the Haase map is based on digitizing paper maps from numerous authors. This led e.g. to artificial breaks along borders, and the persistence of locally separated loess classes such as the alluvial loess in Hungary. Additionally, important loess areas, such as the whole Paris Basin, were not mapped by this approach. Figure 17 includes different categories of aeolian sediments and compares the results of this study with the well-established map of Haase et al. (2007). Differences occur e.g. in north-central France, where some sandy loess and loess derivates are mapped that are not included in our new map. A possible explanation for these discrepancies can be the fact that in France the loess with a minimum thickness of one meter was mapped. For our study, the minimum thickness usually was two meters. These differences are also observed in southern Germany, Austria and Slovenia. Haase et al. (2007) included discontinuous and thin loess sediments in their map (cf. Fink and Nagl, 1979), leading to a more widespread loess distribution. Furthermore, some sandy loess and loess derivates in eastern Germany and southwestern Poland are mapped by Haase et al. (2007), which do not occur in our map. In these areas, loess is often incorporated within loamy and sandy sediments. These polygenetic deposits were not mapped by our approach.

In the southwestern Carpathian Basin, striking differences between the two mapping approaches are visible. This may be due to the uncertain data situation for the area. Most Quaternary deposits are mapped as “Quaternary in general” in the geological map of former Yugoslavia (Federal Geological Institute, 1970), without further differentiation (Lehmkuhl et al., 2018a). This data was used in prior mapping approaches. Our new map includes the newest data from the Croatian geological survey (Croatian Geological Survey, 2009), which have not been available e.g. during data acquisition for the map compiled by Haase et al. (2007). This might explain the differences between the two data sets. Minor differences are found in the southern Lower Danube Basin, as well as the western part of Ukraine and parts of the western Crimea.

Areas that are mapped in our loess map that are not present in the map by Haase et al. (2007) are a consequence of different source data or the combination of aeolian sand and sandy loess in our map. This includes areas in Spain, southern France, Italy, and coastal Croatia, which were not mapped before due to their small extent (Haase et al., 2007). Aeolian sediments in Great Britain and the Netherlands have not been mapped by Haase et al. (2007), but have been included here. Some differences occur in the Central German low mountain ranges, Czech Republic, and southern Poland. These areas are influenced by e.g. slope processes, which can rework loess. We excluded data concerning reworked loess deposits (see Lehmkuhl et al., 2018b), since regional differences hamper a consistent mapping of these sediments. Differences in Hungary are related to the combination of aeolian sands and sandy loess in one unit in our map. In Romania on the other hand loess deposits were not mapped in detail in geological maps. Therefore, the map presented here is based on an approach that uses pedological maps (Lindner et al., 2017) and thus shows different loess distribution patterns. Haase et al. (2007) used a global stream network based on the grid cell boundaries of the GLOBE DEM (Hastings et al., 1999) to extract alluvial plains from the loess distribution. Since this DEM has a resolution of 1 km it is less precise than the pedological map we used in Ukraine (Sokolovsky et al., 1977b), leading to differences between both maps. Generally, we propose that our new map is more precise because in some areas updated maps were used, all data were critically checked by local experts, and our maps has a higher resolution. Nevertheless, it remains challenging to generate an absolutely accurate map since it is impossible to validate the loess distribution in all regions in detail.

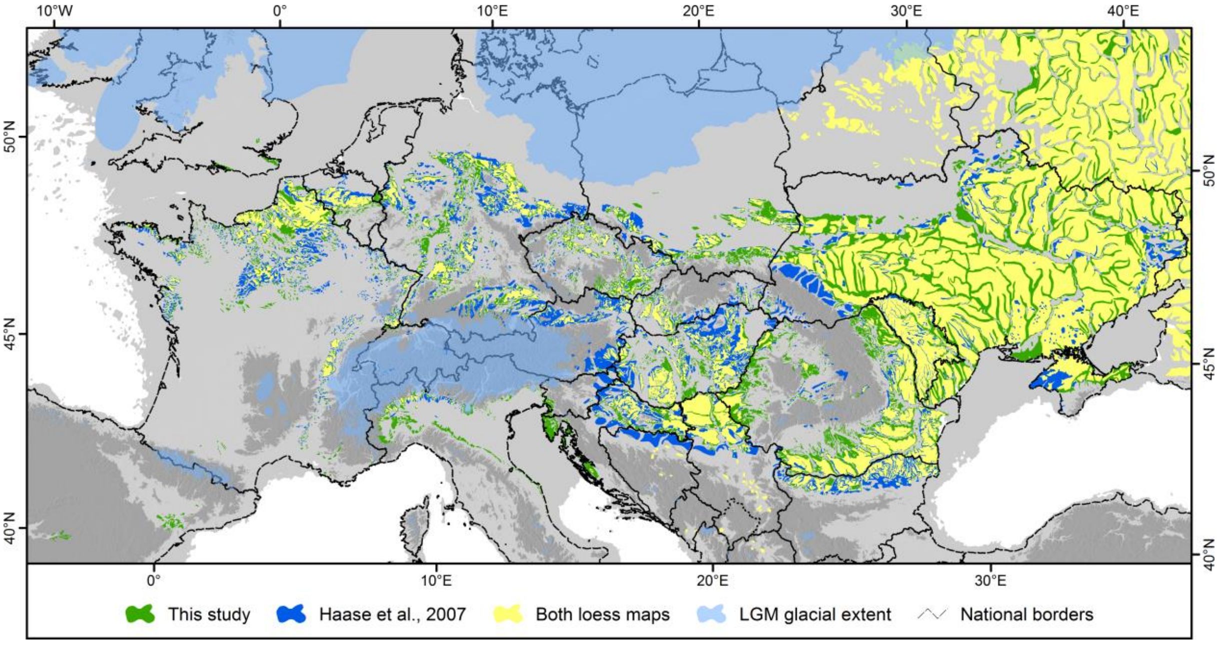

Figure 17: Comparison of our new European loess map to the mapping approach from Haase et al. 2007. Similarities are shown in yellow. The distribution of loess, sandy loess and aeolian sand, and loess derivates that are only evident in our map is depicted in green, while the distribution of loess, loess derivates, sandy and alluvial loess that is only present in the Haase map is shown in blue. The extent of glaciers (Ehlers et al., 2011) and the dry continental shelves (Willmes, 2015) during the LGM are depicted.

4.1.2. Comparison with the mapping approach of Bertran et al. (2016)

Since this study is based on a multitude of geological, geomorphological, and pedological maps (see Chapter 2.1), the detection, removal and smoothing of artificial breaks was one of the main issues. Other recent approaches to map aeolian cover sediments used continuous, European Union wide data. Bertran et al. (2016) used the topsoil textural data from the Land Use and Cover Area frame Statistical survey database (LUCAS, Orgiazzi et al., 2018; Tóth et al., 2013) to extract information about the grain size distribution within the soils and therefore their parent material. The information about clay, silt and sand content were extracted, set in relation and validated for various areas in France and Belgium (Bertran et al., 2016).

In general, the result of our study is comparable to the approach by Bertran et al. (2016). It is, however, obvious that the aeolian sediments mapped by Bertran et al. (2016) cover larger areas. This is especially the case in northwestern France, northern Belgium, the Central German low mountain ranges, southeastern Austria, eastern Slovakia, Transylvania, the eastern Carpathian foreland, southwestern France, northern Spain and the Po plain (Figure 18).

The differences between the two approaches are due to manifold reasons. One of them is due to differing mapping approaches. While the LUCAS database is based on data from top soil samples (Orgiazzi et al., 2018; Tóth et al., 2013), this study is based on inter alia on geological maps. Geological maps usually exclude the uppermost one to two meters below the surface. Therefore, this approach can be expected to miss some of the thin loess and sand covers thinner than one or two meters. This is especially the case in subdomains Ia and IIa. The underrepresentation of aeolian sands, e.g. in northern Germany, is also due to the exploration depth of geological maps, since the thicknesses of these covers are in many cases less than two meters and are therefore not mapped in geological maps (cf. Lehmkuhl et al., 2018b).

As a result of the processing of the LUCAS data set, Bertran et al. (2016) classified aeolian sediments in Europe in four categories: loess, colluviated loess, silty sand and cover sands. These categories were set by combining the different grain size classes from the data set. The differing classification of aeolian sediments by this approach compared to our study hampers a direct comparison of all classes. Therefore, we only compare the classes loess and colluviated loess from Bertran et al. (2016) with the class loess and loess derivates from our study.

Vast covers of colluviated loess are mapped in some areas, such as basins within the Central European low mountain ranges (Figure 18). Colluviated loess is also mapped in e.g. geological maps in Germany (so-called 'Umlagerungsbildungen' or 'Schwemmlöss'; Lehmkuhl et al., 2018b), but their nomenclature is not consistent throughout Europe. Additionally, colluviated loess is usually not mapped in soil maps. To avoid issues and inconsistencies, we disregarded the direct mapping of every form of relocated aeolian sediments. Nevertheless, the class is included in the comparison since it overlaps largely with loess derivates in many regions.

The differences are most striking in the Central European mountain ranges and the Transylvanian Basin. The foothills of e.g. the Ore Mountains, the Sudetes, the Tatra and the Carpathians are affected. Within these regions, the differences are mostly due to mapped colluviated loess. In eastern Slovakia, however, there are vast areas of loess mapped by topsoil data, which were not included in geological maps. There are some areas where the mapped colluviated loess is congruent with loess and loess derivates. The loess deposits of these areas, e.g. the Moldavian plateau and the upper reaches of the Danube River, were mapped as colluviated loess by Bertran et al. (2016) and as loess and loess derivates in this study. Generally, the areas of colluviated loess according to Bertran et al. (2016), which were not mapped by our approach, correspond to areas in which the loess deposits are located in high elevations, compared to their surroundings.

Some inconsistencies between this study and Bertran et al. (2016) are noticeable especially within the Mediterranean realm and the coasts of Normandy and Brittany in northern France. In the Ebro basin in northern Spain and the Po plain in northern Italy, large areas of (colluviated) loess were mapped. This may be due to substrates with a similar granulometric signature as loess, such as weathered marls (Bosq et al., 2018). In studies following Bertran et al. (2016), the thresholds for loess mapping were therefore adjusted (Bosq et al., 2018).

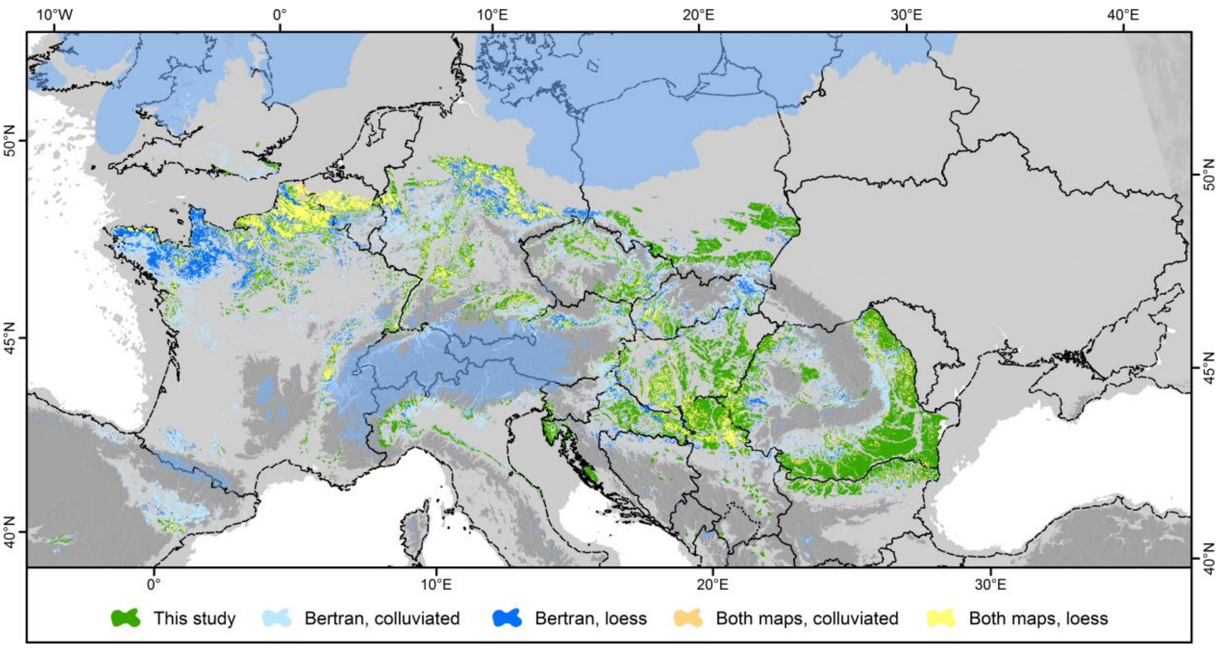

Figure 18: Comparison of our new loess map to the mapping approach from Bertran et al 2016. Please note that only data from the European Union was included due to the extent of the base data. The extent of glaciers (Ehlers et al., 2011) and the dry continental shelves (Willmes, 2015) during the LGM are depicted.

4.1.3. Comparison of the new European loess map with an atmospheric LGM dust model of Schaffernicht et al. (2020)

Here, we compare our map with the recent work by Schaffernicht et al. (2020) presenting an LGM dust cycle model of Europe. According to this study, most of the dust emission occurred in a zone between the Alps, the Black Sea and the southern margin of the ice sheets. Within this zone, the highest deposition rates were located near the southernmost ice sheet margins in domain I and II. Westwards relocation via dust plumes resulted in high modelled deposition rates in western Poland, northern Czech Republic, the Netherlands, the southern North Sea region and northern and central Germany (Figure 19). Relatively high dust production is mainly in domain I in front of the ice sheet margin, while loess accumulation occurred mainly in domain II suggesting the role of higher vegetation density southwards.

Figure 19 compares the atmospheric dust deposition of the dust cycle model (Schaffernicht et al., 2020) with the loess distribution and main domains established by this study. The dust deposition was modelled using a regional climate-dust model. However, this atmospheric dust modeling approach took only (far traveled) dust with small-sized particles of up to 20 µm diameter (fine- to medium silt) into account, while loess deposits mainly contain coarser silt particles. The modeled deposition rates from Schaffernicht et al. (2020), however, are in some contrast to the observed thicknesses of the loess deposits (Figure 19). The thickest loess deposits occur in central-eastern and southeastern Europe and not in the areas with the highest modeled rates. These differences can probably be explained by the degree of preservation. Differences in domain I could be due to insufficient vegetation cover that traps dust in the direct vicinity of the ice margins. Reworking, erosion and relocation of sediment is also present in the periglacially influenced regions of northern Europe. The model also indicates high deposition rates for high mountain areas, which is due to the consideration of only fine silt, since coarse silt is rarely transported to mountainous areas by wind.

Nevertheless, the model can be used to understand the atmospheric circulation patterns and the preservation potential of the different domains, although numerical models, due to their nature of being models, can never constitute complex natural process chains such as the uptake, transport and deposition of aeolian dust in appropriate spatial and temporal resolution. Large-scale models cannot display e.g. short term shifts in atmospheric circulations or sediment availability, which are indeed an important factor in dust deposition and loess formation (Antoine et al., 2009b).

In contrast to the current climatic situation, during the LGM winds from northeast, east and southeast and cyclonic regimes prevailed over central Europe. While potentially a lot of dust deposited within domains I-III, the preservation potential especially in domain I was very low. The continentality and aridity, presumably coupled with appropriate dust traps (e.g. certain vegetation) in domains Ib, IId, IV, and V probably lead to the loess preservation we see in those regions today. However, it should be emphasized that in most climate models the coarse dust as observed during dust fall (Goudie, 1983; Jarke, 1960; Schütz, 1980) is not considered (Adebiyi and Kok, 2020). Additionally, the dust cycle model by Schaffernicht et al. (2020) only includes atmospheric variations during the LGM, whereas dust deposition occurred (sub-)continuously during the last glacial-interglacial cycles, while the hydroclimate fluctuated significantly.

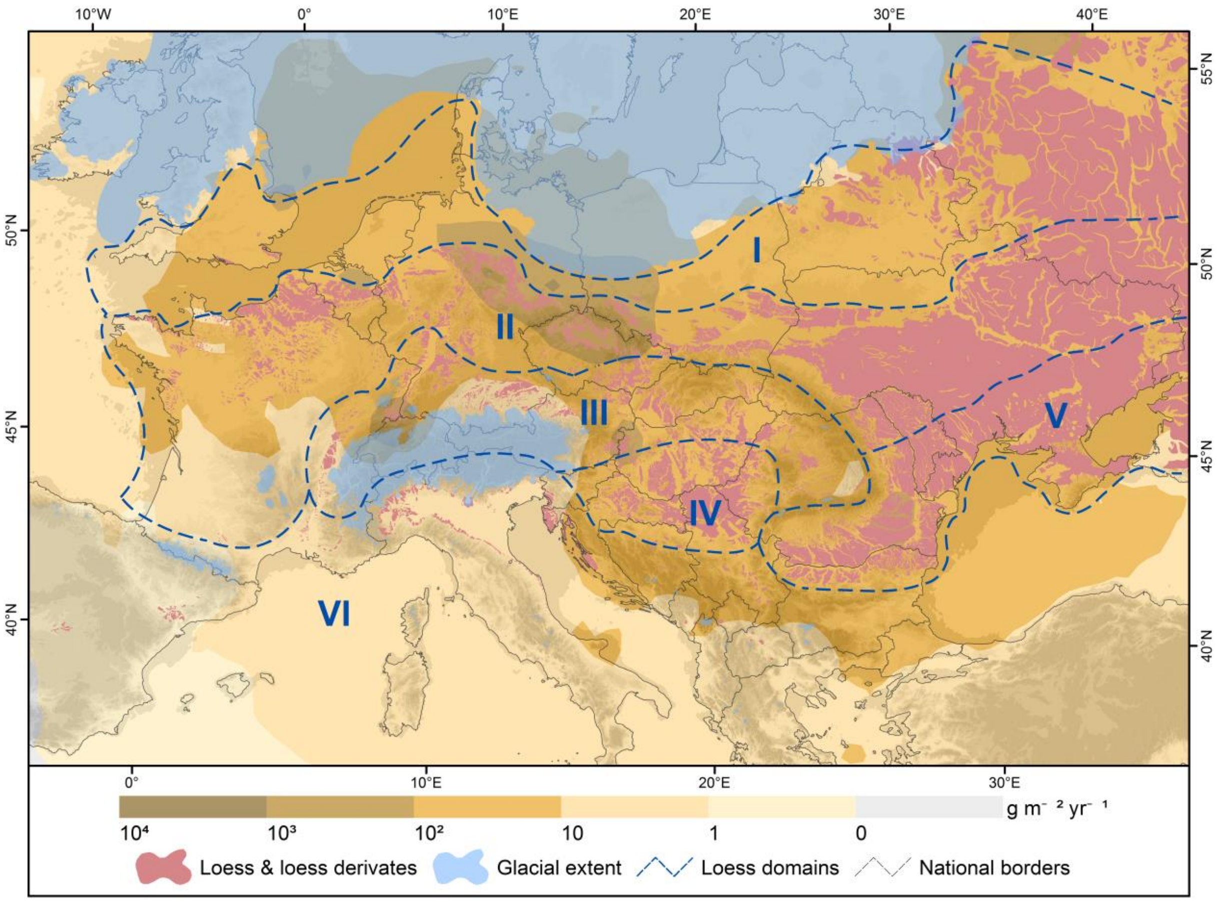

Figure 19: Dust deposition rates for the LGM according to modelled data from Schaffernicht et al. (2020). The dust deposition rates comprise particles of up to 20 µm diameter (FD20) using a dynamic downscaling (FD20 DD). Distribution of loess as well as the boundaries of the main loess domains are given for comparison.

4.2. Discussion of the distribution of loess in Europe

Loess, loess derivates, sandy loess and aeolian sands are widely distributed throughout Europe. In domain I, between the ice sheets and the northern boundary of the European loess belt, patches of loess-like sediments, sandy loess, and widespread sand sheets (cover sands) appear. The boundary between the protogenetic zone and the northern European loess belt is in most regions clearly marked by the transition of sandy loess or sand sheets towards loess. Transitional zones can be found in northern France, Belgium or the Lower Rhine Embayment in Western Germany (subdomain IIa; see Vandenberghe in Schaetzl et al., 2018). In the central parts of domain II, a sharp and clear boundary of the loess distribution occurs - the loess-edge ramp (subdomain IIb, see Figure 9). These marginal steps vary in spatial distribution and shape inter alia due to the influences of and distance to the extending ice sheets. The main distribution of loess within domain II is located at the northern front of Central European low mountain ranges mainly between 105 to 231 m a.s.l (subdomains IIb).

Domain II and III are strongly influenced by periglacial processes and permafrost. The loess accumulation took place in many cases at downwind positions, creating asymmetric valleys (e.g. Figure 6) and covering fluvial terraces (e.g. Figure 12). The influences of periglacial processes gradually diminished southwards and finally disappear. For example, in the Rhône area of subdomain IIIa there is a gradual transition towards domain VIa, where Mediterranean conditions prevailed (Bosq et al., 2020a, 2020b). A similar shift occurs in the Carpathian Basin between domain IIId and IV as well as further east between subdomain IId and domain V in the Eastern European lowlands. These transitions are characterized by increasing temperate to humid subtropical climate conditions with more intensive weathering and soil development in southwestern and southern Europe and to a more semi-arid desert margin environment with lack of humidity in the eastern and southeastern parts of Europe, respectively. In domain IV and V, loess dust accumulation occurred in plateau situations. Due to the local depositional conditions and relative extensive erosional processes, these plateaus were incised by the lowland rivers and are nowadays preserved between the alluvial plains of these rivers. They represent the most complete records of Quaternary paleoclimate and paleoenvironment in Europe beside few lake records. These plateaus are described in the literature (e.g. Marković et al., 2016; Smalley et al., 2011) and their genesis is discussed e.g. by Florea (2010).

The distribution of sand and sandy loess in the domains I and II differs from those e.g. in other domains. Generally, aeolian sands are transported by strong wind systems over short distances. In domain I and II, however, sands are deflated from the outwash plains and other sandy sediments related to Mid-Pleistocene (Saalian and Elsterian) ice extents, as well as (Early) Weichselian deposits. In other loess domains, such as the peri-alpine river valleys (IIIa-c) or Eastern Europe (V), aeolian sands originate from the deposits of larger rivers (e.g. Rhône, Rhine, and Danube River in subdomain III and VI; Dnieper and Dniester in domain V). The Danube River and its tributaries in the Carpathian Basin e.g. provide large quantities of silty and (fine) sandy material. When this material is deflated and subsequently deposited, a complex sedimentary pattern of loess, sandy loess and aeolian sands develops. In this pattern, it is difficult to distinguish between aeolian sand and sandy loess. Therefore, and due to their similar genesis, we combined these two categories in one unit. Nevertheless, one needs to be aware that this is not the case in domain I, e.g. in Northern Germany, where sands, sandy loess and loess are clearly separated. Aeolian sands occur parallel to the ice margin, whereas the northern boundary of loess distribution is further south. Between these two boundaries, sandy loess is found.

Throughout Europe, loess is mostly distributed in the basins and lowlands (northern France, Belgium, Germany, Czech Republic; up to 600 m a.s.l.), the foothills of the Central European low mountain ranges (e.g. Central German low mountain ranges, Carpathian promontory, Fruška Gora Mountains, mainly below 200 m a.s.l.), and in favorable geomorphological settings, e.g. the larger valleys of the Rhône River and upper Rhine River (mainly below 300 to 400 m a.s.l.). In higher elevations, silt-sized particles of aeolian origin are usually mixed with periglacial cover beds building the upper cover bed (Lehmkuhl et al., 2016; Semmel and Terhorst, 2010). In the European Alps, Gild et al. (2018) used the term drape for aeolian mantles in the western part of the Northern Limestone Alps. They described drapes as aeolian covers of a few decimeters in thickness covering different bedrock and Pleistocene sediments. They are slightly modified by initial soil formation and late glacial in age. These drapes have also been described along valleys of the Italian Dolomites (Cremaschi and Lanzinger, 1987, 1984). Usually no or only very limited typical loess deposits occur in the Pleistocene polar deserts in northern Europe of domain I, high-mountain areas or south of the Pleistocene timberline.

The distribution of aeolian sediments is mainly controlled by sediment availability, prevalent wind directions and the presence of suitable dust traps. The sediment availability is dependent on the distance to potential source areas such as larger river systems (e.g. Smalley et al., 2009; Smalley and Leach, 1978), dry shelves (Antoine et al., 2009a) or glacio-fluvial outwash plains of ice sheet margins (e.g. Antoine et al., 2016; Lehmkuhl et al., 2016; Pye, 1995). The vegetation density in the source areas also governs the amount of dust, which can be deflated, since vegetation acts as a dust trap and fixes the sediment. It is obvious that the distribution of loess is closely linked to the distribution of these source areas (Figure 2). The vastest and most prominent loess deposits occur south of the ice margin and along large rivers, where during the Quaternary large amounts of sediment were available with no or very spare vegetation covers.

The local geomorphological setting of sink areas strongly influenced the distribution, preservation and thickness of loess sequences. Several depositional settings such as plateau and interfluve loess, slope loess, colluvial (slope toe) loess, loess sedimentation in depressions and erosion channels (valley loess) were distinguished (see Lehmkuhl et al., 2016 and references therein). Higher accumulation rates were observed e.g. in depressions or on lee sites of topographic barriers, according to the prevailing wind direction (e.g. Figure 6, Antoine et al., 2003). The best developed loess sequences are generally preserved in sediments traps formed by the intersection between alluvial terraces and slopes in stepped terraces systems as in the valleys of Dnieper, Danube, Rhine and other large rivers in Europe (see examples in Figures 6 and 12; e.g. Kukla 1977, 1978). The most thoroughly investigated loess sequences and related archeological findings in the northern parts of Europe are in slope toe or plateau situations. (Lehmkuhl et al., 2016). In domains IV and V dust sedimentation on plateaus is considered continuous since the Middle Pleistocene (Basarin et al., 2014; Marković et al., 2015). The LPS of those deposits can be correlated with the LPS of the Chinese Loess Plateau (Zeeden et al., 2020, 2018).

To summarize, loess in Europe was formed, preserved, overprinted, reworked and relocated through a multitude of different geomorphological, sedimentological and pedological processes. These variations and differences are the results of a complex interplay of paleoclimate, paleoenvironment and geomorphology. Additionally, there is a strong dependence on the distance to the ice sheets and local source areas ((glacio-) fluvial, alluvial, dry shelves), as well as prevailing paleo-wind systems. These conditions control dust accumulation, pedogenesis, preservation, and syngenetic and subsequent erosional events (Maruszczak, 2000; Smalley et al., 2011; Sprafke and Obreht, 2016).

4.3. Discussion of the genesis of loess in Europe

There is a multitude of approaches to differentiate the genesis of loess deposits. Two main directions developed within the centuries: the sedimentological (geological) approach and the pedogenetic one (e.g. Smalley et al., 2011; Smalley and Obreht, 2018; Sprafke and Obreht, 2016). Whereas mainly Pécsi (e.g. 1990) developed many criteria for a loess definition from the latter direction, others like Pye (1995), used a more simple definition for loess as wind-blown dust (see the summarizing discussion in Smalley et al., 2011). Besides the definition of loess itself, which is still under discussion (Sprafke and Obreht, 2016), different modes of loess genesis are described in literature. Muhs and his co-workers summarized, developed and focused on models of "glacial loess" (cold loess, higher latitude loess) and "desert loess" (warm loess) formation (Lancaster, 2020; Muhs, 2013; Muhs and Bettis, 2003; Schaetzl et al., 2018; Wright, 2001). Lately, Li et al. (2020) suggested three modes for the global loess genesis: continental glacier provenance-river transport, mountain provenance-river transport, and mountain provenance-river transport-desert transition.

However, there is not only the "glacial loess" versus "non-glacial" formation in Europe. The main factors for loess formation are the amount of available dust (Crouvi et al., 2010; Maher et al., 2003) and the degree of humidity (semi-arid to semi-humid conditions) as well as its seasonality. In the more humid regions, pedogenesis dominates especially during the interglacials and amounts of incoming far traveled dust are reduced in volume and immediately trapped and altered by soil formation processes. In the semi-arid regions, however, dust can accrete also during interglacial periods lowering but not inhibiting intensity of soil formation (Constantin et al., 2019; Tecsa et al., 2020; Varga et al., 2016). Additionally, (paleo-) environmental factors play an important role for the accumulation and especially the preservation of dust aggradations. They determine the boundaries of vegetation zones and the permafrost distribution, which in turn influence dust trapping, weathering and erosional processes. A conceptual model of glacial loess genesis for Europe was already proposed by Zeuner (1937). Anticyclonal synoptic patterns controlled by the Scandinavian and Alpine ice sheets and their interplay with westerlies are the main element of this concept, in which strong anticyclonal winds are responsible for dust uptake and transport and tundra/steppe vegetation benefitting from humidity brought in by the westerlies controlled trapping and stabilization of dust. According to various authors, the trapping of dust is mostly related to the vegetation cover (e.g. Danin and Ganor, 1991; Hatté et al., 2013; Tsoar and Pye, 1987; Zech et al., 2013) or biocrusts (Svirčev et al., 2019, 2013). As it is assumed that the most common dust traps are grasses (or possibly biocrusts as part of the steppe/tundra flora), the lack of widespread loess deposits south of the northern timberline during the LGM might be explained by this model. In addition to reduced dust sources, there is increasing pedogenesis towards more humid regions. Therefore, the accumulation of dust and the formation of loess is related mainly to tundra and steppe environments.

However, in any loess deposition, after sedimentation and initial fixation of atmospheric mineral dust particles, first post-sedimentary alteration processes occur (Berg, 1916; Pécsi, 1990; Smalley et al., 2011; Svirčev et al., 2013; Smalley and Marković, 2014). It is a matter of debate whether such processes should be assigned to pedogenic or diagenetic process spheres or to a kind of transition zone (Sprafke and Obreht, 2016). However, there is consensus that the typical structure of a loess deposit is caused by these initial alteration processes, whereby the loess differs from primary airborne dust (Pécsi, 1990; Sprafke and Obreht, 2016; Schulte and Lehmkuhl 2018). Besides the factors influencing the mobilization, transport and sedimentation of the loess e.g. distance to source areas or wind velocity (Újvári et al., 2016; Vandenberghe, 2013, 2018), the post-depositional alterations such as chemical weathering or colluviation also have a considerable influence on the grain size composition of the loess deposits (Schulte and Lehmkuhl, 2018; Újvári et al., 2016). Grain-size distribution of loess can serve as an indicator to distinguish among loess and loess-like deposits (Vandenberghe et al., 2018), and may give insight into different acting processes. Coarser deposits formed e.g. under the influence of stronger wind activities or under the influence of non-aeolian processes, such as slope wash or soil creep. High contents of fine material (clay, fine and medium silt) are the result of large distances to the source region, weaker wind conditions, and / or post-depositional alterations such as pedogenesis (Újvári et al., 2016; Vandenberghe, 2013, 2018; Schulte and Lehmkuhl 2018).

4.4. Conceptual model of loess distribution

Finally, based on our observation in Europe and other loess regions, we suggest a conceptual model of loess distribution, loess formation and loess landscapes. In this model, a triangle of the three main ecozones (nival, humid and arid environments, Figure 20) is used to conceptualize the different modes of loess formation as factors of humidity and temperature, mainly controlling the abundance or absence of vegetation, periglacial processes and glaciers. The extreme nival regions with glaciers and the polar desert including the periglacial zone are at the top of the triangle. The more humid regions (densely vegetated and forested at the extreme end) are on the left side and the extreme arid regions (deserts) are on the right side of the triangle. Please note, that there are gradual transitions between the different environments, also towards the extreme regions at the corners.

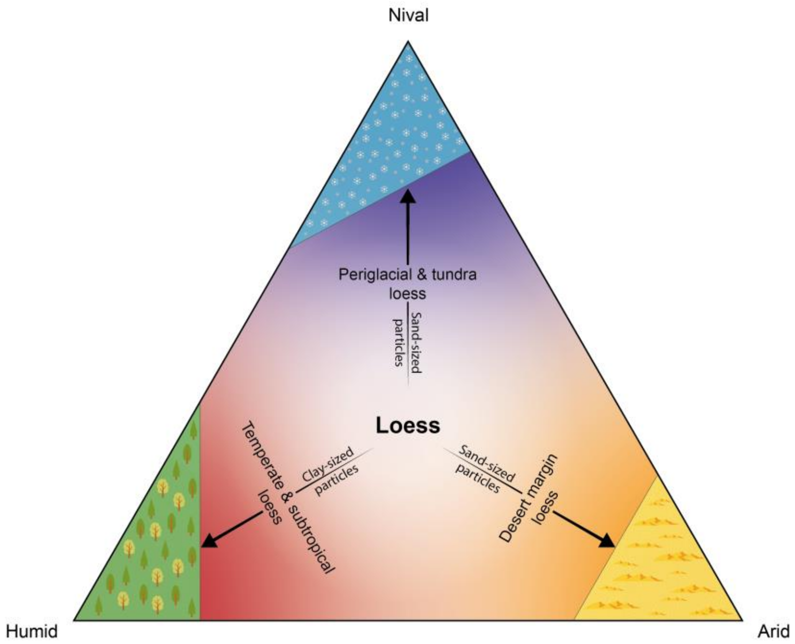

Figure 20: Conceptual model of loess landscapes. Note that the corners represent the extreme end with no loess formation. Top: Glacier with lager extend on the nival-humid axis. Left corner: Forest with larger extend on the humid-nival axis. Right corner: Deserts.

Loess, as predominantly silt-sized aeolian sediment, can have different sources. As loess is found in different environments, a single genetic path cannot explain all loess occurrences. Here we introduce a model that tries to separate loess towards three genetic environments. Typical loess is situated in the center. We propose main loess formation in a balance between nival, humid and arid ecozones and environments.

Permafrost and periglacial environmental conditions, such as the ones found today in the northernmost regions and high mountains of Europe, are indicated towards the top of the triangle (nival regions = glaciers at the extreme end; they have larger extent on the nival-humid axis). These environments included deep freezing during the winter season and freezing-thawing cycles, which influenced the geomorphological and pedogenetic processes resulting in paleosols such as tundra Gley soils (gelic Gleysols) also occurring in loess environments. Fluvial erosion and slope processes (slope wash, sheet flows, solifluction) are enhanced during glacial and periglacial climates. Desiccation due to low temperatures and frost enhanced the availability of small-sized particles (Smalley, 1995). Precipitation mainly occurred as snow during the cold season. This produced high meltwater discharge with its maximum during summer in glacial regions and/or during springtime in periglacial regions, respectively. This resulted in large braided river systems, which fell dry in late summer to autumn and during wintertime. During low water stands, floodplains acted as important sand and silt source areas, especially in autumn (Sima et al., 2009; Smalley et al., 2009). Material from glacial grinding and frost weathering in particular lead to the silt production and accumulation in the floodplains during high discharge seasons (in Europe mainly in the Pleistocene). Therefore, small-sized particles were available but also sands, especially close to rivers, are still found. In general, the dominance of coarse grain sizes (sand-sized particles) increases toward the polar and glacier region. The transport and relocation depended on the humidity, which enforced relocation by slope wash and solifluction. Li et al. (2020) proposed the continental glacier provenance-river transport and mountain provenance-river transport modes for such environments. Although loess-like sediments and loess derivates formed in these environments, the lack of a stabilization process as observed in more arid regions and prevalent geomorphic conditions have caused discordances and hiati. Such loess deposits are very characteristic for domains I – III and mostly formed during cold stadial conditions. Sometimes nivo-aeolian features formed under more humid conditions (depicted as diagonally shaped triangle edge). Other deposits outside of Europe also fall in this part of the conceptual model. For example, the ultimate member on the nival-arid axis are arctic ice silts known as Yedoma deposits. They are found in the permafrost landscapes of Beringia (Central and Eastern Siberia, Alaska and Northern Canada) and contain ice-saturated or supersaturated silt and fine sand sediments (Strauss et al., 2017). They are characterized by a segregation ice content of 30-40% and syngenetic ice wedges (Strauss et al., 2017). Several hypothesis concerning their genesis have been proposed. Researchers working in the Yukon area and Alaska often characterize Yedoma silts as loess or re-transported loess (Péwé, 1955; Sanborn et al., 2006). According to Schirrmeister et al. (2013), a polygenetic hypothesis with a distinct aeolian input is the most popular in the recent scientific literature. Strauss et al. (2017) posed the opinion that the loess and polygenetic concepts could be merged, if the re-transportation of loess (also called secondary loess) is included in the loess concept. We suggest that parts of domain I and IIc-d were influenced by such nival-arid conditions during the Pleistocene. In the Carpathian Basin and eastern Europe there is a gradual transition from the periglacial loess landscapes toward the steppe loess regions (domain III to IV and IId to V, Chapter 4.2) more in the center and right side of the triangle.

The lower right side of the triangle depicts the loess deposits in arid and semi-arid region, e.g. domains V and VIc. These deposits range from silty loess towards more sandy loess in the direction of increasing aridity. The nival-arid axis is distributed more towards the continental areas (domains Ib – IId – V) whereas the humid-arid axis is the transition from domain IV to V. Especially domain IV and the western part of domain V are situated more the center of the triangle. Desert environments are located at the extreme end and are strictly speaking not found in Europe, but it is debatable if some deposits e.g. in Spain and southeastern Europe, were formed under arid and desert margin conditions. In these landscape, dry riverbeds and exposed lacustrine deposits act as source areas for aeolian deflation also for mid- and long-distance transport of silt-sized particles. While in the center of the triangle, that depicts 'typical' loess, continuous and silt-sized dominated loess formation take place (e.g. domain IV, most parts of V), a gradual increase in the contribution of sand-sized particles toward the arid corner is observed. Beside the proximity of source areas (e.g. large streams in Europe; e.g. Jipa, 2014) also a reduced vegetation cover lead to the formation of sandy loess deposits and sand formation especially at the desert margins of the world (e.g. Central Asian deserts, deserts in China). This transition towards the desert margin loess can be found e.g. in eastern and southeastern Europe towards Central Asia (e.g. Sea of Azov (Chen et al., 2020), and Caspian Lowlands (Wei et al., 2020), where the fine and medium silt content of LPS is increased pointing to a contribution of far traveled dust. Moreover, a general and continuous contribution of long range transported dust input stemming from desert margins in the Caspian Lowlands and western Central Asia is likely for southeastern European and western Central Asian Holocene and older interglacial soils (Constantin et al., 2019; Jordanova and Jordanova, 2020; Tecsa et al., 2020; Zhang et al., 2020). Please note that there was and still is also a long range transport of aeolian dust from desert regions (Goudie, 1983, 1978; Schütz, 1980), (Goudie, 1983, 1978; Schütz, 1980), which plays an important role in the global climate system (Lancaster, 2020). The significance of modern, recent and Pleistocene coarse silt transport from the deserts of Central Asia towards the Carpathian area as already reported from the northern Black Sea by Jarke (1960) and also from the Saharan desert towards Europe (Costantini et al., 2018; Longman et al., 2017; Varga et al., 2016, 2013) was unrecognized for many years. However, during the last decade this dust contribution was realized for being relevant for the entire Circum-Saharan realm and hence, also for the loess areas of south and southeastern Europe and may be increased during interglacial times when the deserts tend to expand (Muhs et al., 2010; von Suchodoletz et al., 2010).

On the left side of the triangle (humid = forested regions at the extreme end; they have a larger extend on the humid-nival axis), humid temperate and subtropical (including Mediterranean) landscapes occurred, as in the western and southern parts of Europe (domains IIIa, VIa, VIb) and at higher elevations in central-eastern Europe (domains IV, V). The climatic conditions, especially the availability of moisture and secondarily higher temperatures, lead to a denser vegetation cover resulting in morphodynamic stability and increased chemical weathering and soil development. These processes enhanced the in situ formation of clay-sized particles thereby reducing the amount of coarser (silt-sized) particles. Additionally, higher clay contents of more than 20 % and cementation processes hampered deflation (Pye, 1995). This conceptual zone is limited towards its corner by the timberline, since no loess deposits were formed under dense forest. Our proposed temperate and subtropical loess and the paleosols formed within were mainly developed in regions with a distinct dry season (summer or winter, e.g. towards the Mediterranean regions with winter rainfall or in monsoonal regions with summer rainfall). Dust sources in these regions are and were mainly local and smaller in comparison to the other loess landscapes due to the higher vegetation cover and fewer dry river beds.

Such humid loess deposits can be found at the foothills of the Carpathians in the Romanian Banat (Kels et al., 2014), in Transcarpathia (Ukraine) between steppe and boreal forest at higher elevation (Nawrocki et al., 2016). Such setting with changes between more humid loess environments and more typical loess environment is also developed at the upper reaches of the Dniester between the southern margin of the Scandinavian ice sheet and north of the Carpathian Mountains at the transition of the forest refugia in higher altitudes and the tundra environments towards the ice margin (Łanczont et al., 2019). Another example for subtropical loess and soil formation is the Stalać LPS in subdomain VIc (Bösken et al., 2017; Obreht et al., 2016). Last glacial and penultimate glacial paleosols are strongly weathered and the latter are expressed as reddish Cambisols highlighting the occurrence of humid Mediterranean paleoenvironmental conditions during their formation. A similar setting is realized at the foothills of the southern Alps at the transition to the Po-plain (Zerboni et al., 2015). However, humid loess can be found in the subtropical regions of China (see below) and in South America (e.g. Campodonico et al., 2019). A potential example of humid loess could be also the loess from New Zealand, which is characterized by high contribution of clay and very low carbonate content (Smalley, 1971), probably due to dissolution caused by high amounts of rainfall. Nevertheless, we highlight that the formation of such loess is scarce in Europe during the last glacial cycle, where an increase in humidity in temperate and subtropical areas was mostly related to pedogenesis and weathering resulted in accretionary soils. These soils contain only minor amounts of mineral dust and are therefore strictly speaking no proper loess deposits. In these cases, soil formation outpaced dust accumulation.

Finally, primary or typical loess is usually not formed in any of the extreme conditions (triangle corners) indicated in our conceptual model of loess landscape. We propose that this loess formation occurred mainly during colder periods of the Pleistocene. However, in domain IV and partly in domain V these processes continued at least also during the Holocene (Chen et al., 2018; Tecsa et al., 2020; Zeeden et al., 2018). When conditions become fully nival, humid or arid, already formed loess is strongly altered, and the formation of thick and quasi-continuous silty deposit can be still ongoing. However, conditions indicated as extreme in the triangle have a potential to ultimately alter the loess in a way that its silt-sized origin is largely replaced by finer, strongly weathered material. In case of humid and nival conditions loess could be fully altered into soils due to pedogenesis and reduced dust flux or hampered preservation due to vegetation or snow cover. Under extreme arid conditions, the lack of vegetation and biogenically induced loessification can make loess vulnerable to aeolian deflation and other types of erosion. This includes the preferential deflation of silty material, leaving only coarser components in the source areas.

The conceptual triangle also has relevance if used vertically. Towards higher elevation in more humid mountain regions of Europe, we reach a zone of periglacial and glacial dynamics, yet loess formation is quantitatively reduced by the lack of stable surfaces to support long-lasting dust accumulation (see the discussion in Chapter 4.2 of the distribution of loess in the European Alps; e.g. Gild et al, 2018). In addition, in the rather high mountains and plateaus of arid Central Asia, e.g. the Tibetan Plateau and Qilian Shan, mountain loess deposits are found (Lehmkuhl et al., 2014, 2000; Nottebaum et al., 2015, 2014; Stauch et al., 2012; Yang et al., 2020). The uppermost boundary of loess is periglacial loess, whereas the lowermost parts are desert margin loess (described in Nottebaum et al., 2015, 2014). For these regions, there are still debates on the influence of glaciers and deserts in loess formation.

To further test if the conceptual model is applicable to regions outside Europe, we exemplify here the model for the Chinese Loess Plateau. In the Chinese Loess Plateau there is a gradual transition in grain-size from the more humid monsoonal areas in the Southeast (left side of the triangle in Figure 20) towards the semi-arid and arid regions with desert margin loess in the northwest (right side of the triangle, e.g. Bloemendal et al., 2008; Derbyshire et al., 1995; Yang and Ding, 2003). The thick beds of primary loess in western Manchuria (Obruchev, 1945) and in the mountain areas of western China could be placed in the upper half of our triangle towards the nival environments. These loess landscapes are also influenced by periglacial processes and slope wash (top of the triangle). Moreover, in southern China, e.g. in the Sichuan Basin, there is a debate on subtropical and strongly weathered aeolian (loess) deposits (Feng et al., 2014; Yang et al., 2010). This fits well to the subtropical loess landscapes on the humid-arid axis of our conceptual model. Feng et al. (2014) provides evidence that the Chengdu Clay contains aeolian material of possibly local origin. They assume alluvial sediments in the northwestern Sichuan Basin as the major source and transportation of the material by an ancient katabatic wind over a short distance during glacial and stadial periods (subtropical). Even further north of the desert regions of Central Asia we reach another zone of desert margin loess (e.g. in Tajikistan (Ding et al., 2002) or Kazakhstan (Rao et al., 2013)), whereas in northern Mongolia and Siberia periglacial or mountain loess appears (Andreeva et al., 2011; Lehmkuhl et al., 2012, 2011; Muhs, 2014).

4.5. Aspects of mid-Pleistocene loess formation and distribution in Europe

The new loess map of Europe focusses on processes and paleoenvironments of the LGM as reference period, but as climate changes, the conditions for loess formation and distribution within our conceptual triangle are also shifting. This implies changing environments of loess formation through both, space and time. We want to focus here especially on the Middle Pleistocene environments. For example, ice sheets extended further south during the penultimate and older glaciations compared to the last glacial cycle. Figure 21 indicates the extent of the Saalian and Elsterian ice sheets in the northern part of Europe modified according to Ehlers (2011). The extent of Elsterian and Saalian ice sheets was more than 100 km further south in England and more than 300 km further south in the North Sea west of Denmark when compared to the Weichselian ice sheets. Such extent of ice sheets also influenced the different loess domains, since larger areas were covered by ice (such as IIb and partly IIc) and thus the dust deflation and accumulation areas shifted further south. Furthermore, there were enlarged ice dammed and proglacial lakes close to the ice margins during the Middle Pleistocene. For example, Supplementary Figure S3 shows that a 120,000km² large glacial lake in the southern North Sea existed from around 450,000 to 400,000 years ago (Gibbard, 2007). The North Sea area was covered by both, larger lakes and larger ice sheets during the Elsterian. This area of more than 220,000 km² reduced silt production potential greatly. This is particularly relevant since the same area was a very important potential source of dust at other times (e.g. after the "catastrophic" flooding in MIS 12). Especially the larger extent of ice might be the main reason for the limited accumulation of loess in domain II during the time of older glaciations. For example, older loess deposits in northern France are thin non-calcareous and non-typical sandy loess deposits, which accumulated between about 600 and 420 ka close to the former slopes.

During the end of the Middle Pleistocene (between about 380 and 180 ka), sandy loess was deposited in sediment traps such as sinkholes in the chalk bedrock or more frequently as cover sequences on river terraces and has been preserved until today. Its composition suggests a distinct proportion of local sources (i.e. sands from braided rivers). However, the coarse silt fraction, probably from more distant sources (we speculate that the eastern channel was a main source area), increased in frequency over time. Extensive deposition and preservation of calcareous loess over the plateaus and on downwind slopes of the asymmetric valleys (NE–SE exposures) occurred only during the late Saalian stage (MIS 6, ±150–135 ka; Antoine et al., 2016). They are clearly distinguished from older loess by an especially high amount of green amphibole in the heavy minerals assemblages (Meijs, 2002; Pirson et al., 2018).

The unprecedented increase in loess sedimentation at the end of MIS 6 is also observed in Belgium at Kesselt (Nelissen), where the "B loess" reaches a thickness of 6 to 10 m and contains distinct periglacial features (Meijs, 2002). In Germany, some Middle Pleistocene loess layers have also been preserved, especially in the Lower Rhine Bight (opencast lignite mines Garzweiler and Inden, Fischer et al., 2012) and in the Middle Rhine area (East Eifel volcanic field: e.g. Boenigk and Frechen, 2001a, 2001b).

To summarize, due to changing climate and environmental conditions, the accumulation of aeolian sediments was shifting throughout the Pleistocene. Especially during the Middle Pleistocene, sediment dynamics were strongly influenced by the more southward extension of the ice sheets (Figure 21) and by the occurrence of large ice marginal lakes. Both, lakes and ice extent, reduced the dust production areas in the protogenetic domain (I) and thus they also reduced the potential for loess accumulation in domains II and III.

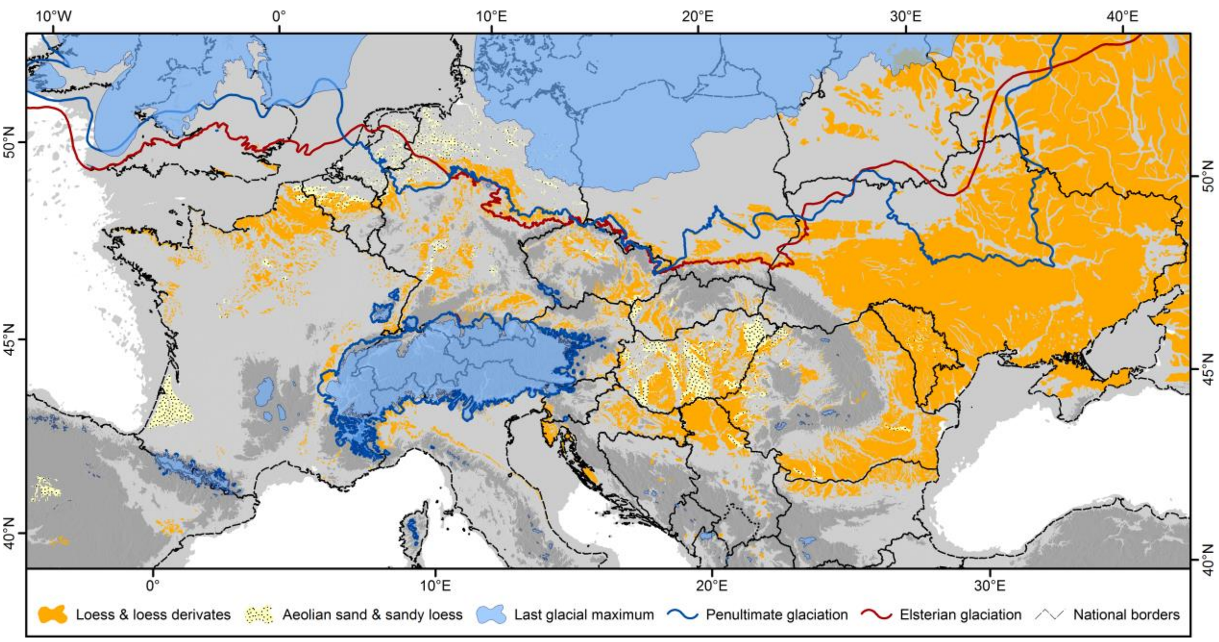

Figure 21: Loess map and extent of Middle Pleistocene glaciation (Saalian / Rissian; Elsterian) according to Ehlers (2011).

5. Conclusion

In this study, we present a new revised map of the distribution of aeolian sediments (mainly loess) and major potential source areas in Europe. We divided the European loess deposits into six major domains and 17 subdomains, based on their facies. Loess facies are differentiated by the silt production area (source), where especially river catchments are important transport agents, and paleoenvironmental factors that influence loess formation, preservation and transformation. By means of the new map and geomorphological cross-sections, we analyzed the various influences of geomorphology and paleoenvironment on loess deposits throughout Europe. The main loess domains in Europe are: (1) The northern European loess belt (domain II), (2) the loess adjacent to Central European high-altitude mountain ranges (domain III), (3) the Middle Danube Basin loess (domain IV), (4) the Pontic East European loess (domain V). Additional important loess regions with less extensive loess covers are the protogenetic zone north of the northern European loess belt (domain I) and areas in the Mediterranean (domain VI). In the Central European low mountain ranges loess occurs in smaller patches in areas above 600 – 800 m a.s.l. thicknesses of less than two meters. In the periglacial zone of northern Europe silty material can also be incorporated in the periglacial cover beds.

The loess deposits in Europe show remarkable differences regarding their distribution and characteristics. These, compared to other loess regions in the world, complex (post-)depositional milieus are mainly due to: (1) the fluctuations of the British and Fennoscandian ice sheets in the north; (2) the permafrost and vegetation boundaries and their fluctuation; (3) the geographical position of Europe bordering the Atlantic Ocean that allows the moist air masses of the westerlies to travel throughout the continent creating a west-east gradient in precipitation, seasonality and continentality; (4) variation in the topography, such as the (low) mountain ranges and the occurrence of extensive lowland basins; and (5) the position of different potential dust sources like the ice sheet margins, mountain glacier forelands, dry shelfs and associated braided river systems, larger river systems and alluvial fans in the more continental areas.

Based on our findings, we suggest a new conceptual model of loess distribution, loess formation and loess landscapes in form of a humid – arid – nival triangle. This model presents three modes of loess formation as factors of humidity, aridity, and temperature. The top of the triangle represents periglacial environments. Although loess-like sediments and loess derivates formed in these environments, the prevalent conditions have caused discordances and hiati. Such loess deposits are very characteristic for domains I – III and mostly formed during cold stadial conditions. The right side of the triangle presents loess in arid and semi-arid regions (e.g. domains V, VIc). These deposits range from silty loess towards more sandy loess in the direction of increasing aridity. The left side of the triangle describes humid temperate and subtropical landscapes as found in the western and southern Europe (domains IIIa, VIa, VIb) and at higher elevations in central-eastern Europe (domains IV, V). The climatic conditions led to a denser vegetation cover resulting in morphodynamic stability and increased chemical weathering and soil development. These processes enhanced the formation of clay-sized particles and reduced the amount of coarser (silt-sized) particles. Finally, typical loess is not formed in any of the extreme conditions and we propose that typical loess formation occurred mainly in domain IV and partly in domain V during colder periods of the Pleistocene.

Even though our map focuses on loess landscapes formed and shaped during the LGM, this study can be related to older loess deposits dating to the Middle Pleistocene. The ice sheets extended further south compared to the last glacial-interglacial cycle. These shifts pushed not only the known paleoclimatic and paleoenrivonmental boundaries such as the permafrost boundary or the timberline further south, they also had crucial ramifications on the size, nature and location of silt production and deposition areas. Additionally, paleogeographic factors such as a vast Elsterian glacial lake in the North Sea Basin, reduced the extent of potential source areas for dust deflation. These factors as well as the periglacial overprinting of loess deposits in subsequent glacial periods, led to the poor preservation of Middle Pleistocene loess deposits, especially in Northern Europe.

6. Acknowledgements

The investigations were carried out in the frame of the CRC 806 “Our way to Europe”, subproject B1 “The Eastern Trajectory”: “Last Glacial Paleogeography and Archaeology of the Eastern Mediterranean and of the Balkan Peninsula”, funded by the Deutsche Forschungsgemeinschaft (DFG, German Research Foundation) – Projektnummer 57444011 – SFB 806). We thank D. Haase for sharing shapefiles of the loess distribution map, P. Bertran for providing the shapefiles of the distribution of aeolian sediments modelled by his team and P. Ludwig providing the data of the LGM regional dust model.

7. Data availability

Our work highlights the value of the compiled geodata, which can be accessed freely at the CRC806 database at https://crc806db.uni-koeln.de/start/

8. Author contributions

Frank Lehmkuhl: Conceptualization, supervision, writing and design of the original draft, funding acquisition Janina J. Nett: Project administration, supervision, methodology, validation, writing original draft. Stephan Pötter: Methodology, validation, data curation, writing original draft. Philipp Schulte: validation, writing original draft, visualization. Tobias Sprafke, Zdzislaw Jary, Pierre Antoine: Resources, writing regional part. Lara Wacha, Daniel Wolf, Andrea Zerboni: Resources, data curation, writing regional part. Jan Hošek, Slobodan B. Marković, Pál Sümegi, Igor Obreht, Daniel Veres: writing regional part. Bruno Boemke: Investigation, data curation, methodology. Viktor Schaubert: Visualization, data curation, formal analysis. Jonas Viehweger: Investigation, data curation, software. Christian Zeeden: validation. Ulrich Hambach: partially designing and contributing to conceptual model, writing regional part, validation. All authors contributed to the discussion and interpretation of the results, reviewed & edited the manuscript.

List of Figures

Figure 1: Modern climatic conditions in Europe. Mean annual air temperature on the upper panel, annual precipitation on the lower panel. Data adapted from Karger et al. (2017).

Figure 2: Distribution of loess and selected Late Pleistocene sediments in Europe. The LGM extent of glaciers (Ehlers et al., 2011) and dry continental shelves (Willmes, 2015), as well as the northern

timberline (modified after Grichuk, 1992) and the boundaries of continuous and discontinuous permafrost (Vandenberghe et al., 2014a) are also mapped.

Figure 3: Major domains (roman numerals) and subdomains (lowercase letters) of loess and loess derivates for the LGM loess landscapes as shown in Figure 2.

Figure 4: N-S transects showing four exemplary loess landscapes across Europe. The location of the transects, the 3-D images (Figs. 7, 8, 10, 11, 13, 14), and the meso-scale loess landscapes is shown in the top map. Meso-scale loess landscape: Valley sections (So = Somme, Northern France Figure 6 and RH = Red Hill, Czech Republic, Figure 12) loess-edge ramp (LS = Lower Saxony, S = Saxony, both Germany, Figure 9).

Figure 5: Transect of 17 selected LPS from northern France to eastern Bulgaria, which span the last glacial cycle in the respective subdomains. For correlation, all sections schematically divided in chrono-climatic units of European loess sequences (Haesaerts and Mestdagh, 2000, Antoine et al., 2013): (Saalian), Interglacial (IG), Earlyglacial (EG), Lower Pleniglacial (LPG), Middle Pleniglacial (MPG) and Upper Pleniglacial (UPG). The interglacials are shown in brown and the glacials in grey scales. The hatchings indicate the soil types. The individual OSL ages can be obtained from the references given above the sequences; countries and subdomain are given as abbreviations. Danube Basin loess stratigraphic nomenclature follows Marković et al. (2015).

Figure 6: Loess stratigraphy in northern France (subdomain IIa) controlled by asymmetric valley topography (modified according to Antoine et al., 2016).

Figure 7: 3-D image of the distribution of loess, sandy deposits, and the late Quaternary floodplain in the southern part of the Lower Rhine Embayment. The size of the 3-D image is 40 x 55 km. Superelevated by factor 1 (no superelevation).

Figure 8: 3-D image of the distribution of loess, sandy deposits, and the late Quaternary floodplain surrounding the Harz Mountains in northern Germany. The size of the 3-D image is 180 x 190 km. Superelevated by factor 20.

Figure 9: Loess-edge ramp (“Lößrandstufe”) in Germany: Examples from Lower Saxony (redrawn and simplified according to Gehrt (1994) and personal communication by E. Gehrt, 2020) and Saxony (redrawn and modified according to Haase et al., 1970).

Figure 10: 3-D image of the distribution of loess, sandy deposits, the Late Pleistocene fluvial deposits and Holocene floodplain in the Upper Rhine Graben, the Kraichgau and Neckar Basin. The size of the 3-D image is 95 x 155km. Superelevated by factor 1 (no superelevation).

Figure 11: 3-D image of the distribution of loess, sandy deposits, the Late Pleistocene fluvial deposits and Holocene floodplain in Lower Austria. The size of the 3-D image is 35 x 70 km. Superelevated by factor 1 (no superelevation).

Figure 12: Redrawn and modified sketch from Kukla (1977, 1978) showing the Červený kopec (Red Hill) section at Brno Czech Republic with the terraces CK 1 -5 covered with LPS. The section was exposed in an excavation front of a brickyard pit and in boreholes.

Figure 13: 3-D image of the loess landscape in the Vojvodina (northern Serbia) showing the distribution of loess, loess derivates, the late Quaternary floodplain and numerous investigated loess sequences. The size of the 3-D image is 53 x 57 km. Superelevated by factor 1 (no superelevation).

Figure 14: 3-D image of the distribution of loess and late Quaternary floodplain deposits in the Lower Danube Basin. The size of the 3-D image is 50 x 55 km. Superelevated by factor 1 (no superelevation).

Figure 15: Box plots of the elevation (ordinate) of loess and loess derivates in Europe per subdomain (abscissae). To exclude extreme outliers, the upper and lower limit in the whisker was set to 1% (cf. Supplementary Tab. S3).

Figure 16: Frequency distributions of the elevation of loess and loess derivates per main and subdomain. The ordinate shows the relative proportion of each elevation that is depicted on the horizontal axis. A color legend is given for the subdomains. Note that the ordinated of domain 4 uses a different scale.

Figure 17: Comparison of our new European loess map to the mapping approach from Haase et al. 2007. Similarities are shown in yellow. The distribution of loess, sandy loess and aeolian sand, and loess derivates that are only evident in our map is depicted in green, while the distribution of loess, loess derivates, sandy and alluvial loess that is only present in the Haase map is shown in blue. The extent of glaciers (Ehlers et al., 2011) and the dry continental shelves (Willmes, 2015) during the LGM are depicted.

Figure 18: Comparison of our new loess map to the mapping approach from Bertran et al 2016. Please note that only data from the European Union was included due to the extent of the base data. The extent of glaciers (Ehlers et al., 2011) and the dry continental shelves (Willmes, 2015) during the LGM are depicted.

Figure 19: Dust deposition rates for the LGM according to modelled data from Schaffernicht et al. (2020). The dust deposition rates comprise particles of up to 20 µm diameter (FD20) using a dynamic downscaling (FD20 DD). Distribution of loess as well as the boundaries of the main loess domains are given for comparison.

Figure 20: Conceptual model of loess landscapes. Note that the corners represent the extreme end with no loess formation. Top: Glacier with lager extend on the nival-humid axis. Left corner: Forest with larger extend on the humid-nival axis. Right corner: Deserts.

Figure 21: Loess map and extent of Middle Pleistocene glaciation (Saalian / Rissian; Elsterian) according to Ehlers (2011).

List of Tables

Table 1: Surface statistics of the distribution of loess and selected Late Pleistocene sediments in Europe (Figure 2) per domain and subdomain.

References

Adebiyi, A.A., Kok, J.F., 2020. Climate models miss most of the coarse dust in the atmosphere. Sci. Adv. 6, eaaz9507. https://doi.org/10.1126/sciadv.aaz9507

Amit, R., Zerboni, A., 2013. Report on the INQUA-AEOMED field trip workshop “Reconsidering Loess in Northern Italy” (Po Plain, 1-3 July 2013). Alpine and Mediterranean Quaternary 26, xi–xv.

Andreeva, D.B., Leiber, K., Glaser, B., Hambach, U., Erbajeva, M., Chimitdorgieva, G.D., Tashak, V., Zech, W., 2011. Genesis and properties of black soils in Buryatia, southeastern Siberia, Russia. Quaternary International 243, 313–326. https://doi.org/10.1016/j.quaint.2010.12.017

Anechitei-Deacu, V., Timar-Gabor, A., Fitzsimmons, K., Veres, D., Hambach, U., 2014. Multi-method luminescence investigations on quartz grains of different sizes extracted from a loess section in Southeast Romania interbedding the Campanian Ignimbrite ash layer. Geochronometria 41, 1–14. https://doi.org/10.2478/s13386-013-0143-4

Antoine, P., Bonifay, E., Conchon, O., Lautridou, J.P., Macaire, J.J., Mandier, P., Monnier, J.L., Morzadec, M.T., Revel, J.C., Sommé, J., Tastet, J.-P., Legigan, P., 1999a. Extension des loess et sables éoliens à 18±2 ka en France. La France pendant les deux derniers extrêmes climatiques, variabilité naturelle des environnements.

Antoine, P., Catt, J., Lautridou, J.-P., Sommé, J., 2003. The loess and coversands of northern France and southern England. J. Quaternary Sci. 18, 309–318. https://doi.org/10.1002/jqs.750

Antoine, P., Coutard, S., Guerin, G., Deschodt, L., Goval, E., Locht, J.-L., Paris, C., 2016. Upper Pleistocene loess-palaeosol records from Northern France in the European context: Environmental background and dating of the Middle Palaeolithic. Quaternary International 411, 4–24. https://doi.org/10.1016/j.quaint.2015.11.036

Antoine, P., Goval, E., Jamet, G., Coutard, S., Moine, O., Hérisson, D., Auguste, P., Guérin, G., Lagroix, F., Schmidt, E., Robert, V., Debenham, N., Meszner, S., Bahain, J.-J., 2014. Les séquences loessiques pléistocène supérieur d’Havrincourt (Pas-de-Calais, France) : stratigraphie, paléoenvironnements, géochronologie et occupations paléolithiques. Quaternaire 321–368. https://doi.org/10.4000/quaternaire.7278

Antoine, P., Lagroix, F., Jordanova, D., Jordanova, N., Lomax, J., Fuchs, M., Debret, M., Rousseau, D.-D., Hatté, C., Gauthier, C., Moine, O., Taylor, S.N., Till, J.L., Coutard, S., 2019. A remarkable Late Saalian (MIS 6) loess (dust) accumulation in the Lower Danube at Harletz (Bulgaria). Quaternary Science Reviews 207, 80–100. https://doi.org/10.1016/j.quascirev.2019.01.005

Antoine, P., Rousseau, D.-D., Degeai, J.-P., Moine, O., Lagroix, F., Kreutzer, S., Fuchs, M., Hatté, C., Gauthier, C., Svoboda, J., Lisá, L., 2013. High-resolution record of the environmental response to climatic variations during the Last Interglacial–Glacial cycle in Central Europe: the loess-palaeosol sequence of Dolní Věstonice (Czech Republic). Quaternary Science Reviews 67, 17–38. https://doi.org/10.1016/j.quascirev.2013.01.014

Antoine, P., Rousseau, D.-D., Fuchs, M., Hatté, C., Gauthier, C., Marković, S.B., Jovanović, M., Gaudenyi, T., Moine, O., Rossignol, J., 2009a. High-resolution record of the last climatic cycle in the southern Carpathian Basin (Surduk, Vojvodina, Serbia). Quaternary International 198, 19–36. https://doi.org/10.1016/j.quaint.2008.12.008

Antoine, P., Rousseau, D.-D., Lautridou, J.-P., Hatté, C., 1999b. Last interglacial-glacial climatic cycle in loess-palaeosol successions of north-western France. Boreas 28, 551–563. https://doi.org/10.1111/j.1502-3885.1999.tb00241.x

Antoine, P., Rousseau, D.-D., Moine, O., Kunesch, S., Hatté, C., Lang, A., Tissoux, H., Zöller, L., 2009b. Rapid and cyclic aeolian deposition during the Last Glacial in European loess: a high-resolution record from Nussloch, Germany. Quaternary Science Reviews 28, 2955–2973. https://doi.org/10.1016/j.quascirev.2009.08.001

Antoine, P., Rousseau, D.-D., Zöller, L., Lang, A., Munaut, A.-V., Hatté, C., Fontugne, M., 2001. High-resolution record of the last interglacial–glacial cycle in the Nussloch loess–palaeosol sequences, Upper Rhine Area, Germany. Quaternary International 76, 211–229.

Antonioli, F., Vai, G.B., 2004. Litho-Paleoenvironmental Maps of Italy During the Last Two Climatic Extremes. ENEA.
Assadi-Langroudi, A., 2019. A conceptual model for loess in England: Principles and applications. Proceedings of the Geologists' Association 130, 115–125. https://doi.org/10.1016/j.pgeola.2018.12.003
Badino, F., Pini, R., Ravazzi, C., Margaritora, D., Arrighi, S., Bortolini, E., Figus, C., Giaccio, B., Lugli, F., Marciani, G., Monegato, G., Moroni, A., Negrino, F., Oxilia, G., Peresani, M., Romandini, M., Ronchitelli, A., Spinapolice, E.E., Zerboni, A., Benazzi, S., 2019. An overview of Alpine and Mediterranean palaeogeography, terrestrial ecosystems and climate history during MIS 3 with focus on the Middle to Upper Palaeolithic transition. Quaternary International S1040618219307608. https://doi.org/10.1016/j.quaint.2019.09.024
Badura, J., Jary, Z., Smalley, I., 2013. Sources of loess material for deposits in Poland and parts of Central Europe: The lost Big River. Quaternary International 296, 15–22. https://doi.org/10.1016/j.quaint.2012.06.019
Balasch, J.C., Poch, R.M., Rodríguez, R., Plata, J.M., Jiménez, D., Castelltort, X., Aran, M., Ascaso, E., Boixadera, J., 2019. Els sòls del loess -Unes notes en el front de batalla Itinerari edàfic per la Terra Alta i la Ribera d'Ebre. Departament de Medi Ambient i Ciències del Sòl. Universitat de Lleida.
Banak, A., Mandic, O., Sprovieri, M., Lirer, F., Pavelić, D., 2016. Stable isotope data from loess malacofauna: Evidence for climate changes in the Pannonian Basin during the Late Pleistocene. Quaternary International 415, 15–24. https://doi.org/10.1016/j.quaint.2015.10.102
Barta, G., 2014. Paleoenvironmental reconstruction based on the morphology and distribution of secondary carbonates of the loess-paleosol sequence at Süttő, Hungary. Quaternary International, Loess Research and Lithostratigraphy in Hungary 319, 64–75. https://doi.org/10.1016/j.quaint.2013.08.019
Basarin, B., Buggle, B., Hambach, U., Marković, S.B., Dhand, K.O., Kovačević, A., Stevens, T., Guo, Z., Lukić, T., 2014. Time-scale and astronomical forcing of Serbian loess–paleosol sequences. Global and Planetary Change 122, 89–106. https://doi.org/10.1016/j.gloplacha.2014.08.007
Basarin, B., Vandenberghe, D.A.G., Marković, S.B., Catto, N., Hambach, U., Vasiliniuc, S., Derese, C., Rončević, S., Vasiljević, Dj.A., Rajić, Lj., 2011. The Belotinac section (Southern Serbia) at the southern limit of the European loess belt: Initial results. Quaternary International, The Second Loessfest (2009) 240, 128–138. https://doi.org/10.1016/j.quaint.2011.02.022
Bellwood, P.S., 2005. First Farmers: the origins of agricultural societies. Blackwell Pub, Malden, MA.
Bertran, P., Liard, M., Sitzia, L., Tissoux, H., 2016. A map of Pleistocene aeolian deposits in Western Europe, with special emphasis on France: Pleistocene aeolian deposits in western Europe. Journal of Quaternary Science 31, 844–856. https://doi.org/10.1002/jqs.2909
BGR [Bundesanstalt für Geowissenschaften und Rohstoffe], 2005. Soil Regions of the European Union and Adjacent Countries 1 : 5 000 000 (EUSR5000) Version 2.0. Special Publication, Ispra. EU catalogue number S.P.I.05.134.
Bibus, E., 2002. Zum Quartär im mittleren Neckarraum: Reliefentwicklung, Löß/Paläobodensequenzen, Paläoklima, Tübinger geowissenschaftliche Arbeiten. Geographisches Institut der Universität.
Bibus, E., Rähle, W., Wedel, J., 2002. Profilaufbau, Molluskenführung und Parallelisierungsmöglichkeiten des Altwürmabschnitts im Lössprofil Mainz-Weisenau. https://doi.org/10.23689/FIDGEO-1147
Bloemendal, J., Liu, X., Sun, Y., Li, N., 2008. An assessment of magnetic and geochemical indicators of weathering and pedogenesis at two contrasting sites on the Chinese Loess plateau. Palaeogeography, Palaeoclimatology, Palaeoecology 257, 152–168. https://doi.org/10.1016/j.palaeo.2007.09.017

Boenigk, W., Frechen, M., 2001a. The loess record in sections at Koblenz–Metternich and Tönchesberg in the Middle Rhine Area. Quaternary International 76–77, 201–209. https://doi.org/10.1016/S1040-6182(00)00103-8
Boenigk, W., Frechen, M., 2001b. Zur Geologie der Kärlich Hauptwand. Mainzer geowissenschaftliche Mitteilungen 30, 123–194.
Boixadera, J., Poch, R.M., Lowick, S.E., Balasch, J.C., 2015. Loess and soils in the eastern Ebro Basin. Quaternary International, Rates of soil forming processes and the role of aeolian influx 376, 114–133. https://doi.org/10.1016/j.quaint.2014.07.046
Bokhorst, M.P., Beets, C.J., Marković, S.B., Gerasimenko, N.P., Matviishina, Z.N., Frechen, M., 2009. Pedo-chemical climate proxies in Late Pleistocene Serbian–Ukranian loess sequences. Quaternary International, Loess in the Danube Region and Surrounding Loess Provinces: The Marsigli Memorial Volume 198, 113–123. https://doi.org/10.1016/j.quaint.2008.09.003
Bokhorst, M.P., Vandenberghe, J., Sümegi, P., Łanczont, M., Gerasimenko, N.P., Matviishina, Z.N., Marković, S.B., Frechen, M., 2011. Atmospheric circulation patterns in central and eastern Europe during the Weichselian Pleniglacial inferred from loess grain-size records. Quaternary International 234, 62–74. https://doi.org/10.1016/j.quaint.2010.07.018
Boretto, G., Zanchetta, G., Ciulli, L., Bini, M., Fallick, A.E., Lezzerini, M., Colonese, A.C., Zembo, I., Trombino, L., Regattieri, E., Sarti, G., 2017. The loess deposits of Buca Dei Corvi section (Central Italy): Revisited. Catena 151, 225–237. https://doi.org/10.1016/j.catena.2017.01.001
Borsy, Z., Felszerfalvi, J., Szabo, P.P., 1979. Thermoluminescence dating of several layers of the loess sequences at Paks and Mende (Hungary). Acta Geologica Academiae Scientiarum Hungaricae 29, 451–459.
Bösken, J., Klasen, N., Zeeden, C., Obreht, I., Marković, S.B., Hambach, U., Lehmkuhl, F., 2017. New luminescence-based geochronology framing the last two glacial cycles at the southern limit of European Pleistocene loess in Stalać (Serbia). Geochronometria 44, 150–161. https://doi.org/10.1515/geochr-2015-0062
Bösken, J., Obreht, I., Zeeden, C., Klasen, N., Hambach, U., Sümegi, P., Lehmkuhl, F., 2019. High-resolution paleoclimatic proxy data from the MIS3/2 transition recorded in northeastern Hungarian loess. Quaternary International 502, 95–107. https://doi.org/10.1016/j.quaint.2017.12.008
Bosq, M., Bertran, P., Degeai, J.-P., Kreutzer, S., Queffelec, A., Moine, O., Morin, E., 2018. Last Glacial aeolian landforms and deposits in the Rhône Valley (SE France): Spatial distribution and grain-size characterization. Geomorphology 318, 250–269. https://doi.org/10.1016/j.geomorph.2018.06.010
Bosq, M., Bertran, P., Degeai, J.-P., Queffelec, A., Moine, O., 2020a. Geochemical signature of sources, recycling and weathering in the Last Glacial loess from the Rhône Valley (southeast France) and comparison with other European regions. Aeolian Research 42, 100561. https://doi.org/10.1016/j.aeolia.2019.100561
Bosq, M., Kreutzer, S., Bertran, P., Degeai, J.-P., Dugas, P., Kadereit, A., Lanos, P., Moine, O., Pfaffner, N., Queffelec, A., Sauer, D., 2020b. Chronostratigraphy of two Late Pleistocene loess-palaeosol sequences in the Rhône Valley (southeast France). Quaternary Science Reviews 245, 106473. https://doi.org/10.1016/j.quascirev.2020.106473
Botti, D., 2018. A phytoclimatic map of Europe. cybergeo. https://doi.org/10.4000/cybergeo.29495
British Geological Survey, 2013. Onshore Digital Geological Map of Great Britain, BGS Geology 625k/ DiGMapGB-625.
Bronger, A., 2003. Correlation of loess–paleosol sequences in East and Central Asia with SE Central Europe: towards a continental Quaternary pedostratigraphy and paleoclimatic history. Quaternary International 106, 11–31.
Bruno, L., Marchi, M., Bertolini, I., Gottardi, G., Amorosi, A., 2020. Climate control on stacked paleosols in the Pleistocene of the Po Basin (northern Italy). J. Quaternary Sci 35, 559–571. https://doi.org/10.1002/jqs.3199

Buggle, B., Glaser, B., Zöller, L., Hambach, U., Marković, S., Glaser, I., Gerasimenko, N., 2008. Geochemical characterization and origin of Southeastern and Eastern European loesses (Serbia, Romania, Ukraine). Quaternary Science Reviews 27, 1058–1075. https://doi.org/10.1016/j.quascirev.2008.01.018

Buggle, B., Hambach, U., Glaser, B., Gerasimenko, N., Marković, S.B., Glaser, I., Zöller, L., 2009. Stratigraphy, and spatial and temporal paleoclimatic trends in Southeastern/Eastern European loess–paleosol sequences. Quaternary International, Lower Latitudes Loess-Dust Transport Past and Present 196, 86–106. https://doi.org/10.1016/j.quaint.2008.07.013

Buggle, B., Hambach, U., Kehl, M., Marković, S.B., Zöller, L., Glaser, B., 2013. The progressive evolution of a continental climate in southeast-central European lowlands during the Middle Pleistocene recorded in loess paleosol sequences. Geology 41, 771–774. https://doi.org/10.1130/G34198.1

Buggle, B., Hambach, U., Müller, K., Zöller, L., Marković, S.B., Glaser, B., 2014. Iron mineralogical proxies and Quaternary climate change in SE-European loess–paleosol sequences. Catena, Loess and dust dynamics, environments, landforms, and pedogenesis: a tribute to Edward Derbyshire 117, 4–22. https://doi.org/10.1016/j.catena.2013.06.012

Catt, J.A., 1985. Soil particle size distribution and mineralogy as indicators of pedogenic and geomorphic history: examples from the loessial soils of England and Wales., in: Richard K.S., Arnet R.R., Ellis S. (Eds): Geomorphology and Soils. G. Allen & Unwin, London, pp. 202–218.

Catt, J.A., 1977. Loess and coversand. In: Shotton, F.W., (ed.), British Quaternary Studies - Recent Advances. Clarendon Press, Oxford, pp. 221–229.

Cegła, J., 1972. Sedymentacja lessów Polski (Loess sedimentation in Poland), Acta Universitatis Wratislaviensis.

Chen, J., Yang, T., Matishov, G.G., Velichko, A.A., Zeng, B., He, Y., Shi, P., 2018. Luminescence chronology and age model application for the upper part of the Chumbur-Kosa loess sequence in the Sea of Azov, Russia. J. Mt. Sci. 15, 504–518. https://doi.org/10.1007/s11629-017-4689-0

Chen, J., Yang, T., Qiang, M., Matishov, G.G., Velichko, A.A., Zeng, B., Xu, M., Shi, P., 2020. Interpretation of sedimentary subpopulations extracted from grain size distributions in loess deposits at the Sea of Azov, Russia. Aeolian Research 45, 100597. https://doi.org/10.1016/j.aeolia.2020.100597

Cheshitev, G., Kânčev, I., Vâlkov, V., Marinova, R., Shilyafova, J., Russeva, M., Iliev, K., 1989. Geological Map of P.R. Bulgaria.

Christ, P., 1944. Geologische Generalkarte der Schweiz - Blatt 1 Neuchâtel. Notice explicative par D. Aubert & H. Badoux, 1956.

Christ, P., 1942. Geologische Gerneralkarte der Schweiz - Blatt 2 Basel-Bern. Erläuterungen von A. Buxtorf, 1951.

Christ, P., Nabholz, W., 1950. Geologische Generalkarte der Schweiz - Blatt 3 Zürich-Glarus. Erläuterungen von A. Buxtorf, mit Beiträgen von W. Nabholz, 1957.

Chu, W., 2018. The Danube Corridor Hypothesis and the Carpathian Basin: Geological, Environmental and Archaeological Approaches to Characterizing Aurignacian Dynamics. Journal of World Prehistory 31, 117–178. https://doi.org/10.1007/s10963-018-9115-1

Clark, P.U., Dyke, A.S., Shakun, J.D., Carlson, A.E., Clark, J., Wohlfarth, B., Mitrovica, J.X., Hostetler, S.W., McCabe, A.M., 2009. The Last Glacial Maximum. Science 325, 710–714. https://doi.org/10.1126/science.1172873

Constantin, D., Begy, R., Vasiliniuc, S., Panaiotu, C., Necula, C., Codrea, V., Timar-Gabor, A., 2014. High-resolution OSL dating of the Costineşti section (Dobrogea, SE Romania) using fine and coarse quartz. Quaternary International 334–335, 20–29. https://doi.org/10.1016/j.quaint.2013.06.016

Constantin, D., Timar-Gabor, A., Veres, D., Begy, R., Cosma, C., 2012. SAR-OSL dating of different grain-sized quartz from a sedimentary section in southern Romania interbedding the

Campanian Ignimbrite/Y5 ash layer. Quaternary Geochronology 10, 81–86. https://doi.org/10.1016/j.quageo.2012.01.012
Constantin, D., Veres, D., Panaiotu, C., Anechitei-Deacu, V., Groza, S.M., Begy, R., Kelemen, S., Buylaert, J.-P., Hambach, U., Marković, S.B., Gerasimenko, N., Timar-Gabor, A., 2019. Luminescence age constraints on the Pleistocene-Holocene transition recorded in loess sequences across SE Europe. Quaternary Geochronology 49, 71–77. https://doi.org/10.1016/j.quageo.2018.07.011
Costantini, E.A.C., Carnicelli, S., Sauer, D., Priori, S., Andreetta, A., Kadereit, A., Lorenzetti, R., 2018. Loess in Italy: Genesis, characteristics and occurrence. Catena 168, 14–33. https://doi.org/10.1016/j.catena.2018.02.002
Costantini, E.A.C., L'Abate, G., Barbetti, R., Fantappié, M., Lorenzetti, R., Magini, S., 2012. Mappa dei Suoli d'Italia – Soil Map of Italy 1:1,000,000. Consiglio per la Ricerca e la Sperimentazione in Agricoltura, Ministero delle Politiche Agricole Alimentari e Forestali.
Coutard, S., Antoine, P., Hérisson, D., Pirson, S., Balescu, S., Forget Brisson, L., Spagna, P., Debenham, N., Barré, M., Chantreau, Y., Giros, R., Lamothe, M., 2018. La séquence loessique Pléistocène moyen à supérieur d'Etricourt‑ Manancourt (Picardie, France) : un enregistrement pédo‑ sédimentaire de référence pour les derniers 350 ka. Quaternaire 29/4, 311–346. https://doi.org/10.4000/quaternaire.10569
Cremaschi, M., 2004. Late Pleistocene loess, in: Litho-Palaeoenvironmental Maps of Italy During the Last Two Climatic Extremes. Climex Maps Italy. Antonioli F., Vai G.B. (Eds.), Museo Geologico Giovanni Cappellini, Bologna, Italy.
Cremaschi, M. (Ed.), 1990a. The Loess in Northern and Central Italy: a Loess basin between the Alps and the Mediterranean region ; (guide-book to the excursion in Northern and Central Italy, September - October 1988), 1st ed, Quaderni di Geodinamica Alpina e Quaternaria. Centro di Studio per la Stratigrafia e Petrografia delle Alpi Centrale, Milano, Italy.
Cremaschi, M., 1990b. Stratigraphy and palaeoenvironmental significance of the loess deposits on Susak Island (Dalmatian archipelago). Quaternary International 5, 97–106. https://doi.org/10.1016/1040-6182(90)90029-4
Cremaschi, M., 1987. Loess deposits of the Plain of the Po and of the adjoining Adriatic basin (Northern Italy)., in: Loess and Periglacial Phenomena. Pecsi M., French H.M. (Eds.), Akademiai Kiado, Budapest, pp. 125–140.
Cremaschi, M., Fedoroff, N., Guerreschi, A., Huxtable, J., Colombi, N., Castelletti, L., Maspero, A., 1990. Sedimentary and pedological processes in the Upper Pleistocene loess of northern Italy. The Bagaggera sequence. Quaternary International 5, 23–38. https://doi.org/10.1016/1040-6182(90)90022-V
Cremaschi, M., Ferraro, F., 2007. The upper Pleistocene in the Paglicci Cave (Gargano, southern Italy): loess and tephra in the anthropogenic sequence. Attie della Societa Toscana di Scienze Naturalie Memorie Serie A, 153–163.
Cremaschi, M., Lanzinger, M., 1987. Studio pedostratigrafico e geomorfologico dell'area circostante il sito tardo Paleolitico-Mesolitico di Terlago (Trento). Studi Trentini Scienze Naturali. Acta Geol. 64, 99–120.
Cremaschi, M., Lanzinger, M., 1984. La successione stratigrafica e le fasi pedogenetiche del sito epigravettiano di Andalo, i loess tardiglaciali della Val d'Adige. Preistoria Alpina 19, 179–188.
Cremaschi, M., Van Vliet-Lanoë, B., 1990. Traces of frost activity and ice segregation in Pleistocene loess deposits and till of northern Italy: Deep seasonal freezing or permafrost? Quaternary International 5, 39–48. https://doi.org/10.1016/1040-6182(90)90023-W
Cremaschi, M., Zerboni, A., Nicosia, C., Negrino, F., Rodnight, H., Spötl, C., 2015. Age, soil-forming processes, and archaeology of the loess deposits at the Apennine margin of the Po plain (northern Italy): New insights from the Ghiardo area. Quaternary International 376, 173–188. https://doi.org/10.1016/j.quaint.2014.07.044
Croatian Geological Survey, 2009. Geological map of the Republic of Croatia, scale 1 : 300,000.

Crouvi, O., Amit, R., Enzel, Y., Gillespie, A.R., 2010. Active sand seas and the formation of desert loess. Quaternary Science Reviews 29, 2087–2098. https://doi.org/10.1016/j.quascirev.2010.04.026

Danin, A., Ganor, E., 1991. Trapping of airborne dust by mosses in the Negev Desert, Israel. Earth Surf. Process. Landforms 16, 153–162. https://doi.org/10.1002/esp.3290160206

de San José Mancha, M.A., 1973. Mapa Geológico de España nº 606 (Chinchón), 1 : 50,000.

Delpiano, D., Peresani, M., Bertola, S., Cremaschi, M., Zerboni, A., 2019. Lashed by the wind: short-term Middle Palaeolithic occupations within the loess-palaeosoil sequence at Monte Netto (Northern Italy). Quaternary International 502, 137–147. https://doi.org/10.1016/j.quaint.2019.01.026

Derbyshire, E., Kemp, R., Meng, X., 1995. Variations in loess and palaeosol properties as indicators of palaeoclimatic gradients across the Loess Plateau of North China. Quaternary Science Reviews 14, 681–697. https://doi.org/10.1016/0277-3791(95)00077-1

Ding, Z.L., Ranov, V., Yang, S.L., Finaev, A., Han, J.M., Wang, G.A., 2002. The loess record in southern Tajikistan and correlation with Chinese loess. Earth and Planetary Science Letters 200, 387–400. https://doi.org/10.1016/S0012-821X(02)00637-4

Dobrzański, B., Kowaliński, S., Kuznicki, F., Witek, T., Zawadzki, S., 1974. Soil Map of Poland, 1 : 1,000,000.

Durn, G., Rubinić, V., Wacha, L., Patekar, M., Frechen, M., Tsukamoto, S., Tadej, N., Husnjak, S., 2018. Polygenetic soil formation on Late Glacial Loess on the Susak Island reflects paleo-environmental changes in the Northern Adriatic area. Quaternary International 494, 236–247. https://doi.org/10.1016/j.quaint.2017.06.072

Ehlers, J., Gibbard, P.L., Hughes, P.D., 2011. Quaternary Glaciations - Extent and Chronology, 1st Edition. ed. Elsevier.

Einwögerer, T., Friesinger, H., Händel, M., Neugebauer-Maresch, C., Simon, U., Teschler-Nicola, M., 2006. Upper Palaeolithic infant burials. Nature 444, 285–285. https://doi.org/10.1038/444285a

EMODnet - Bathymetry, 2019. . Understanding the topography of the European seas. https://portal.emodnet-bathymetry.eu/.

European Soils Bureau Network, 2005. Soil Atlas of Europe. European Commission, Office for Official Publications of the European Communities, Luxembourg.

Federal Geological Institute, 1970. Geological map of SFR Yugoslavia, 1:500,000. Prepared by Institute for geological and mining exploration and investigation of nuclear and other raw materials, Belgrade.

Feng, J.-L., Hu, Z.-G., Ju, J.-T., Lin, Y.-C., 2014. The dust provenance and transport mechanism for the Chengdu Clay in the Sichuan Basin, China. CATENA 121, 68–80. https://doi.org/10.1016/j.catena.2014.04.018

Fenn, K., Durcan, J.A., Thomas, D.S.G., Banak, A., 2020. A 180 ka record of environmental change at Erdut (Croatia): a new chronology for the loess–palaeosol sequence and its implications for environmental interpretation. J. Quaternary Sci 35, 582–593. https://doi.org/10.1002/jqs.3201

Ferraro, F., 2009. Age, sedimentation, and soil formation in the Val Sorda loess sequence, Northern Italy. Quaternary International 204, 54–64. https://doi.org/10.1016/j.quaint.2008.12.002

Fink, J., 1965. The pleistocene in eastern Austria. Geological Society of America Special Papers 84, 179–200.

Fink, J., 1954. Die fossilen Böden im österreichischen Löß. Quartär 6, 85–108.

Fink, J., Haase, G., Ruske, R., 1977. Bemerkung zur Lößkarte von Europa 1:2,5 Mio. Petermanns Geographische Mitteilungen 2, 81–97.

Fink, J., Kukla, G.J., 1977. Pleistocene climates in central Europe: At least 17 interglacials after the Olduvai event. Quaternary Research 7, 363–371. https://doi.org/10.1016/0033-5894(77)90027-8

Fink, J., Nagl, H., 1979. Quartäre Sedimente und Formen (Quaternary sediments and forms), 1:1,000,000. In: Österreichische Akademie der Wissenschaften (ÖAW). Kommission für Raumforschung, Atlas der Republik Österreich 1:1,000,000, Nr. II/6.

Fischer, P., Hilgers, A., Protze, J., Kels, H., Lehmkuhl, F., Gerlach, R., 2012. Formation and geochronology of Last Interglacial to Lower Weichselian loess/palaeosol sequences - case studies from the Lower Rhine Embayment, Germany. E&G Quaternary Science Journal 61, 48–63. https://doi.org/10.3285/eg.61.1.04

Fitzsimmons, K.E., Marković, S.B., Hambach, U., 2012. Pleistocene environmental dynamics recorded in the loess of the middle and lower Danube basin. Quaternary Science Reviews 41, 104–118. https://doi.org/10.1016/j.quascirev.2012.03.002

Flint, R.F., 1971. Glacial and Quaternary geology. Wiley, New York.

Florea, N., 2010. Loess was formed, but not sedimented. Rev. Roum. Geogr. 54, 159–169.

Florea, N., Conea, A., Munteanu, I., 1971. Harta Pedologica a Republicii Socialiste Romania (Soil Map of Romania), 1 : 500,000.

Flügel, W.W., Neubauer, F.R., 1984. Geologische Karte der Steiermark 1:200 000. Geologische Bundesanstalt.

Forno, M.G., 1990. Aeolian and reworked loess in the Turin Hills (northwestern Italy). Quaternary International 5, 81–87. https://doi.org/10.1016/1040-6182(90)90027-2

Franc, O., Moine, O., Fülling, A., Auguste, P., Pasty, J., Gadiolet, P., Gaertner, V., Robert, V., 2017. Les séquences alluvio-lœssiques du Würm moyen/supérieur de Quincieux et de Lyon (Rhône-Alpes, France) : premières interprétations paléoenvironnementales et corrélations. Quaternaire 423–453. https://doi.org/10.4000/quaternaire.8453

Frechen, M., Horváth, E., Gábris, G., 1997. Geochronology of Middle and Upper Pleistocene Loess Sections in Hungary. Quaternary Research 48, 291–312. https://doi.org/10.1006/qres.1997.1929

Frechen, M., Oches, E.A., Kohfeld, K.E., 2003. Loess in Europe—mass accumulation rates during the Last Glacial Period. Quaternary Science Reviews, Loess and the Dust Indicators and Records of Terrestrial and Mari ne Palaeoenvironments (DIRTMAP) database 22, 1835–1857. https://doi.org/10.1016/S0277-3791(03)00183-5

Frechen, M., Schirmer, W., 2011. Luminescence Chronology of the Schwalbenberg II Loess in the Middle Rhine Valley. E&G Quaternary Sci. J. 60, 78–89. https://doi.org/10.3285/eg.60.1.05

Fuček, L., Matičec, D., Vlahović, I., Oštrić, N., Prtoljan, B., Kobar, T., Husinec, A., Palenik, D., 2014. Basic Geological Map of the Republic of Croatia Scale 1: 50.000 Sheet Cres 4. Croatian Geological Survey (Department of Geology).

Fuchs, M., Kreutzer, S., Rousseau, D.-D., Antoine, P., Hatté, C., Lagroix, F., Moine, O., Gauthier, C., Svoboda, J., Lisá, L., 2013. The loess sequence of Dolní Věstonice, Czech Republic: A new OSL-based chronology of the Last Climatic Cycle: Loess sequence of Dolní Věstonice, Czech Republic: OSL chronology. Boreas 42, 664–677. https://doi.org/10.1111/j.1502-3885.2012.00299.x

Fuchs, M., Rousseau, D.-D., Antoine, P., Hatté, C., Gauthier, C., Marković, S., Zoeller, L., 2008. Chronology of the Last Climatic Cycle (Upper Pleistocene) of the Surduk loess sequence, Vojvodina, Serbia. Boreas 37, 66–73. https://doi.org/10.1111/j.1502-3885.2007.00012.x

Gaar, D., Preusser, F., 2017. Age of the Most Extensive Glaciation of Northern Switzerland: Evidence from the scientific drilling at Möhliner Feld. E&G Quaternary Sci. J. 66, 1–5. https://doi.org/10.3285/eg.66.1.er1

Gallet, S., Jahn, B., Torii, M., 1996. Geochemical characterization of the Luochuan loess-paleosol sequence, China, and paleoclimatic implications. Chemical Geology 133, 67–88. https://doi.org/10.1016/S0009-2541(96)00070-8

Galović, L., 2016. Sedimentological and mineralogical characteristics of the Pleistocene loess/paleosol sections in the Eastern Croatia. Aeolian Research 20, 7–23. https://doi.org/10.1016/j.aeolia.2015.10.007

Galović, L., Frechen, M., Halamić, J., Durn, G., Romić, M., 2009. Loess chronostratigraphy in Eastern Croatia—A luminescence dating approach. Quaternary International 198, 85–97. https://doi.org/10.1016/j.quaint.2008.02.004

Galović, L., Frechen, M., Peh, Z., Durn, G., Halamić, J., 2011. Loess/palaeosol section in Šarengrad, Croatia – A qualitative discussion on the correlation of the geochemical and magnetic susceptibility data. Quaternary International, The Second Loessfest (2009) 240, 22–34. https://doi.org/10.1016/j.quaint.2011.02.003

Gehrt, E., 1994. Die äolischen Sedimente im Bereich der nördlichen Lößgrenze zwischen Leine und Oker und deren Einflüsse auf die Bodenentwicklung, Diss. Univ. Göttingen. Göttingen.

Gehrt, E., Hagedorn, J., 1996. Zur Entstehung der nördlichen Lößgrenze in Mitteleuropa. – in: Böden als Zeugen der Landschaftsentwicklung., in: Festschrift Zum 80. Geburtstag von Prof. Dr. H. E. Stremme. Landesamt Für Natur Und Umwelt Des Landes Schleswig-Holstein, Abt. Geologie/Boden. Kiel, pp. 59–66.

Gibbard, P., 2007. Europe cut adrift. Nature 448, 259–260. https://doi.org/10.1038/448259a

Gild, C., Geitner, C., Sanders, D., 2018. Discovery of a landscape-wide drape of late-glacial aeolian silt in the western Northern Calcareous Alps (Austria): First results and implications. Geomorphology 301, 39–52. https://doi.org/10.1016/j.geomorph.2017.10.025

Gouda, G., 1962. Untersuchungen an Lössen der Nordschweiz. Geographica Helvetica 17, 137–221.

Goudie, A.S., 1983. Dust storms in space and time. Progress in Physical Geography: Earth and Environment 7, 502–530. https://doi.org/10.1177/030913338300700402

Goudie, A.S., 1978. Dust storms and their geomorphological implications. Journal of Arid Environments 1, 291–311. https://doi.org/10.1016/S0140-1963(18)31712-9

Gozhik, P., Komar, M., Łanczont, M., Fedorowicz, S., Bogucki, A., Mroczek, P., Prylypko, S., Kusiak, J., 2014. Paleoenvironmental history of the Middle Dnieper Area from the Dnieper to Weichselian Glaciation: A case study of the Maksymivka loess profile. Quaternary International 334–335, 94–111. https://doi.org/10.1016/j.quaint.2013.11.037

Grahmann, R., 1932. Der Löss in Europa, Mitteilungen Gesellschaft für Erdkunde. Duncker & Humblot, Leipzig.

Grichuk, V.P., 1992. Main types of vegetation (ecosystems) for the maximum cooling of the last glaciation., in: In: Frenzel, B., Pecsi, B. Velichko, A.A. (Eds.): Atlas of Palaeoclimates and Palaeoenvironments of the Northern Hemisphere. NQUA/Hungarian Academy of Sciences, Budapest, pp. 123–124.

Guenther, E.W., 1987. Zur Gliederung der Lösse des südlichen Oberrheintals. E&G – Quaternary Science Journal 37, 67–77. http://dx.doi.org/10.23689/fidgeo-1291

Haase, D., Fink, J., Haase, G., Ruske, R., Pécsi, M., Richter, H., Altermann, M., Jäger, K.-D., 2007. Loess in Europe—its spatial distribution based on a European Loess Map, scale 1:2,500,000. Quaternary Science Reviews 26, 1301–1312. https://doi.org/10.1016/j.quascirev.2007.02.003

Haase, G., Lieberoth, I., Ruske, R., 1970. Sedimente und Paläoböden im Lößgebiet., in: Richter, H., Haase, G., Lieberoth, I. & Ruske, R. (Eds.): Periglazial – Löß – Paläolithikum Im Jungpleistozän Der Deutschen Demokratischen Republik, Ergänzungsheft Zu Petermanns Geographischen Mitteilungen. VEB Hermann Haack, pp. 99–212.

Haesaerts, P., Borziak, I., Chirica, V., Damblon, F., Koulakovska, L., Van der Plicht, J., 2003. The east Carpathian loess record : a reference for the middle and late pleniglacial stratigraphy in central Europe [La séquence loessique du domaine est-carpatique : une référence pour le Pléniglaciaire moyen et supérieur d'Europe centrale.]. Quaternaire 14, 163–188. https://doi.org/10.3406/quate.2003.1740

Haesaerts, P., Damblon, F., Gerasimenko, N., Spagna, P., Pirson, S., 2016. The Late Pleistocene loess-palaeosol sequence of Middle Belgium. Quaternary International 411, 25–43. https://doi.org/10.1016/j.quaint.2016.02.012

Haesaerts, P., Damblon, F., Sinitsyn, A., van der Plicht, J., 2004. Kostienki 14 (Voronezh, Central Russia): new data on stratigraphy and radiocarbon chronology. BAR International Series 1240, 169–180.

Haesaerts, P., Mestdagh, H., 2000. Pedosedimentary evolution of the last interglacial and early glacial sequence in the European loess belt from Belgium to central Russia. Netherlands Journal of Geosciences 79, 313–324. https://doi.org/10.1017/S001677460002179X

Haesaerts, P., Pirson, S., Meijs, E.P.M., 2011. New Proposal for the Quaternary Lithostratigraphic Units (Belgium). National Commission for Stratigraphy, Subcommission Quaternary.

Hastings, D.A., Dunbar, P.K., Elphingstone, G.M., Bootz, M., Murakami, H., Maruyama, H., Masaharu, H., Holland, P., Payne, J., Bryant, N.A., Logan, T.L., Muller, J.-P., Schreier, G., MacDonald, J.S., 1999. The Global Land Onekilometer Base Elevation (GLOBE) Digital Elevation Model, Version 1.0.

Hatté, C., Gauthier, C., Rousseau, D.-D., Antoine, P., Fuchs, M., Lagroix, F., Markovic, S.B., Moine, O., Sima, A., 2013. Excursions to C_4 vegetation recorded in the Upper Pleistocene loess of Surduk (Northern Serbia): an organic isotope geochemistry study. Clim. Past 9, 1001–1014. https://doi.org/10.5194/cp-9-1001-2013

Hauck, T.C., Lehmkuhl, F., Zeeden, C., Bösken, J., Thiemann, A., Richter, J., 2017. The Aurignacian way of life: Contextualizing early modern human adaptation in the Carpathian Basin. Quaternary International 485, 150–166. https://doi.org/10.1016/j.quaint.2017.10.020

Henze, N., 1998. Kennzeichnung des Oberwürmlösses der Niederrheinischen Bucht, Kölner Forum für Geologie und Paläontologie. Geologisches Institut der Universität zu Köln, Dissertation, Köln.

Hilgers, A., Gehrt, E., Janotta, A., Radtke, U., 2001a. A contribution to the dating of the northern boundary of the Weichselian Loess Belt in Northern Germany by luminescence dating and pedological analysis. Quaternary International 76–77, 191–200. https://doi.org/10.1016/S1040-6182(00)00102-6

Hilgers, A., Murray, A.S., Schlaak, N., Radtke, U., 2001b. Comparison of quartz OSL protocols using Lateglacial and Holocene dune sands from Brandenburg, Germany. Quaternary Science Reviews 20, 731–736. https://doi.org/10.1016/S0277-3791(00)00050-0

Hirniak, J.N., Smith, E.I., Johnsen, R., Ren, M., Hodgkins, J., Orr, C., Negrino, F., Riel-Salvatore, J., Fitch, S., Miller, C.E., Zerboni, A., Mariani, G.S., Harris, J.A., Gravel-Miguel, C., Strait, D., Peresani, M., Benazzi, S., Marean, C.W., 2020. Discovery of cryptotephra at Middle–Upper Paleolithic sites Arma Veirana and Riparo Bombrini, Italy: a new link for broader geographic correlations. J. Quaternary Sci. 35, 199–212. https://doi.org/10.1002/jqs.3158

Hošek, J., Hambach, U., Lisá, L., Grygar, T.M., Horáček, I., Meszner, S., Knésl, I., 2015. An integrated rock-magnetic and geochemical approach to loess/paleosol sequences from Bohemia and Moravia (Czech Republic): Implications for the Upper Pleistocene paleoenvironment in central Europe. Palaeogeography, Palaeoclimatology, Palaeoecology 418, 344–358. https://doi.org/10.1016/j.palaeo.2014.11.024

Hošek, J., Lisá, L., Hambach, U., Petr, L., Vejrostová, L., Bajer, A., Grygar, T.M., Moska, P., Gottvald, Z., Horsák, M., 2017. Middle Pleniglacial pedogenesis on the northwestern edge of the Carpathian basin: A multidisciplinary investigation of the Bíňa pedo-sedimentary section, SW Slovakia. Palaeogeography, Palaeoclimatology, Palaeoecology 487, 321–339. https://doi.org/10.1016/j.palaeo.2017.09.017

Hughes, M.W., Almond, P.C., Roering, J.J., Tonkin, P.J., 2010. Late Quaternary loess landscape evolution on an active tectonic margin, Charwell Basin, South Island, New Zealand. Geomorphology 122, 294–308. https://doi.org/10.1016/j.geomorph.2009.09.034

Hughes, P.D., Woodward, J.C., van Calsteren, P.C., Thomas, L.E., 2011. The glacial history of the Dinaric Alps, Montenegro. Quaternary Science Reviews 30, 3393–3412. https://doi.org/10.1016/j.quascirev.2011.08.016

Iovita, R., Fitzsimmons, K.E., Dobos, A., Hambach, U., Hilgers, A., Zander, A., 2012. Dealul Guran: evidence for Lower Palaeolithic (MIS 11) occupation of the Lower Danube loess steppe. Antiquity 86, 973–989.

Jahn, A., 1950. Less, jego pochodzenie i związek z klimatem epoki lodowej (Loess, its origin and connection with the climate of the glacial epoch). Acta Geologica Polonica I, 257–310.
Jakab, S., 2007. Chrono-toposequences of soils on the river terraces in Transylvania (Romania). Catena 71, 406–410. https://doi.org/10.1016/j.catena.2007.03.016
Jarke, J., 1960. Staubfall auf dem Schwarzen Meer. Deutsche Hydrographische Zeitschrift 13, 225–229. https://doi.org/10.1007/BF02224720
Jary, Z., 2010. Loess-soil sequences as a source of climatic proxies: an example from SW Poland. Geologija 52, 40–45. https://doi.org/10.2478/v10056-010-0004-2
Jary, Z., 2009. Periglacial markers within the Late Pleistocene loess–palaeosol sequences in Poland and Western Ukraine. Quaternary International 198, 124–135. https://doi.org/10.1016/j.quaint.2008.01.008
Jary, Z., 2007. Record of Climate Changes in Upper Pleistocene loess-soil sequences in Poland and western part of Ukraine. Treatise of the Institute of Geography and Regional Development of the University of Wrocław 1 (in Polish with English summary).
Jary, Z., 1996. Chronostratigraphy and the course of loess sedimentation in SW Poland on the example of the Glubczyce Upland and Trzebnica Hills. Acta Universitatis Wratislaviensis 1766, Studia Geograficzne 63, 103 pp. (in Polish with English summary).
Jary, Z., Ciszek, D., 2013. Late Pleistocene loess–palaeosol sequences in Poland and western Ukraine. Quaternary International 296, 37–50. https://doi.org/10.1016/j.quaint.2012.07.009
Jary, Z., Kida, J., 2000. Loess particles sources, transport and deposition on the example of SW Poland. Acta Universitatis Wratislaviensis 2269, 71–77.
Jary, Z., Kida, J., Snihur, M., 2002. Loess and loess-derived sediments in SW Poland. Loess in Lower Silesia, Czasopismo Geograficzne 63-100. (in Polish with English summary).
Jary, Z., Krawczyk, M., Raczyk, J., Ryzner, K., 2016. Loess in Lower Silesia., in: Berlin, Geozon Science Media, 57-73., In: Dominik Faust and Katja Heller [Eds]: Erkundungen in Sachsen Und Schlesien: Quartäre Sedimente Im Landschaftsgenetischen Kontext. Geozon Science Media, Berlin, pp. 57–73.
JAXA EORC, 2016. ALOS Global Digital Surface Model “ALOS World 3D - 30m” (AW3D30). URL http://www.eorc.jaxa.jp/ALOS/en/aw3d30/index.htm (accessed 2.15.18).
Jersak, J., 1973. Litologia i stratygrafia lessu wyżyn południowej Polski (Lithology and stratigraphy of the loess on the Southern Polish Uplands), Acta Geographica Lodziensia. Państwowe Wydawn, Lódź.
Jipa, D.C., 2014. The conceptual sedimentary model of the Lower Danube loess basin: Sedimentogenetic implications. Quaternary International, Loess and the record of upper Palaeolithic cultures in the Danube Basin 351, 14–24. https://doi.org/10.1016/j.quaint.2013.06.008
Jordanova, D., Jordanova, N., 2020. Diversity and peculiarities of soil formation in eolian landscapes – Insights from the mineral magnetic records. Earth and Planetary Science Letters 531, 115956. https://doi.org/10.1016/j.epsl.2019.115956
Juvigné, E., Tallier, E., Haesaerts, P., Pirson, S., 2008. Un nouveau stratotype du téphra de Rocourt dans la carrière de Romont (Eben/ Bassenge, Belgique). Quaternaire. Revue de l’Association française pour l’étude du Quaternaire 19/2, 133–139. https://doi.org/10.4000/quaternaire.2742
Kadereit, A., Kind, C.-J., Wagner, G.A., 2013. The chronological position of the Lohne Soil in the Nussloch loess section – re-evaluation for a European loess-marker horizon. Quaternary Science Reviews 59, 67–86. https://doi.org/10.1016/j.quascirev.2012.10.026
Karger, D.N., Conrad, O., Böhner, J., Kawohl, T., Kreft, H., Soria-Auza, R.W., Zimmermann, N.E., Linder, H.P., Kessler, M., 2017. Climatologies at high resolution for the earth’s land surface areas. Scientific Data 4, 170122.
Kels, H., 2007. Bau und Bilanzierung der Lössdecke am westlichen Niederrhein. Heinrich-Heine-Universität Düsseldorf, Düsseldorf.

Kels, H., Protze, J., Sitlivy, V., Hilgers, A., Zander, A., Anghelinu, M., Bertrams, M., Lehmkuhl, F., 2014. Genesis of loess-like sediments and soils at the foothills of the Banat Mountains, Romania – Examples from the Paleolithic sites Româneşti and Coşava. Quaternary International, Loess and the record of upper Palaeolithic cultures in the Danube Basin 351, 213–230. https://doi.org/10.1016/j.quaint.2014.04.063

Koeniger, P., Barta, G., Thiel, C., Bajnóczi, B., Novothny, Á., Horváth, E., Techmer, A., Frechen, M., 2014. Stable isotope composition of bulk and secondary carbonates from the Quaternary loess-paleosol sequence in Süttő, Hungary. Quaternary International, Loess Research and Lithostratigraphy in Hungary 319, 38–49. https://doi.org/10.1016/j.quaint.2012.06.038

Kolfschoten, T. van, Roebroeks, W., Vandenberghe, J., 1993. The Middle and Late Pleistocene sequence at Maastricht-Belvédère: the Type Locality of the Belvédère Interglacial. Mededelingen Rijks Geologische Dienst 47, 81–91.

Košťálik, J., 1989. Spraše a fosílne pôdy Východného Slovenska, ich genéza, charakteristika, chronostratigrafia a využitie v národnom hospodárstve (The loess and fossils of Eastern Slovakia, their genesis, characteristics, chronostratigraphy and use in the national economy). PhD thesis. VŠP Nitra.

Koster, E.A., 2005. Recent advances in luminescence dating of Late Pleistocene (cold-climate) aeolian sand and loess deposits in western Europe. Permafrost and Periglacial Processes 16, 131–143. https://doi.org/10.1002/ppp.512

Kostić, N., Protić, N., 2000. Pedology and mineralogy of loess profiles at Kapela-Batajnica and Stalać, Serbia. Catena 41, 217–227. https://doi.org/10.1016/S0341-8162(00)00102-8

Kozarski, S., Nowaczyk, B., 1991. Lithofacies variation and chronostratigraphy of Late Vistulian and Holocene aeolian phenomena in northwestern Poland. Z. Geomorph. N.F., Suppl.-Bd 90, 107–122.

Krauß, L., Kappenberg, A., Zens, J., Kehl, M., Schulte, P., Zeeden, C., Eckmeier, E., Lehmkuhl, F., 2017. Reconstruction of Late Pleistocene paleoenvironments in southern Germany using two high-resolution loess-paleosol records. Palaeogeography, Palaeoclimatology, Palaeoecology 509, 58–76. https://doi.org/10.1016/j.palaeo.2017.11.043

Krauß, L., Zens, J., Zeeden, C., Schulte, P., Eckmeier, E., Lehmkuhl, F., 2016. A multi-proxy analysis of two loess-paleosol sequences in the northern Harz foreland, Germany. Palaeogeography, Palaeoclimatology, Palaeoecology 461, 401–417. https://doi.org/10.1016/j.palaeo.2016.09.001

Krenmayr, H.G., Schnabel, W. (coordination), Reitner, J.M., van Husen, D., Finger, F., Linner, M., Krenmayr, H.G., Roetzel, R., Rupp, Ch., Egger, H., Schnabel, W., Bryda, G., Mandl, G.W., Nowotny, A., Pestal, G., Schuster, R. (regional cartographers), 2006. Geological Map of Upper Austria (Geologische Karte von Oberösterreich), 1 : 200,000.

Krolopp, E., Sümegi, P., 2002. A ságvári lösz-rétegsor csigafaunája (The mollusc fauna of the Ságvár loess profile). Malakológiai Tájékoztató 20, 7–14.

Krupenikov, I.A., Novak, T.S., Rodina, A.K., Ursu, A.F., 1969. Soil Map of the Soviet Socialist Republic Moldavia.

Kukla, G., 1978. The classical European glacial stages: correlation with deep-sea sediments. Transactions of the Nebraska Academy of Science and Affiliated Societies VI, 57–93.

Kukla, G., Cílek, V., 1996. Plio-Pleistocene megacycles: record of climate and tectonics. Palaeogeography, Palaeoclimatology, Palaeoecology 120, 171–194. https://doi.org/10.1016/0031-0182(95)00040-2

Kukla, G.J., 1977. Pleistocene land—sea correlations I. Europe. Earth-Science Reviews 13, 307–374. https://doi.org/10.1016/0012-8252(77)90125-8

Kukla, G.J., 1975. Loess stratigraphy of Central Europe. In: K.W. Butzer and G.LI. Isaac (Editors), After the Australopithecines. Mouton, The Hague, pp. 99–188.

Küster, M., Preusser, F., 2010. Late Glacial and Holocene aeolian sands and soil formation from the Pomeranian outwash plain (Mecklenburg, NE-Germany). E&G – Quaternary Science Journal 58, 156–163. https://doi.org/10.23689/fidgeo-1050

Lancaster, N., 2020. On the formation of desert loess. Quat. res. 96, 105–122. https://doi.org/10.1017/qua.2020.33
Łanczont, M., Bogucki, A., Yatsyshyn, A., Terpiłowski, S., Mroczek, P., Orłowska, A., Hołub, B., Zieliński, P., Komar, M., Woronko, B., Kulesza, P., Dmytruk, R., Tomeniuk, O., 2019. Stratigraphy and chronology of the periphery of the Scandinavian ice sheet at the foot of the Ukrainian Carpathians. Palaeogeography, Palaeoclimatology, Palaeoecology 530, 59–77. https://doi.org/10.1016/j.palaeo.2019.05.024
Łanczont, M., Wojtanowicz, J., 2009. Typologia przestrzenna lessów Europy (Spatial typology of European loess). [In:] A. Kostrzewski, R. Paluszkiewicz (ed.), Geneza, litologia i stratygrafia utworów czwartorzędowych, t. V, Seria Geografia nr 88. pp. 301–314.
Lautridou, J.-P., 1987. Données nouvelles sur le Quaternaire de Normandie. Quaternaire 24, 161–164. https://doi.org/10.3406/quate.1987.1843
Leger, M., 1990. Loess landforms. Quaternary International 7–8, 53–61. https://doi.org/10.1016/1040-6182(90)90038-6
Lehmkuhl, F., Bösken, J., Hošek, J., Sprafke, T., Marković, S.B., Obreht, I., Hambach, U., Sümegi, P., Thiemann, A., Steffens, S., Lindner, H., Veres, D., Zeeden, C., 2018a. Loess distribution and related Quaternary sediments in the Carpathian Basin. Journal of Maps 14, 661–670. https://doi.org/10.1080/17445647.2018.1526720
Lehmkuhl, F., Hilgers, A., Fries, S., Hülle, D., Schlütz, F., Shumilovskikh, L., Felauer, T., Protze, J., 2011. Holocene geomorphological processes and soil development as indicator for environmental change around Karakorum, Upper Orkhon Valley (Central Mongolia). Catena 87, 31–44. https://doi.org/10.1016/j.catena.2011.05.005
Lehmkuhl, F., Hülle, D., Knippertz, M., 2012. Holocene geomorphic processes and landscape evolution in the lower reaches of the Orkhon River (northern Mongolia). Catena 98, 17–28. https://doi.org/10.1016/j.catena.2012.06.003
Lehmkuhl, F., Klinge, M., Rees-Jones, J., Rhodes, E.J., 2000. Late Quaternary aeolian sedimentation in central and south-eastern Tibet. Quaternary International, Nat Rutter Honorarium 68–71, 117–132. https://doi.org/10.1016/S1040-6182(00)00038-0
Lehmkuhl, F., Pötter, S., Pauligk, A., Bösken, J., 2018b. Loess and other quaternary sediments in Germany. Journal of Maps 14, 330–340. https://doi.org/10.1080/17445647.2018.1473817
Lehmkuhl, F., Schulte, P., Zhao, H., Hülle, D., Protze, J., Stauch, G., 2014. Timing and spatial distribution of loess and loess-like sediments in the mountain areas of the northeastern Tibetan Plateau. Catena, Loess and dust dynamics, environments, landforms, and pedogenesis: a tribute to Edward Derbyshire 117, 23–33. https://doi.org/10.1016/j.catena.2013.06.008
Lehmkuhl, F., Zens, J., Krauß, L., Schulte, P., Kels, H., 2016. Loess-paleosol sequences at the northern European loess belt in Germany: Distribution, geomorphology and stratigraphy. Quaternary Science Reviews 153, 11–30. https://doi.org/10.1016/j.quascirev.2016.10.008
Leonova, N., Nesmeyanov, S., Vinogradova, E., Voeykova, O., 2015. Upper Paleolithic subsistence practices in the southern Russian Plain: paleolandscapes and settlement system of Kamennaya Balka sites. Quaternary International 355, 175–187. https://doi.org/10.1016/j.quaint.2014.10.004
Li, Y., Shi, W., Aydin, A., Beroya-Eitner, M.A., Gao, G., 2020. Loess genesis and worldwide distribution. Earth-Science Reviews 201, 102947. https://doi.org/10.1016/j.earscirev.2019.102947
Liang, Y., Yang, T., Velichko, A.A., Zeng, B., Shi, P., Wang, L., He, Y., Chen, J., Chen, Y., 2016. Paleoclimatic record from Chumbur-Kosa section in Sea of Azov region since Marine Isotope Stage 11. J. Mt. Sci. 13, 985–999. https://doi.org/10.1007/s11629-015-3738-9
Lindner, H., Lehmkuhl, F., Zeeden, C., 2017. Spatial loess distribution in the eastern Carpathian Basin: a novel approach based on geoscientific maps and data. Journal of Maps 13, 173–181. https://doi.org/10.1080/17445647.2017.1279083

Lindner, L., Bogutsky, A., Gozhik, P., Marciniak, B., Marks, L., Lanczont, M., Wojtanowicz, J., 2002. Correlation of main climatic glacial-interglacial and loess-palaeosol cycles in the Pleistocene of Poland and Ukraine. Acta Geologica Polonica 52, 459–469.

Little, E.C., Lian, O.B., Velichko, A.A., Morozova, T.D., Nechaev, V.P., Dlussky, K.G., Rutter, N.W., 2002. Quaternary stratigraphy and optical dating of loess from the east European Plain (Russia). Quaternary Science Reviews 21, 1745–1762. https://doi.org/10.1016/S0277-3791(01)00151-2

Liu, J., Liu, W., 2017. Soil nitrogen isotopic composition of the Xifeng loess-paleosol sequence and its potential for use as a paleoenvironmental proxy. Quaternary International 440, 35–41. https://doi.org/10.1016/j.quaint.2016.04.018

Lomax, J., Fuchs, M., Antoine, P., Rousseau, D.-D., Lagroix, F., Hatté, C., Taylor, S.N., Till, J.L., Debret, M., Moine, O., Jordanova, D., 2019. A luminescence-based chronology for the Harletz loess sequence, Bulgaria. Boreas 48, 179–194. https://doi.org/10.1111/bor.12348

Longman, J., Veres, D., Ersek, V., Salzmann, U., Hubay, K., Bormann, M., Wennrich, V., Schäbitz, F., 2017. Periodic input of dust over the Eastern Carpathians during the Holocene linked with Saharan desertification and human impact. Clim. Past 13, 897–917. https://doi.org/10.5194/cp-13-897-2017

Macoun, J., Šibrava, V., Tyráček, J., Kneblová-Vodičková, V., 1965. Kvartér Ostravska a Moravské brány. ÚÚG, Prague.

Maher, B.A., MengYu, H., Roberts, H.M., Wintle, A.G., 2003. Holocene loess accumulation and soil development at the western edge of the Chinese Loess Plateau: implications for magnetic proxies of palaeorainfall. Quaternary Science Reviews 22, 445–451. https://doi.org/10.1016/S0277-3791(02)00188-9

Makeev, A.O., 2009. Pedogenic alteration of aeolian sediments in the upper loess mantles of the Russian Plain. Quaternary International 209, 79–94. https://doi.org/10.1016/j.quaint.2009.03.007

Malicki, A., 1950. Geneza i rozmieszczenie lessów w środkowej i wschodniej Polsce (The origin and distribution of loess in Central and Eastern Poland). Annales UMCS, sec. B, 4, 8, 4, 8 195–228.

Marechal, R., Tavernier, R., 1970. Associations de sols – pédologie, 1:500.000, Atlas de Belguique, Planche 11B. L'Institut Géographique Militaire.

Marković, S.B., Bokhorst, M.P., Vandenberghe, J., McCoy, W.D., Oches, E.A., Hambach, U., Gaudenyi, T., Jovanović, M., Zöller, L., Stevens, T., Machalett, B., 2008. Late Pleistocene loess-palaeosol sequences in the Vojvodina region, north Serbia. Journal of Quaternary Science 23, 73–84. https://doi.org/10.1002/jqs.1124

Marković, S.B., Fitzsimmons, K.E., Sprafke, T., Gavrilović, D., Smalley, I.J., Jović, V., Svirčev, Z., Gavrilov, M.B., Bešlin, M., 2016. The history of Danube loess research. Quaternary International 399, 86–99.

Marković, S.B., Hambach, U., Stevens, T., Kukla, G.J., Heller, F., McCoy, W.D., Oches, E.A., Buggle, B., Zöller, L., 2011. The last million years recorded at the Stari Slankamen (Northern Serbia) loess-palaeosol sequence: revised chronostratigraphy and long-term environmental trends. Quaternary Science Reviews 30, 1142–1154. https://doi.org/10.1016/j.quascirev.2011.02.004

Marković, S.B., Korač, M., Mrđič, N., Buylaert, J.-P., Thiel, C., McLaren, S.J., Stevens, T., Tomič, N., Petič, N., Jovanovič, M., Vasiljević, D.A., Sümegi, P., Gavrilov, M.B., Obreht, I., 2014. Palaeoenvironment and geoconservation of mammoths from the Nosak loess–palaeosol sequence (Drmno, northeastern Serbia): Initial results and perspectives. Quaternary International 334–335, 30–39. https://doi.org/10.1016/j.quaint.2013.05.047

Marković, S.B., Oches, E., Sümegi, P., Jovanović, M., Gaudenyi, T., 2006. An introduction to the Middle and Upper Pleistocene loess–paleosol sequence at Ruma brickyard, Vojvodina, Serbia. Quaternary International 149, 80–86. https://doi.org/10.1016/j.quaint.2005.11.020

Marković, S.B., Oches, E.A., McCoy, W.D., Frechen, M., Gaudenyi, T., 2007. Malacological and sedimentological evidence for "warm" glacial climate from the Irig loess sequence, Vojvodina, Serbia. Geochemistry, Geophysics, Geosystems 8, Q09008. https://doi.org/10.1029/2006GC001565

Marković, S.B., Stevens, T., Kukla, G.J., Hambach, U., Fitzsimmons, K.E., Gibbard, P., Buggle, B., Zech, M., Guo, Z., Hao, Q., Wu, H., O'Hara Dhand, K., Smalley, I.J., Újvári, G., Sümegi, P., Timar-Gabor, A., Veres, D., Sirocko, F., Vasiljević, D.A., Jary, Z., Svensson, A., Jović, V., Lehmkuhl, F., Kovács, J., Svirčev, Z., 2015. Danube loess stratigraphy — Towards a pan-European loess stratigraphic model. Earth-Science Reviews 148, 228–258. https://doi.org/10.1016/j.earscirev.2015.06.005

Marković, S.B., Stevens, T., Mason, J., Vandenberghe, J., Yang, S., Veres, D., Újvári, G., Timar-Gabor, A., Zeeden, C., Guo, Z., Hao, Q., Obreht, I., Hambach, U., Wu, H., Gavrilov, M.B., Rolf, C., Tomić, N., Lehmkuhl, F., 2018a. Loess correlations – Between myth and reality. Palaeogeography, Palaeoclimatology, Palaeoecology 509, 4–23. https://doi.org/10.1016/j.palaeo.2018.04.018

Marković, S.B., Sümegi, P., Stevens, T., Schaetzl, R.J., Obreht, I., Chu, W., Buggle, B., Zech, M., Zech, R., Zeeden, C., Gavrilov, M.B., Perić, Z., Svirčev, Z., Lehmkuhl, F., 2018b. The Crvenka loess-paleosol sequence: A record of continuous grassland domination in the southern Carpathian Basin during the Late Pleistocene. Palaeogeography, Palaeoclimatology, Palaeoecology 509, 33–46. https://doi.org/10.1016/j.palaeo.2018.03.019

Marton, P., 1979. Paleomagnetism of the Mende brickyard exposure. Unknown Journal 55–61.

Maruszczak, H., 2000. Definition and classification of loesses and loess-like deposits (in Polish with Englisch summary). Przegląd Geologiczny 48, 580–586.

Maruszczak, H., 1991. Ogólna charakterystyka lessów w Polsce (General features of the loesses in Poland), in: Maruszczak, H., (Ed.), Podstawowe Profile Lessów w Polsce (Main Section of Loesses in Poland). Wyd. UMCS, Lublin, pp. 1–12.

Maruszczak, H., 1985. Main genetic features and relief of loess covers in southern Poland, in: Maruszczak, H., (Ed.), Problems of the Stratigraphy and Paleogeography of Loesses, Guide-Book of the International Symposium. UMCS Lublin, pp. 9–37.

Maruszczak, H., 1969. Une analyse paléogéographique de la répartition du loess polonaise et de ses caractéres lithologiques directifs (A paleogeographic analysis of the distribution of the Polish loess and its directive lithological characters). Biuletyn Peryglacjalny 20, 133–152.

Matenco, L., Munteanu, I., ter Borgh, M., Stanica, A., Tilita, M., Lericolais, G., Dinu, C., Oaie, G., 2016. The interplay between tectonics, sediment dynamics and gateways evolution in the Danube system from the Pannonian Basin to the western Black Sea. Science of The Total Environment 543, 807–827. https://doi.org/10.1016/j.scitotenv.2015.10.081

Mayr, C., Matzke-Karasz, R., Stojakowits, P., Lowick, S.E., Zolitschka, B., Heigl, T., Mollath, R., Theuerkauf, M., Weckend, M.-O., Bäumler, R., Gregor, H.-J., 2017. Palaeoenvironments during MIS 3 and MIS 2 inferred from lacustrine intercalations in the loess–palaeosol sequence at Bobingen (southern Germany). E&G Quaternary Sci. J. 66, 73–89. https://doi.org/10.5194/egqsj-66-73-2017

Meijs, E.P.M., 2002. Loess stratigraphy in Dutch and Belgian Limburg. E&G – Quaternary Science Journal 51, 114–130. http://dx.doi.org/10.23689/fidgeo-1322

Meijs, E.P.M., Peer, P. van, Warrimont, J.P.L.M.N. de, 2013. Geomorphologic context and proposed chronostratigraphic position of Lower Palaeolithic artefacts from the Op de Schans pit near Kesselt (Belgium) to the west of Maastricht. Netherlands Journal of Geosciences 91, 137–157. https://doi.org/10.1017/S0016774600001554

Meszner, S., Kreutzer, S., Fuchs, M., Faust, D., 2014. Identifying depositional and pedogenetic controls of Late Pleistocene loess-paleosol sequences (Saxony, Germany) by combined grain size and microscopic analyses. zeit fur geo supp 58, 63–90. https://doi.org/10.1127/0372-8854/2014/S-00169

Meszner, S., Kreutzer, S., Fuchs, M., Faust, D., 2013. Late Pleistocene landscape dynamics in Saxony, Germany: Paleoenvironmental reconstruction using loess-paleosol sequences. Quaternary International 296, 94–107. https://doi.org/10.1016/j.quaint.2012.12.040

Mikulčić Pavlaković, S., Crnjaković, M., Tibljaš, D., Šoufek, M., Wacha, L., Frechen, M., Lacković, D., 2011. Mineralogical and geochemical characteristics of Quaternary sediments from the Island of Susak (Northern Adriatic, Croatia). Quaternary International 234, 32–49. https://doi.org/10.1016/j.quaint.2010.02.005

Moine, O., Antoine, P., Hatté, C., Landais, A., Mathieu, J., Prud'homme, C., Rousseau, D.-D., 2017. The impact of Last Glacial climate variability in west-European loess revealed by radiocarbon dating of fossil earthworm granules. Proc Natl Acad Sci USA 114, 6209–6214. https://doi.org/10.1073/pnas.1614751114

Morozova, T.D., Nechaev, V.P., 1997. The valdai periglacial zone as an area of cryogenic soil formation. Quaternary International 41–42, 53–58. https://doi.org/10.1016/S1040-6182(96)00036-5

Moska, P., Adamiec, G., Jary, Z., 2012. High resolution dating of loess profile from Biały Kościół, south–west Poland. Quaternary Geochronology 10, 87–93. https://doi.org/10.1016/j.quageo.2012.04.003

Moska, P., Adamiec, G., Jary, Z., 2011. OSL dating and lithological characteristics of loess deposits from Biały Kościół. Geochronometria 38, 162–171. https://doi.org/10.2478/s13386-011-0013-x

Moska, P., Jary, Z., Adamiec, G., Bluszcz, A., 2019. Chronostratigraphy of a loess-palaeosol sequence in Biały Kościół, Poland using OSL and radiocarbon dating. Quaternary International 502, 4–17. https://doi.org/10.1016/j.quaint.2018.05.024

Muhs, D.R., 2014. Origins and Properties of Quaternary Loess Deposits, in: Reference Module in Earth Systems and Environmental Sciences. Elsevier. https://doi.org/10.1016/B978-0-12-409548-9.09431-8

Muhs, D.R., 2013. The geologic records of dust in the Quaternary. Aeolian Research 9, 3–48. https://doi.org/10.1016/j.aeolia.2012.08.001

Muhs, D.R., Bettis, E.A., 2003. Quaternary loess-Paleosol sequences as examples of climate-driven sedimentary extremes, in: Special Paper 370: Extreme Depositional Environments: Mega End Members in Geologic Time. Geological Society of America, pp. 53–74. https://doi.org/10.1130/0-8137-2370-1.53

Muhs, D.R., Budahn, J., Avila, A., Skipp, G., Freeman, J., Patterson, D., 2010. The role of African dust in the formation of Quaternary soils on Mallorca, Spain and implications for the genesis of Red Mediterranean soils. Quaternary Science Reviews 29, 2518–2543. https://doi.org/10.1016/j.quascirev.2010.04.013

Nawrocki, J., Bogucki, A.B., Gozhik, P., Łanczont, M., Pańczyk, M., Standzikowski, K., Komar, M., Rosowiecka, O., Tomeniuk, O., 2019. Fluctuations of the Fennoscandian Ice Sheet recorded in the anisotropy of magnetic susceptibility of periglacial loess from Ukraine. Boreas 48, 940–952. https://doi.org/10.1111/bor.12400

Nawrocki, J., Gozhik, P., Łanczont, M., Pańczyk, M., Komar, M., Bogucki, A., Williams, I.S., Czupyt, Z., 2018. Palaeowind directions and sources of detrital material archived in the Roxolany loess section (southern Ukraine). Palaeogeography, Palaeoclimatology, Palaeoecology 496, 121–135. https://doi.org/10.1016/j.palaeo.2018.01.028

Nawrocki, J., Łanczont, M., Rosowiecka, O., Bogucki, A.B., 2016. Magnetostratigraphy of the loess-palaeosol key Palaeolithic section at Korolevo (Transcarpathia, W Ukraine). Quaternary International 399, 72–85. https://doi.org/10.1016/j.quaint.2014.12.063

Necula, C., Dimofte, D., Panaiotu, C., 2015a. Rock magnetism of a loess-palaeosol sequence from the western Black Sea shore (Romania). Geophys. J. Int. 202, 1733–1748. https://doi.org/10.1093/gji/ggv250

Necula, C., Panaiotu, C., Schinteie, G., Palade, P., Kuncser, V., 2015b. Reconstruction of superparamagnetic particle grain size distribution from Romanian loess using frequency dependent magnetic susceptibility and temperature dependent Mössbauer spectroscopy. Global and Planetary Change 131, 89–103. https://doi.org/10.1016/j.gloplacha.2015.05.009

Neugebauer-Maresch, C., 2008. Krems-Hundssteig – Mammutjägerlager der Eiszeit. Ein Nutzungsareal paläolithischer Jäger- und Sammler(innen) vor 41.000–27.000 Jahren, Mitteilungen der Prähistorischen Kommission. ÖAW,. Wien.
Neugebauer-Maresch, C., 1993. Zur altsteinzeitlichen Besiedlungsgeschichte des Galgenberges von Stratzing/Krems-Rehberg. Archäologie Österreichs 4, 10–19.
Neugebauer-Maresch, C., Hambach, U., Anghelinu, M., 2014. Loess and the record of Upper Palaeolithic cultures in the Danube Basin. Quaternary International 351, 1–4. https://doi.org/10.1016/j.quaint.2014.10.041
Nigst, P.R., Haesaerts, P., Damblon, F., Frank-Fellner, C., Mallol, C., Viola, B., Götzinger, M., Niven, L., Trnka, G., Hublin, J.-J., 2014. Early modern human settlement of Europe north of the Alps occurred 43,500 years ago in a cold steppe-type environment. PNAS 201412201. https://doi.org/10.1073/pnas.1412201111
Nottebaum, V., Lehmkuhl, F., Stauch, G., Hartmann, K., Wünnemann, B., Schimpf, S., Lu, H., 2014. Regional grain size variations in aeolian sediments along the transition between Tibetan highlands and north-western Chinese deserts – the influence of geomorphological settings on aeolian transport pathways. Earth Surf. Process. Landforms 39, 1960–1978. https://doi.org/10.1002/esp.3590
Nottebaum, V., Stauch, G., Hartmann, K., Zhang, J., Lehmkuhl, F., 2015. Unmixed loess grain size populations along the northern Qilian Shan (China): Relationships between geomorphologic, sedimentologic and climatic controls. Quaternary International 372, 151–166. https://doi.org/10.1016/j.quaint.2014.12.071
Novothny, Á., Frechen, M., Horváth, E., Bradák, B., Oches, E.A., McCoy, W.D., Stevens, T., 2009. Luminescence and amino acid racemization chronology of the loess–paleosol sequence at Süttő, Hungary. Quaternary International 198, 62–76. https://doi.org/10.1016/j.quaint.2008.01.009
Novothny, Á., Frechen, M., Horváth, E., Wacha, L., Rolf, C., 2011. Investigating the penultimate and last glacial cycles of the Süttő loess section (Hungary) using luminescence dating, high-resolution grain size, and magnetic susceptibility data. Quaternary International, Loess in Eurasia 234, 75–85. https://doi.org/10.1016/j.quaint.2010.08.002
Novothny, Á., Horváth, E., Frechen, M., 2002. The loess profile at Albertirsa, Hungary—improvements in loess stratigraphy by luminescence dating. Quaternary International, Inception: Mechanisms, patterns and timing of ice sheet inception 95–96, 155–163. https://doi.org/10.1016/S1040-6182(02)00036-8
Obreht, I., Buggle, B., Catto, N., Marković, S.B., Bösel, S., Vandenberghe, D.A.G., Hambach, U., Svirčev, Z., Lehmkuhl, F., Basarin, B., Gavrilov, M.B., Jović, G., 2014. The Late Pleistocene Belotinac section (southern Serbia) at the southern limit of the European loess belt: Environmental and climate reconstruction using grain size and stable C and N isotopes. Quaternary International 334–335, 10–19. https://doi.org/10.1016/j.quaint.2013.05.037
Obreht, I., Hambach, U., Veres, D., Zeeden, C., Bösken, J., Stevens, T., Marković, S.B., Klasen, N., Brill, D., Burow, C., Lehmkuhl, F., 2017. Shift of large-scale atmospheric systems over Europe during late MIS 3 and implications for Modern Human dispersal. Scientific Reports 7, 5848. https://doi.org/10.1038/s41598-017-06285-x
Obreht, I., Zeeden, C., Hambach, U., Veres, D., Marković, S.B., Bösken, J., Svirčev, Z., Bačević, N., Gavrilov, M.B., Lehmkuhl, F., 2016. Tracing the influence of Mediterranean climate on Southeastern Europe during the past 350,000 years. Scientific Reports 6, 36334. https://doi.org/10.1038/srep36334
Obreht, I., Zeeden, C., Hambach, U., Veres, D., Marković, S.B., Lehmkuhl, F., 2019. A critical reevaluation of palaeoclimate proxy records from loess in the Carpathian Basin. Earth-Science Reviews 190, 498–520. https://doi.org/10.1016/j.earscirev.2019.01.020
Obruchev, V.A., 1945. Loess types and their origin. American Journal of Science 243, 256–262. https://doi.org/10.2475/ajs.243.5.256

Oliva, M., Palacios, D., Fernández-Fernández, J.M., Rodríguez-Rodríguez, L., García-Ruiz, J.M., Andrés, N., Carrasco, R.M., Pedraza, J., Pérez-Alberti, A., Valcárcel, M., Hughes, P.D., 2019. Late Quaternary glacial phases in the Iberian Peninsula. Earth-Science Reviews 192, 564–600. https://doi.org/10.1016/j.earscirev.2019.03.015

Orgiazzi, A., Ballabio, C., Panagos, P., Jones, A., Fernández-Ugalde, O., 2018. LUCAS Soil, the largest expandable soil dataset for Europe: a review: LUCAS Soil, pan-European open-access soil dataset. European Journal of Soil Science 69, 140–153. https://doi.org/10.1111/ejss.12499

Orth, A., 1872. Geognostische Durchforschung des Schlesischen Schwemmlandes zwischen dem Zobtener und Trebnitzer Gebirge. Wiegandt u. Hempel, Berlin, LVIII.

Ovejanu, I., Candrea, B., Crăciunescu, V., 1968. Harta Geologica a Reppublicii Socialiste Romania (Geological Map of the Socialist Republic of Romania) 1:200.000. Bukarest: Comittul de stat al geologiei Institutul geologic (State Geological Survey).

Pascher, G.A., 1999. Geologische Karte des Burgenlandes 1:200 000. Geologische Bundesanstalt.

Pécsi, M., 1990. Loess is not just the accumulation of dust. Quaternary International 7, 1–21.

Pécsi, M., 1987. The loess-paleosol and related subaereal sequence in Hungary. GeoJournal 15, 151–162. https://doi.org/10.1007/BF00157941

Pécsi, M., Richter, G., 1996. Löss - Herkunft - Gliederung - Landschaften. Zeitschrift für Geomorphologie, Supplementary Issues 98.

Pendea, I.F., Gray, J.T., Ghaleb, B., Tantau, I., Badarau, A.S., Nicorici, C., 2009. Episodic build-up of alluvial fan deposits during the Weichselian Pleniglacial in the western Transylvanian Basin, Romania and their paleoenvironmental significance. Quaternary International 198, 98–112. https://doi.org/10.1016/j.quaint.2008.05.002

Pendea, I.F., Tantau, I., Gray, J., Ghaleb, B., Beldean, C., Badarau, A.S., Miclea, A., Balc, R., Toth, A., 2008. Middle Weichselian paleoenvironments in north-western Transylvania: Sedimentology, palynology and malacofauna analysis. Acta Palaeontologica Romaniae 6, 349–358.

Peresani, M., Cremaschi, M., Ferraro, F., Falguères, C., Bahain, J.-J., Gruppioni, G., Sibilia, E., Quarta, G., Calcagnile, L., Dolo, J.-M., 2008. Age of the final Middle Palaeolithic and Uluzzian levels at Fumane Cave, Northern Italy, using 14C, ESR, 234U/230Th and thermoluminescence methods. Journal of Archaeological Science 35, 2986–2996. https://doi.org/10.1016/j.jas.2008.06.013

Péwé, T.L., 1955. Origin of the upland silt near Fairbanks, Alaska. Geol Soc America Bull 66, 699. https://doi.org/10.1130/0016-7606(1955)66[699:OOTUSN]2.0.CO;2

Pirson, S., Baele, J.-M., Balescu, S., Haesaerts, P., Juvigné, E., Meijs, E., Spagna, P., 2018. Green amphibole distribution as a stratigraphic tool in loess sequences from Belgium: A review. Quaternary International 485, 183–198. https://doi.org/10.1016/j.quaint.2017.06.026

Pouclet, A., Juvigne, E., 2009. The Eltville tephra, a late Pleistocene widespread tephra layer in Germany, Belgium and The Netherlands; symptomatic compositions of the minerals. Geol. Belg. 12, 93–103.

Profe, J., Neumann, L., Novothny, Á., Barta, G., Rolf, C., Frechen, M., Ohlendorf, C., Zolitschka, B., 2018a. Paleoenvironmental conditions and sedimentation dynamics in Central Europe inferred from geochemical data of the loess-paleosol sequence at Süttő (Hungary). Quaternary Science Reviews 196, 21–37. https://doi.org/10.1016/j.quascirev.2018.07.034

Profe, J., Wacha, L., Frechen, M., Ohlendorf, C., Zolitschka, B., 2018b. XRF scanning of discrete samples – A chemostratigraphic approach exemplified for loess-paleosol sequences from the Island of Susak, Croatia. Quaternary International 494, 34–51. https://doi.org/10.1016/j.quaint.2018.05.006

Prud'homme, C., Lécuyer, C., Antoine, P., Moine, O., Hatté, C., Fourel, F., Martineau, F., Rousseau, D.-D., 2016. Palaeotemperature reconstruction during the Last Glacial from δ 18 O of earthworm calcite granules from Nussloch loess sequence, Germany. Earth and Planetary Science Letters 442, 13–20. https://doi.org/10.1016/j.epsl.2016.02.045

Pye, K., 1995. The nature, origin and accumulation of loess. Quaternary Science Reviews, Aeolian Sediments in the Quaternary Record 14, 653–667. https://doi.org/10.1016/0277-3791(95)00047-X

R Core Team, 2014. R: A Language and Environment for Statistical Computing.

Rao, Z., Xu, Y., Xia, D., Xie, L., Chen, F., 2013. Variation and paleoclimatic significance of organic carbon isotopes of Ili loess in arid Central Asia. Organic Geochemistry 63, 56–63. https://doi.org/10.1016/j.orggeochem.2013.08.007

Roesner, U., 1990. Die Mainfränkische Lößprovinz. Sedimentologische, pedologische und morphodynamische Prozesse der Lößbildung während des Pleistozäns in Mainfranken. Mitteilungen der Fränkischen Geographischen Gesellschaft 37, 1–290.

Rolf, C., Hambach, U., Novothny, Á., Horváth, E., Schnepp, E., 2014. Dating of a Last Glacial loess sequence by relative geomagnetic palaeointensity: A case study from the Middle Danube Basin (Süttő, Hungary). Quaternary International, Loess Research and Lithostratigraphy in Hungary 319, 99–108. https://doi.org/10.1016/j.quaint.2013.08.050

Rousseau, D.-D., 2001. Loess biostratigraphy: new advances and approaches in mollusk studies. Earth-Science Reviews, Recent research on loess and palaeosols, pure and applied 54, 157–171. https://doi.org/10.1016/S0012-8252(01)00046-0

Rousseau, D.-D., 1987. Paleoclimatology of the Achenheim series (middle and upper pleistocene, Alsace, France) A. malacological analysis. Palaeogeography, Palaeoclimatology, Palaeoecology 59, 293–314.

Rousseau, D.-D., Antoine, P., Boers, N., Lagroix, F., Ghil, M., Lomax, J., Fuchs, M., Debret, M., Hatté, C., Moine, O., Gauthier, C., Jordanova, D., Jordanova, N., 2020. Dansgaard-Oeschger-like events of the penultimate climate cycle: the loess point of view. Clim. Past 16, 713–727. https://doi.org/10.5194/cp-16-713-2020

Rousseau, D.-D., Antoine, P., Gerasimenko, N., Sima, A., Fuchs, M., Hatté, C., Moine, O., Zoeller, L., 2011. North Atlantic abrupt climatic events of the last glacial period recorded in Ukrainian loess deposits. Clim. Past 7, 221–234. https://doi.org/10.5194/cp-7-221-2011

Rousseau, D.-D., Chauvel, C., Sima, A., Hatté, C., Lagroix, F., Antoine, P., Balkanski, Y., Fuchs, M., Mellett, C., Kageyama, M., Ramstein, G., Lang, A., 2014. European glacial dust deposits: Geochemical constraints on atmospheric dust cycle modeling: European Glacial Dust Deposits. Geophys. Res. Lett. 41, 7666–7674. https://doi.org/10.1002/2014GL061382

Rousseau, D.-D., Derbyshire, E., Antoine, P., Hatté, C., 2013. LOESS RECORDS | Europe, in: Mock, S.A.E.J. (Ed.), Encyclopedia of Quaternary Science (Second Edition). Elsevier, Amsterdam, pp. 606–619.

Rousseau, D.-D., Gerasimenko, N., Matviischina, Z., Kukla, G., 2001. Late Pleistocene Environments of the Central Ukraine. Quat. res. 56, 349–356. https://doi.org/10.1006/qres.2001.2270

Rousseau, D.-D., Puisségur, J.-J., 1990. A 350,000-year climatic record from the loess sequence of Achenheim, Alsace, France. Boreas 19, 203–216. https://doi.org/10.1111/j.1502-3885.1990.tb00446.x

Rousseau, D.-D., Sima, A., Antoine, P., Hatté, C., Lang, A., Zöller, L., 2007. Link between European and North Atlantic abrupt climate changes over the last glaciation. Geophys. Res. Lett. 34, L22713. https://doi.org/10.1029/2007GL031716

Rousseau, D.-D., Svensson, A., Bigler, M., Sima, A., Steffensen, J.P., Boers, N., 2017. Eurasian contribution to the last glacial dust cycle: how are loess sequences built? Clim. Past 13, 1181–1197. https://doi.org/10.5194/cp-13-1181-2017

Rousseau, D.-D., Zöller, L., Valet, J.-P., 1998. Late Pleistocene Climatic Variations at Achenheim, France, Based on a Magnetic Susceptibility and TL Chronology of Loess. Quaternary Research 49, 255–263. https://doi.org/10.1006/qres.1998.1972

Rubinić, V., Galović, L., Lazarević, B., Husnjak, S., Durn, G., 2018. Pseudogleyed loess derivates – The most common soil parent materials in the Pannonian region of Croatia. Quaternary International 494, 248–262. https://doi.org/10.1016/j.quaint.2017.06.044

Ruszkiczay-Rüdiger, Z., Kern, Z., 2015. Permafrost or seasonal frost? A review of paleoclimate proxies of the last glacial cycle in the East Central European lowlands. Quaternary International 415, 241–252. https://doi.org/10.1016/j.quaint.2015.07.027

Rutter, N.W., Rokosh, D., Evans, M.E., Little, E.C., Chlachula, J., Velichko, A., 2003. Correlation and interpretation of paleosols and loess across European Russia and Asia over the last interglacial–glacial cycle. Quat. res. 60, 101–109. https://doi.org/10.1016/S0033-5894(03)00069-3

Šajgalík, J., Modlitba, I., 1983. Spraše Podunajskej nížiny a ich vlastnosti (The loess of the Danube lowlands and their properties). VEDA. Bratislava.

Sanborn, P.T., Smith, C.A.S., Froese, D.G., Zazula, G.D., Westgate, J.A., 2006. Full-glacial paleosols in perennially frozen loess sequences, Klondike goldfields, Yukon Territory, Canada. Quat. res. 66, 147–157. https://doi.org/10.1016/j.yqres.2006.02.008

Săndulescu, M., Kräutner, H., Borcoș, M., Năstăseanu, S., Patrulius, D., Ștefănescu, M., Ghenea, C., Lupu, M., Savu, H., Bercia, I., Marinescu, F., 1978. România - Atlas geologic foaia 1 (Geological Atlas of Romania), scale 1:1,000,000.

Sauer, D., Kadereit, A., Kühn, P., Kösel, M., Miller, C.E., Shinonaga, T., Kreutzer, S., Herrmann, L., Fleck, W., Starkovich, B.M., Stahr, K., 2016. The loess-palaeosol sequence of Datthausen, SW Germany: Characteristics, chronology, and implications for the use of the Lohne Soil as a marker soil. Catena, Dan H. Yaalon Memorial Issue 146, 10–29. https://doi.org/10.1016/j.catena.2016.06.024

Schaetzl, R.J., Bettis, E.A., Crouvi, O., Fitzsimmons, K.E., Grimley, D.A., Hambach, U., Lehmkuhl, F., Marković, S.B., Mason, J.A., Owczarek, P., Roberts, H.M., Rousseau, D.-D., Stevens, T., Vandenberghe, J., Zárate, M., Veres, D., Yang, S., Zech, M., Conroy, J.L., Dave, A.K., Faust, D., Hao, Q., Obreht, I., Prud'homme, C., Smalley, I., Tripaldi, A., Zeeden, C., Zech, R., 2018. Approaches and challenges to the study of loess—Introduction to the LoessFest Special Issue. Quaternary Research 89, 563–618. https://doi.org/10.1017/qua.2018.15

Schaffernicht, E.J., Ludwig, P., Shao, Y., 2020. Linkage between dust cycle and loess of the Last Glacial Maximum in Europe. Atmospheric Chemistry and Physics 20, 4969–4986. https://doi.org/10.5194/acp-20-4969-2020

Schatz, A.-K., Buylaert, J.-P., Murray, A., Stevens, T., Scholten, T., 2012. Establishing a luminescence chronology for a palaeosol-loess profile at Tokaj (Hungary): A comparison of quartz OSL and polymineral IRSL signals. Quaternary geochronology 10, 68–74.

Schatz, A.-K., Qi, Y., Siebel, W., Wu, J., Zöller, L., 2015a. Tracking potential source areas of Central European loess: examples from Tokaj (HU), Nussloch (D) and Grub (AT). Open Geosciences 7, 678–720. https://doi.org/10.1515/geo-2015-0048

Schatz, A.-K., Scholten, T., Kühn, P., 2015b. Paleoclimate and weathering of the Tokaj (Hungary) loess–paleosol sequence. Palaeogeography, Palaeoclimatology, Palaeoecology 426, 170–182. https://doi.org/10.1016/j.palaeo.2015.03.016

Schatz, A.-K., Zech, M., Buggle, B., Gulyás, S., Hambach, U., Marković, S.B., Sümegi, P., Scholten, T., 2011. The late Quaternary loess record of Tokaj, Hungary: Reconstructing palaeoenvironment, vegetation and climate using stable C and N isotopes and biomarkers. Quaternary International, The Second Loessfest (2009) 240, 52–61. https://doi.org/10.1016/j.quaint.2010.10.009

Schirmer, W., 2016. Late Pleistocene loess of the Lower Rhine. Quaternary International 411, 44–61. https://doi.org/10.1016/j.quaint.2016.01.034

Schirmer, W., 2012. Rhine loess at Schwalbenberg II–MIS 4 and 3. Eiszeitalter & Gegenwart/Quaternary Science Journal 61.

Schirmer, W., 2003. Die Eben-Zone im Oberwürmlöss zwischen Maas und Rhein, in: Landschaftsgeschichte Im Europäischen Rheinland. pp. 351–416.

Schirrmeister, L., Froese, D., Tumskoy, V., Grosse, G., Wetterich, S., 2013. Permafrost and periglacial features | Yedoma: Late Pleistocene Ice-Rich Syngenetic Permafrost of Beringia, in:

Encyclopedia of Quaternary Science. Elsevier, pp. 542–552. https://doi.org/10.1016/B978-0-444-53643-3.00106-0
Schulte, P., Lehmkuhl, F., 2018. The difference of two laser diffraction patterns as an indicator for post-depositional grain size reduction in loess-paleosol sequences. Palaeogeography, Palaeoclimatology, Palaeoecology 509, 126–136. https://doi.org/10.1016/j.palaeo.2017.02.022
Schütz, L., 1980. Long range transport of dester dust with special emphasis on the Sahara. Ann NY Acad Sci 338, 515–532. https://doi.org/10.1111/j.1749-6632.1980.tb17144.x
Sebe, K., Csillag, G., Ruszkiczay-Rüdiger, Z., Fodor, L., Thamó-Bozsó, E., Müller, P., Braucher, R., 2011. Wind erosion under cold climate: A Pleistocene periglacial mega-yardang system in Central Europe (Western Pannonian Basin, Hungary). Geomorphology 134, 470–482. https://doi.org/10.1016/j.geomorph.2011.08.003
Semmel, A., 1998. Zur paläopedologischen Grundgliederung des älteren Würmlösses in Mitteleuropa. Mitteilungen deutscher bodenkundlichen Gesellschaft 88, 449–452.
Semmel, A., Terhorst, B., 2010. The concept of the Pleistocene periglacial cover beds in central Europe: A review. Quaternary International 222, 120–128. https://doi.org/10.1016/j.quaint.2010.03.010
Sima, A., Rousseau, D.-D., Kageyama, M., Ramstein, G., Schulz, M., Balkanski, Y., Antoine, P., Dulac, F., Hatté, C., 2009. Imprint of North-Atlantic abrupt climate changes on western European loess deposits as viewed in a dust emission model. Quaternary Science Reviews 28, 2851–2866. https://doi.org/10.1016/j.quascirev.2009.07.016
Skurzyński, J., Jary, Z., Kenis, P., Kubik, R., Moska, P., Raczyk, J., Seul, C., 2020. Geochemistry and mineralogy of the Late Pleistocene loess-palaeosol sequence in Złota (near Sandomierz, Poland): Implications for weathering, sedimentary recycling and provenance. Geoderma 375, 114459. https://doi.org/10.1016/j.geoderma.2020.114459
Smalley, I., 1995. Making the material: The formation of silt sized primary mineral particles for loess deposits. Quaternary Science Reviews 14, 645–651. https://doi.org/10.1016/0277-3791(95)00046-1
Smalley, I., Leach, J.A., 1978. The origin and distribution of the loess in the Danube basin and associated regions of East-Central Europe — A review. Sedimentary Geology 21, 1–26. https://doi.org/10.1016/0037-0738(78)90031-3
Smalley, I., Marković, S.B., Svirčev, Z., 2011. Loess is [almost totally formed by] the accumulation of dust. Quaternary International 240, 4–11. https://doi.org/10.1016/j.quaint.2010.07.011
Smalley, I., Obreht, I., 2018. The formation of loess ground by the process of loessification: a history of the concept. Geologos 24, 163–170. https://doi.org/10.2478/logos-2018-0015
Smalley, I., O'Hara-Dhand, K., Wint, J., Machalett, B., Jary, Z., Jefferson, I., 2009. Rivers and loess: The significance of long river transportation in the complex event-sequence approach to loess deposit formation. Quaternary International 198, 7–18. https://doi.org/10.1016/j.quaint.2008.06.009
Smalley, I.J., 1971. "In-situ" theories of loess formation and the significance of the calcium-carbonate content of loess. Earth-Science Reviews 7, 67–85. https://doi.org/10.1016/0012-8252(71)90082-1
Sokolovsky, A.N., Krupsky, N.K., Voronin, A.V., Bogdanovich, V.G., 1977a. Soil Map of Ukraine.
Sokolovsky, A.N., Krupsky, N.K., Voronin, A.V., Bogdanovich, V.G., 1977b. Soil Map of Ukraine.
Sprafke, T., 2016. Löss in Niederösterreich – Archiv quartärer Klima- und Landschaftsveränderungen (Loess in Lower Austria - archive of Quaternary climate and landscape development). Würzburg University Press, Würzburg.
Sprafke, T., Obreht, I., 2016. Loess: Rock, sediment or soil – What is missing for its definition? Quaternary International 399, 198–207. https://doi.org/10.1016/j.quaint.2015.03.033
Sprafke, T., Thiel, C., Terhorst, B., 2014. From micromorphology to palaeoenvironment: The MIS 10 to MIS 5 record in Paudorf (Lower Austria). Catena 117, 60–72. https://doi.org/10.1016/j.catena.2013.06.024

Stauch, G., IJmker, J., Pötsch, S., Zhao, H., Hilgers, A., Diekmann, B., Dietze, E., Hartmann, K., Opitz, S., Wünnemann, B., Lehmkuhl, F., 2012. Aeolian sediments on the north-eastern Tibetan Plateau. Quaternary Science Reviews 57, 71–84. https://doi.org/10.1016/j.quascirev.2012.10.001

Steup, R., Fuchs, M., 2017. The loess sequence at Münzenberg (Wetterau/Germany): A reinterpretation based on new luminescence dating results. Zeitschrift für Geomorphologie, Supplementary Issues 61, 101–120. https://doi.org/10.1127/zfg_suppl/2016/0408

Stojak, J., McDevitt, A.D., Herman, J.S., Searle, J.B., Wójcik, J.M., 2015. Post-glacial colonization of eastern Europe from the Carpathian refugium: evidence from mitochondrial DNA of the common vole Microtus arvalis. Biol J Linn Soc 115, 927–939. https://doi.org/10.1111/bij.12535

Strauss, J., Schirrmeister, L., Grosse, G., Fortier, D., Hugelius, G., Knoblauch, C., Romanovsky, V., Schädel, C., Schneider von Deimling, T., Schuur, E.A.G., Shmelev, D., Ulrich, M., Veremeeva, A., 2017. Deep Yedoma permafrost: A synthesis of depositional characteristics and carbon vulnerability. Earth-Science Reviews 172, 75–86. https://doi.org/10.1016/j.earscirev.2017.07.007

Strunk, H., 1990. Das Quartärprofil von Hagelstadt im Bayerischen Tertiärhügelland. Eiszeitalter und Gegenwart 40, 85–96.

Sümegi, P., Gulyás, S., Molnár, D., Náfrádi, K., Törőcsik, T., Sümegi, B.P., Müller, T., Szilágyi, G., Varga, Z., 2017. Ice Age Terrestrial and Freshwater Gastropod Refugia in the Carpathian Basin, Central Europe. Biological Resources of Water. https://doi.org/10.5772/intechopen.71910

Sümegi, P., Gulyás, S., Persaits, G., GergelyPáll, D., Molnár, D., 2011. The loess-paleosol sequence of Basaharc (Hungary) revisited: Mollusc-based paleoecological results for the Middle and Upper Pleistocene. Quaternary International 240, 181–192. https://doi.org/10.1016/j.quaint.2011.05.005

Sümegi, P., Krolopp, E., 2002. Quatermalacological analyses for modeling of the Upper Weichselian palaeoenvironmental changes in the Carpathian Basin. Quaternary International 91, 53–63. https://doi.org/10.1016/S1040-6182(01)00102-1

Sümegi, P., Magyari, E., Dániel, P., Molnár, M., Törőcsik, T., 2013. Responses of terrestrial ecosystems to Dansgaard–Oeshger cycles and Heinrich-events: A 28,000-year record of environmental changes from SE Hungary. Quaternary International, Advancing Pleistocene and Holocene climate change research in the Carpathian-Balkan region 293, 34–50. https://doi.org/10.1016/j.quaint.2012.07.032

Sümegi, P., Marković, S.B., Molnár, D., Sávai, S., Náfrádi, K., Szelepcsényi, Z., Novák, Z., 2016a. Črvenka loess-paleosol sequence revisited: local and regional Quaternary biogeographical inferences of the southern Carpathian Basin. Open Geosciences 8, 390–404. https://doi.org/10.1515/geo-2016-0031

Sümegi, P., Rudner, E., Beszeda, I., 2000. Stratigraphical and palaeoecological investigation of the fossil soil comprising Upper Palaeolithic tools at Bodrogkeresztúr – Henye, in: Dobosi, T. V. (Ed.) Bodrogkeresztúr – Henye (NE Hungary) Upper Palaeolithic Site. Magyar Nemzeti Múzeum Kiadványa, Budapest, pp. 217–220.

Sümegi, P., Törőcsik, T., Náfrádi, K., Sümegi, B., Majkut, P., Molnár, D., Tapody, R., 2016b. Radiocarbon dated complex paleoecological and geoarcheological analyses at the Bodrogkeresztúr-Henye Gravettian site (NE Hungary). Archeometriai Műhely 2016/XIII./1., 31–41.

Svirčev, Z., Dulić, T., Obreht, I., Codd, G.A., Lehmkuhl, F., Marković, S.B., Hambach, U., Meriluoto, J., 2019. Cyanobacteria and loess—an underestimated interaction. Plant Soil 439, 293–308. https://doi.org/10.1007/s11104-019-04048-3

Svirčev, Z., Marković, S.B., Stevens, T., Codd, G.A., Smalley, I., Simeunović, J., Obreht, I., Dulić, T., Pantelić, D., Hambach, U., 2013. Importance of biological loess crusts for loess formation in semi-arid environments. Quaternary International, Closing the gap - North Carpathian loess traverse in the Eurasian loess belt 6th Loess Seminar, Wrocław, Poland Dedicated to Prof. Henryk Maruszczak 296, 206–215. https://doi.org/10.1016/j.quaint.2012.10.048

Sycheva, S., Frechen, M., Terhorst, B., Sedov, S., Khokhlova, O., 2020. Pedostratigraphy and chronology of the Late Pleistocene for the extra glacial area in the Central Russian Upland (reference section Aleksandrov quarry). Catena 194, 104689. https://doi.org/10.1016/j.catena.2020.104689

Tecsa, V., Gerasimenko, N., Veres, D., Hambach, U., Lehmkuhl, F., Schulte, P., Timar-Gabor, A., 2020. Revisiting the chronostratigraphy of Late Pleistocene loess-paleosol sequences in southwestern Ukraine: OSL dating of Kurortne section. Quaternary International. https://doi.org/10.1016/j.quaint.2020.03.001

Terhorst, B., 2013. A stratigraphic concept for Middle Pleistocene Quaternary sequences in Upper Austria. E&G Quaternary Science Journal 62, 4–13. https://doi.org/10.3285/eg.62.1.01

Terhorst, B., Sedov, S., Sprafke, T., Peticzka, R., Meyer-Heintze, S., Kühn, P., Solleiro Rebolledo, E., 2015. Austrian MIS 3/2 loess–palaeosol records—Key sites along a west–east transect. Palaeogeography, Palaeoclimatology, Palaeoecology 418, 43–56. https://doi.org/10.1016/j.palaeo.2014.10.020

Terhorst, B., Thiel, C., Peticzka, R., Sprafke, T., Frechen, M., Fladerer, F.A., Roetzel, R., Neugebauer-Maresch, C., 2011. Casting new light on the chronology of the loess/paleosol sequences in Lower Austria. E&G Quaternary Science Journal 60, 270–277. https://doi.org/10.3285/eg.60.2-3.04

Torre, G., Gaiero, D.M., Cosentino, N.J., Coppo, R., 2020. The paleoclimatic message from the polymodal grain-size distribution of late Pleistocene-early Holocene Pampean loess (Argentina). Aeolian Research 42, 100563. https://doi.org/10.1016/j.aeolia.2019.100563

Tóth, G., Jones, A., Montanarella, L., European Commission, Joint Research Centre, Institute for Environment and Sustainability, 2013. LUCAS topsoil survey: methodology, data and results. Publications Office, Luxembourg.

Tsatskin, A., Heller, F., Hailwood, E.A., Gendler, T.S., Hus, J., Montgomery, P., Sartori, M., Virina, E.I., 1998. Pedosedimentary division, rock magnetism and chronology of the loess/palaeosol sequence at Roxolany (Ukraine). Palaeogeography, Palaeoclimatology, Palaeoecology 143, 111–133. https://doi.org/10.1016/S0031-0182(98)00073-X

Tsoar, H., Pye, K., 1987. Dust transport and the question of desert loess formation. Sedimentology 34, 139–153. https://doi.org/10.1111/j.1365-3091.1987.tb00566.x

Tutkovsky, P.A., 1899. K woprosu o sposobje obrazovanija lossa (The question of the origin of loess). Zemlevedenie 1–2, 213–311.

Újvári, G., Kok, J.F., Varga, G., Kovács, J., 2016. The physics of wind-blown loess: Implications for grain size proxy interpretations in Quaternary paleoclimate studies. Earth-Science Reviews 154, 247–278. https://doi.org/10.1016/j.earscirev.2016.01.006

Újvári, G., Kovács, J., Varga, G., Raucsik, B., Marković, S.B., 2010. Dust flux estimates for the Last Glacial Period in East Central Europe based on terrestrial records of loess deposits: a review. Quaternary Science Reviews 29, 3157–3166. https://doi.org/10.1016/j.quascirev.2010.07.005

Újvári, G., Stevens, T., Molnár, M., Demény, A., Lambert, F., Varga, G., Jull, A.J.T., Páll-Gergely, B., Buylaert, J.-P., Kovács, J., 2017. Coupled European and Greenland last glacial dust activity driven by North Atlantic climate. PNAS 114, E10632–E10638. https://doi.org/10.1073/pnas.1712651114

Újvári, G., Varga, A., Balogh-Brunstad, Z., 2008. Origin, weathering, and geochemical composition of loess in southwestern Hungary. Quaternary Research 69, 421–437. https://doi.org/10.1016/j.yqres.2008.02.001

van Baelen, A., 2017. The Lower to Middle Palaeolithic Transition in Northwestern Europe: Evidence from Kesselt-Op de Schans, 01 ed. Leuven University Press, Leuven, Belgium.

Vancampenhout, K., Langohr, R., Slaets, J., Buurman, P., Swennen, R., Deckers, J., 2013. Paleo-pedological record of the Rocourt Pedosequence at Veldwezelt–Hezerwater (Belgian

Pleistocene loess belt): Part 1 — Evolution of the parent material. CATENA 107, 118–129. https://doi.org/10.1016/j.catena.2013.02.005

Vandenberghe, J., French, H.M., Gorbunov, A., Marchenko, S., Velichko, A.A., Jin, H., Cui, Z., Zhang, T., Wan, X., 2014a. The Last Permafrost Maximum (LPM) map of the Northern Hemisphere: permafrost extent and mean annual air temperatures, 25-17 ka BP: The Last Permafrost Maximum (LPM) map of the Northern Hemisphere. Boreas 43, 652–666. https://doi.org/10.1111/bor.12070

Vandenberghe, J., Huijzer, B.S., Mücher, H., Laan, W., 1998. Short climatic oscillations in a western European loess sequence (Kesselt, Belgium). J. Quaternary Sci. 13, 471–485. https://doi.org/10.1002/(SICI)1099-1417(1998090)13:5<471::AID-JQS401>3.0.CO;2-T

Vandenberghe, J., Markovič, S.B., Jovanovič, M., Hambach, U., 2014b. Site-specific variability of loess and palaeosols (Ruma, Vojvodina, northern Serbia). Quaternary International, ED@80: Loess in China and Europe - A Tribute to Edward Derbyshire 334–335, 86–93. https://doi.org/10.1016/j.quaint.2013.10.036

Vandenberghe, J., Renssen, H., van Huissteden, K., Nugteren, G., Konert, M., Lu, H., Dodonov, A., Buylaert, J.-P., 2006. Penetration of Atlantic westerly winds into Central and East Asia. Quaternary Science Reviews 25, 2380–2389. https://doi.org/10.1016/j.quascirev.2006.02.017

Vandenberghe, J., Sun, Y., Wang, X., Abels, H.A., Liu, X., 2018. Grain-size characterization of reworked fine-grained aeolian deposits. Earth-Science Reviews 177, 43–52. https://doi.org/10.1016/j.earscirev.2017.11.005

Varga, G., Cserháti, C., Kovács, J., Szalai, Z., 2016. Saharan dust deposition in the Carpathian Basin and its possible effects on interglacial soil formation. Aeolian Research 22, 1–12.

Varga, G., Kovács, J., Újvári, G., 2013. Analysis of Saharan dust intrusions into the Carpathian Basin (Central Europe) over the period of 1979–2011. Global and Planetary Change 100, 333–342. https://doi.org/10.1016/j.gloplacha.2012.11.007

Varga, G., Újvári, G., Kovács, J., 2019. Interpretation of sedimentary (sub)populations extracted from grain size distributions of Central European loess-paleosol series. Quaternary International 502, 60–70. https://doi.org/10.1016/j.quaint.2017.09.021

Vaškovský, I., 1977. Kvartér Slovenska. – Geologický ústav Dionýza Štúra. Bratislava. 247 pp. in Slovak. Bratislava.

Velichko, A.A., 1990. Loess-paleosol formation on the Russian plain. Quaternary International 7–8, 103–114. https://doi.org/10.1016/1040-6182(90)90044-5

Velichko, A.A., Catto, N.R., Yu Kononov, M., Morozova, T.D., Yu Novenko, E., Panin, P.G., Ya Ryskov, G., Semenov, V.V., Timireva, S.N., Titov, V.V., Tesakov, A.S., 2009. Progressively cooler, drier interglacials in southern Russia through the Quaternary: Evidence from the Sea of Azov region. Quaternary International 198, 204–219. https://doi.org/10.1016/j.quaint.2008.06.005

Velichko, A.A., Morozova, T.D., Nechaev, V.P., Rutter, N.W., Dlusskii, K.G., Little, E.C., Catto, N.R., Semenov, V.V., Evans, M.E., 2006. Loess/paleosol/cryogenic formation and structure near the northern limit of loess deposition, East European Plain, Russia. Quaternary International 152–153, 14–30. https://doi.org/10.1016/j.quaint.2005.12.003

Veres, D., Lane, C.S., Timar-Gabor, A., Hambach, U., Constantin, D., Szakács, A., Fülling, A., Onac, B.P., 2013. The Campanian Ignimbrite/Y5 tephra layer–A regional stratigraphic marker for Isotope Stage 3 deposits in the Lower Danube region, Romania. Quaternary International 293, 22–33.

Veres, D., Tecsa, V., Gerasimenko, N., Zeeden, C., Hambach, U., Timar-Gabor, A., 2018. Short-term soil formation events in last glacial east European loess, evidence from multi-method luminescence dating. Quaternary Science Reviews 200, 34–51. https://doi.org/10.1016/j.quascirev.2018.09.037

Vetters, H., 1933. Geologische Karte der Republik Österreich und der Nachbargebiete (Die Ostalpen, ihre Ausläufer und Vorlande nebst den angrenzenden Teilen der fränkischen Alb und des böhmischen Massivs). (Geological Map of the Austrian Republic and its neighbouring regions

- the eastern alps, its foothills and forelands, the neighbouring parts of Franconian Jura and the Bohemian Massif). 1 : 500,000.

von Suchodoletz, H., Oberhänsli, H., Hambach, U., Zöller, L., Fuchs, M., Faust, D., 2010. Soil moisture fluctuations recorded in Saharan dust deposits on Lanzarote (Canary Islands) over the last 180ka. Quaternary Science Reviews 29, 2173–2184. https://doi.org/10.1016/j.quascirev.2010.05.014

Wacha, L., Frechen, M., 2011. The geochronology of the “Gorjanović loess section” in Vukovar, Croatia. Quaternary International, The Second Loessfest (2009) 240, 87–99. https://doi.org/10.1016/j.quaint.2011.04.010

Wacha, L., Galović, L., Koloszár, L., Magyari, Á., Chikán, G., Marsi, I., 2013. The chronology of the Šarengrad II loess-palaeosol section (Eastern Croatia). Geol Cro 66, 191–203. https://doi.org/10.4154/GC.2013.18

Wacha, L., Mikulčić Pavlaković, S., Frechen, M., Crnjaković, M., 2011a. The Loess Chronology of the Island of Susak, Croatia. Quaternary Science Journal - EuG 60, 153–169. https://doi.org/10.3285/eg.60.1.11

Wacha, L., Mikulčić Pavlaković, S., Novothny, Á., Crnjaković, M., Frechen, M., 2011b. Luminescence dating of Upper Pleistocene loess from the Island of Susak in Croatia. Quaternary International 234, 50–61. https://doi.org/10.1016/j.quaint.2009.12.017

Wacha, L., Rolf, C., Hambach, U., Frechen, M., Galović, L., Duchoslav, M., 2018. The Last Glacial aeolian record of the Island of Susak (Croatia) as seen from a high-resolution grain–size and rock magnetic analysis. Quaternary International 494, 211–224. https://doi.org/10.1016/j.quaint.2017.08.016

Wagner, M., M, W., 1979. Mollusc Fauna of the Mende Loess Profile.

Walter, H., 1974. Die Vegetation Osteuropas, Nord- und Zentralasiens, Vegetationsmonographien der einzelnen Grossräume. G. Fischer, Stuttgart.

Wei, H., Wang, L., Azarmdel, H., Khormali, F., Frechen, M., Li, G., Chen, F., 2020. Quartz OSL dating of loess deposits since the late glacial in the Southeast of Caspian Sea. Quaternary International S1040618220302068. https://doi.org/10.1016/j.quaint.2020.04.042

Whittle, A.W.R., Whittle, A.W.R., 1996. Europe in the Neolithic: the creation of new worlds, Cambridge world archaeology. Cambridge University Press, Cambridge ; New York.

Willmes, C., 2015. LGM sealevel change (HiRes), CRC806 database, Collaborative Research Centre 806.

Wolf, D., Kolb, T., Alcaraz-Castaño, M., Heinrich, S., Baumgart, P., Calvo, R., Sánchez, J., Ryborz, K., Schäfer, I., Bliedtner, M., Zech, R., Zöller, L., Faust, D., 2018. Climate deteriorations and Neanderthal demise in interior Iberia. Sci Rep 8, 7048. https://doi.org/10.1038/s41598-018-25343-6

Wolf, D., Ryborz, K., Kolb, T., Zapata, R.C., Vizcaino, J.S., Zöller, L., Faust, D., 2019. Origins and genesis of loess deposits in central Spain, as indicated by heavy mineral compositions and grain-size variability. Sedimentology 66, 1139–1161. https://doi.org/10.1111/sed.12539

Wright, J.S., 2001. “Desert” loess versus “glacial” loess: quartz silt formation, source areas and sediment pathways in the formation of loess deposits. Geomorphology 36, 231–256. https://doi.org/10.1016/S0169-555X(00)00060-X

Yang, Fei, Zhang, G.-L., Sauer, D., Yang, Fan, Yang, R.-M., Liu, F., Song, X.-D., Zhao, Y.-G., Li, D.-C., Yang, J.-L., 2020. The geomorphology – sediment distribution – soil formation nexus on the northeastern Qinghai-Tibetan Plateau: Implications for landscape evolution. Geomorphology 354, 107040. https://doi.org/10.1016/j.geomorph.2020.107040

Yang, S., Fang, X., Shi, Z., Lehmkuhl, F., Song, C., Han, Y., Han, W., 2010. Timing and provenance of loess in the Sichuan Basin, southwestern China. Palaeogeography, Palaeoclimatology, Palaeoecology 292, 144–154. https://doi.org/10.1016/j.palaeo.2010.03.039

Yang, S.L., Ding, Z.L., 2003. Color reflectance of Chinese loess and its implications for climate gradient changes during the last two glacial-interglacial cycles: Color Reflectance of Chinese Loess. Geophys. Res. Lett. 30. https://doi.org/10.1029/2003GL018346

Zagwijn, W.H., Van Staalduinen, C.J., 1975. Toelichtingen bij the geologische overzichtskarten van Nederland.

Zech, R., Zech, M., Marković, S., Hambach, U., Huang, Y., 2013. Humid glacials, arid interglacials? Critical thoughts on pedogenesis and paleoclimate based on multi-proxy analyses of the loess–paleosol sequence Crvenka, Northern Serbia. Palaeogeography, Palaeoclimatology, Palaeoecology 387, 165–175. https://doi.org/10.1016/j.palaeo.2013.07.023

Zeeberg, J., 1998. The European sand belt in eastern Europe - and comparison of Late Glacial dune orientation with GCM simulation results. Boreas 27, 127–139. https://doi.org/10.1111/j.1502-3885.1998.tb00873.x

Zeeden, C., Hambach, U., Veres, D., Fitzsimmons, K., Obreht, I., Bösken, J., Lehmkuhl, F., 2018. Millennial scale climate oscillations recorded in the Lower Danube loess over the last glacial period. Palaeogeography, Palaeoclimatology, Palaeoecology 509, 164–181. https://doi.org/10.1016/j.palaeo.2016.12.029

Zeeden, C., Kels, H., Hambach, U., Schulte, P., Protze, J., Eckmeier, E., Marković, S.B., Klasen, N., Lehmkuhl, F., 2016. Three climatic cycles recorded in a loess-palaeosol sequence at Semlac (Romania) – Implications for dust accumulation in south-eastern Europe. Quaternary Science Reviews 154, 130–142. https://doi.org/10.1016/j.quascirev.2016.11.002

Zeeden, C., Obreht, I., Veres, D., Kaboth-Bahr, S., Hošek, J., Marković, S.B., Bösken, J., Lehmkuhl, F., Rolf, C., Hambach, U., 2020. Smoothed millennial-scale palaeoclimatic reference data as unconventional comparison targets: Application to European loess records. Sci Rep 10, 5455. https://doi.org/10.1038/s41598-020-61528-8

Zeman, A., Bezvodová, B., Havlíček, P., Minaříková, D., Růžičková, E., Fejfar, O., Kovanda, J., 1986. Zpráva o přehledném výzkumu kvartéru a geomorfologie v úseku Jih se zaměřením na morfostrukturní analýzu pro vyhledávání ložisek přírodních uhlovodíků (Report on Quaternary geometrical and geomorphological research in the south section with a focus on morphostructural analysis for the search of natural hydrocarbon deposits). Czech Geological Survey, Praha.

Zeman, A., Havlíček, P., Minaříková, D., Růžička, M., Fejfar, O., 1980. Kvartérní sedimenty střední Moravy (Quaternary sediments of Central Moravia). Anthropozoic 13, 3791.

Zens, J., Schulte, P., Klasen, N., Krauß, L., Pirson, S., Burow, C., Brill, D., Eckmeier, E., Kels, H., Zeeden, C., Spagna, P., Lehmkuhl, F., 2018. OSL chronologies of paleoenvironmental dynamics recorded by loess-paleosol sequences from Europe: Case studies from the Rhine-Meuse area and the Neckar Basin. Palaeogeography, Palaeoclimatology, Palaeoecology 509, 105–125. https://doi.org/10.1016/j.palaeo.2017.07.019

Zens, J., Zeeden, C., Römer, W., Fuchs, M., Klasen, N., Lehmkuhl, F., 2017. The Eltville Tephra (Western Europe) age revised: Integrating stratigraphic and dating information from different Last Glacial loess localities. Palaeogeography, Palaeoclimatology, Palaeoecology 466, 240–251. https://doi.org/10.1016/j.palaeo.2016.11.033

Zerboni, A., Amit, R., Baroni, C., Coltorti, M., Ferrario, M.F., Fioraso, G., Forno, M.G., Frigerio, C., Gianotti, F., Irace, A., Livio, F., Mariani, G.S., Michetti, A.M., Monegato, G., Mozzi, P., Orombelli, G., Perego, A., Porat, N., Rellini, I., Trombino, L., Cremaschi, M., 2018. Towards a map of the Upper Pleistocene loess of the Po Plain Loess Basin (Northern Italy). Alpine and Mediterranean Quaternary 31, 253–256.

Zerboni, A., Trombino, L., Frigerio, C., Livio, F., Berlusconi, A., Michetti, A.M., Rodnight, H., Spötl, C., 2015. The loess-paleosol sequence at Monte Netto: a record of climate change in the Upper Pleistocene of the central Po Plain, northern Italy. J Soils Sediments 15, 1329–1350. https://doi.org/10.1007/s11368-014-0932-2

Zeuner, F.E., 1956. Loess and Palaeolithic Chronology. Proc. Prehist. Soc. 21, 51–64. https://doi.org/10.1017/S0079497X00017400

Zeuner, F.E., 1937. The climate of the countries adjoining the ice-sheet of the Pleistocene. Proceedings of the Geologists' Association 48, 379–395. https://doi.org/10.1016/S0016-7878(37)80049-8

Zhang, J., Rolf, C., Wacha, L., Tsukamoto, S., Durn, G., Frechen, M., 2018. Luminescence dating and palaeomagnetic age constraint of a last glacial loess-palaeosol sequence from Istria, Croatia. Quaternary International 494, 19–33. https://doi.org/10.1016/j.quaint.2018.05.045

Zhang, X.-X., Claiborn, C., Lei, J.-Q., Vaughan, J., Wu, S.-X., Li, S.-Y., Liu, L.-Y., Wang, Z.-F., Wang, Y.-D., Huang, S.-Y., Zhou, J., 2020. Aeolian dust in Central Asia: Spatial distribution and temporal variability. Atmospheric Environment 238, 117734. https://doi.org/10.1016/j.atmosenv.2020.117734

Zöller, L., Semmel, A., 2001. 175 years of loess research in Germany—long records and "unconformities." Earth-Science Reviews, Recent research on loess and palaeosols, pure and applied 54, 19–28. https://doi.org/10.1016/S0012-8252(01)00039-3

Zollinger, Gaby, 1991. Die Lößdeckschichten der Ziegelei in Allschwil (Kanton Basel - Landschaft/Schweiz) - Ein Beitrag zur Quartärstratigraphie am südlichen Oberrheingraben. Ber. Naturf. Ges. Freiburg i. Br. 79, 165–176.

Figure 1

Click here to access/download;Figure;Fig01_Clima.png

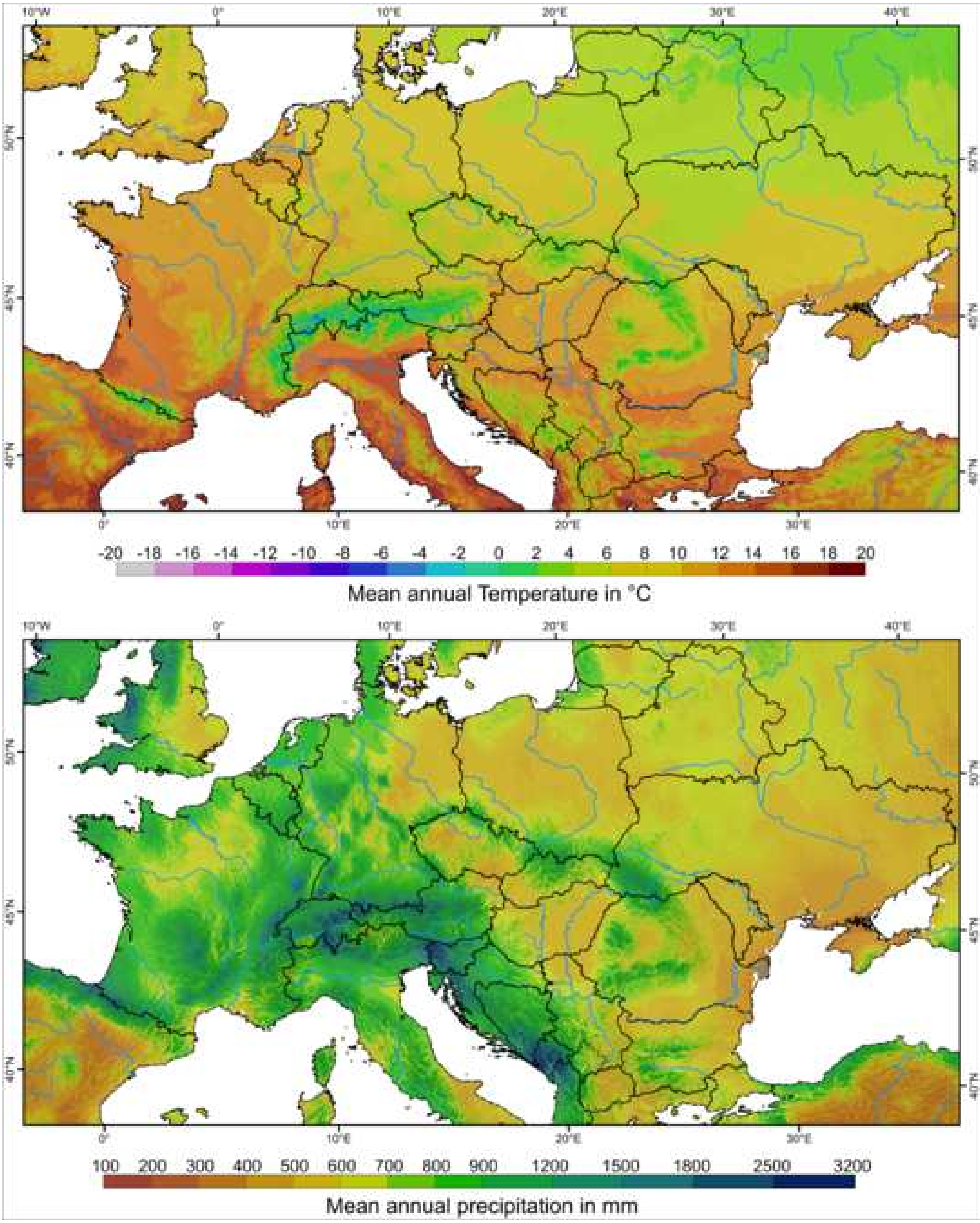

Figure 2

Click here to access/download;Figure;Fig02_Loessmap_Europe_alluvium.png

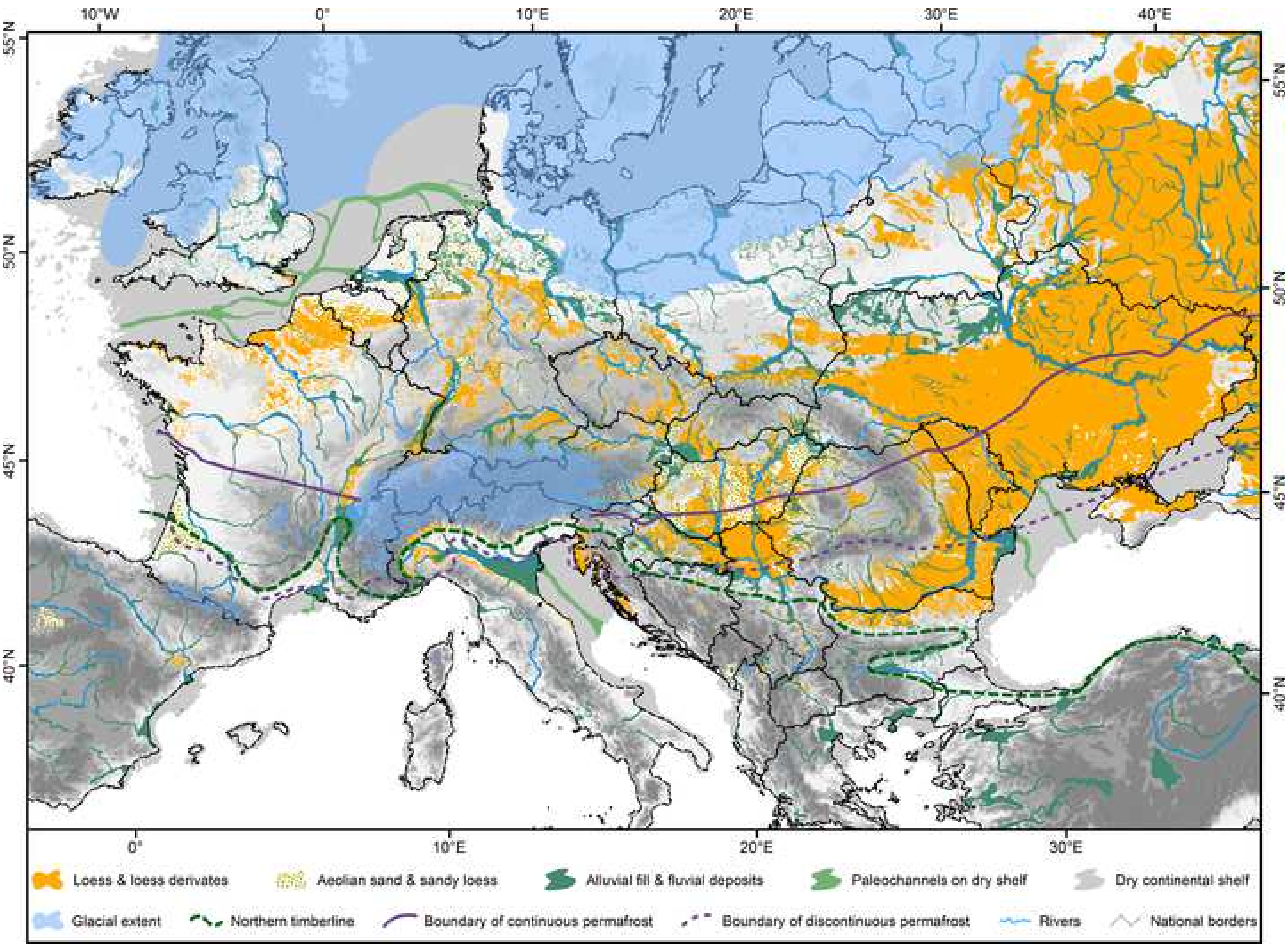

Figure 3

Click here to access/download;Figure;Fig03_Loessmap_Europe_domains.jpg

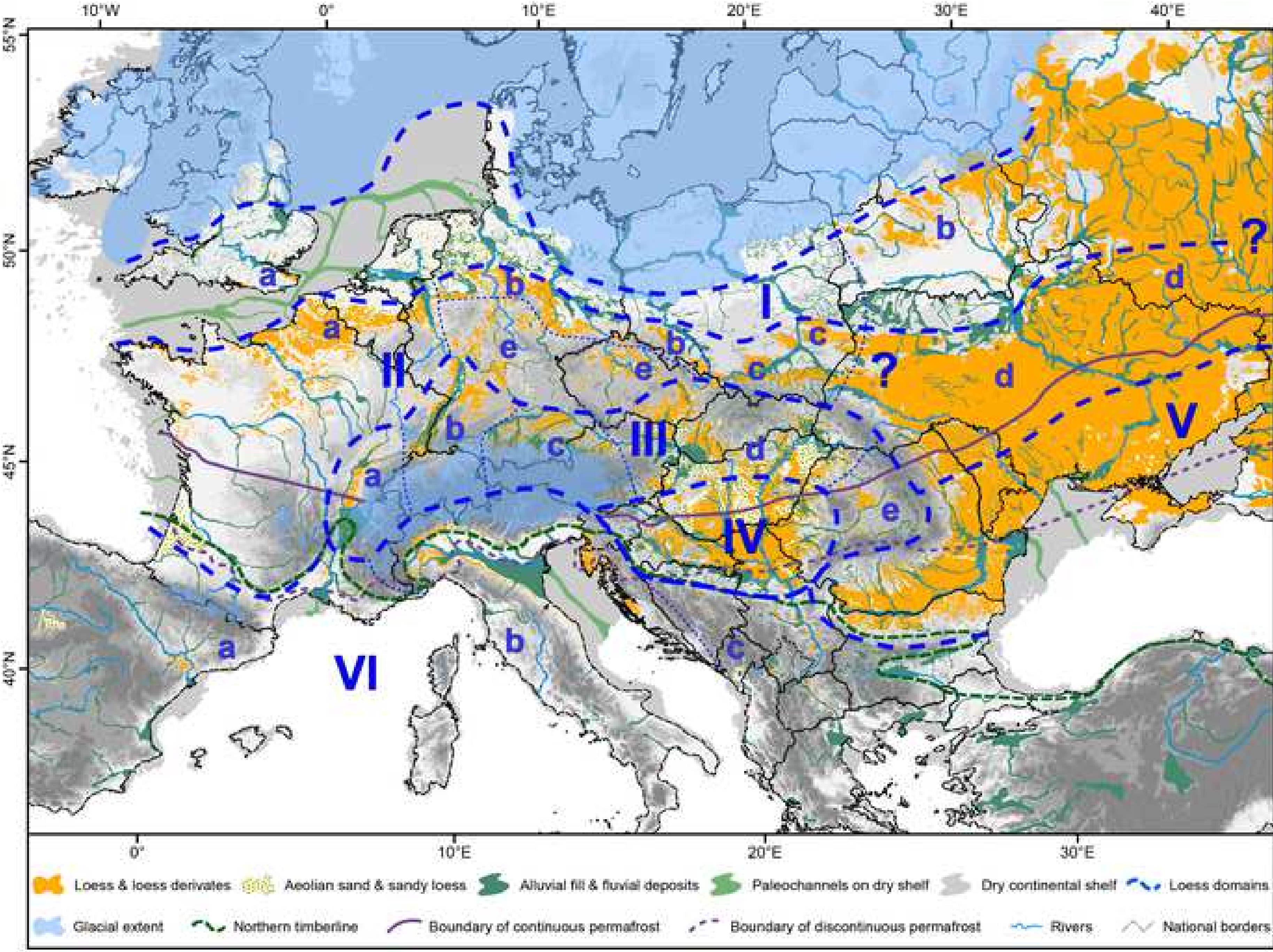

Figure 4

Click here to access/download;Figure;Fig04_Map and transectss.jpg

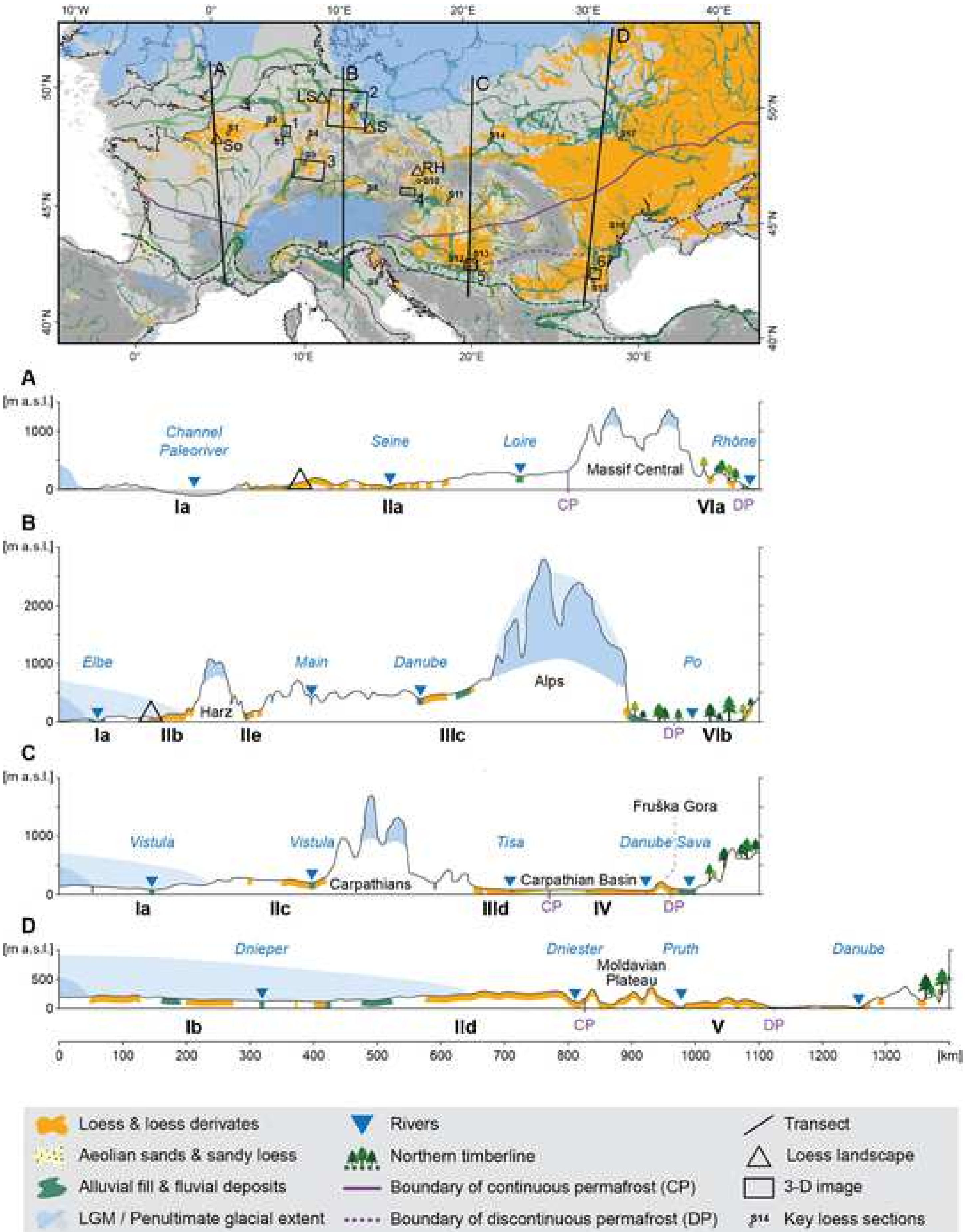

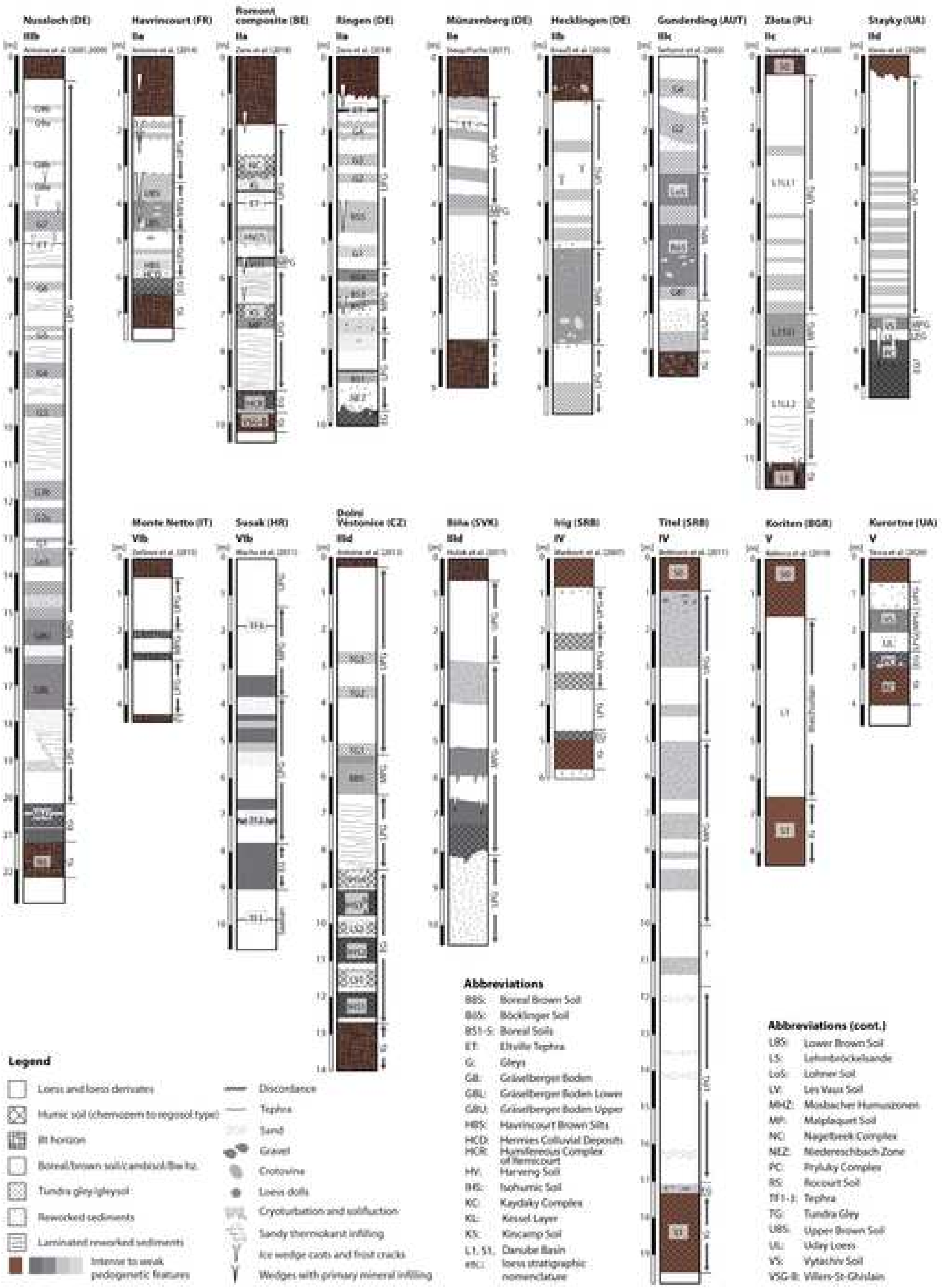
Nussloch (DE)
Havrincourt (FR)
Remont composite (BE)
Ringen (DE)
Münzenberg (DE)
Hecklingen (DE)
Gunderding (AUT)
Złota (PL)
Stayky (UA)
Monte Netto (IT)
Susak (HR)
Dolni Vestonice (CZ)
Biňa (SVK)
Irig (SRB)
Titel (SRB)
Koriten (BGR)
Kurortne (UA)
Legend
Loess and loess derivates
Humic soil (chernozem to regosol type)
Bt horizon
Boreal/brown soil/cambisol/Bw hz.
Tundra gley/gleysol
Reworked sediments
Laminated reworked sediments
Intense to weak pedogenetic features
Discordance
Tephra
Sand
Gravel
Crotovina
Loess dolls
Cryoturbation and solifluction
Sandy thermokarst infilling
Ice wedge casts and frost cracks
Wedges with primary mineral infilling
Abbreviations
BBS: Boreal Brown Soil
BöS: Böcklinger Soil
BS1-5: Boreal Soils
ET: Eltville Tephra
G: Gleys
GB: Gräselberger Boden
GBL: Gräselberger Boden Lower
GBU: Gräselberger Boden Upper
HBS: Havrincourt Brown Silts
HCD: Hermies Colluvial Deposits
HCR: Humiferous Complex of Remicourt
HV: Harveng Soil
IHS: Isohumic Soil
KC: Kaydaky Complex
KL: Kessel Layer
KS: Kincamp Soil
L1, S1, etc.: Danube Basin loess stratigraphic nomenclature
Abbreviations (cont.)
LBS: Lower Brown Soil
LS: Lehmbröckelsande
LoS: Lohner Soil
LV: Les Vaux Soil
MHZ: Mosbacher Humuszonen
MP: Malplaquet Soil
NC: Nagelbeek Complex
NEZ: Niedereschbach Zone
PC: Pryluky Complex
RS: Rocourt Soil
TF1-3: Tephra
TG: Tundra Gley
UBS: Upper Brown Soil
UL: Uday Loess
VS: Vytachiv Soil
VSG-B: Villers-St-Ghislain

Figure 6

Click here to access/download;Figure;Fig06 asymmetric valley.jpg

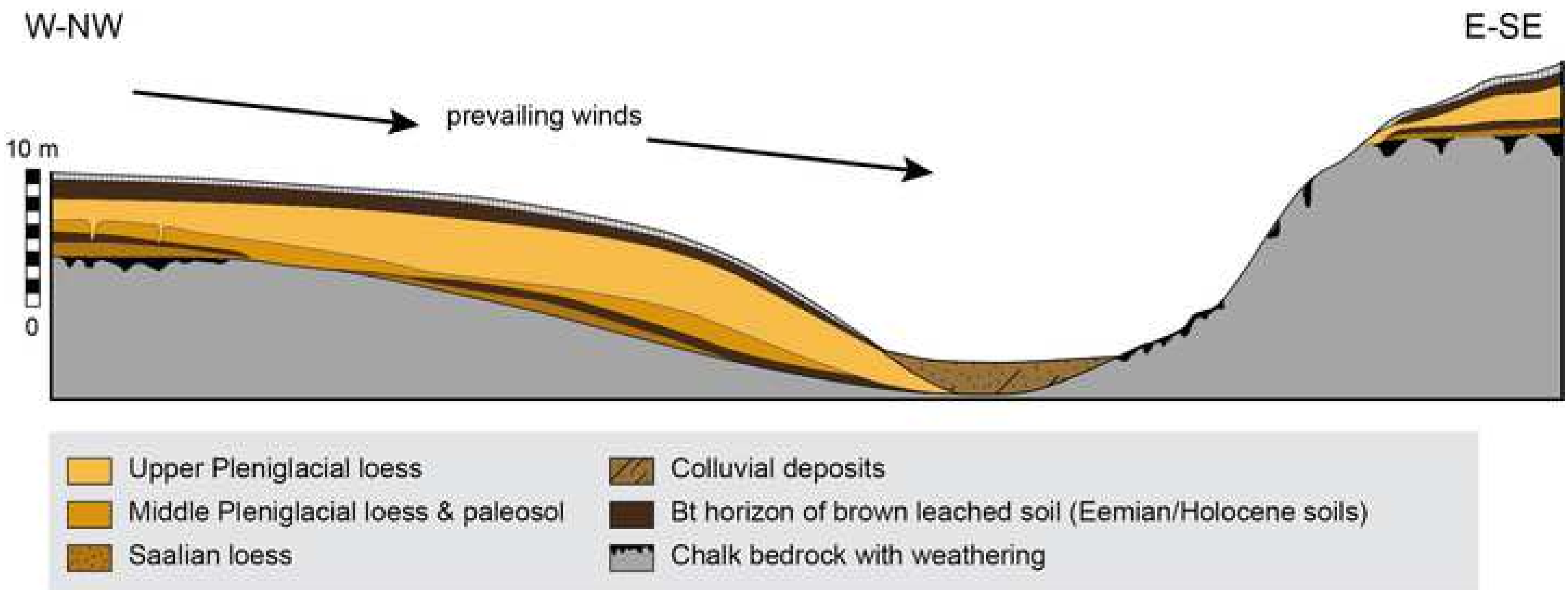

Figure 7

Click here to access/download;Figure;Fig07_Blockbild_Remagen.jpg

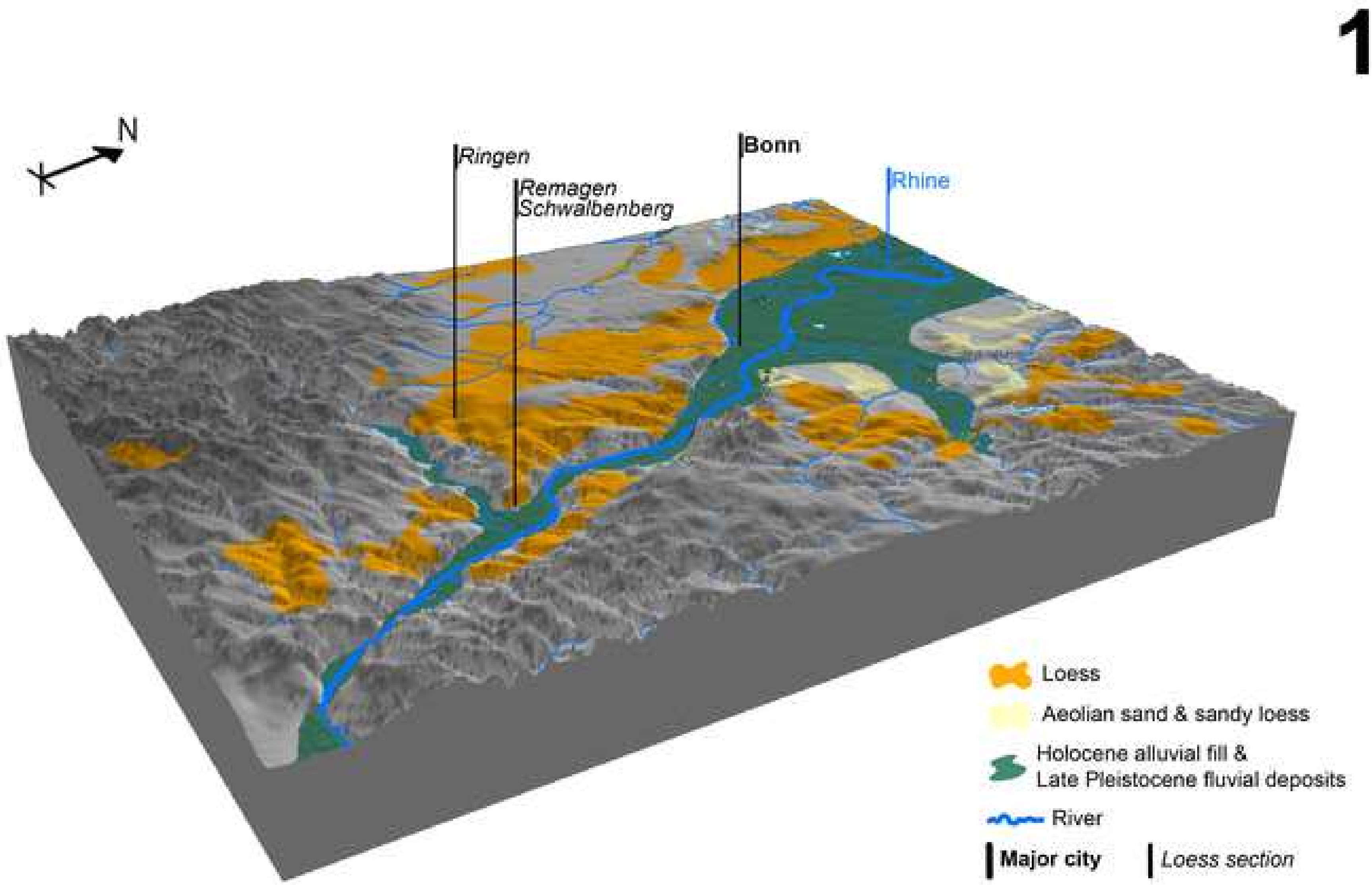

Figure 8

Click here to access/download;Figure;Fig08_Blockbild_Harzvorland.jpg

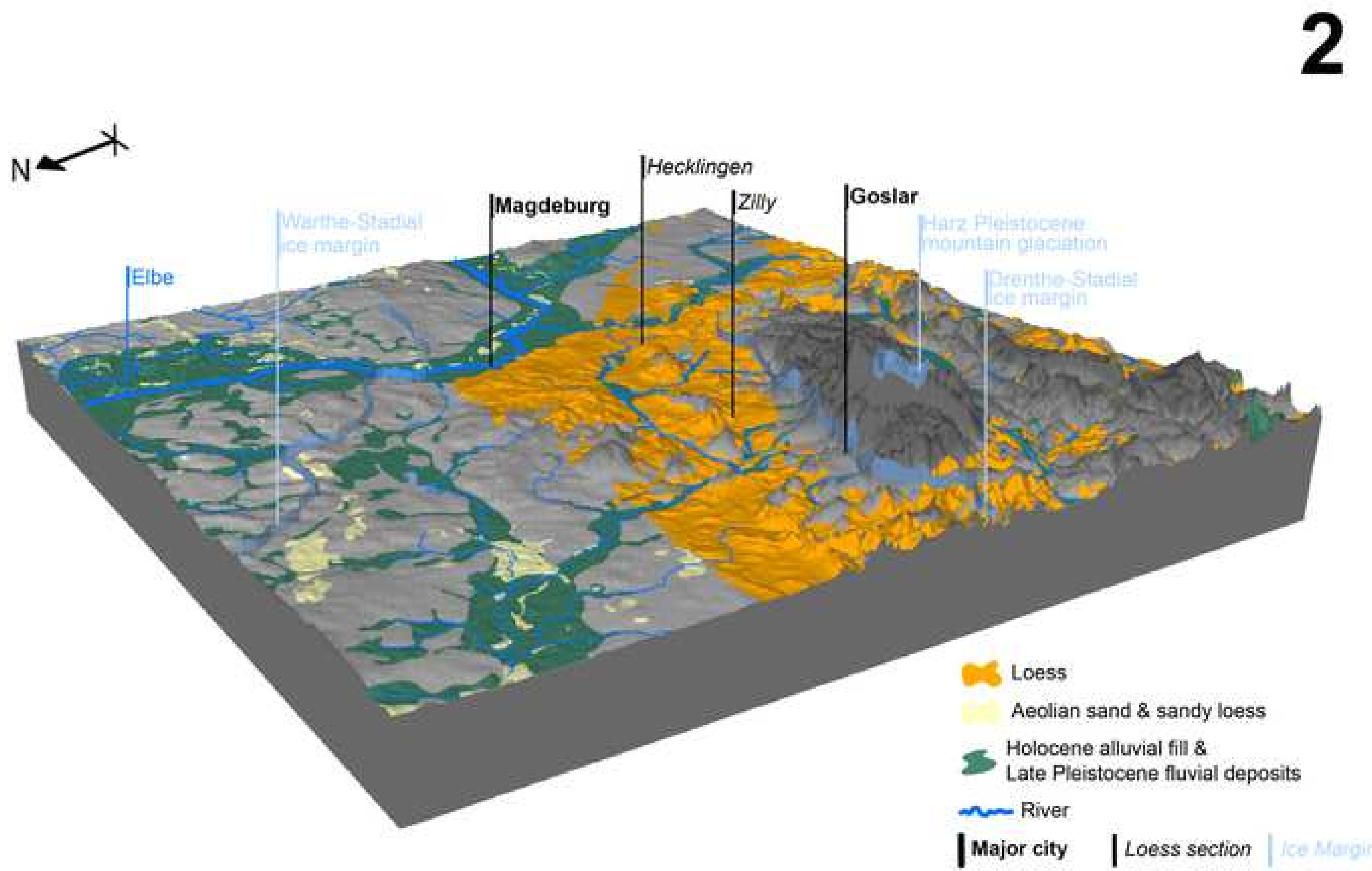

Figure 9

Click here to access/download;Figure;Fig09 Loss marginal ramp.jpg

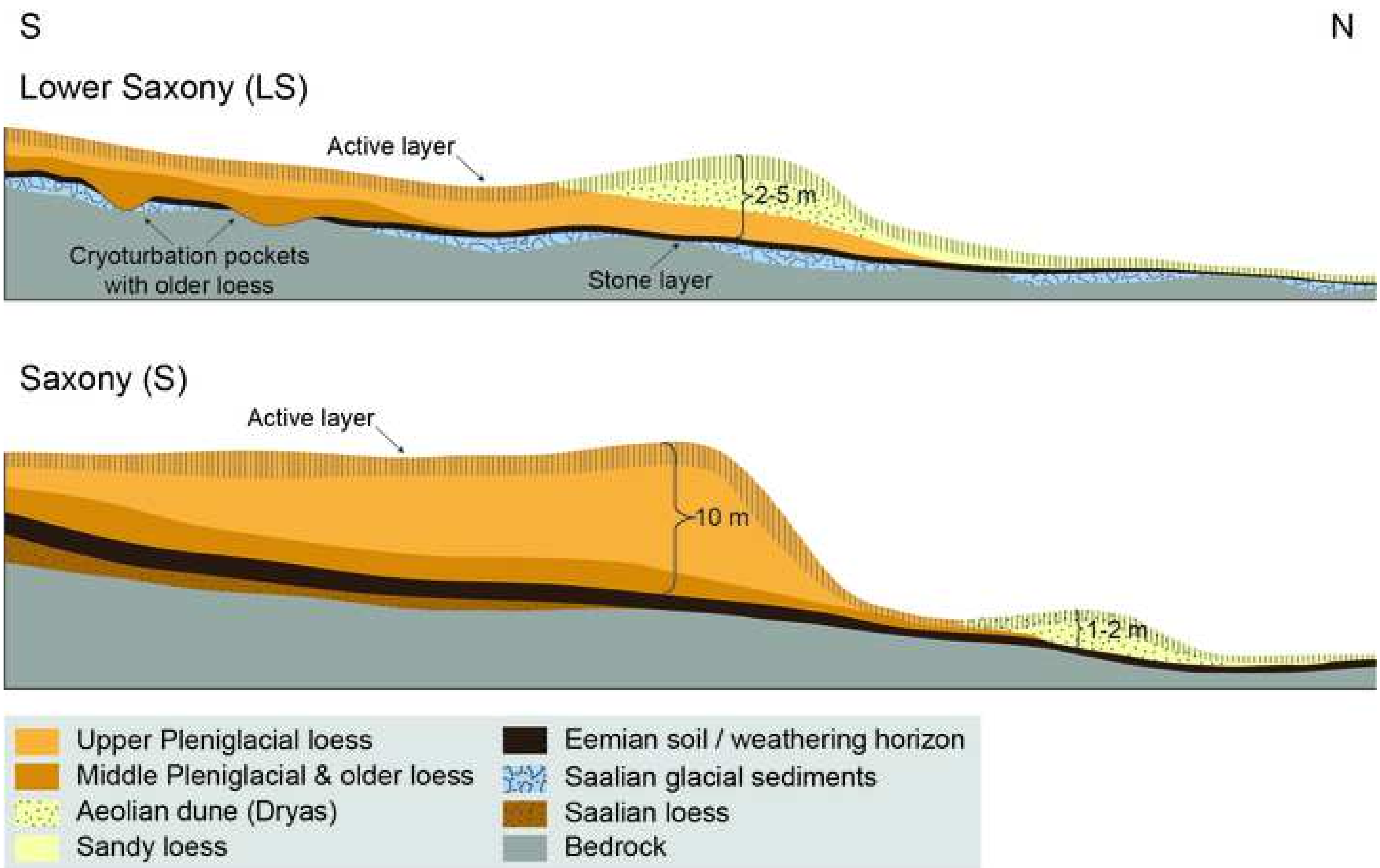

Figure 10

Click here to access/download;Figure;Fig10_Blockbild_Kraichgau.jpg

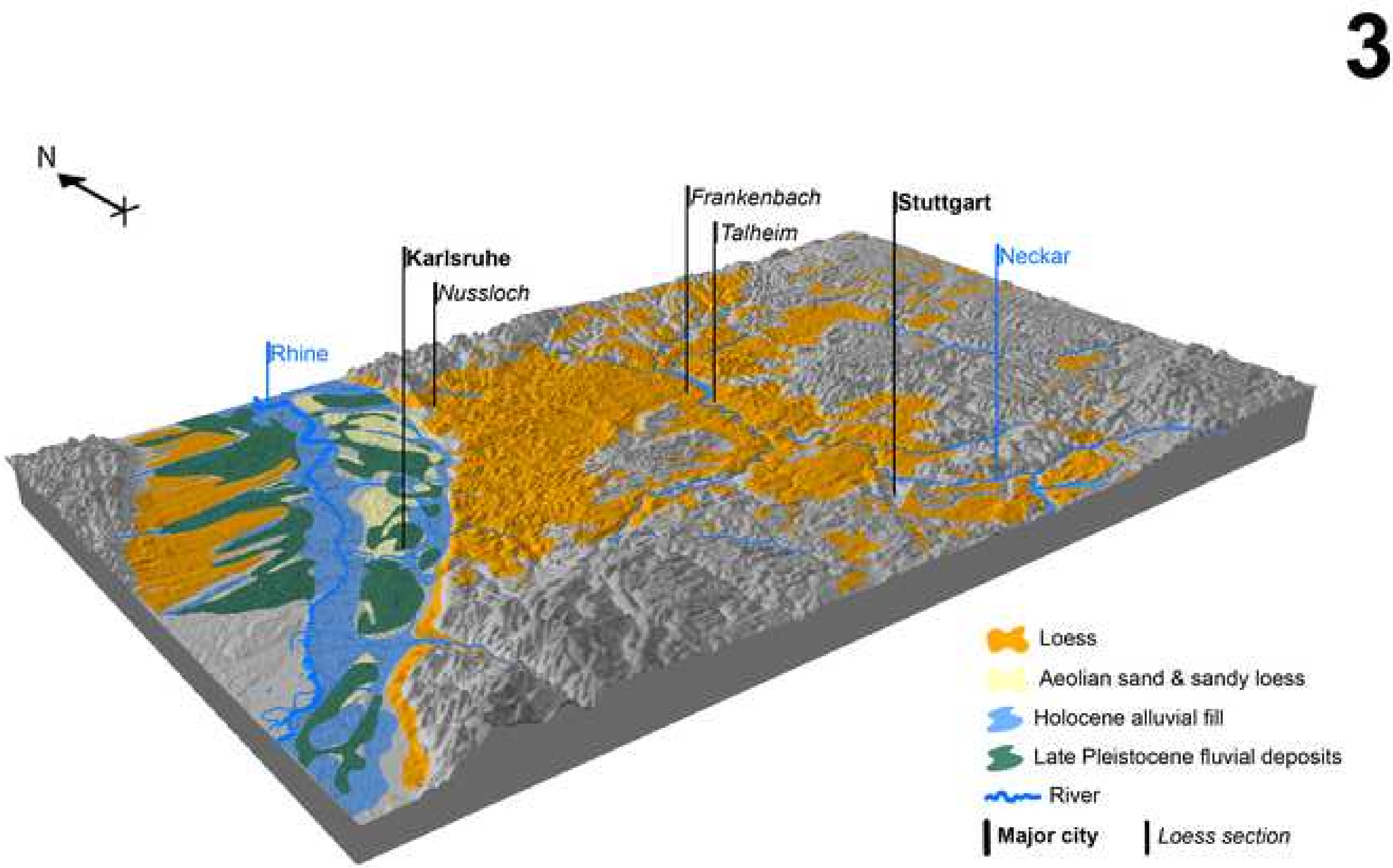

Figure 11 Click here to access/download;Figure;Fig11_Blockbild_Wiener_Pforte.png

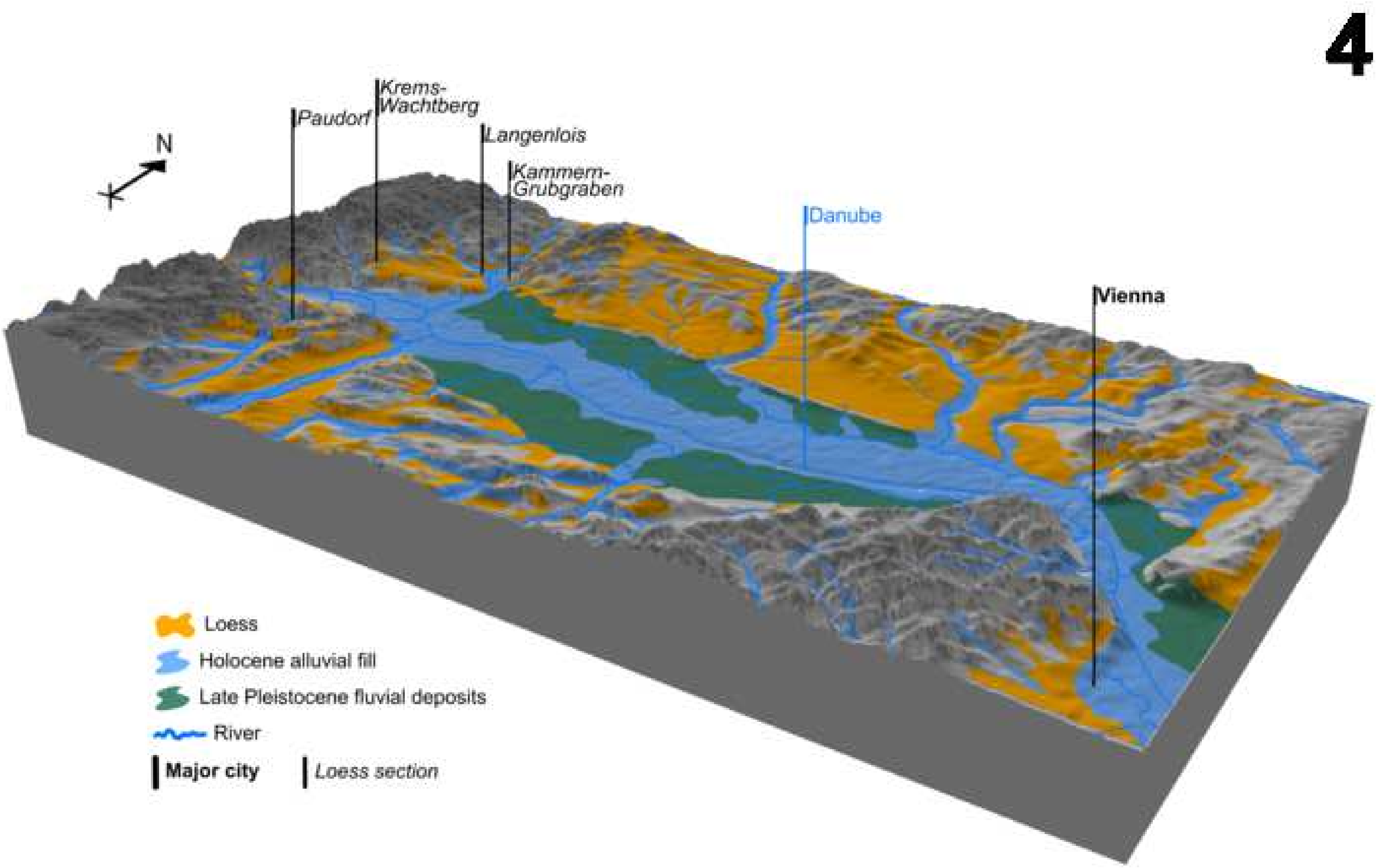

Figure 12

Click here to access/download;Figure;Fig12 KUKLA 69 Loess Terrasses.jpg

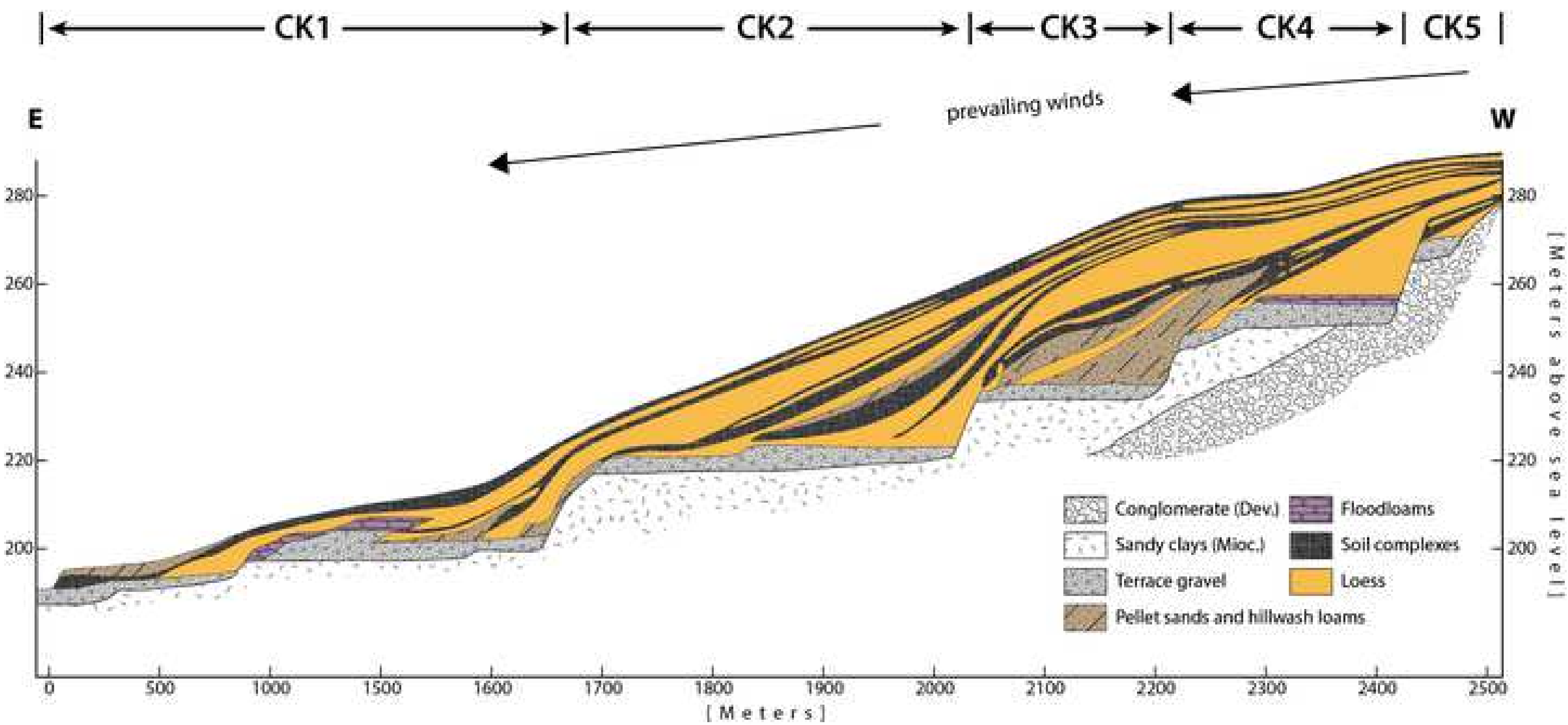

Figure 13

Click here to access/download;Figure;Fig13_Blockbild_Irig_Titel.png

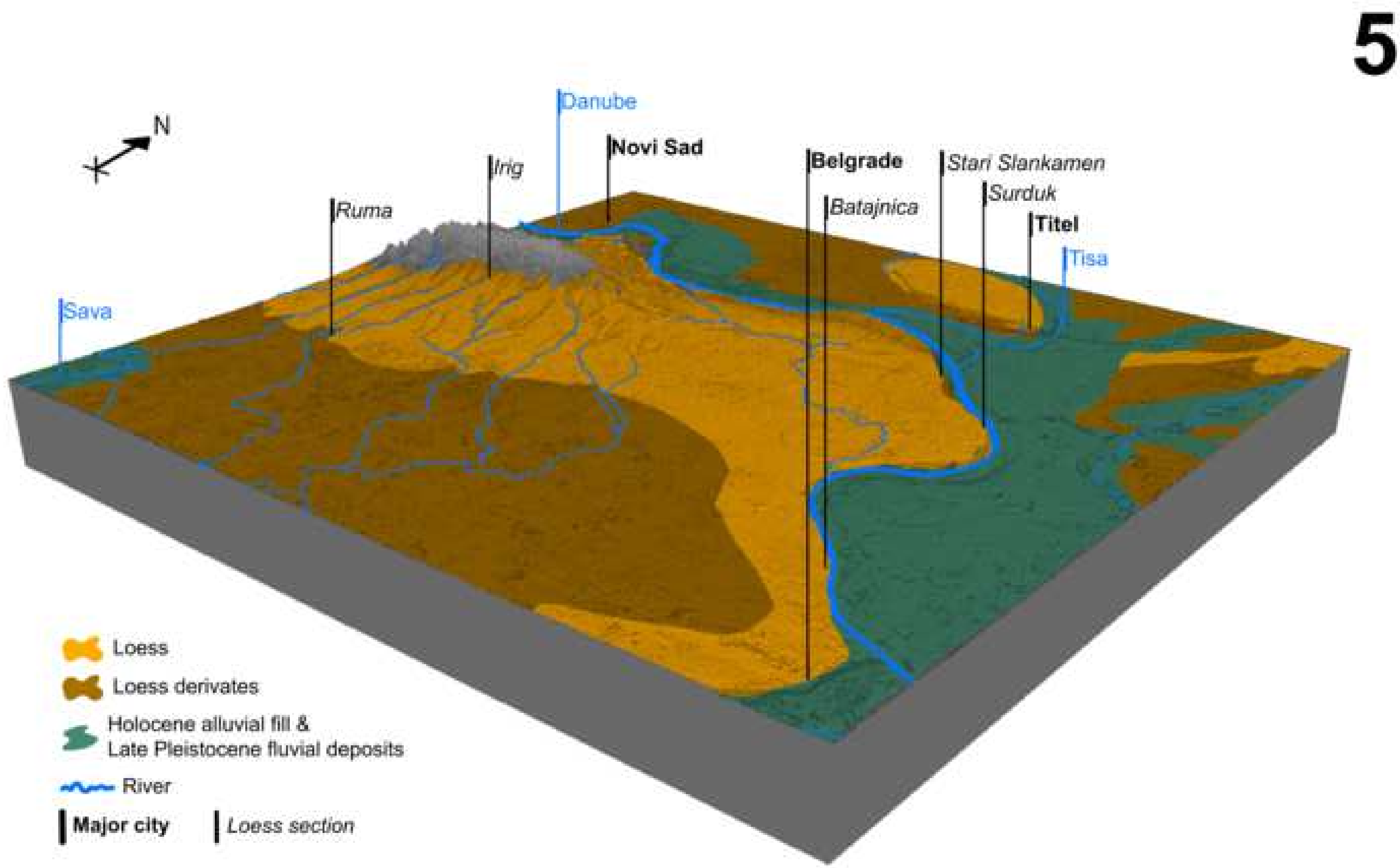

Figure 14

Click here to access/download;Figure;Fig14_Blockbild_Vlasca.jpg

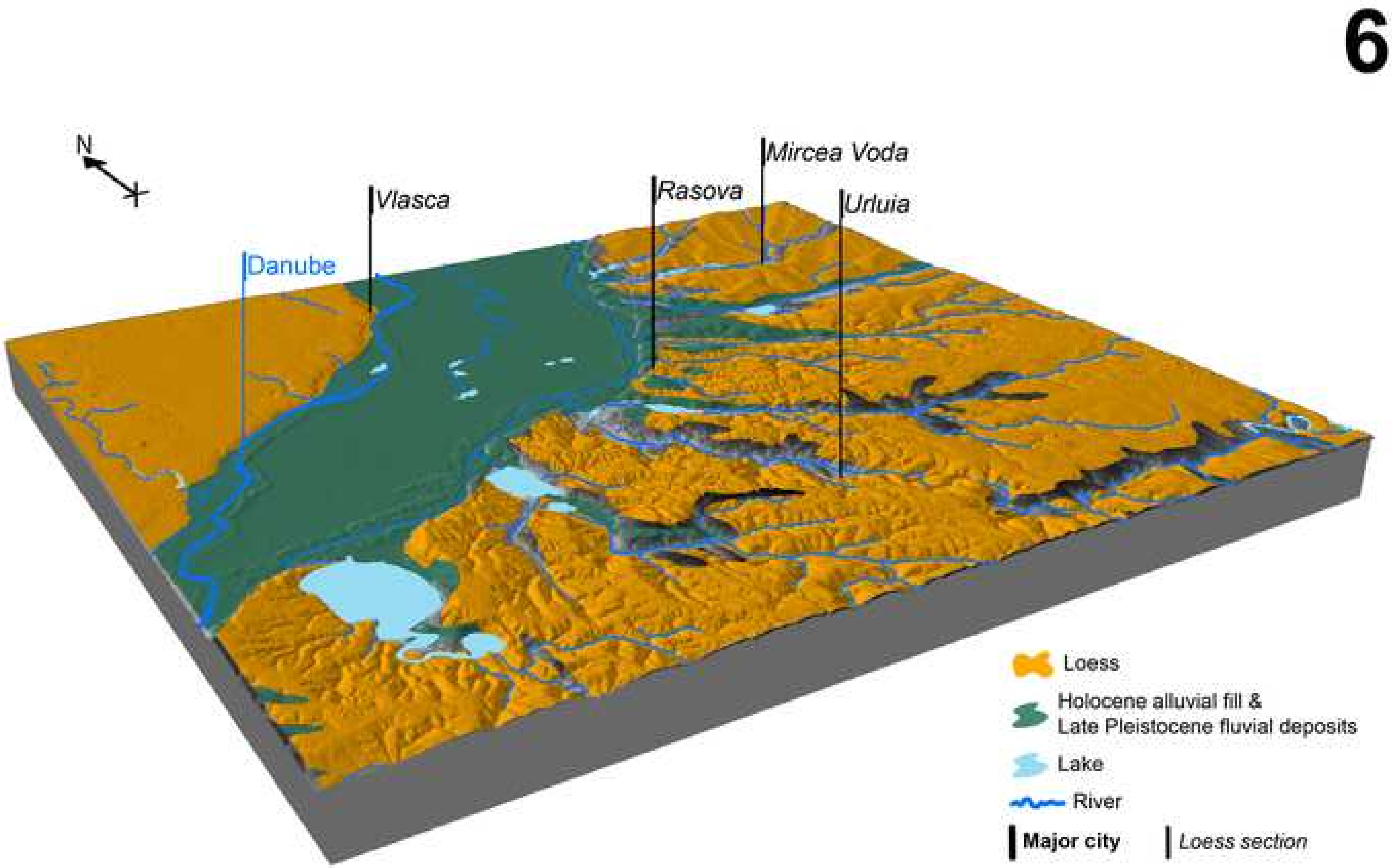

Figure 15

Click here to access/download;Figure;Fig15_Boxplots_Hoehenverteilung.png

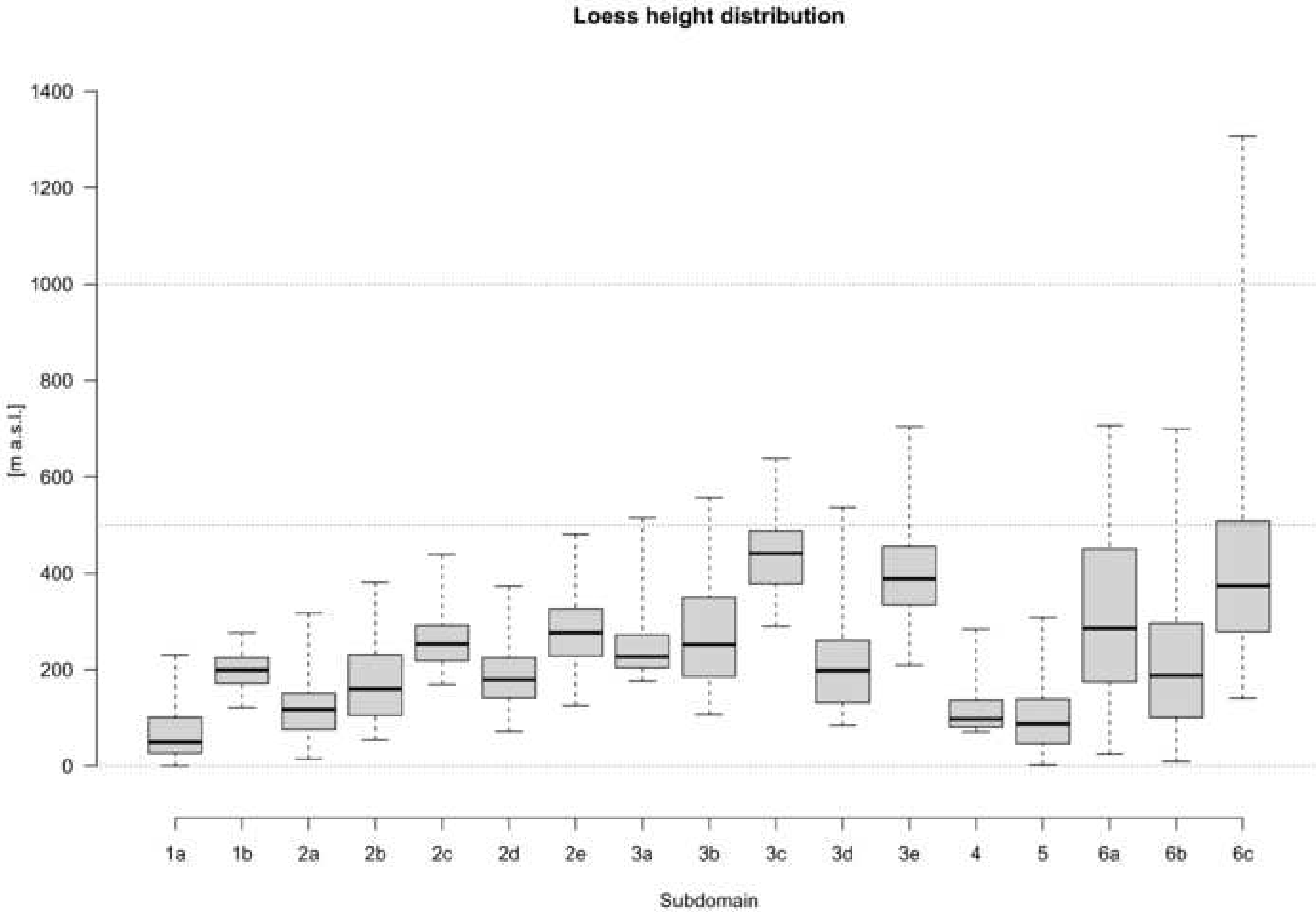

Figure 16

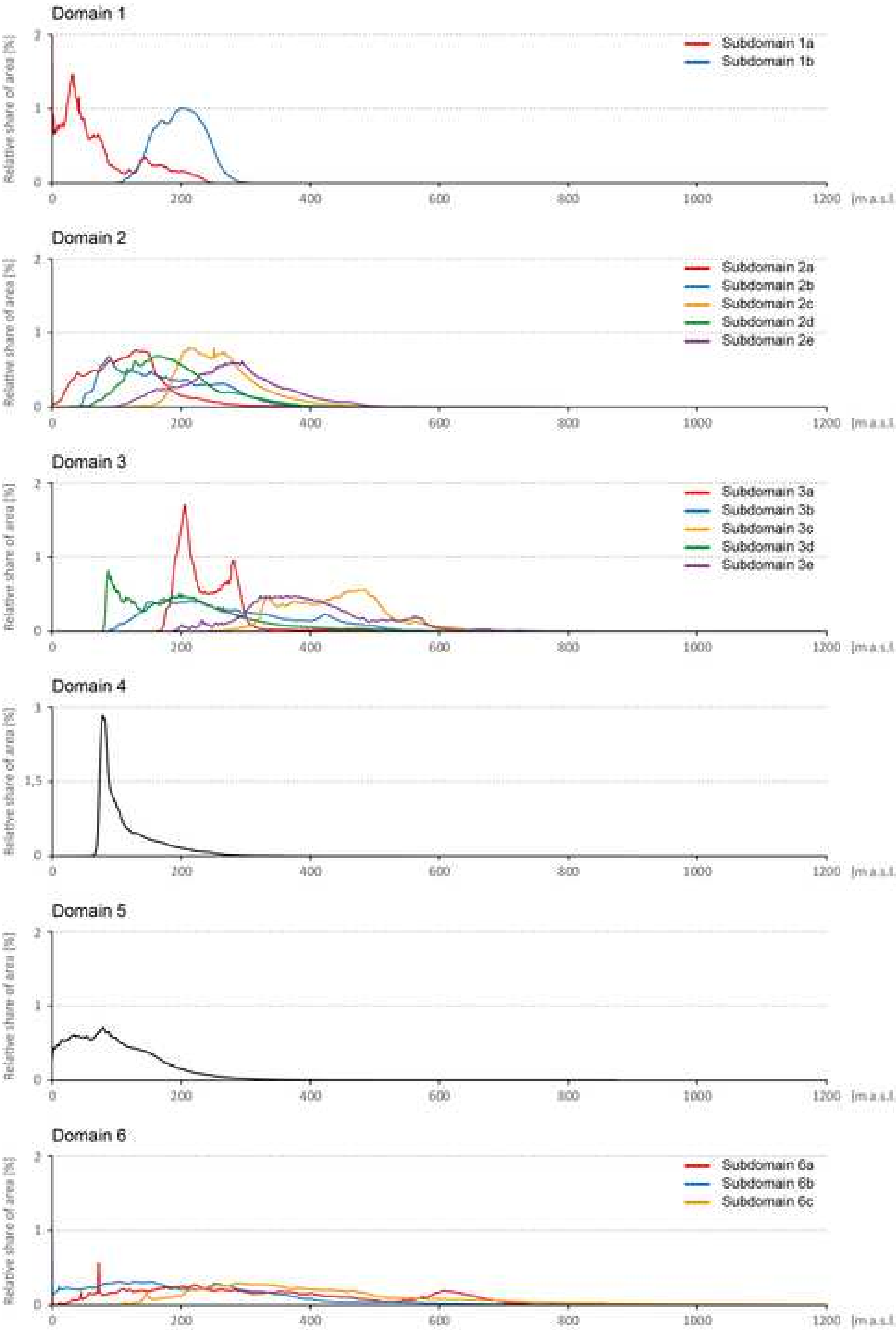
Domain 1
Subdomain 1a
Subdomain 1b
Domain 2
Subdomain 2a
Subdomain 2b
Subdomain 2c
Subdomain 2d
Subdomain 2e
Domain 3
Subdomain 3a
Subdomain 3b
Subdomain 3c
Subdomain 3d
Subdomain 3e
Domain 4
Domain 5
Domain 6
Subdomain 6a
Subdomain 6b
Subdomain 6c
Relative share of area [%]
0
200
400
600
800
1000
1200
[m a.s.l.]
0
1
2
1,5
3

Figure 17

Click here to access/download;Figure;Fig17_Loessmap_Vergleich_Haase.png

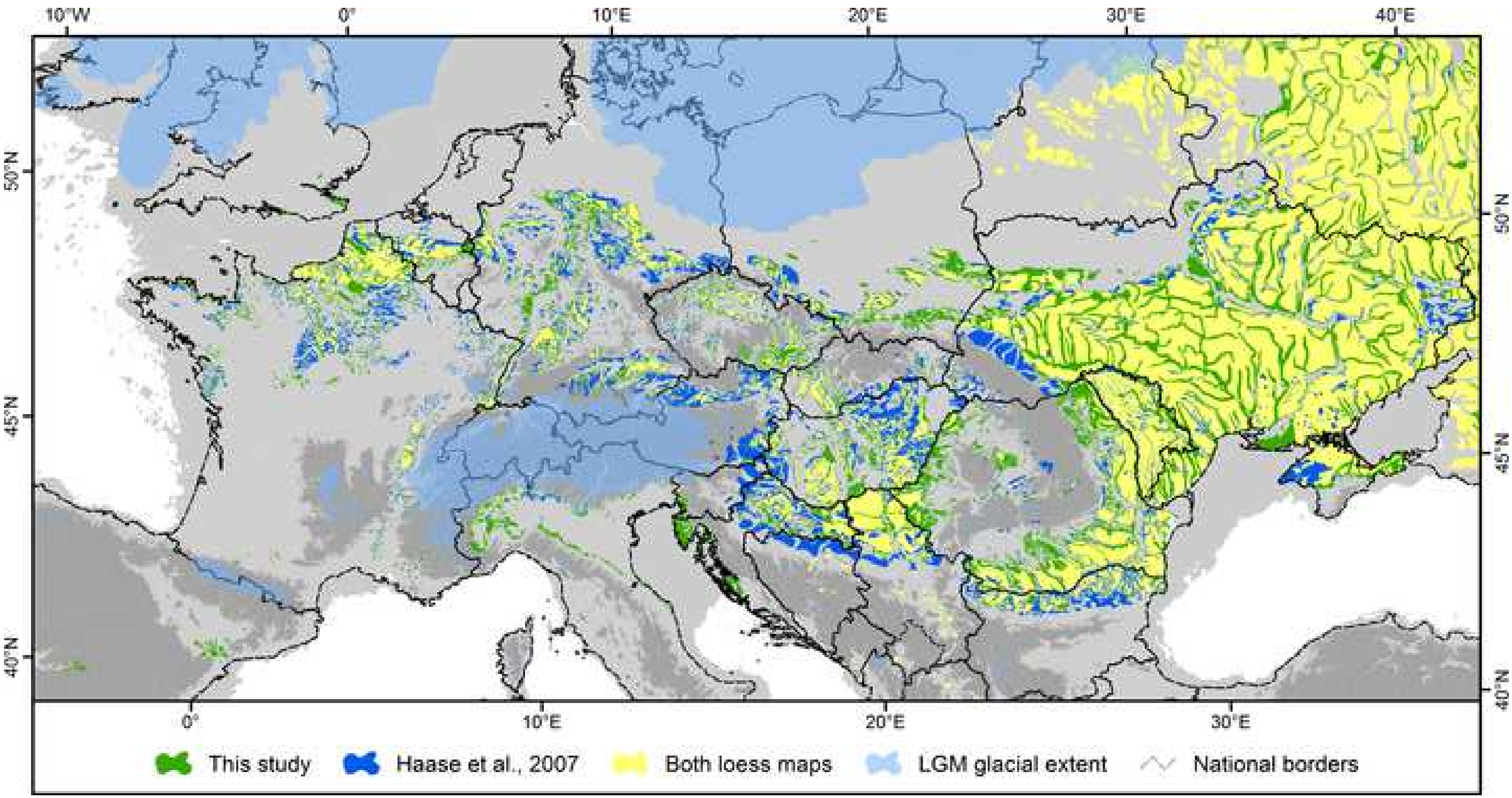

Figure 18

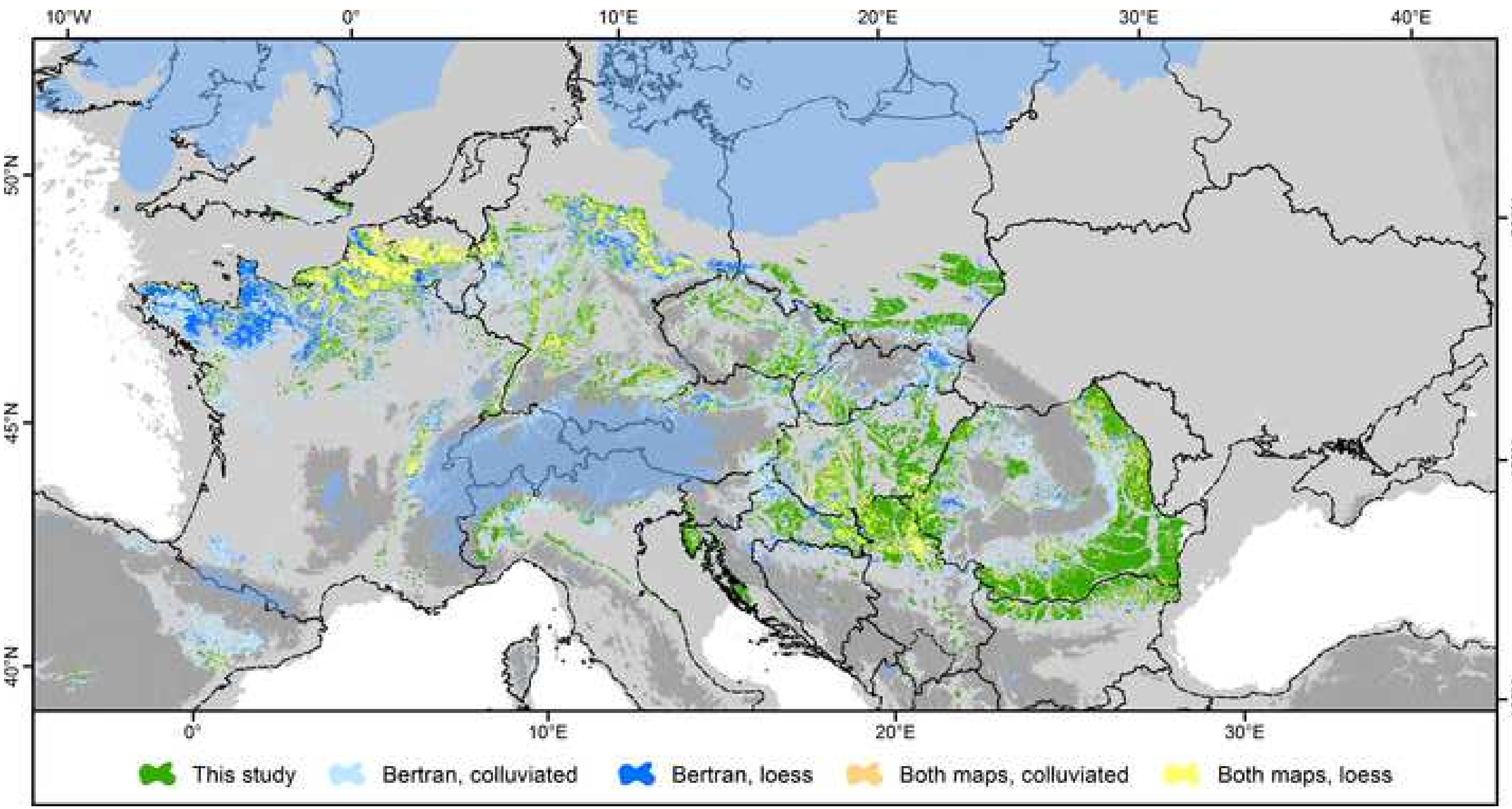
10°W
0°
10°E
20°E
30°E
40°E
50°N
45°N
40°N
This study
Bertran, colluviated
Bertran, loess
Both maps, colluviated
Both maps, loess

Figure 19

Click here to access/download;Figure;Fig19_Loessmap_Europe_dust_deposition.png

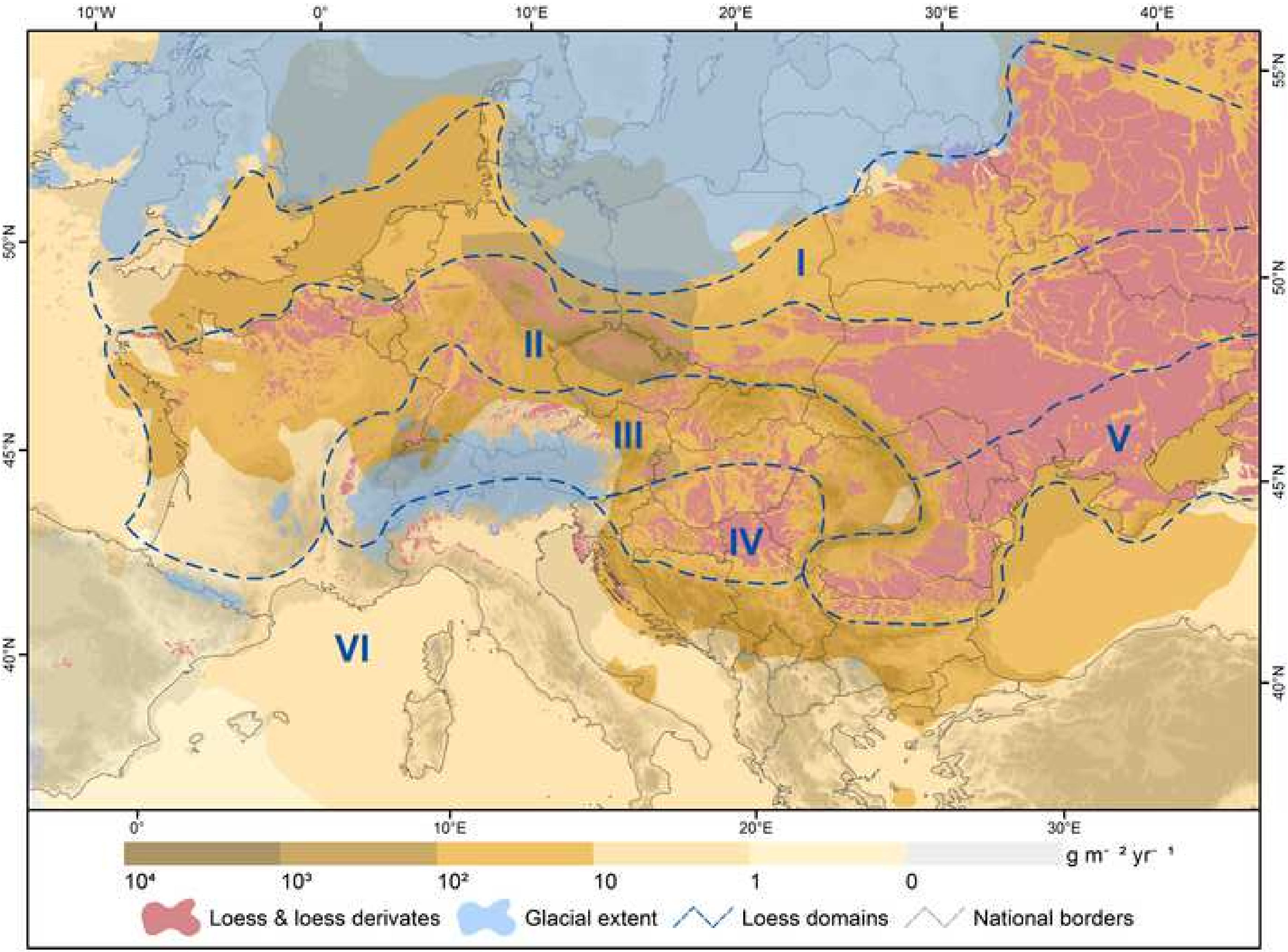

Figure 20

Click here to access/download;Figure;Fig20 Loess model.jpg

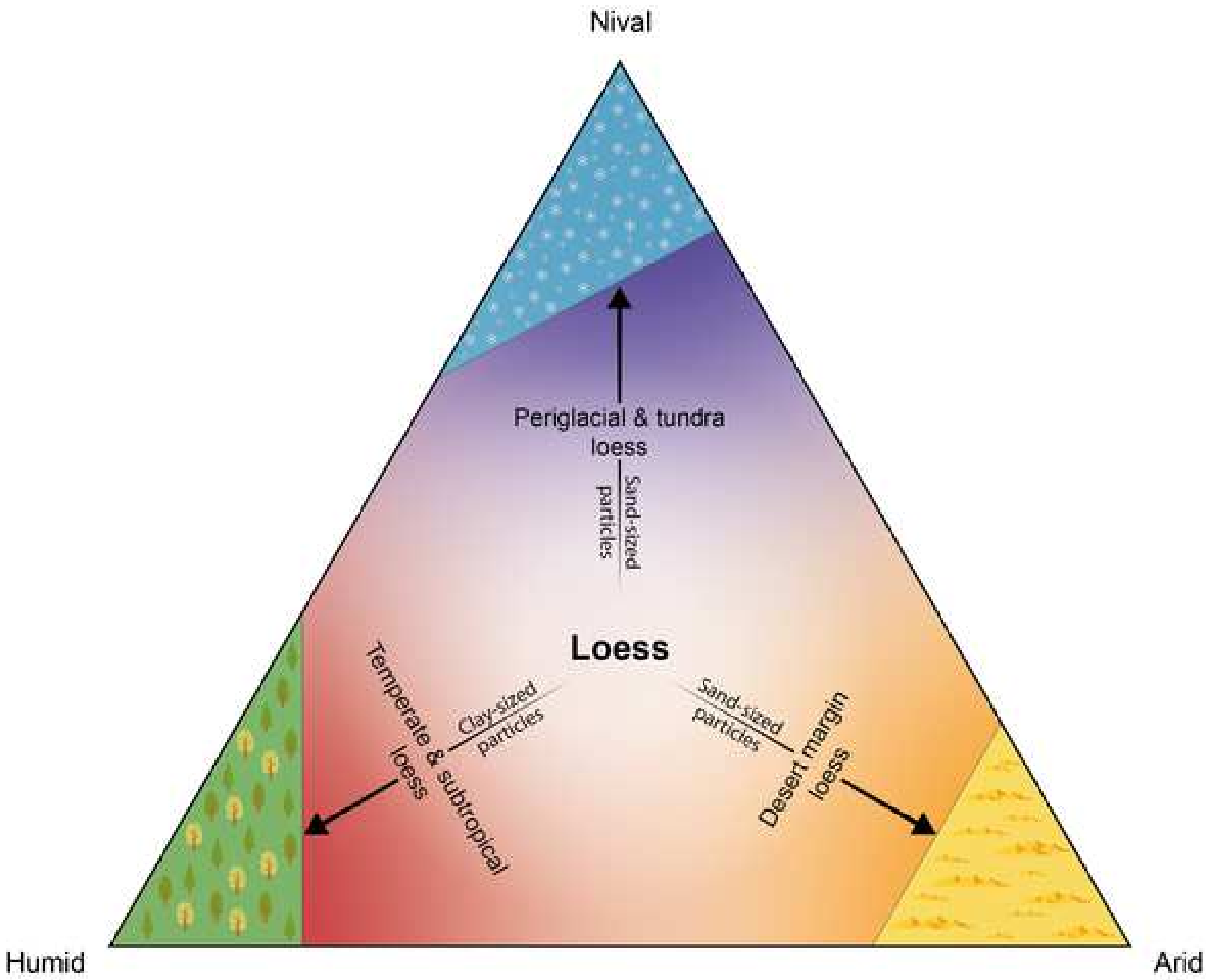

Figure 21

Click here to access/download;Figure;Fig21_Loessmap_Europe_glaciation.png

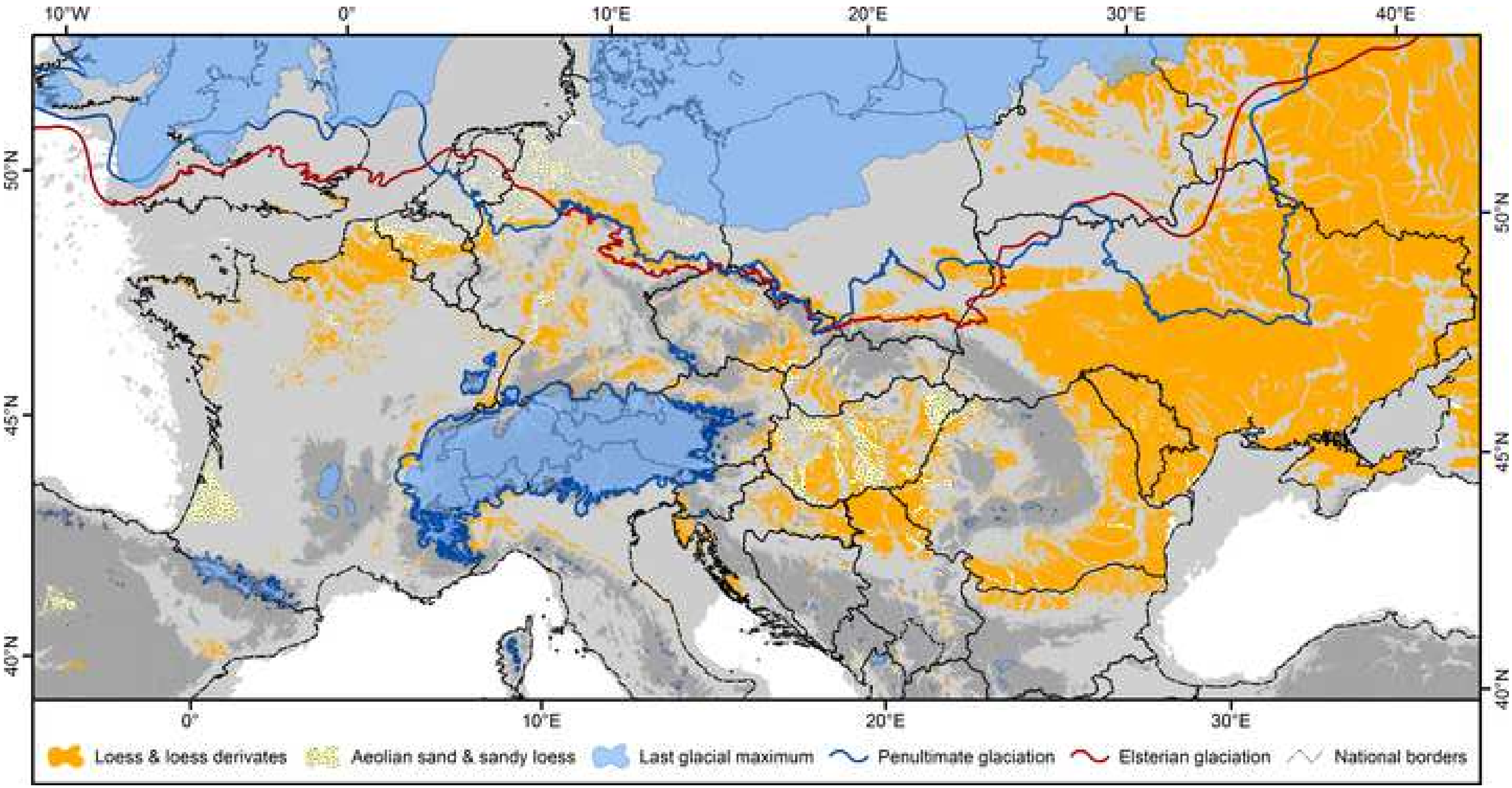

Conflict of interest

The authors declare that the research was conducted in the absence of any commercial or financial relationships that could be construed as a potential conflict of interest.

On behalf of all authors

Prof. Dr. Frank Lehmkuhl
Corresponding author

Click here to access/download
Supplementary Material
Lehmkuhl et al Suppl.pdf